Old Dominion University
ODU Digital Commons

OES Theses and Dissertations | Ocean & Earth Sciences

Spring 2005

Correlation and Causes of Fifth Order Cycles Within the Upper Cretaceous Eagle Formation, Bighorn Basin of Wyoming

Kimberly Ann Johnson
Old Dominion University

Follow this and additional works at: https://digitalcommons.odu.edu/oeas_etds

 Part of the Geology Commons

Recommended Citation

Johnson, Kimberly A.. "Correlation and Causes of Fifth Order Cycles Within the Upper Cretaceous Eagle Formation, Bighorn Basin of Wyoming" (2005). Doctor of Philosophy (PhD), Dissertation, Ocean & Earth Sciences, Old Dominion University, DOI: 10.25777/3m7g-1s87
https://digitalcommons.odu.edu/oeas_etds/55

This Dissertation is brought to you for free and open access by the Ocean & Earth Sciences at ODU Digital Commons. It has been accepted for inclusion in OES Theses and Dissertations by an authorized administrator of ODU Digital Commons. For more information, please contact digitalcommons@odu.edu.

CORRELATION AND CAUSES OF FIFTH ORDER CYCLES WITHIN THE UPPER CRETACEOUS EAGLE FORMATION, BIGHORN BASIN OF WYOMING

by

Kimberly Ann Johnson
B.A. August 1992, Old Dominion University
M.S. May 1995, Old Dominion University

A Dissertation Submitted to the Faculty of
Old Dominion University in Partial Fulfillment of the
Requirement for the Degree of

DOCTOR OF PHILOSOPHY

OCEAN, EARTH AND ATMOSPHERIC SCIENCES

OLD DOMINION UNIVERSITY
May 2005

Approved by:

Donald J.P. Swift (Director)

Dennis Darby (Member)

James Castle (Member)

Chester Grosch (Member)

Reproduced with permission of the copyright owner. Further reproduction prohibited without permission.

ABSTRACT

CORRELATION AND CAUSES OF FIFTH ORDER CYCLES
WITHIN THE UPPER CRETACEOUS EAGLE FORMATION,
BIGHORN BASIN OF WYOMING

Kimberly Ann Johnson
Old Dominion University, 2005
Director: Dr. Donald J.P. Swift

Cyclic stratification was examined in the Upper Cretaceous (Santonian-Campanian) section (Eagle Formation) within the Bighorn Basin of Wyoming. Of particular concern was the 10^3 to 10^4 year band, which in marine settings has been attributed to orbital forcing (Milankovitch cyclicity). A series of 19 sections were measured through the Virgelle Member of the Eagle Formation. Most were measured on the "J"-shaped escarpment that constitutes the nose and north flank of the Thermopolis anticline. Several others were measured at sites up to 30 km to the northwest along paleo-shoreline. In the study, detailed thickness data of all sections and grain size data of three sections were used to test the hypothesis that fifth-order cycles are of eustatic origin. Spectral analysis of limited grain size data clearly indicated a strong 41,000-year Milankovitch cycle (the obliquity cycle) along with a well-defined 20,000-year Milankovitch cycle (the precession cycle). The Sherman statistic, a statistic which tests whether events are periodic or random, was used on the more extensive thickness data. Results indicated the presence of Milankovitch events at periodicities of 41,000 and 20,000-years, and these events have been correlated along paleo-shoreline as well as into the basin. This data has been interpreted as a result of varying monsoonal strength often ascribed to precessional control. Variation in monsoonal strength may have caused the rate of sediment input to vary, or may have caused sea level to vary, or both.

Reproduced with permission of the copyright owner. Further reproduction prohibited without permission.

This dissertation is dedicated to my stepfather Steve Forster, a fellow geologist who has influenced me in more ways that can he can imagine.

Reproduced with permission of the copyright owner. Further reproduction prohibited without permission.

ACKNOWLEDGMENTS

There are several people who have helped to make this dissertation possible. I would like to thank my dissertation committee members individually. Dr. Donald Swift for introducing me to the Bighorn Basin and believing in me always. Dr. Dennis Darby for his insights and helping me to become a better writer. Dr. Chet Grosch for his amazing contribution with respect to time series analysis. Dr. Jim Castle for the friendly comments and willingness to be an outside reader. I would also like to thank the students and faculty of Old Dominion University and Tidewater Community College for their help in the field, in the lab and with logistics. To my mother and my sister Amanda for their unconditional support during the last five years. To Carol Peterson, Sherry Johnson, Sharon DuBois, Rob Gucwa and Lisa Van Kylen for all their support during the ups and downs in the field, in the lab and during the writing process. And finally to Mike Howell, my rock, my best friend and the reason I enjoy life.

Reproduced with permission of the copyright owner. Further reproduction prohibited without permission.

TABLE OF CONTENTS

Page

Reproduced with permission of the copyright owner. Further reproduction prohibited without permission.

TABLE OF CONTENTS (continued)

Page

Reproduced with permission of the copyright owner. Further reproduction prohibited without permission.

LIST OF TABLES

Table Page

Reproduced with permission of the copyright owner. Further reproduction prohibited without permission.

LIST OF FIGURES

Reproduced with permission of the copyright owner. Further reproduction prohibited without permission.

Reproduced with permission of the copyright owner. Further reproduction prohibited without permission.

Reproduced with permission of the copyright owner. Further reproduction prohibited without permission.

Reproduced with permission of the copyright owner. Further reproduction prohibited without permission.

LIST OF PLATES

Plate

Reproduced with permission of the copyright owner. Further reproduction prohibited without permission.

INTRODUCTION

The purpose of this study is to investigate the origin of high-frequency stratigraphic cyclicity in the Cretaceous Foreland Basin of the North American western interior (Figure 1). The unit involved is the Upper Cretaceous (Santonian-Campanian) section (Eagle Formation) within the Bighorn Basin of Wyoming (Figure 2). Of particular concern is the 10^3 to 10^4 year band, the fifth-order cycles of Van Wagoner et al. (1990) and Plint (1996) in which tectonics, eustasy, and sediment supply have all been suggested as forcing mechanisms. The first step has been to determine how far such fifth-order cycles can be correlated in order to establish whether or not the forcing is therefore of at least regional scale. The question then becomes, what factors (or forces) are controlling sedimentation at the fifth-order scale? Possible factors included allocyclic factors (forces outside the basin), autocyclic factors (forces within the basin), or both. Allocyclicity may involve eustasy (long-period or Milankovitch band), or may involve hydrological mechanisms within the basin such as river avulsion or groundwater storage during climatic events involving large volumes of precipitation (monsoonal). Autocyclicity may involve tectonic forces within the basin.

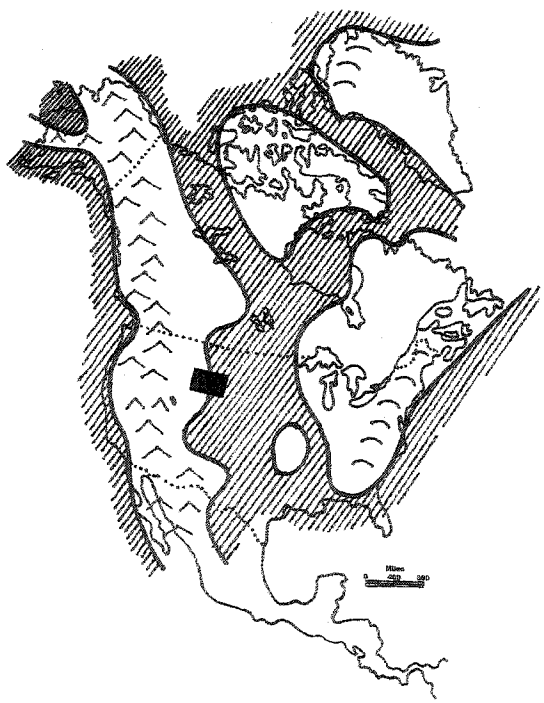

Figure 1. Paleogeographic map of the North American continent during the Upper Cretaceous, showing the location and extent of the Western Interior Seaway. Black box denotes the state of Wyoming (modified from Williams and Stelck, 1975).

The model journal used for this dissertation was American Association of Petroleum Geologists Bulletin.

Reproduced with permission of the copyright owner. Further reproduction prohibited without permission.

In the study, grain size distribution data and data for the spectral analysis of bed thickness in vertical profiles will be used to analyze the cyclic shales and sands within the Virgelle Member of the Eagle Formation. While the study is seen as complete in itself, it is designed to serve as a basis for exploring problems outside the Bighorn Basin, which can be pursued in following years. The Virgelle Member, coupled with the detailed measured sections in a small geographic area, serves as a control area for further studies. Once the cyclicity has been established for the control area, it is possible to investigate whether or not these cycles correlate within the basin, outside the basin, to other Upper Cretaceous units within the United States, and if possible, globally.

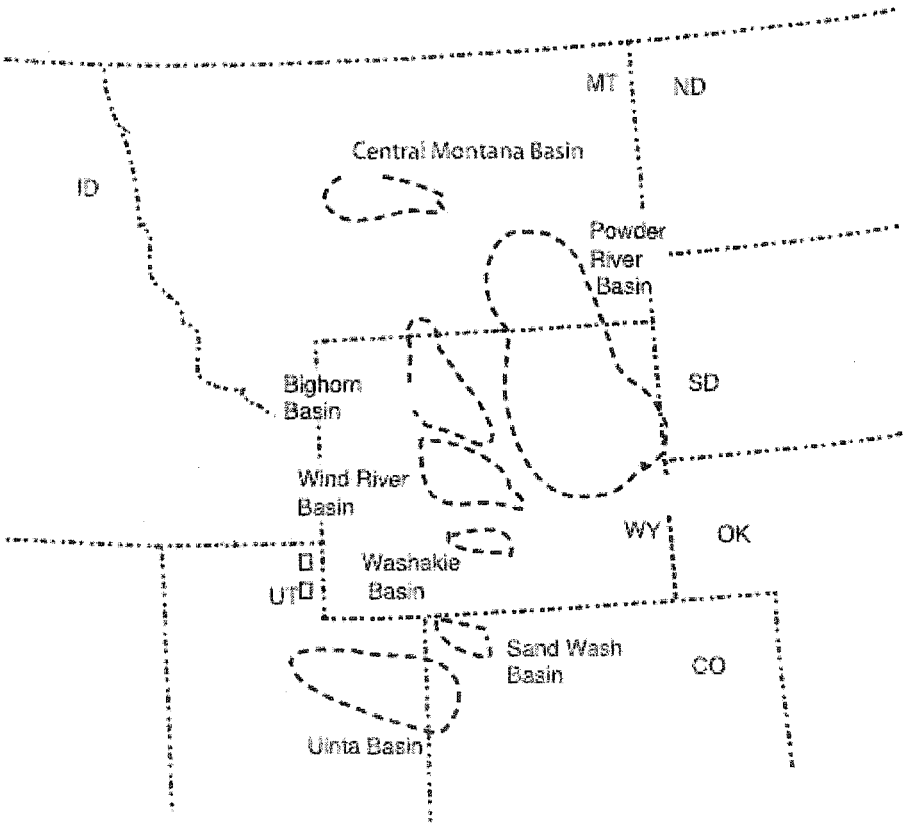

Figure 2. Location of the Bighorn Basin in relation to other Laramide basins.

Reproduced with permission of the copyright owner. Further reproduction prohibited without permission.

DESCRIPTION OF THE PROBLEM

GEOLOGIC HISTORY

Overview of the Cretaceous Western Interior Seaway

The Cretaceous Western Interior basin has been described as the result of a retroarc thrust belt resulting in architecture of a foreland basin. Retroarc basins form along the continental-interior flanks of continental margin orogenic belts (Jordan, 1995). The Cretaceous Western Interior Basin is an accessible, unusually large, and well-exposed example of a retroarc basin, about which an extensive literature has developed. The basin formed during the late Mesozoic westward drift of the North American plate, as the actively deforming leading edge was repeatedly thrust over the craton, resulting in flexural subsidence of the latter and the development of a retroarc foreland basin (Figure 3). The basin deposits are series of "clastic wedges" (King, 1959) whose sandstones and gravels fill the western foredeep, and interfinger with the shales and limestones of the central and eastern portion of the basin. The Cretaceous Western Interior Basin has served as the testing ground for recent ideas concerning the controlling forces of stratigraphic successions, and it has become a natural laboratory for "high resolution" sequence stratigraphers. Its stratigraphic interval, the Cretaceous period, is an important one in which to study the effects of eustasy; the existence of a "Great Cretaceous Transgression" was first suggested by Edward Suess (1875, in Howell and Flint, 2003), and later shown to be related to an interval of faster sea floor spreading rates (Pitman, 1978). The time interval is well documented; "... [this] is one of the best biostratigraphically constrained basins in the World" (Krystinik and DeJarnett, 1995).

A tectonic component in stratigraphic patterns of the Cretaceous western interior has long been inferred. The thick clastic wedges of the Upper Cretaceous were initially thought to mark periods of tectonic activity and sediment production in the source terrain (Armstrong, 1968), but arguments have been made that during much of the upper Cretaceous, tectonic activity meant thrust loading of the foreland with consequent subsidence (Heller et al., 1988). Gravels might accumulate at the thrust front, but subsidence would extend several hundred kilometers into the foreland, the distance depending on the flexural rigidity of the lithosphere. The resulting accommodation space would be filled by far-traveled fine sediment transported laterally along the basin axis. A clastic wedge would not prograde into the basin until after thrust loading ceased and isostatic uplift could begin. In this model, the proximal and distal stratigraphic sections would be out of phase with each other and the immediate signature of tectonic activity would, counter-intuitively, be the accumulation of shale (Heller et al., 1988). The situation becomes more

Reproduced with permission of the copyright owner. Further reproduction prohibited without permission.

complex in the Campanian, as thin-skinned Sevier tectonics (thrusting) gave way to thick-skinned Laramide tectonics (basement uplifts). Within the Washakie and Red Desert Basins, contrasting

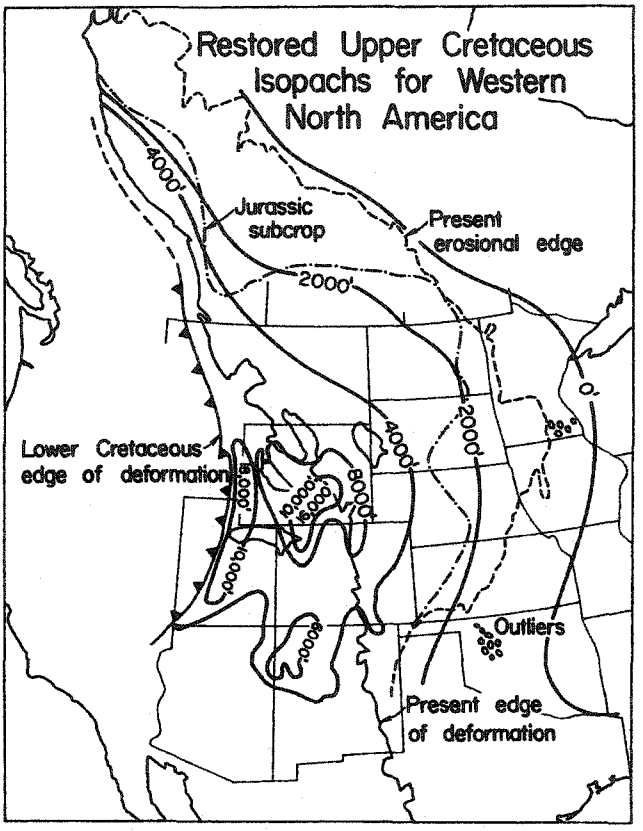

Figure 3. Isopach map illustrating the depositional width of the Western Interior Basin during the late Cretaceous. From Beaumont et al., 1993.

depositional patterns of sedimentation during this period, as thrust-driven flexural subsidence (thin-skinned tectonics) and the new basement uplift processes interact (Devlin et al., 1993).

Geodynamics of thrust belts associated with the Cretaceous Western Interior Seaway have led to more complex insights into retroarc foreland dynamics in more recent studies. In regions far removed from thrust loading, in this case east of the Sevier Orogeny beyond the forebulge, subsidence would occur not due entirely to crustal loading, but from dynamic processes in the mantle, called dynamic subsidence (DeCelles, 2004; Figure 4). Subsidence over a broad region (large wavelength) is controlled by the downward migration of the oceanic plate to the west, taking with it the adjacent asthenosphere causing a vertical "pull" of the lithosphere above. This would then create accommodation space in a depocenter east of the foredeep and beyond the

Reproduced with permission of the copyright owner. Further reproduction prohibited without permission.

forbulge (DeCelles, 2004). Deposits of the foredeep, forebulge and backbulge (large wavelength) are well represented in the Western Interior Seaway (Figure 3).

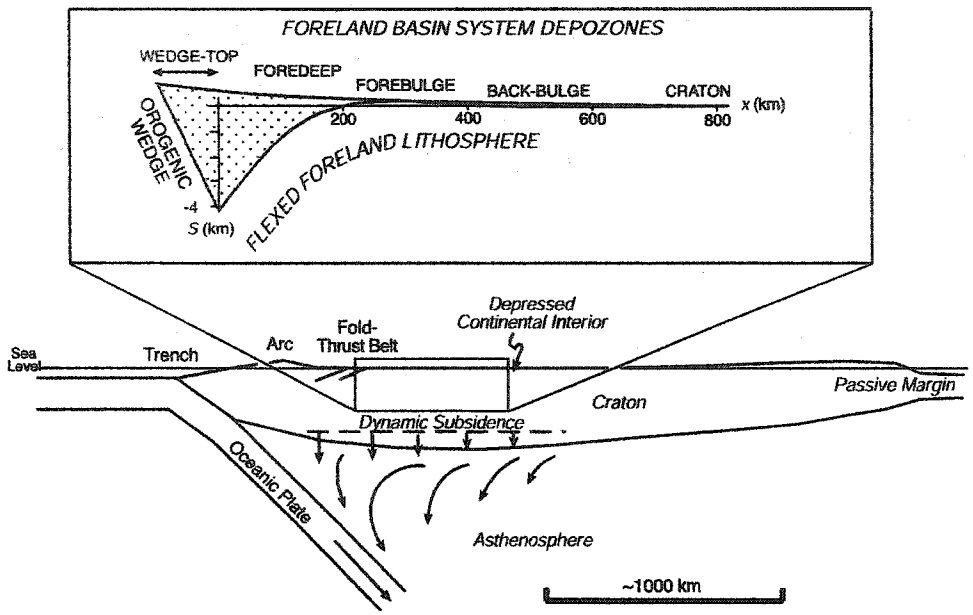

Figure 4. Schematic cross sections illustrating the principal mechanisms of subsidence in retroarc foreland basins (modified from DeCelles and Giles, 1996).

Cyclic sedimentation in the Western Interior Basin is well documented; however, the relationship between sequence stratigraphy and cyclostratigraphy is not well understood. Orbital forcing (Milankovitch cyclicity) related to sedimentation is popular for the carbonate deposition in the eastern portion of the Western Interior Seaway; however, limited studies have been done on the clastics of the western portion of the Seaway. Deeper water deposits with good time constraints often provide clear evidence of orbital signals but not so clear sea level changes. The opposite is also true; shallow water deposits often provided clear evidence of sea level changes but not well-developed orbital signals (Gale et al., 2002). The clastic deposits of the Virgelle sandstone tongues and the Telegraph Creek Shales are potentially the record keepers of such signals. The methods and results of this project serve as tools for studying Milankovitch cyclicity in clastic depositional environments.

Paleoclimatology and Paleoceanography

The second half of the Cretaceous was a time of warm stable climate, often described at a greenhouse climate (Barron and Washington, 1982). Evidence includes geography of terrestrial plants (Parrish and Spicer, 1988) as well as marine organisms (Barnard, 1973; Kauffman, 1973;

Reproduced with permission of the copyright owner. Further reproduction prohibited without permission.

Mutterlose, 1992). Other evidence includes sea level position, which was the highest in the Mesozoic. These extraordinarily high sea levels would lead to the notion that there were no ice caps and that temperatures must have been much warmer than they are today. A contradiction to this notion suggests that glacial-eustatic changes are the only explanation for the large and rapid changes in sea level (Miller et al., 2004); however, he also mentions that more studies need to be completed in order to fully explain sea level changes prior to the Eocene. Through the use of paleogeographic reconstructions and CO_2 estimates, climate models have also predicted significantly reduced thermal gradients (Barron and Washington, 1982; Barron, 1983; Crowley and North, 1991). These reduced atmospheric thermal gradients would then affect the ocean circulation producing a sluggish deep water circulation leading to the deposition of organic rich sediments in oxygen-deficient deep-ocean waters (Ryan and Cita, 1976; Arthur and Schlanger, 1979; Brass et al., 1982; Wilde and Berry, 1982). Changes in monsoon intensity have been shown to occur on Milankovitch frequencies (Clemens et al., 1991; Jacobs and Sahagian, 1995; Reinhardt and Ricken, 2000), and it has been suggested that changes in continental water storage on a Milankovitch scale is a possible mechanism for sea level changes equivalent to those seen with changing ice volumes (Jacobs and Sahagian, 1995). Monsoons driven on a precessional scale can produce enough precipitation that is stored in lakes and groundwater to influence sea level fluctuations. Calculations of such water storage suggests that sea level can change 2 to 8 meters, sufficient enough to cause the thickness variations in the carbonate deposits on the eastern side of the Western Interior Basin (Jacobs and Sahagian, 1995).

Surface circulation was generated for the Turonian through the application of modeling using five forcing fields: the wind field, latitudinal temperature gradient, precipitation minus evaporation, runoff and mixing of Boreal and Tethyan waters (Kump and Slingerland, 1999). These forcings coupled with a general circulation model for coastal areas produced a circulation pattern where runoff from the eastern side of the western interior exited to the north, and runoff from the western side exited to the south. The pattern generates two counterclockwise gyres, nearly connected, for the Western Interior Seaway (Figure 5). During fair-weather conditions, fine-grained suspended sediment was then transported primarily to the southeast. A well-developed shelf-slope morphology existed along the western margin of the seaway during Campanian time (Asquith, 1970). During storms, northeasterly winds generated south-trending, downwelling, geostrophically balanced flows that were capable of transporting sand southward along the shelf and offshore (Swift and Parsons, 1995).

Reproduced with permission of the copyright owner. Further reproduction prohibited without permission.

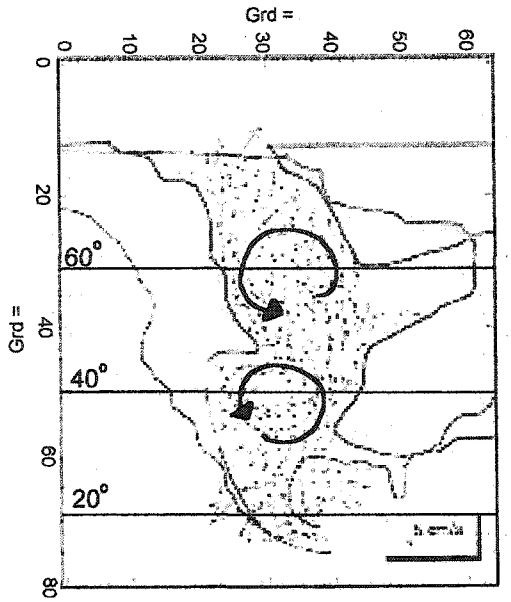

Figure 5. Circulation in the upper 10 m of water column during the Cretaceous (from Slingerland et al., 1996).

The Upper Cretaceous of Wyoming

The modern day Bighorn Basin is a large-scale syncline that formed as a result of several Tertiary Laramide uplifts including the Abrasoka, Owl Creek, Bighorn and Crazy Horse ranges. These uplifts exposed several Mesozoic sections including the Upper Cretaceous Mesaverde Group (Figure 6), which contains continuous outcrop exposure for several kilometers along paleoshoreline as well as several kilometers into the basin. The Mesaverde Group is comprised of two formations, the Eagle and Judith River Formations (Fitzsimmons and Johnson, 2000; Figure 7). The lowermost Eagle Formation offers repetitive sandstone-shale successions with well-developed cyclicity at multiple scales (Figures 8). The focus of this research is the Virgelle Member and the interfingering Telegraph Creek Shale of the Eagle Formation, which presents an excellent expression of high frequency cyclicity (Fitzsimmons and Johnson, 2000). The Virgelle is separated by the overlying Gebo Member by a sequence boundary called the Shannon Surface. The Shannon Surface is a Type II sequence boundary (Van Wagoner et al., 1990) meaning it is a surface of sea level fall that can be traced several kilometers along paleoshoreline and several kilometers into the basin. This surface was used as the datum for comparing and correlating the 19 measured sections that were completed for this project.

The Virgelle includes eight down-dip sandstone tongues composed of shallow marine facies that pinch out and interfinger with the Telegraph Creek Shale (Figure 8). In sequence stratigraphic terms each of these tongues would represent a progradation of the shoreline due to sea level fall

Reproduced with permission of the copyright owner. Further reproduction prohibited without permission.

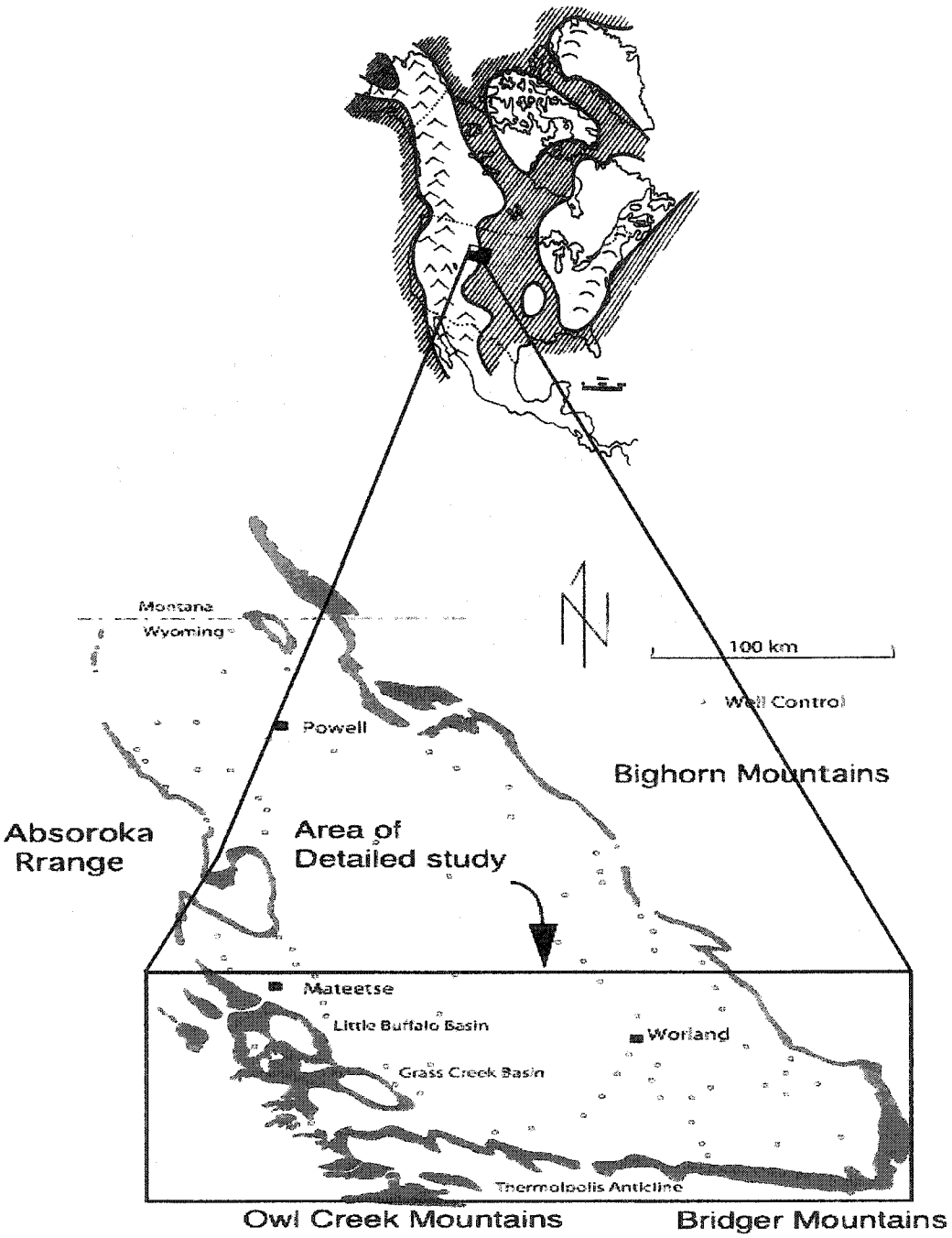

Figure 6. Study area showing outcrop belt of the Mesaverde Group (dark band) in the Bighorn Basin.

Reproduced with permission of the copyright owner. Further reproduction prohibited without permission.

AGE	STAGE	GROUP	FORMATION	MEMBER	AGE (Ma)	AMMONITE ZONE
CRETACEOUS	CAMPANIAN	MESAVERDE	JUDITH RIVER	TEAPOT	76 Ma	Baculites scottii
				UNNAMED		
				CLAGGETT	79.5 Ma	Baculites obtusus
						Baculites sp. (weak ribs)
			EAGLE	GEBO	80.54 (+/- 0.55) Ma	
				VIRGELLE		Baculites sp. (smooth)
				TELEGRAPH CREEK		
				FISHTOOTH	83.1 (+/- 0.5) Ma	Scaphites hippocrepis 2
		CODY	CODY			Scaphites hippocrepis 1

Figure 7. Stratigraphy of the Mesaverde Group within the Bighorn Basin. Based on Gill and Cobban (1966 a & b, 1973) and Fitzsimmons and Johnson (2000). Dates based on nomenclature by Obradovitch (1993).

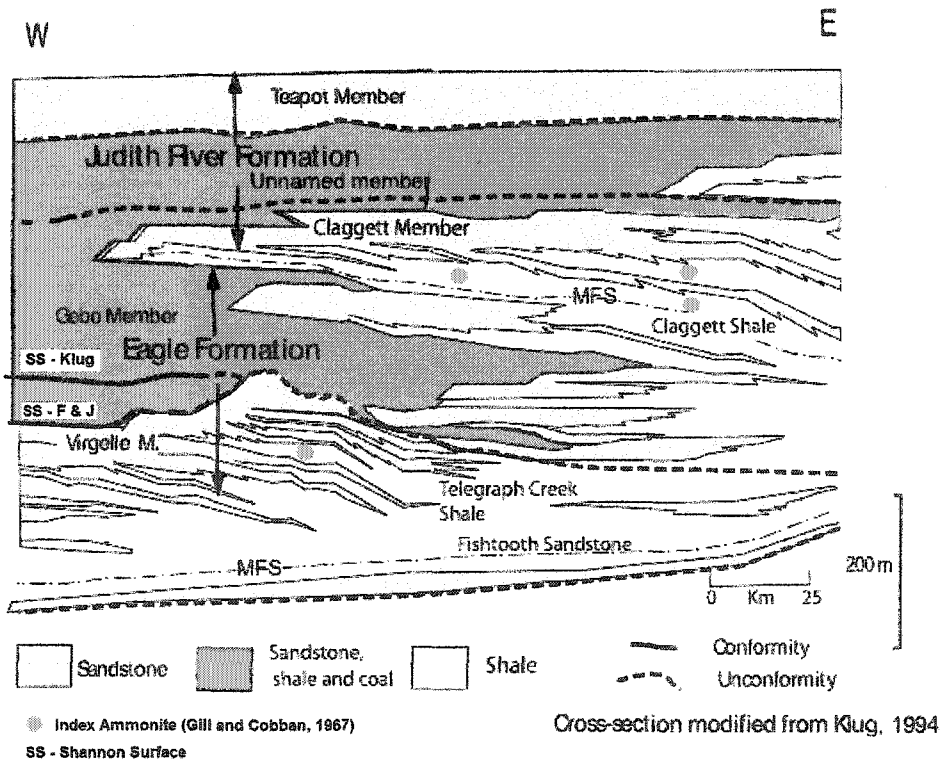

Figure 8. Simplified lithostratigraphic cross section through the depositional dip of the Eagle Formation within the Bighorn basin (modified from Klug, 1994).

Reproduced with permission of the copyright owner. Further reproduction prohibited without permission.

followed by a succession of shoaling upward depositional facies called a parasequence (open marine, offshore transition, lower shoreface, middle shoreface, upper shoreface, foreshore and finally coastal plain deposits), capped by a marine flooding surface. The Virgelle tongues however, do not record the shoaling nature of facies succession normally found in a parasequence. Instead, there is a sharp base separating the open marine deposits from the shoreface deposits and only the offshore transition, and in some cases the lower shoreface, is preserved which is immediately followed by open marine deposits for several meters prior to the next sharp base (the next Virgelle sandstone tongue). These have been termed high frequency sequences (Fitzsimmons and Johnson, 2000), and the sharp base between the open marine and lower shoreface deposits is termed a regressive ravinement (Swift et al., 1991; Swift et al., 2003). This results in storm wave action on the sea floor due to a relative drop in sea level and decrease in accommodation space (Swift et al., 1991).

Reproduced with permission of the copyright owner. Further reproduction prohibited without permission.

CYCLICITY

Historical Background

From the beginning of stratigraphy, it has been recognized that stratification is often cyclic; sediment types (sand, shale, or limestone) alternate (Grabau, 1913). Furthermore, the repetitions are hierarchical; small-scale alternations and large-scale alternations occur in the same deposits. Earlier workers had assumed that vertical variation in sediments is due mainly to tectonism (mountain building). In 1909, Chamberlain famously stated that "diastrophism [elevation change] is the ultimate basis of correlation". By mid-century, however interest had developed in eustasy (global sea level change) as an alternate explanation. Students of the Carboniferous began to talk about "cyclothems" (Schwarzacher, 1964; Duff et al., 1967; Peach, 1988). The sedimentary portion of the North American craton was divided into 5 major eustatic sequences (Sloss, 1963). These ideas eventually crystallized as "sequence stratigraphy" in which eustasy is seen as the dominant driving force. (Vail et al., 1977).

Cyclicity and the Western Interior Basin

Cyclicity in the Cretaceous Western Interior Basin occurs through a range of spatial scales (Table 1). The basin fill as a whole has been designated by Sloss (1962) as the Zuñi supersequence. Second-order sequences (probable periodicities of 10^7 yrs; Van Wagoner et al., 1990), were referred to as cyclothems (Kauffman, 1977). Such low-frequency sequences are in turn composed of third order sequences (probable periodicities of 10^6 yrs; Van Wagoner et al., 1990); also known as alloformations (Plint, 1996). These units may be bundled into fourth-order sequences (Van Wagoner et al., 1990). Fourth-order periodicities are on the order of 10^5 yrs (Van Wagoner et al., 1988). Fourth-order sequences are also known as parasequence sets or high-frequency sequences, (O'Byrne and Flint, 1995), or allomembers (Bhattacharya and Walker, 1991). These last two terms are not fully synonymous; high frequency sequences are bounded by unconformities, while parasequences are bounded by flooding surfaces. Upward-coarsening bed sets have been described as fifth-order sequences or parasequences (Van Wagoner et al., 1990); or as shingles (Bhattacharya and Walker, 1991). Fifth-order periodicities are on the order of 10^3 to 10^4 yr (Schwans, 1995; Fitzsimmons and Johnson, 2000).

Reproduced with permission of the copyright owner. Further reproduction prohibited without permission.

Table 1. Scales of cyclic sedimentation in the Cretaceous Western Interior Basin

Order	Duration	Descriptive terms	Reference	Assumed Forcing
2nd	10^6-10^7	Sequences, Cyclothems Clastic Wedges	Kauffman, 1977;Van Wagoner et al., 1990; Ryer, 1993; Plint, 1996	Eustatic
3rd	10^5-10^6	Sequences, sequence sets, Alloformations	Van Wagoner et al., 1990; Plint, 1996	Tectonic
4th	10^4-10^5	Sequences, high frequency sequences, allomembers (Milankovich band)	Van Wagoner et al., 1990; Plint, 1996	Tectonic, Lobe-switching or Milankovitch
5^{th}	10^3-10^4	Parasequences, shingles (Milankovich band)	Van Wagoner et al., 1990; Plint, 1996	Milankovitch

Higher orders of complexity can be observed as the western margin of the basin is approached (Van Wagoner et al., 1988). The shoreline serves as a low-pass filter, which passes the effects of low frequency sea level motions onto the terrestrial environment, but filters out the high frequency motions (Fitzsimmons and Johnson, 2000). The cyclicity considered in this study occurs in the cliff-forming sandstones and intervening shales of the western margin of the basin. Here the cyclicity occurs as shaley bed sets centimeters to meters in thickness, whose member beds increase upward in sand content. Fifth-order cyclicity in this setting has not been previously studied.

Attempts have been made to identify third and fourth-order cycles for the Mesaverde Group. Four third order sequences have been identified in the Mesaverde located at the top of the Fishtooth, the top of the Virgelle, the top of the Claggett and the top of the unnamed Member of the Judith River (Fitzsimmons and Johnson, 2000). Each of the eight sandstone tongues of the

Reproduced with permission of the copyright owner. Further reproduction prohibited without permission.

Virgelle are interpreted to be fourth-order cycles (Fitzsimmons and Johnson, 2000). Therefore, the natural location for fifth-order cycles would then be within the Telegraph Creek Shale that interfingers each of the fourth order Virgelle sandstone tongues. The Telegraph Creek Shale is often ignored with respect to outcrop detail and generally lumped into a thick shale unit. It is quite often easy to recognize the third and fourth order cycles due to significant changes in lithogies, whereas subtle changes in shales are not as apparent in outcrop expression. Large-scale storms, such as those generated by monsoons with periodicities on the fifth order scale could potentially drive both grain size and bed thickness changes within the Telegraph Creek Shale. Therefore, the subtle changes in bed thickness and grain size changes may represent the surfaces of fifth order cycles.

Storm Stratification

Numerical simulations by Storms and Swift (2003) indicate that fourth-order beds enshroud the successive highstand systems tracts of prograding high-frequency sequences (Figure 9).

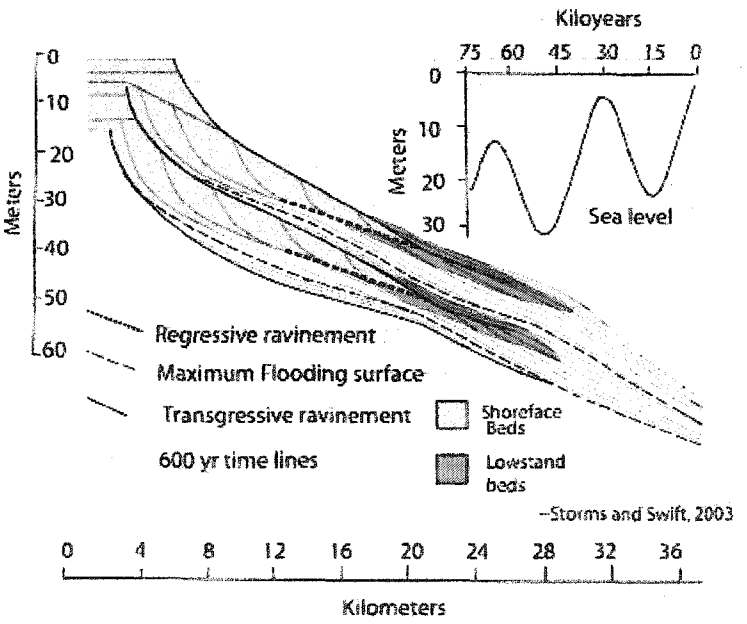

Figure 9. Numerical simulation of two high-frequency (fourth order) sequences deposited over a 75,000 yr period. Curvilinear time lines equal 600 yr intervals. They show the progressive development of the deposit at 15, 000 yr intervals. Notice how the lowstand beds (closely spaced time lines) envelope the highstand deposits (widely spaced time lines). Modified from Storms and Swift, 2003.

In the lowstand beds, fifth-order cyclicity is generally overprinted onto storm stratification patterns. The spacing of storm beds within the lowstand bed succession should vary randomly because the

Reproduced with permission of the copyright owner. Further reproduction prohibited without permission.

ocean and atmosphere comprise a coupled chaotic system (Zhang et al., 1997), and the intensity and frequency of storms is not predictable, but modulation by changes in relative sea level leads to characteristic patterns.

In one such pattern, there is a wide but regular spacing of storm beds (up to 3 m) in the shales between fourth-order sandstone tongues (Figure 10). Storm beds in this distal setting can only be deposited during fifth-order lowstand when the shoreline has arrived at its closest approach to the site of observation. A second style occurs within fourth-order sandstones (Figure 11). In this case, storm beds are closely spaced (1-2 m). Storm bed thickness increases in thickness and decreases in spacing up to the horizon of closest shoreline approach, followed by a repeat of the cycle.

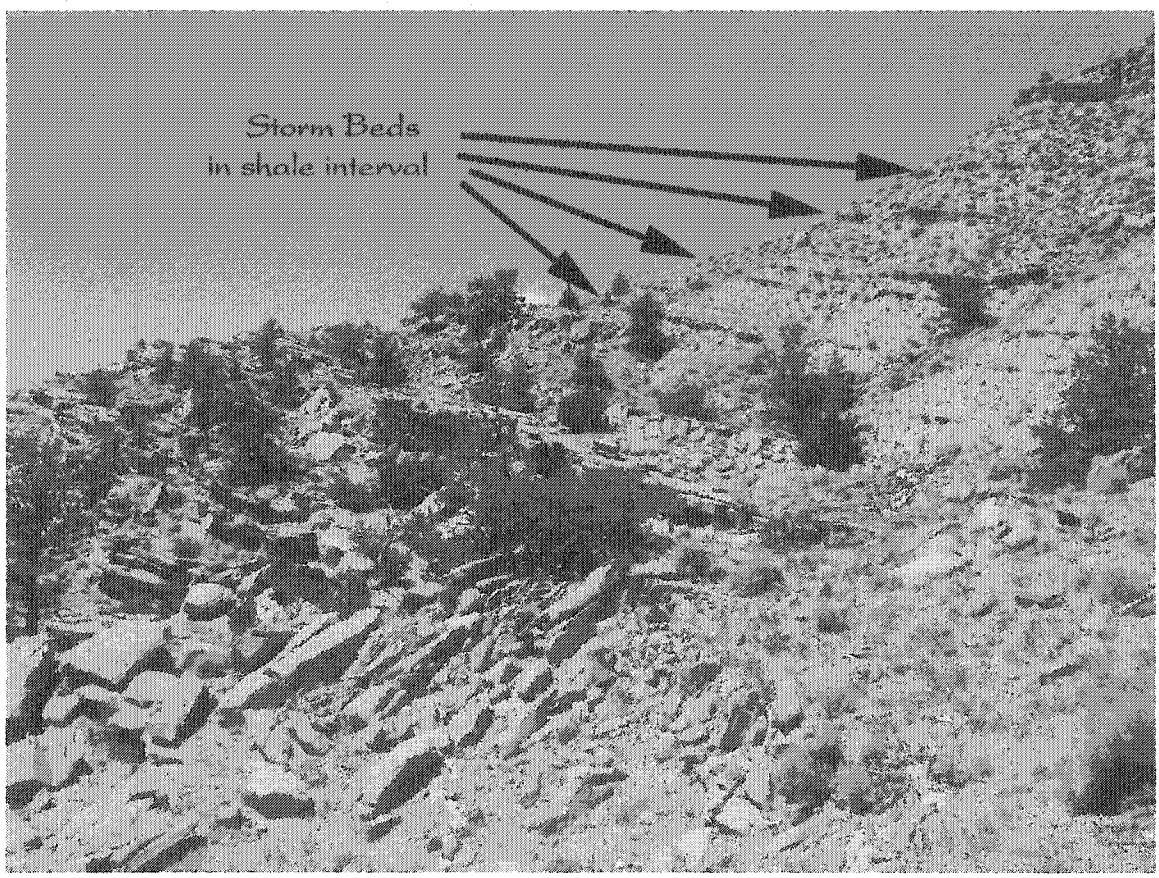

Figure 10. Shale interval above the Virgelle tongue. Notice the widely spaced storm beds (fifth-order) in the shale interval. Approximately 2.5 – 3 meters between arrows.

Reproduced with permission of the copyright owner. Further reproduction prohibited without permission.

Numerical simulations have shown that pseudo-cyclicity can appear in purely random storm bed successions (Thorne et al., 1991). Feedback between the grain size characteristics of the seabed after storm bed deposition, and erosion during the next event can generate a kind of autocyclicity. Consequently, an important aspect of this study will be separating the deterministic fifth-order signal from the random storm bed signal.

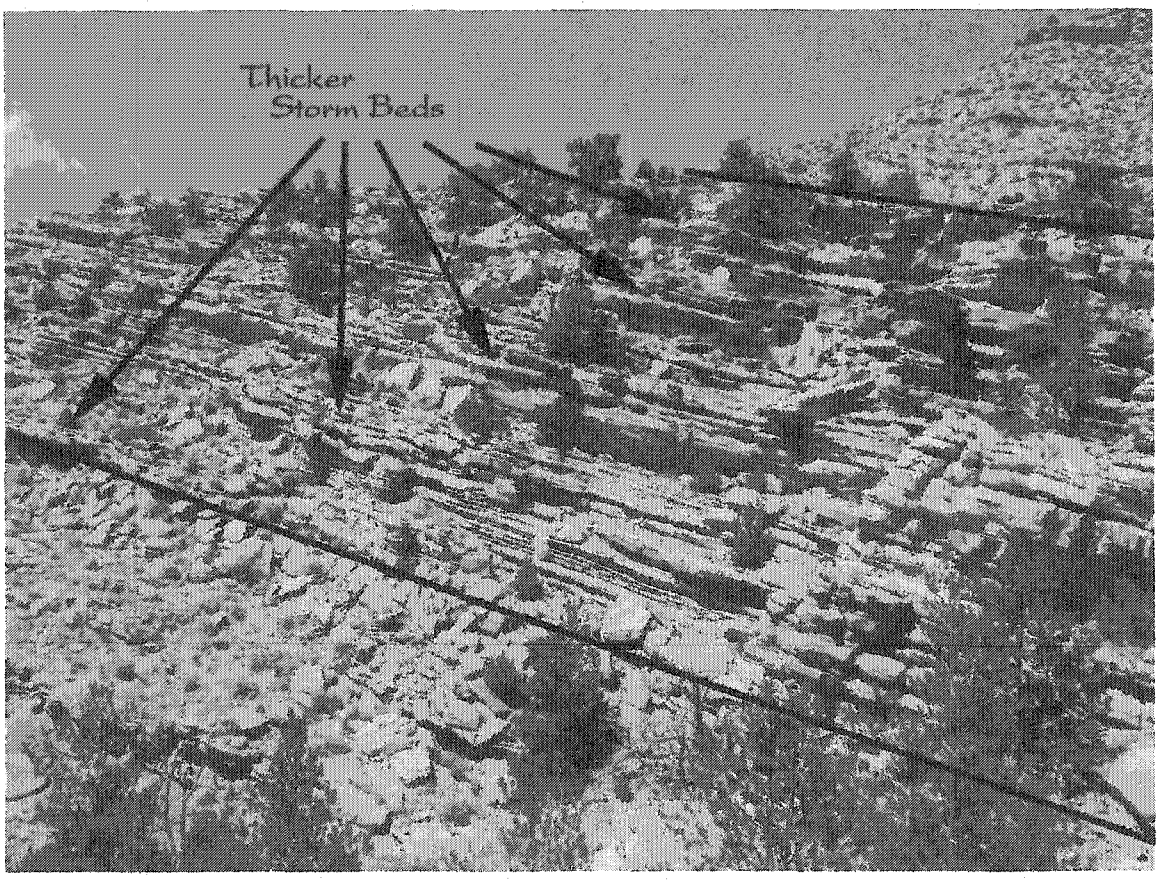

Figure 11. A fourth-order tongue in the Virgelle (marked by solid black lines). Notice the regular spacing of thicker (fifth-order) storm beds. Approximately 1 – 1.5 meters between arrows.

Causes of high-frequency Cyclicity: a Survey of the literature

Fifth-order cyclicity is often attributed to climatic variations driven by the Milankovitch mechanism of precession, obliquity and eccentricity (Figure 12). Precession is the "wobble" in the Earth's rotation (de Boer and Smith, 1994). The period in which precession occurs is 19,000 to 23,000 years. Obliquity is the shift in the tilt of Earth's axis from 22 to 24.5 degrees with a periodicity of 41,000 years. Finally, eccentricity is the path of Earth's orbit around the sun, which shifts from

Reproduced with permission of the copyright owner. Further reproduction prohibited without permission.

more circular to more elliptical over a period of 100,000 years. Each of these mechanisms cause the amount of solar radiation absorbed at a point on the Earth's surface to vary.

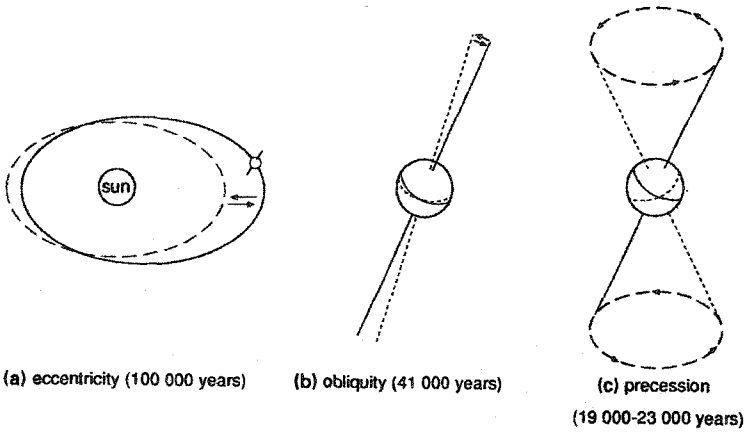

Figure 12. Diagram showing the astronomical variables that influence Earth's climate (from de Boer, 1983).

The most authoritative statement concerning fifth-order cyclicity compared bedding rhythms in Germany, Italy, and the Cretaceous Western Interior (Fischer, 1993)..."21 ky. (precessional) cycles are widely recorded in bedding couplets in the Niobrara Formation of the Western Interior", but cautioned that "even though plain to the eye, this frequency does not generally emerge from time series analysis, due to... irregularity in the precessional period [and] variations in accumulation rate." Frequency ratios in bed thickness, or bundling has been used to establish orbital forcing (Sageman et al., 1997). In the Bridge Creek Member of the Greenhorn Formation five precessional cycles are seen for every 100,000-year eccentricity cycle, called the precessional index (Sageman et al., 1997). Ideally, the precession and eccentricity terms as described by Milankovitch would interact to give a 1:2:5 ratio of cyclicity (Fischer, 1993). Impact of these cycles on climate invokes variations in water density and biological productivity, and sediment supply rather than glacioeustasy (Fischer, 1993). In the absence of worldwide fluctuations of glacial ice, climatic cycles in the mountains to the west of the basin could be expected to send brackish water across the seaway, producing bottom anoxia that would suppress carbonate production and would be accompanied by increased clastics (Fischer, 1993).

In contrast, interpretations of stratigraphic cyclicity as a response to tectonism is strongly supported (Yoshida et al., 1996). Modeling responses to periodic changes in interplate stress and flexural load on time scales down to that corresponding to the spacing of individual

Reproduced with permission of the copyright owner. Further reproduction prohibited without permission.

earthquakes (10^{-1} to10^{4} yr), making a case for tectonic cyclicity that could explain 4th and 5th order cycles (Peper et al., 1992). For instance, fourth-order cyclicity and fifth-order cyclicity could be tied to tectonism through the mechanism of in-phase and out-of-phase thrusting (Houston et al., 2000). Thrusts are usually sequentially younger towards the foreland, but much of the sediment load generated during each thrust movement is trapped on intra-orogen (piggyback) basins (fifth-order cyclicity?). However, the less frequent out-of-sequence thrusts, breaking out in the already-thrusted hinterland, elevate earlier thrust plates, and much more sediment is released (fourth-order cyclicity?).

Tectonism and eustasy are allocyclic mechanisms (driven by forces from outside the basin, beyond the actual Seaway). High-frequency cyclicity might also be driven by such autocyclic mechanisms as delta avulsion and lobe switching (Boyd et al., 1989). Numerical experiments by Hampson and Storms (2003) have shown that high frequency changes in sediment supply may result from delta avulsion or rhythmic beach ridge progradation, and may generate surfaces of discontinuity in shallow marine successions. So do high frequency changes in sea level or wave regime, but the allocyclic mechanisms generate facies shifts that are apparent across the surface of discontinuity, while changes in sediment supply do not. The change in sediment supply may not be the same across the entire basin, sediment supply is dependent on the orbitally-intensified monsoonal circulation, as well as position of river mouths, which supply to sediment to the basin.

Biostratigraphic control

A detailed ammonite zonation for the Cretaceous Western Interior basin (Figure 13) has been developed (Gill and Cobban, 1966a, 1966b, 1973). A careful comparison of this ammonite evolution with radiochronology (Obradovitch 1993) has been undertaken (Krystinik and DeJarnett 1995). They note that the radiometric dates are spread unevenly through the Upper Cretaceous section. Throughout much of the section, resolution is on the order of 0.5 my per ammonite zone. In the late Santonian through lower Campanian, however, our section of maximum interest, the resolution increases to 300,000 years per ammonite zone, equivalent to the duration of longer 4th order cycles. The Telegraph Creek, Cody, and Claggett Shales of the Bighorn basin have yielded complete faunal successions of the Western interior Ammonite index fossils. Several faunal zones contain K/Ar dated bentonites (Obradovich and Cobban, 1975; Obradovich, 1988). The most serious limitation for the study lies in the difficulty of independently constraining thrust timing in the Sevier hinterland to less that 1 or 2 my (see analyses of Witschko and Dorr, 1983; Jordan, 1988). The role of thrusting must therefore be supported by multiple lines of evidence.

Reproduced with permission of the copyright owner. Further reproduction prohibited without permission.

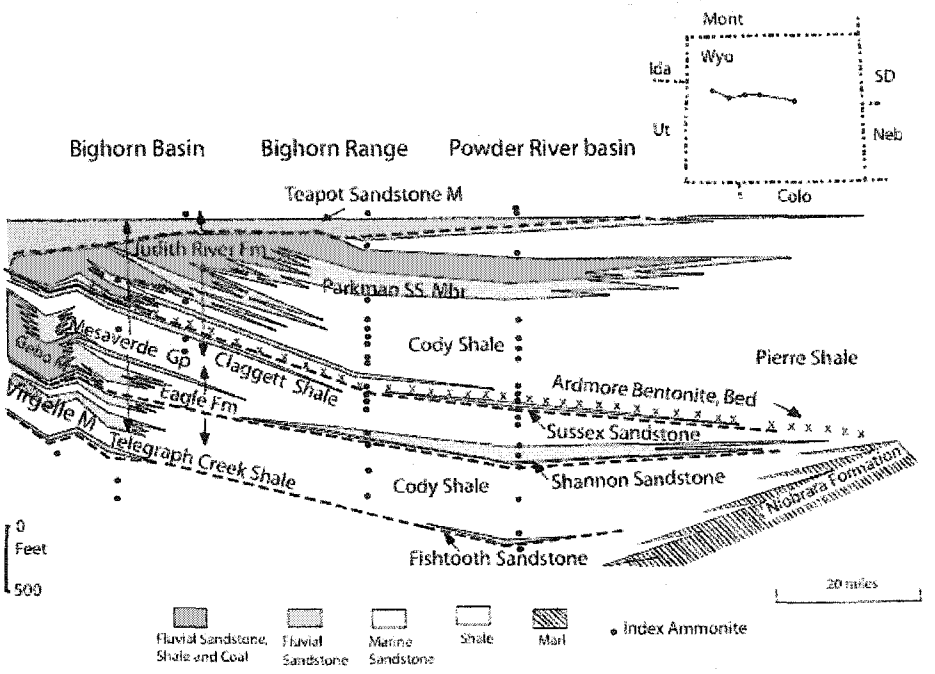

Figure 13. The great Wyoming cross-section, extending 176 miles across the Bighorn and Powder River basins (after Gill and Cobban, 1966a).

The Mesaverde Group falls between the *Scaphites hippocrepis* and *Baculites* sp. (smooth) ammonite biozones (Gill and Cobban 1973). This range encompasses approximately 2 million years of time (Kauffman et al., 1993) of which the Virgelle (based on thickness) envelops approximately one half of that range. Assuming a constant sedimentation rate, the time between each of the eight sandstone tongues would be approximately 100,000 to 125,000 years.

Reproduced with permission of the copyright owner. Further reproduction prohibited without permission.

FORMULATING THE HYPOTHESIS

Given the rich diversity of approach and opinion concerning the origin of stratigraphic cyclicity how can the problem be reduced to manageable proportions? I reduced it by limiting my effort to the fifth-order cyclicity of the high-frequency cyclicity imprinted on the lowstand systems tract on the western margin of The Cretaceous seaway. In this study, I investigate the extent to which these fifth-order cycles in the Bighorn basin are responses to tectonic, eustatic (orbital), climatic (monsoonal) or autocyclic (delta building), specifically the interval between the first (V-1) and second (V-2) Virgelle tongues were investigated. I present as an hypothesis the proposition that the fifth-order cycles of the southern Bighorn basin are a result of orbital forcing and are potentially of eustatic origin.

TESTING THE HYPOTHESIS

Criteria for Orbital Forcing

Eustatic sea level changes due to orbital forcing have been demonstrated in many stratigraphic settings (Laferriere and Hattin, 1987; Kominz and Bond, 1990; Herbert et al., 1999; D'Argenio et al., 1999). Milankovitch cycles can lead either to changes in sea level or sediment supply. The bundling of beds at 5:1 ratios (five-20,000 year precession cycles within one-100,000 year eccentricity cycle) is diagnostic of orbital forcing (Laffierre and Hattin, 1987). Slight departures from the 5:1 ratio (i.e. 3:1, 7:1 and 9:1) may reflect orbital parameters at slightly different periodicities. These orbitally induced packages could theoretically be correlated along paleoshoreline and have been shown to correlate from the basin axis to the western margin (Elder et al., 1994; see Table 2).

Changes in monsoonal strength at Milankovitch frequencies has been a proposed to cause a 2 to 8 meters of sea level change, due to increased precipitation of monsoons on a precessional scale will then increase the amount of water storage in lakes and groundwater systems, ultimately affecting the level of the shoreline. This has been shown to explain the sea level cycles in nearshore carbonates (Jacobs and Sahagian, 1995), however the literature lacks support for cycles of this nature in nearshore to offshore clastics.

Criteria for Tectonic Forcing

Tectonic forces in foreland basins can cause an alternation between uplift and subsidence across a range of temporal scales, with decadal to million year periodicities (Peper et al., 1992). Short-term vertical motions are related to small-scale thrust events, while long-term vertical motions are

Reproduced with permission of the copyright owner. Further reproduction prohibited without permission.

induced by larger scale deformation in the overriding thrust wedge. At these various temporal scales, uplift and subsidence alternate in pseudo-periodic fashion in response to cycles of stress accumulation, rupture, and relaxation. These pseudo-cycles could mimic Milankovitch cyclicity in the associated sedimentary deposits (Peper et al., 1992). Since multiple time scales are present in the tectonic forcing (individual fault movements, successive in-sequence thrusts, episodic out –of –sequence thrusts) stratal bundling is at least theoretically possible (Houston et al., 2000). Since the tectonic events in question are not truly periodic and the presumed time interval for this project is no more than 250,000 years, such pseudocycles would presumably exhibit greater statistical variance in properties such as stratal thickness and grain size, and might be localized in areal extent over tens of kilometers (see Table 2).

Criteria for Autocyclic Shoreline Repetition

Delta lobe switching by channel avulsion, and rhythmic beach ridge accretion are pseudo-periodic shoreline processes that can lead to cyclic sedimentation (Hampson and Storms, 2003). As in the case of tectonic cycles, such pseudocycles would presumably exhibit greater statistical variance in properties such as stratal thickness and grain size. Modern coasts analogous to the western margin of the seaway such as the Costa de Nararit (Curray et al., 1969) suggest that such pseudocycles might be localized in areal extent to within ten km of the shoreline, with alongshore extents of 10 km or less, therefore stratal bundling is unlikely (see Table 2).

Criteria for Regional Variations in Sediment Supply

In depositional settings where delta lobe switching does not occur, sediment is transported into the basin via river systems and is dispersed along a continental shelf by storms. Storms have a significant influence on sediment supply from a terrigenous source. Intense storms erode a greater amount of continental material and carry a greater volume of sediment onto the continental shelf environment than weaker, short-lived storms. Intense storms during periods of intensified monsoons then, have the potential to disperse coarser grained material further seaward than during fair weather conditions. Monsoon conditions, which are large-scale sustained wind systems driven primarily by solar insolation, are seen today as seasonal patterns of climate change in Africa (Tuenter, et al., 2003) and Asia (Wang et al., 2003). Monsoonal strength variations on a Milankovitch scale have also been described in the Quaternary (Bloemendal and deMenocal, 1989; Quade et al., 1989; Clemens et al., 1991). During Pangaean time (Upper Triassic), the single landmass coupled with the location of the Tethys Sea produced a mega-monsoon circulation pattern (Parrish and Curtis, 1982; Crowley et al., 1989; Kutzback

Reproduced with permission of the copyright owner. Further reproduction prohibited without permission.

and Gallimore, 1989; Parrish, 1993; Kutzbach, 1994). Varying degrees of monsoonal activity were also seen in the Upper Triassic playa deposits of Germany (Reinhardt and Ricken, 2000).

To date, the literature does not contain sufficient information regarding clastic deposition on a continental shelf as an indicator of the variation in sediment supply on a period scale such as the Milankovitch scale. If orbital forcing shifts the amount of solar insolation on the surface of the Earth, which is reflected by shifts in climate, then these monsoonal cycles, which have been related to Milankovitch periodicity (Reinhardt and Ricken, 2000), could then provide a mechanism by which coarser grained sediments are transported offshore. These clastic sediments in vertical section will then punctuate normal sedimentation (clays) in a periodic fashion, but of course rivers would be carrying more sediment also.

Table 2. Decision Table

	5:1 thickness bundling	3:1, 7:1 or 9:1 thickness bundling	Slight departure from 3:1, 5:1, 7:1 or 9:1 thickness bundling	Significant departure from 3:1, 5:1, 7:1 or 9:1 thickness bundling	Correlate along paleoshoreline	Correlate to basin axis
Eustasy	Possibly Orbital forcing	Possibly Interference of orbital forcing at different frequencies	Possibly orbital forcing	_____	Yes	Yes
Tectonics	_____	_____	_____	Yes	Moderately	Possibly
Lobe-switching	_____	_____	_____	Yes	No	No
Sediment supply	Yes – Orbital forcing	Yes – Orbital forcing	_____	_____	Yes	Yes

_____ = not applicable

Reproduced with permission of the copyright owner. Further reproduction prohibited without permission.

METHODS

FIELD PROCEDURES

Measured Sections

During the summers of 2002 and 2003 a total of 19 measured sections within the Thermopolis area of the Bighorn Basin of Wyoming were completed. Measurements began at the top of the Virgelle 1 (V1) sand and extended to the Shannon Surface, which is the stratigraphic boundary between the Virgelle and Gebo Members (see Figure 7 for the stratigraphic succession investigated in this study). Individual sites were pre-selected, but, accessibility problems either prevented the measuring of an entire section or resulted in the shifting of some locations. Names, designations and GPS locations of each section are outlined in Table 3. All measured sections with detailed descriptions were drafted in LogPlot2003™ and are located in Appendix A.

Table 3. Names, designations and locations of measured sections

Place Name	Section Designation	Measured	Sampled for Grain Size	GPS Location (UTM)
Wagonhound Bench	WH Central	X	X	N 0686191, W 4853837
	WH North – 1	X		N 0685998, W 4854669
	WH North – 2	X		N 0685877, W 4855043
	WH North – 3	X	X	N 0686083, W 4856226
	WH South – 1	X		N 0686313, W 4853491
	WH South – 2	X		N 0687091, W 4852265
	WH South – 3	X	X	N 0687404, W 4851618
	WH East – 1	X		N 0686960, W 4856567
	WH East – 2	X	X	N 0687564, W 4856241
	WH East – 3	X		N 0688616, W 4855835
	WH East – 4	X		N 0689302, W 4855593
	WH East – 5	X		N 0695146, W 4856485
	WH East – 6	X		N 0696724, W 4855948
	WH East – 7	X		N 0697159, W 4855862
Sand Draw	SD	X		N 0708399, W 4854384
Grass Creek	GC	X		N 0691375, W 4868091
Little Buffalo Basin	LBB	X		N 0675751, W 4885663
Sunshine Reservoir	SR	X		N 0656524, W 4880623
Zimmerman Butte	ZB	X		N 0260823, W 4848507

Reproduced with permission of the copyright owner. Further reproduction prohibited without permission.

GPS coordinates and strike/dip measurements were recorded for each location prior to measuring. Measurements were made using a Jacob Staff with centimeter increments and a Brunton compass. Strike and dip measurements were used to ensure proper and correct thickness of beds. A bed-by-bed thickness was acquired and detailed descriptions of lithology, grain size and sedimentary structures were noted. Lithologies consisted of primarily sandstones and shale. Grain size was obtained using a hand lens and the American/Canadian Stratigraphic field grain size chart. Sedimentary structures noted ranged from no structures seen, planar bedding, hummocky cross stratification, trough cross bedding, wavy and climbing ripples, and trace fossils. Beds that were 2 cm in thickness or less were not recorded and noted as interbeds where appropriate. Care was taken that all parties involved were instructed on the proper techniques for data gathering and recording.

Grain Size Sampling

A total of 314 samples were collected from the Telegraph Creek Shale between the Virgelle -1 and Virgelle - 2 sandstone tongues (WHCentral, WH South-3 and WH East-2). Samples were collected every 0.5 meter and obtained by digging 30-50 cm into the section to ensure a fresh, undisturbed sample (based on appearance). Approximately 400-500 grams of sample were placed in a canvas sample bag, labeled and transported back to the lab.

LAB PROCEDURES

Measured Sections

All field data was transferred to computer files through the use of LogPlot2003™, plotting software written by Rockware, Inc. Sections include lithologic symbols, grain size data and detailed descriptions. All measured sections are located in Appendix A. Excel spreadsheets were created with thickness data to be used for statistical analysis.

Grain Size

The procedure used to obtain grain size measurements of each sample is located in Appendix B (modified from Folk, 1968). There were three samples, which could not be processed due to a significant amount of cement involved. Data for those three points were extrapolated based on the average grain size of the sample above and below.

Reproduced with permission of the copyright owner. Further reproduction prohibited without permission.

ANALYSIS AND RESULTS

MEASURED SECTION DESCRIPTION

Measured section locations are depicted on Figure 14. A total of 19 measured sections were completed and from this point forward the following acronyms will be used: Wagonhound Central (WHC), Wagonhound North (WHN), Wagonhound South (WHS), Wagonhound East (WHE), Sunshine Reservoir (SR), Little Buffalo Basin (LBB), Grass Creek (GC), Sand Draw (SD) and Zimmerman Butte (ZB). WHN-3 and WHE-1 are sections that are geographically located within the nose of the Thermopolis anticline, and these sections were most likely altered and shortened during structural deformation and were not used for statistical analysis. The data sheet for the measured section for Wagonhound Central is shown in Figure 15. All other measured sections are located in Appendix A.

Within the Virgelle Member of the Eagle Formation there are a total of eight sandstone tongues that interfinger with the Telegraph Creek Shale (Fitzsimmons and Johnson, 2000; see Figure 8 in Description of the Problem section). Fitzsimmons and Johnson have labeled each of the sandstone tongues of the Virgelle Member Virgelle 1 (V1) through Virgelle 8 (V8). Sections including WHC, all WHN, all WHS, all WHE, GC, LBB and SR contain V1 through V3, each separated by a tongue of the Telegraph Creek Shale. SD contains V3 through V5, and Zimmerman Butte contains V8 only.

The base of each of the measured sections began with the V-1 tongue if it were present. When V-1 was buried, the base of the outcrop slope was the starting point. V-1 ranged in thickness from 2 to 3 meters with sedimentary structures that included planar bedding at the base grading into blocky structure. The Telegraph Creek Shale (Figure 16) between V1 and V2 is primarily shale punctuated by thin (up to 5cm thick) silty sands, fine sands, and a few medium sands. No body fossils were found and sedimentary structures within these thin sands included planar bedding and hummocky bedding, climbing ripples and in some lenses planar bedding grading into climbing ripples (Figure 17 - 19). These sand lenses are interpreted as storm beds with rapidly accelerating flow and erosion creating a sharp base followed by rapidly waning flow producing the climbing ripples and hummocks. This type of storm sedimentation has been studied and the sedimentary structures are similar to those modeled on modern continental shelves (Myrow and Southard, 1996). Sand lenses tended to thicken toward V-2 (Figure 20). Overall, the Telegraph Creek Shale between V-1 and V-2 ranged in thickness from 50 to 60 meters. V-2 consisted of what appears to be amalgamated thin (50-100cm) blocky sand beds, separated by thin (2-10 cm) shale beds. These sands included sedimentary structures such as ripple marks, planar blocky bedding and bioturbation. The Telegraph Creek shale between V-2 and V-3 was similar in nature

Reproduced with permission of the copyright owner. Further reproduction prohibited without permission.

to the interval between V-1 and V-2, except that the sand lenses were thicker, on the order of 50-100 cm thick. The top of each of the thicker sand lenses was usually capped by a resistant ledge-forming layer with well developed ripples at the top, which represents a flooding surface (Figure 21). Sand lenses thickened toward V-3 and V-3 was similar in nature to V-2 and was capped by the Shannon Surface. The Gebo Member found above this surface included a succession of two thick amalgamated sandstones (Figure 22) often bleached white, with large iron concretions throughout. These stacked sandstones are a distinguishing feature of this section that can be seen at great distance. The bottom sand is V-3 and the top two sands are interpreted to be estuarine sands (Fitzsimmons and Johnson, 2000). The boundary between V-3 and the Gebo, interpreted here at the Shannon Surface was the datum used for correlation.

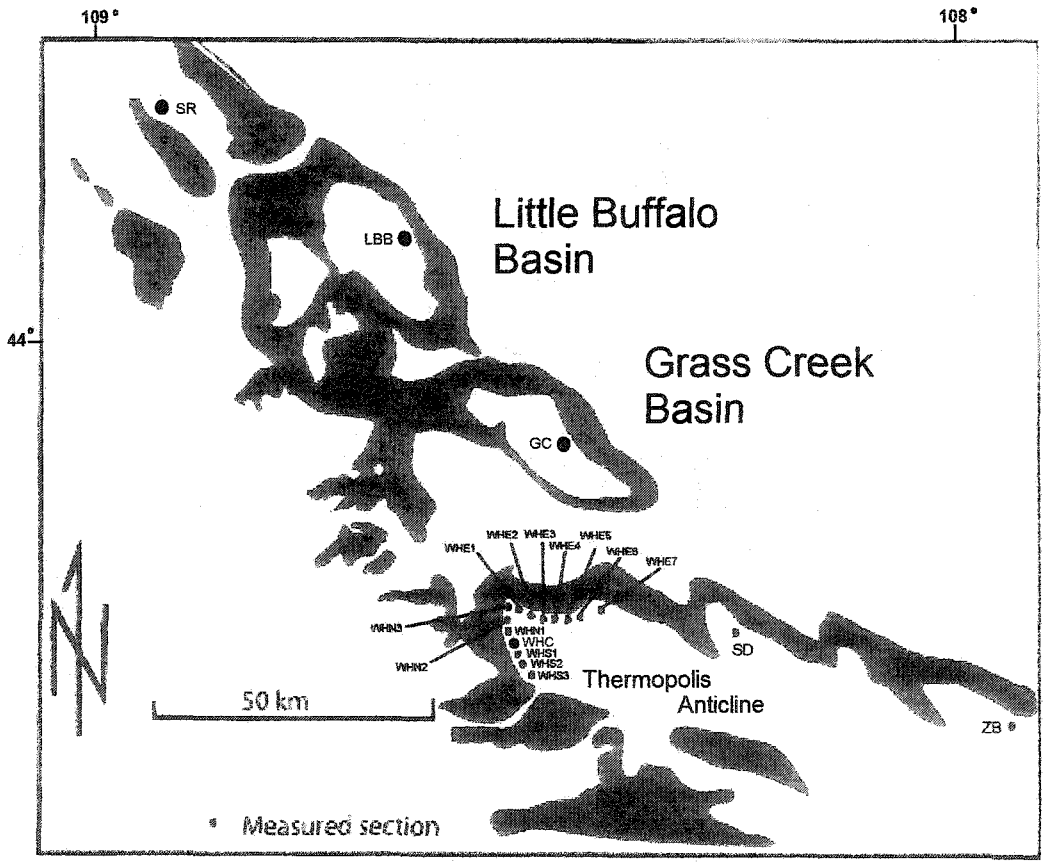

Figure 14. Generalized map of location of exposed Upper Cretaceous Eagle Formation (shaded black area) with location of measured sections. (adapted from Fitzsimmons and Johnson, 2000).

Reproduced with permission of the copyright owner. Further reproduction prohibited without permission.

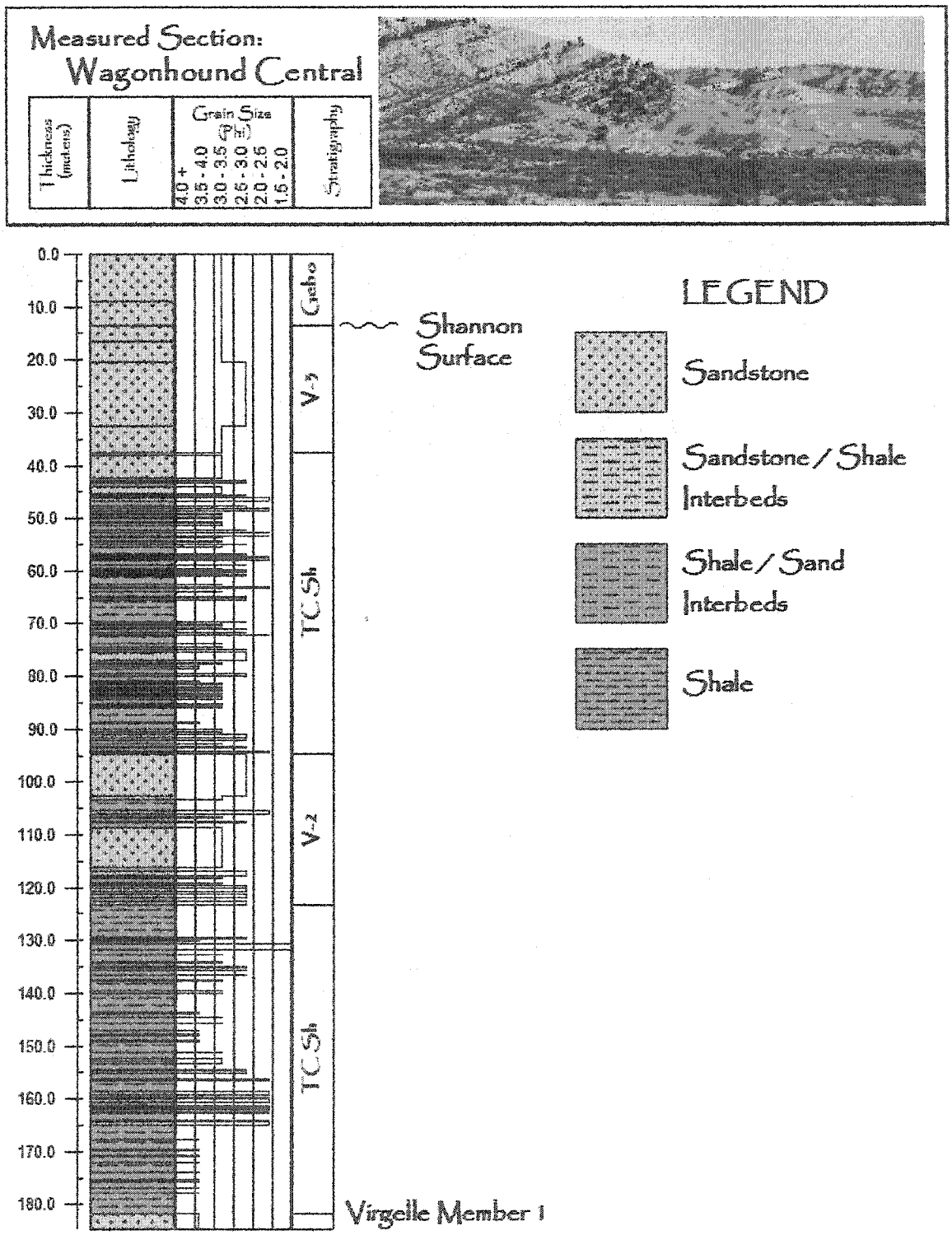

Figure 15. Wagonhound Central measured section.

Reproduced with permission of the copyright owner. Further reproduction prohibited without permission.

Figure 16. Typical overall expression of the Telegraph Creek Shale between V-1 and V-2.

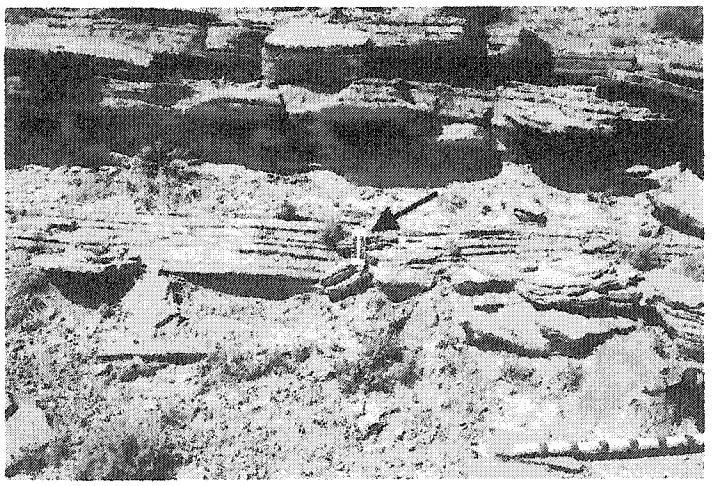

Figure 17. Planar bedding in the Telegraph Creek Shale located between V-2 and V-3. Blue section on scale card is 10 cm (indicated by black arrow).

Reproduced with permission of the copyright owner. Further reproduction prohibited without permission.

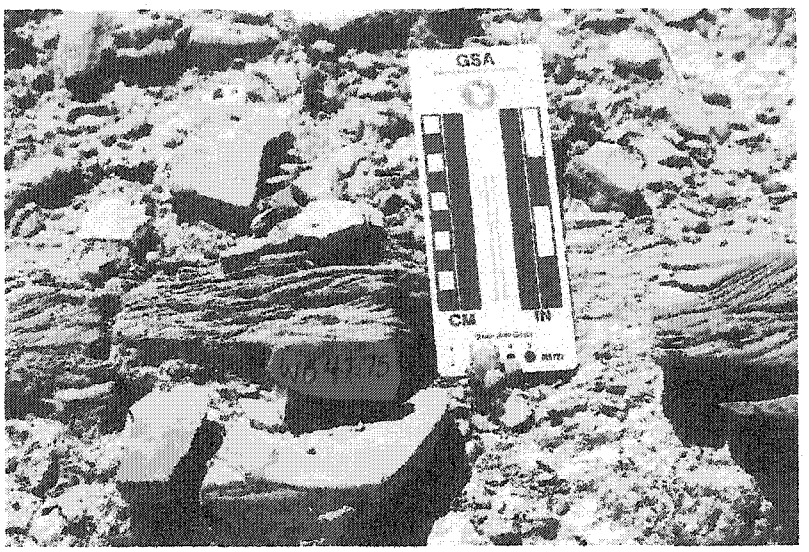

Figure 18. Climbing ripples in sandstone beds within the Telegraph Creek Shale between V-1 and V-2 measuring between 2-6 cm thick.

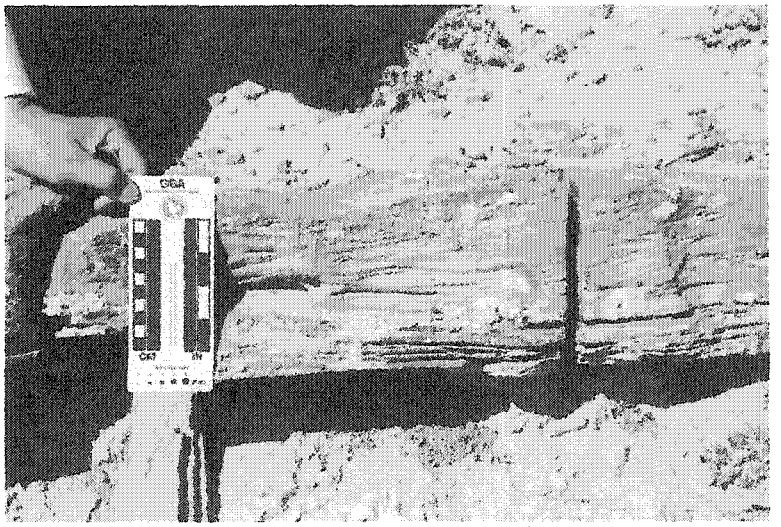

Figure 19. Planar beds at base grading into climbing ripples in the Telegraph Creek Shale between V-1 and V-2 measuring between 8-10 cm thick.

Reproduced with permission of the copyright owner. Further reproduction prohibited without permission.

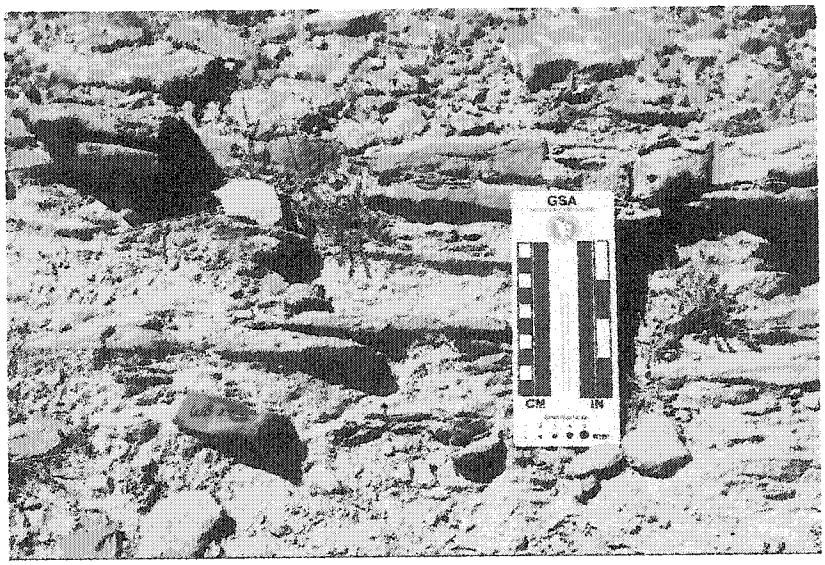

Figure 20. Sandstone beds thickening upward toward the tongue of the Virgelle Member V-2.

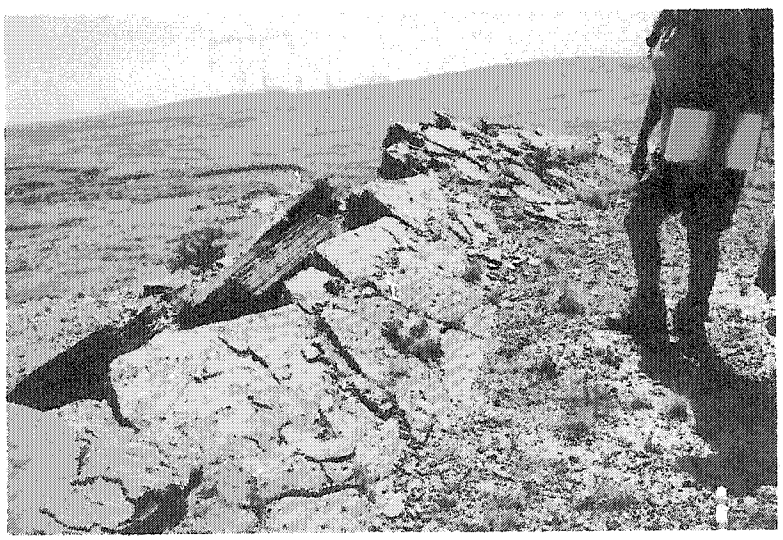

Figure 21. Ripple marks on a flooding surface at the top of a resistant sandstone bed in the Telegraph Creek Shale between V-2 and V-3.

Reproduced with permission of the copyright owner. Further reproduction prohibited without permission.

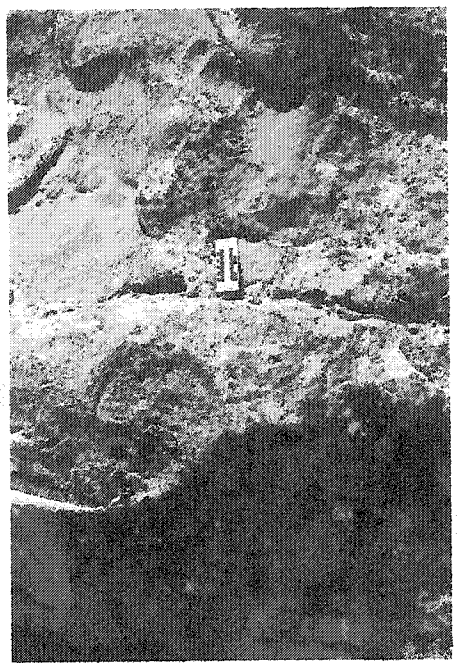

Figure 22. Amalgamated sandstone of the Gebo Member at Wagonhound Central 1 meter above the Shannon Surface.

Reproduced with permission of the copyright owner. Further reproduction prohibited without permission.

ANALYSIS OF GRAIN SIZE DATA

Field and laboratory work in this project has lead to a limited amount of labor-intensive grain size profiles, and a more extensive series of bed thickness profiles. Though limited in extent, the grain size data is valuable because it is evenly spaced, and can be subjected to spectral analysis. This is not possible for the thickness data, since beds of different thickness are beds of different duration, but the results of spectral analysis of the grain size data can be used to resolve periodicities in the thickness data as well.

Preparation of the Grain Size Data

Three of the four sections used for grain size sampling were then used for statistical analysis; WHC, WHS-3 and WHE-2 (see Figure 14). Raw data for average grain size data, "tuned" time, sand fraction (expressed in percent), silt fraction and clay fraction for the WHC, WHS-3 and WHE-2 sections are located in Appendix C. Once average grain size data were obtained (refer to Methods Section), several steps were taken in order to process the data used for statistical analyses. Those included (1) reviewing a simple plot of the grain size data for possible trends (2) an f-test to determine the significance of linear and quadratic trends (3) spectral analysis using the maximum entropy method (MEM). Each of these methods was also completed for the sand fraction, silt fraction and clay fraction.

With time series analysis, a plot of the data is necessary in order to visually determine if there are possible trends. For WHC, WHS-3 and WHE-2, the mean for each section was first removed, followed by an f-test, which determined if the data had linearity or quadratic trends. For all three sections, a linear trend was found to be present and was removed. A very minimal quadratic trend was present and was also removed. Figures 23 through 25 represent the graphical plots of the WHC section for the raw data of average grain size, average grain size data with the mean removed and average grain size with the mean removed showing a linear trend. On the x-axis, time in years is expressed from 0 to $1x10^5$, which is 0 to 100,000 years. The 0 represents the beginning of the section, going back in time to a maximum of 100,000 years. Figures 26 through 28 represent the same graphical plots for WHS-3, and figures 29 through 31 for WHE-2. Figures 32, 33 and 34 are the plots of the WHC, WHS-3 and WHE-2 sections respectively, with the mean and linear trends removed. The data represented in figures 32 through 34 were then used for spectral analysis. Graphical plots for fraction of sand, silt and clay are located in Appendix D.

Reproduced with permission of the copyright owner. Further reproduction prohibited without permission.

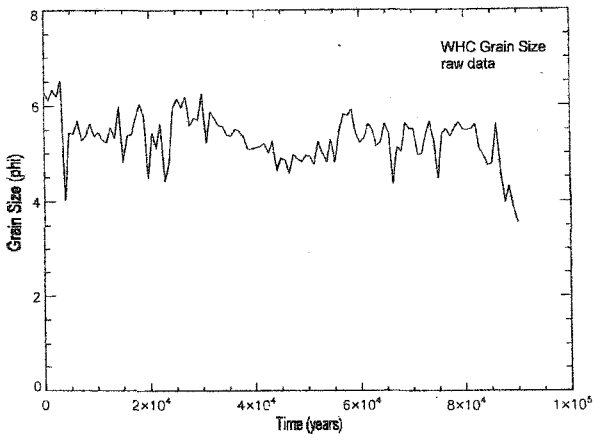

Figure 23. Graphical plot of the raw data for average grain size for WHC.

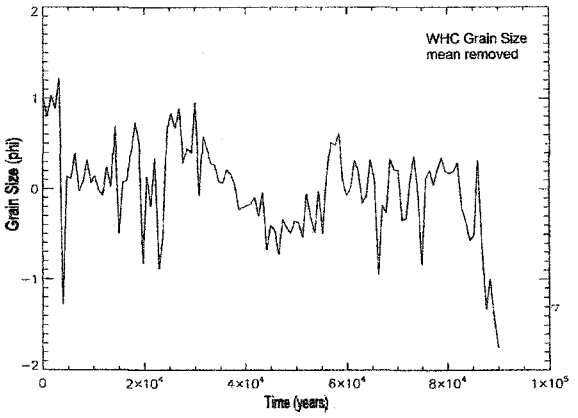

Figure 24. Graphical plot of the average grain size for WHC with the mean removed.

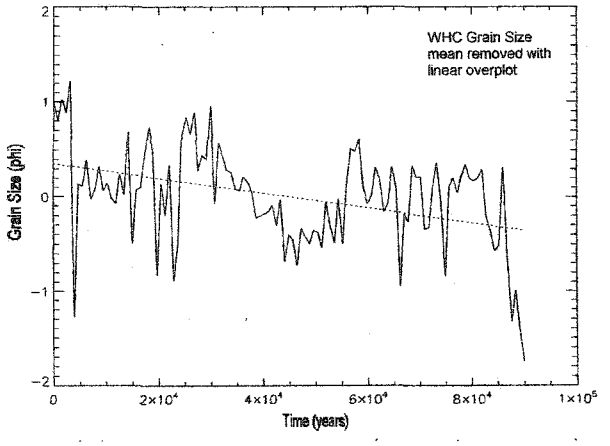

Figure 25. Graphical plot of the average grain size for WHC with mean removed showing a linear trend.

Reproduced with permission of the copyright owner. Further reproduction prohibited without permission.

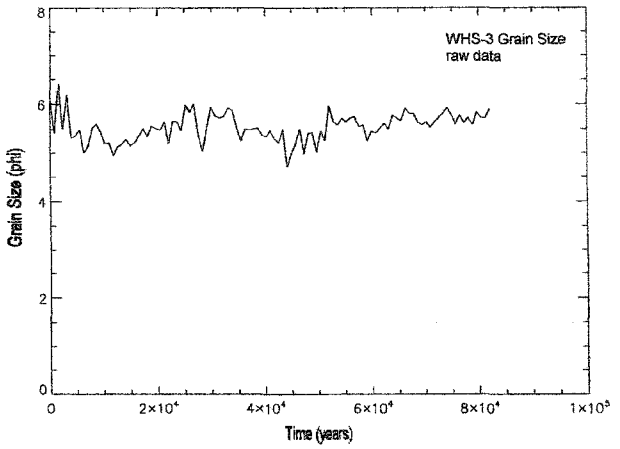

Figure 26. Graphical plot of the raw data for average grain size for WHS-3.

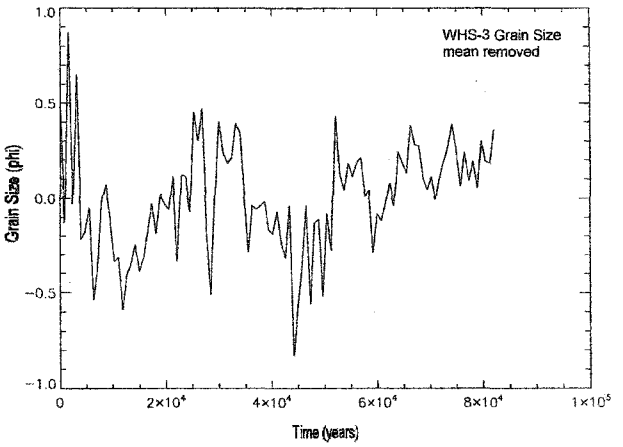

Figure 27. Graphical plot of the average grain size for WHS-3 with the mean removed.

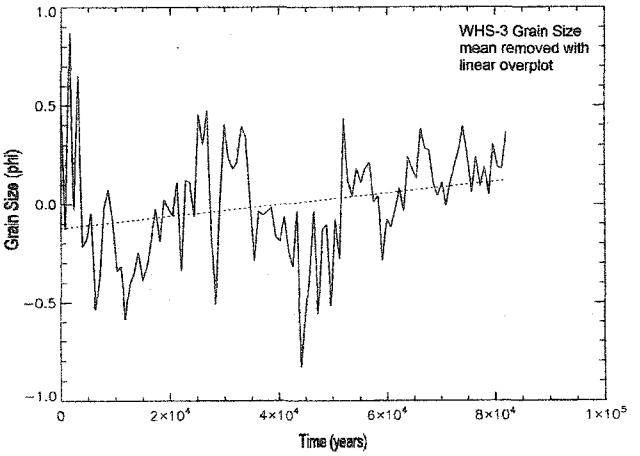

Figure 28. Graphical plot of the average grain size for WHS-3 with mean removed showing a linear trend.

Reproduced with permission of the copyright owner. Further reproduction prohibited without permission.

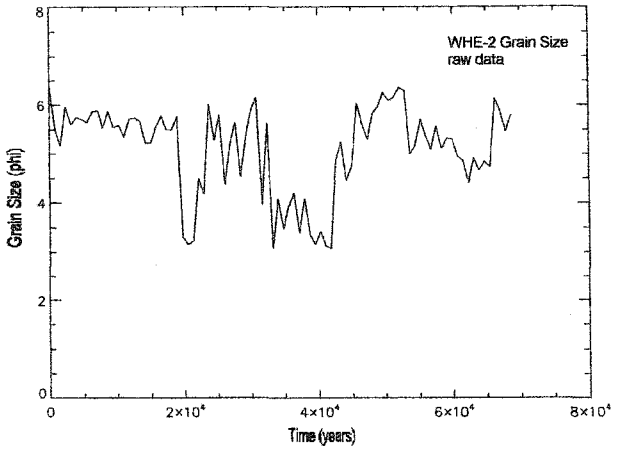

Figure 29. Graphical plot of the raw data for average grain size for WHE-2.

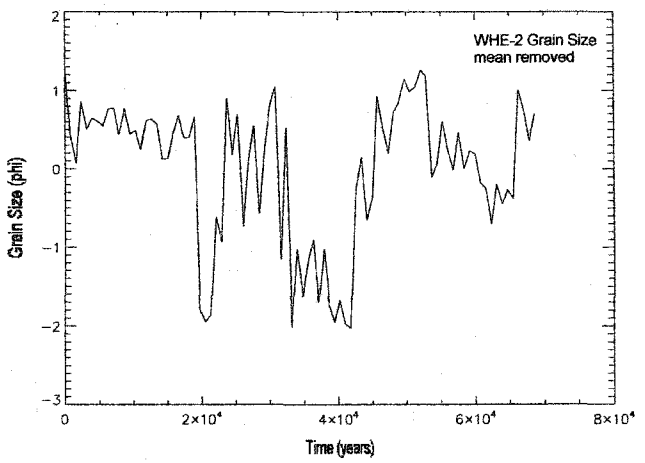

Figure 30. Graphical plot of the average grain size data for WHE-2 with the mean removed.

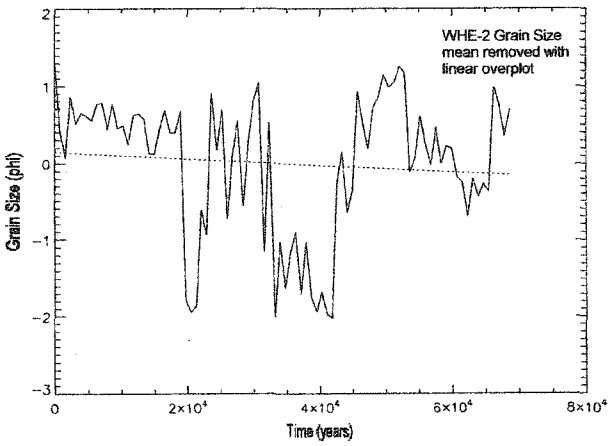

Figure 31. Graphical plot of the average grain size for WHE-2 with the mean removed showing a linear trend.

Reproduced with permission of the copyright owner. Further reproduction prohibited without permission.

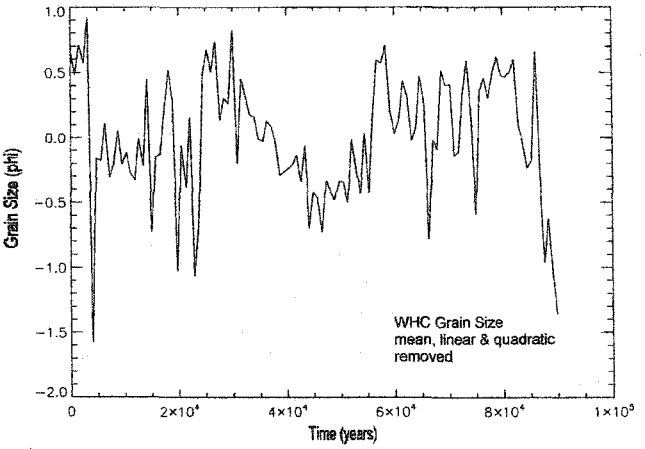

Figure 32. Graphical plot for the average grain size of WHC with mean, linear and quadratic removed.

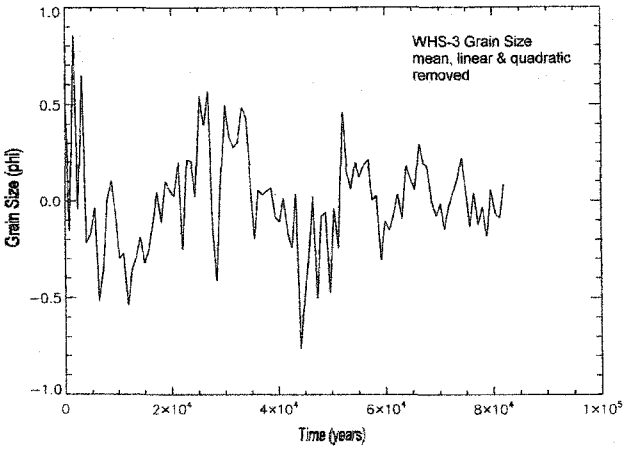

Figure 33. Graphical plot for the average grain size of WHS-3 with mean, linear and quadratic removed.

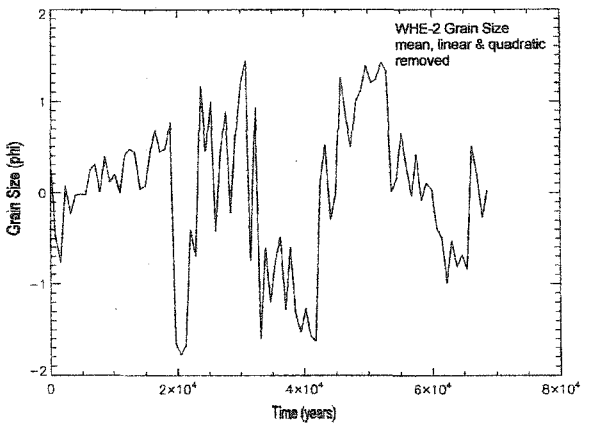

Figure 34. Graphical plot for the average grain size of WHE-2 with mean, linear and quadratic removed.

Reproduced with permission of the copyright owner. Further reproduction prohibited without permission.

Spectral Analysis

Spectral analysis is used to partition the variance of a time series as a function of frequency. For a stochastic time series, contributions from the different frequency components are measured in terms of the power (energy per unit frequency; Emery and Thompson, 1997). For the purposes of this research, Maximum Entropy Method (MEM) was used (Ulrych & Bishop, 1975). MEM was completed on mean grain size (Figures 35 through 37), sand fraction (Figures 38 through 40), silt fraction (Figures 41 through 43) and clay fraction (Figures 44 through 46) for WHC, WHS-3 and WHE-2. WHC and WHE-2 showed the best results, indicating that the 40,000 and 20,000 year cycles are present above the 95% confidence interval. WHS-3 did not produce results as convincing as WHC and WHE-2. In all cases the percent clay proved to be ambiguous.

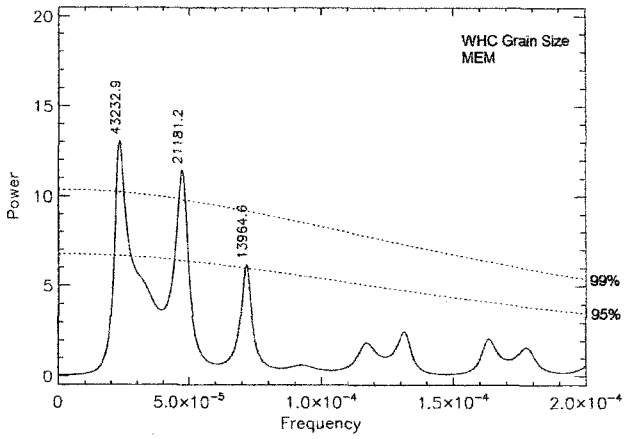

Figure 35. Spectral analysis results for WHC average grain size data.

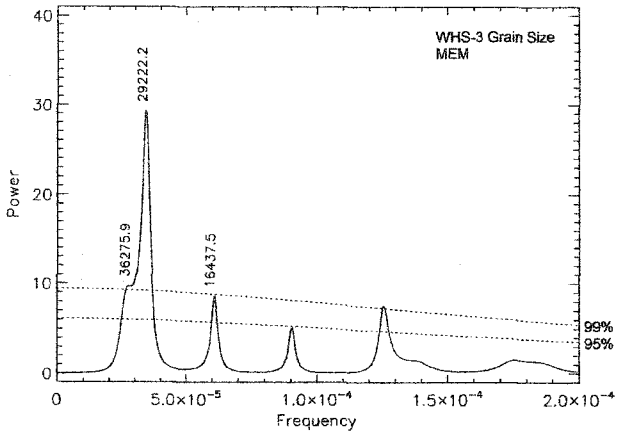

Figure 36. Spectral analysis results for WHS-3 average grain size data.

Reproduced with permission of the copyright owner. Further reproduction prohibited without permission.

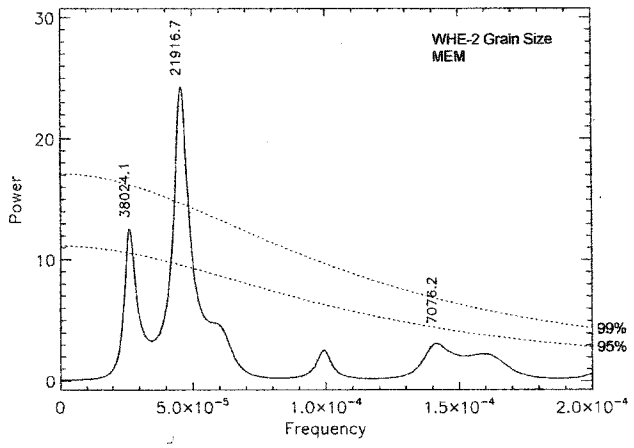

Figure 37. Spectral analysis results for WHE-2 average grain size data.

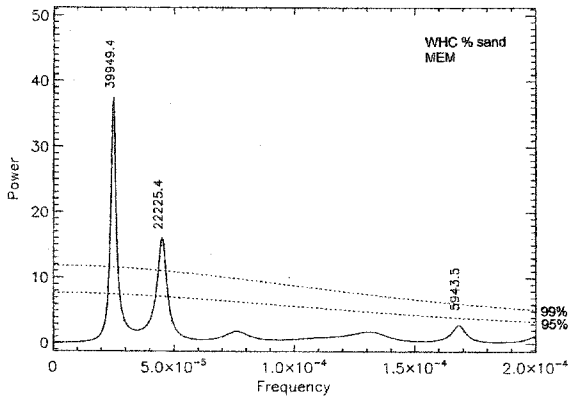

Figure 38. Spectral analysis results for WHC sand fraction data.

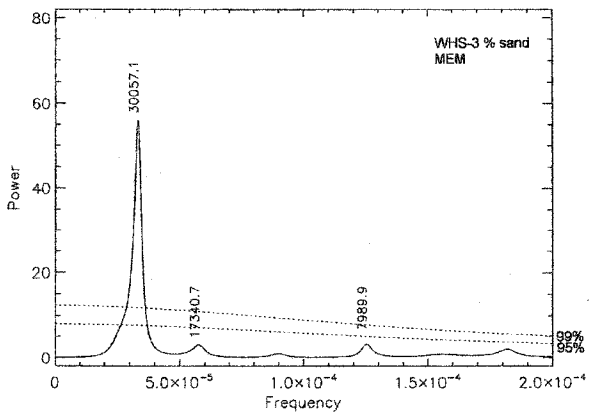

Figure 39. Spectral analysis results for WHS-3 sand fraction data.

Reproduced with permission of the copyright owner. Further reproduction prohibited without permission.

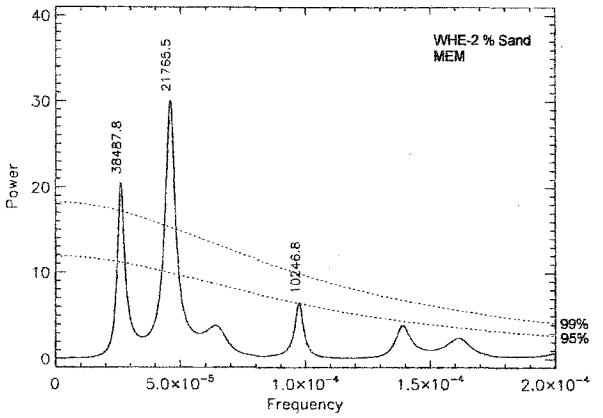

Figure 40. Spectral analysis results for WHE-2 sand fraction data.

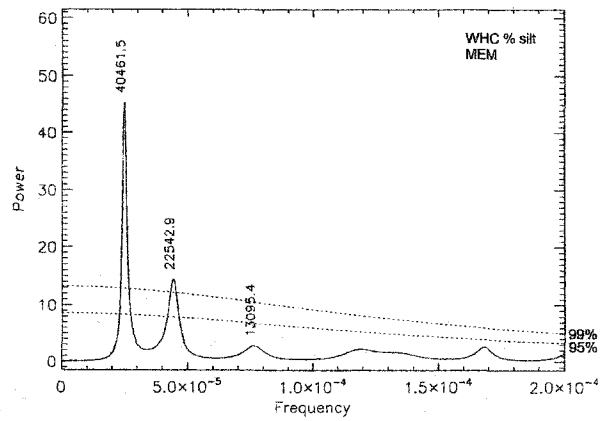

Figure 41. Spectral analysis results for WHC silt fraction data.

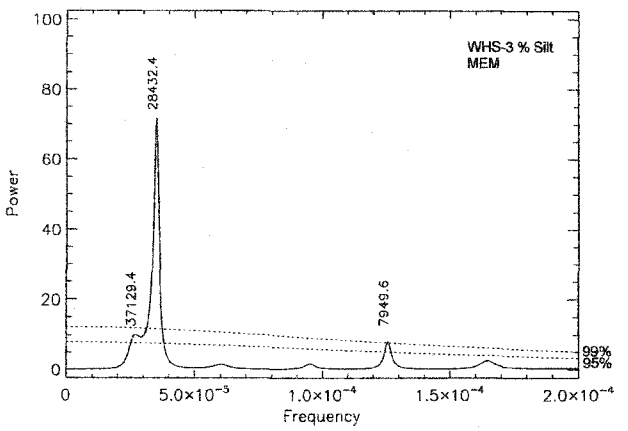

Figure 42. Spectral analysis results for WHS-3 silt fraction data.

Reproduced with permission of the copyright owner. Further reproduction prohibited without permission.

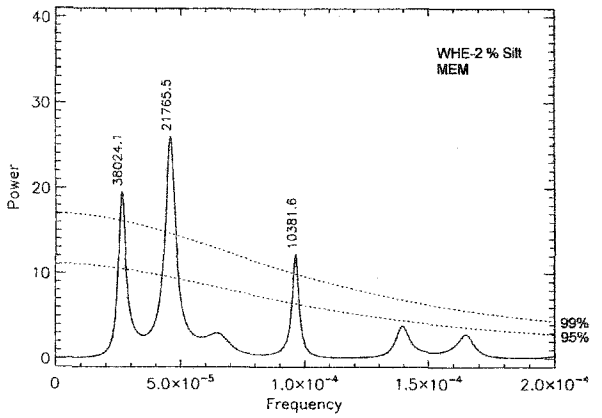

Figure 43. Spectral analysis results for WHE-2 silt fraction data.

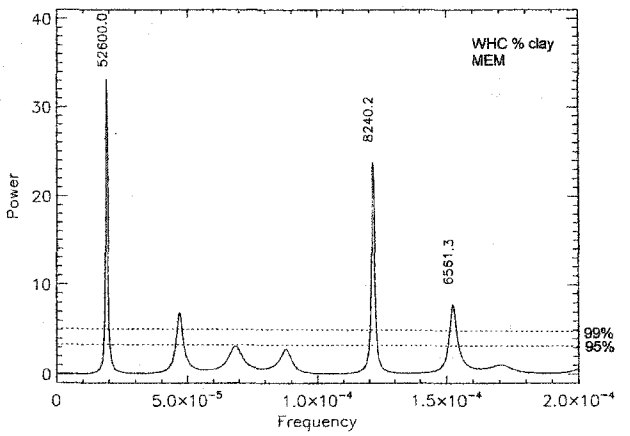

Figure 44. Spectral analysis results for WHC clay fraction data.

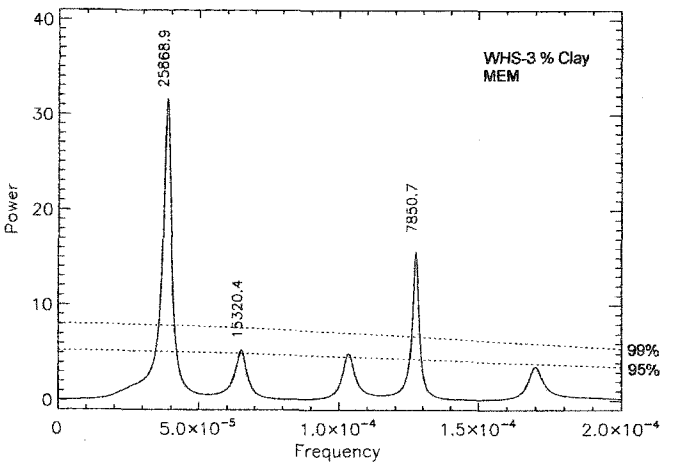

Figure 45. Spectral analysis results for WHS-3 clay fraction data.

Reproduced with permission of the copyright owner. Further reproduction prohibited without permission.

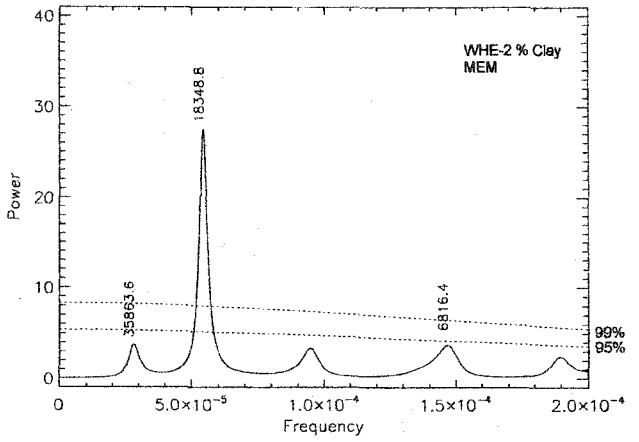

Figure 46. Spectral analysis results for WHE-2 clay fraction data.

Tuning the analysis

Time series analysis of data is a powerful method of determining whether cyclicity occurs in sedimentary successions. Time series methods have been developed based on events whose position in time are known. Age control for geologic events can pose a significant problem and certain assumptions must be made. In outcrop expression, events, such as the sand lenses within the Telegraph Creek Shale may be equally spaced based on thickness, but may not be equally spaced in time. For this project a constant sedimentation rate and a constant subsidence rate is assumed. This assumption will allow for the comparison and possible correlation of fifth-order events from one measured section to the next.

There are several methods for time series analysis, most of which were developed for engineering purposes with high frequency data sets. Using the biostratigraphic information provided by Obradovich (1993; Figure 8) the duration of the Virgelle Member has been determined to be approximately 1 million years (between 82.5 and 81.5 million years old). Dividing this time between the eight sandstone tongues yields approximately 100,000 to 125,000 years for each tongue. Grain size data were collected from the Telegraph Creek Shale at 0.5 meter intervals between sandstone tongue V1 and sandstone tongue V2 in sections WHC, WHS-3 and WHE-2. This interval yielded between 100,000 and 125,000 potential years of time to work with, allowing the possibility for five 20,000 to 22,000 yr cycles, three 40,000 to 43,000 yr cycles and one 100,000 year Milankovitch cycle to occur. Thickness data were collected from V1 to the Shannon Surface. For grain size analysis the Maximum Entropy Method (MEM; Ulrych and Bishop, 1975) was used and for thickness data the Sherman statistic was used (Sherman, 1950; Bartholomew, 1954; Sherman, 1957; Lamb, 1972). A detailed explanation of data and results are presented below.

Reproduced with permission of the copyright owner. Further reproduction prohibited without permission.

Before a detailed statistical analysis can be performed on each section, the amount of time (duration) represented in each section must be known. Time for each section must be "tuned" by means of an assumed sedimentation rate, calculations of which will be described in a later section, and an iterative procedure using an initial MEM spectral analysis. The analysis was completed on the grain size data for the WHC section using an estimate of 100,000 years as the amount of time represented for the sampled interval. The MEM results of the spectral analysis (Figure 47) clearly showed two distinct peaks above the 99% confidence interval. Confidence intervals are based on a "red noise" spectrum derived from an auto regression process AR(1) with coefficient equal to the autocorrelation of the data at lag 1 (Ulrych and Bishop, 1975). Each peak is denoted by a number, which corresponds to a periodicity based on the estimated duration of the interval in years. The periods 46,753 years and 25,714 years were relatively close to the 2:1 ratio of the obliquity and precession period, 43,000 years and 21,000 years, generated by orbital forcing (Fischer, 1993). Therefore, assuming that these are in fact obliquity and precession periodicities, the true duration of the interval must be 90,000 years (89,946 years calculated). This is close to the 100,000 year predicted time with an error of +/- 10 %.

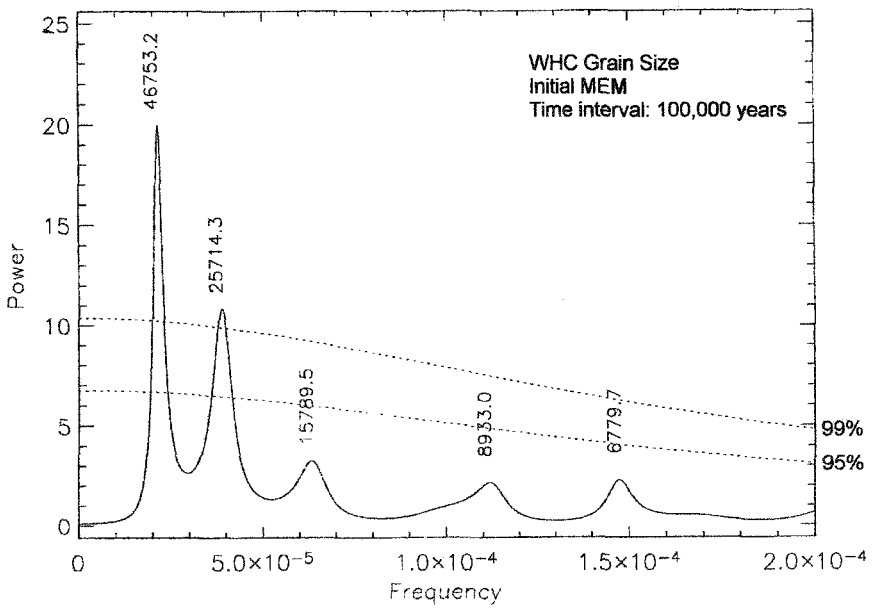

Figure 47. Initial spectral analysis results using 100,000 years for an estimated duration. The number associated with each peak is years.

Reproduced with permission of the copyright owner. Further reproduction prohibited without permission.

Verification of the Tuning Process: Sedimentation Rates

The sediment accumulation rate typically reaches a maximum on the inner shelf (Swift et al., 2003; Storms and Swift, 2003). Landward of the maximum, sediment discharge is high, but the fluid power expended on the sea floor by waves is correspondingly higher; much of the sediment is bypassed seaward. Seaward of the maximum, fluid power is lower, but the transport load is depleted, and there is less sediment to deposit. Recent studies of modern shelves suggest values on the order of 0.03 cm/yr to 0.06 cm/yr (Wheatcroft and Drake, 2003) at the inner shelf maximum. Numerical simulations suggest similar values (Storms and Swift, 2003).

Sedimentation rates were calculated for sections WHC, WHS-3 and WHE-2 using the thickness of the sampled interval and the amount of time represented for that interval. This information was used to develop a more detailed timeline for the entire measured section at each location. For example, the shale section for WHC in which grain size samples were collected was approximately 57 meters thick, and results from the spectral analysis revealed that there were 90,000 years (89,946 years calculated) represented. This then produces a net sedimentation rate of .06 cm/yr, similar to modern analogs. For WHS-3 the shale section in which grain size samples were taken was approximately 53 meters thick with 82,000 years (82,056 years calculated) represented yielding a sedimentation rate of .06 cm/yr. WHE-2 had a sampled interval of 44 meters with 69,000 years (69,078 years calculated) represented yielding a sedimentation rate of 0.06 cm/yr (Figure 48).

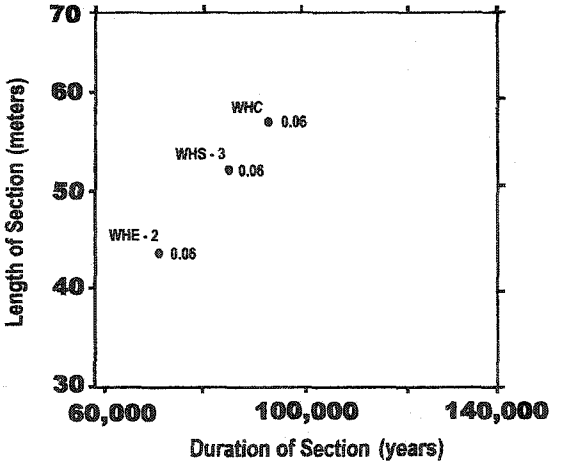

Figure 48. Plot of accumulation rates for WHC, WHS-3 and WHE-2.

Reproduced with permission of the copyright owner. Further reproduction prohibited without permission.

Storm bed thickness follows a power law distribution of the form $\Delta\eta = a \bullet T^P$ (Thorne, 1988; Thorne et al., 1991), where $\Delta\eta$ is bed thickness for a storm of a given return period (T). P is return period power and *a* is the return period intercept, or the minimum bed thickness, equivalent to the thickness of the one year return period bed (Figure 49). For a moderate, mid-latitude wave climate such as the New Jersey shelf wave climate a value of 10 cm is reasonable (Niedoroda et al., 1989). Each of the sand layers was considered to be a storm event, and a sedimentation rate of 10 cm/yr was used. Once the timeline was established for each section, statistical analysis was completed on the thickness data. Calculated time lines for each section are located in Appendix E.

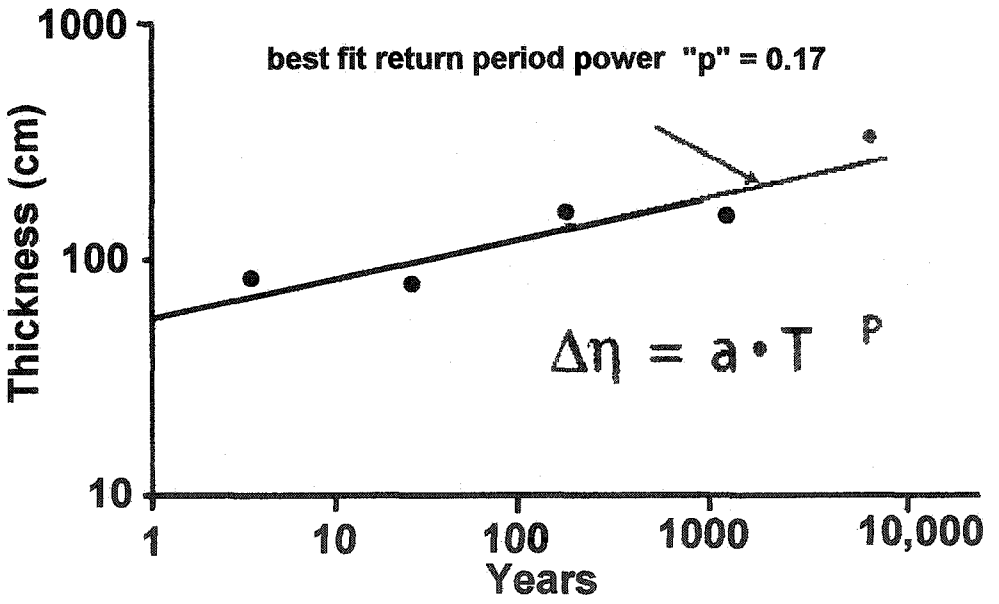

Figure 49. Plot of power law for stratal thickness (from Thorne, 1988).

Reproduced with permission of the copyright owner. Further reproduction prohibited without permission.

ANALYSIS OF BED THICKNESS DATA

It is not possible to undertake spectral analysis of the thickness data, because the successive, discrete, thickness measurements of beds do not represent a constant time interval. However, since spectral analysis of the grain size data shows that obliquity and precessional cycles (41,000 yr and 20,000 yr cycles) are present, it is possible to map these cycles through the Telegraph Creek Shale, using other statistical methods. As noted in the previous section, storm beds form randomly spaced sequences, but their stacking patterns are likely to be modulated by shoreline shifts driven by orbital forcing. At a given depth, storm bed thickness is proportional to storm intensity. Parameterized as maximum wave height (Niedoroda et al., 1989; Thorne et al., 1991). Storm beds are liable to occur each year, with 5, 10, 20, 50, and 100-year return period beds interspersed with the 1-year return period beds. As water depth increased the shorter return beds drop out (Niedoroda et al., 1989). Modulation of the random storm bed succession would occur with at least a 20,000 year period, so thickness analysis must begin with identification of the very long return period beds, here termed "rare events", and determination of whether the rare event beds are periodic or random.

Rare Events

In order to determine which beds were to be considered rare events, thickness bins were set up. For example, the value for bin #1 contains the number of beds that measured between 0 and 5 cm, the value for bin #2 contains the number of beds that measured between 6 and 10 cm, and so on. A plot for WHC is shown on Figure 51 and it can be seen that data in bins 10 and beyond are most likely rare events. All other sections are located in Appendix G. A program called Powell's Method (Press et al., 1992) fitted an empirical exponential probability distribution to the 'number of beds per bin' values and determined at which point the bins began to be rare. The majority of the rare events were the thick shale layers. Deposited at the top of each of those rare shale layers was a 2-4 cm sand layer. Therefore, the top of those rare events were then assigned an age, based on the calculation method described in the 'Verification of the Tuning Process: Sedimentation Rates' section, and a Sherman statistic was completed to determine if those rare events were in fact periodic or random (Sherman, 1957).

Reproduced with permission of the copyright owner. Further reproduction prohibited without permission.

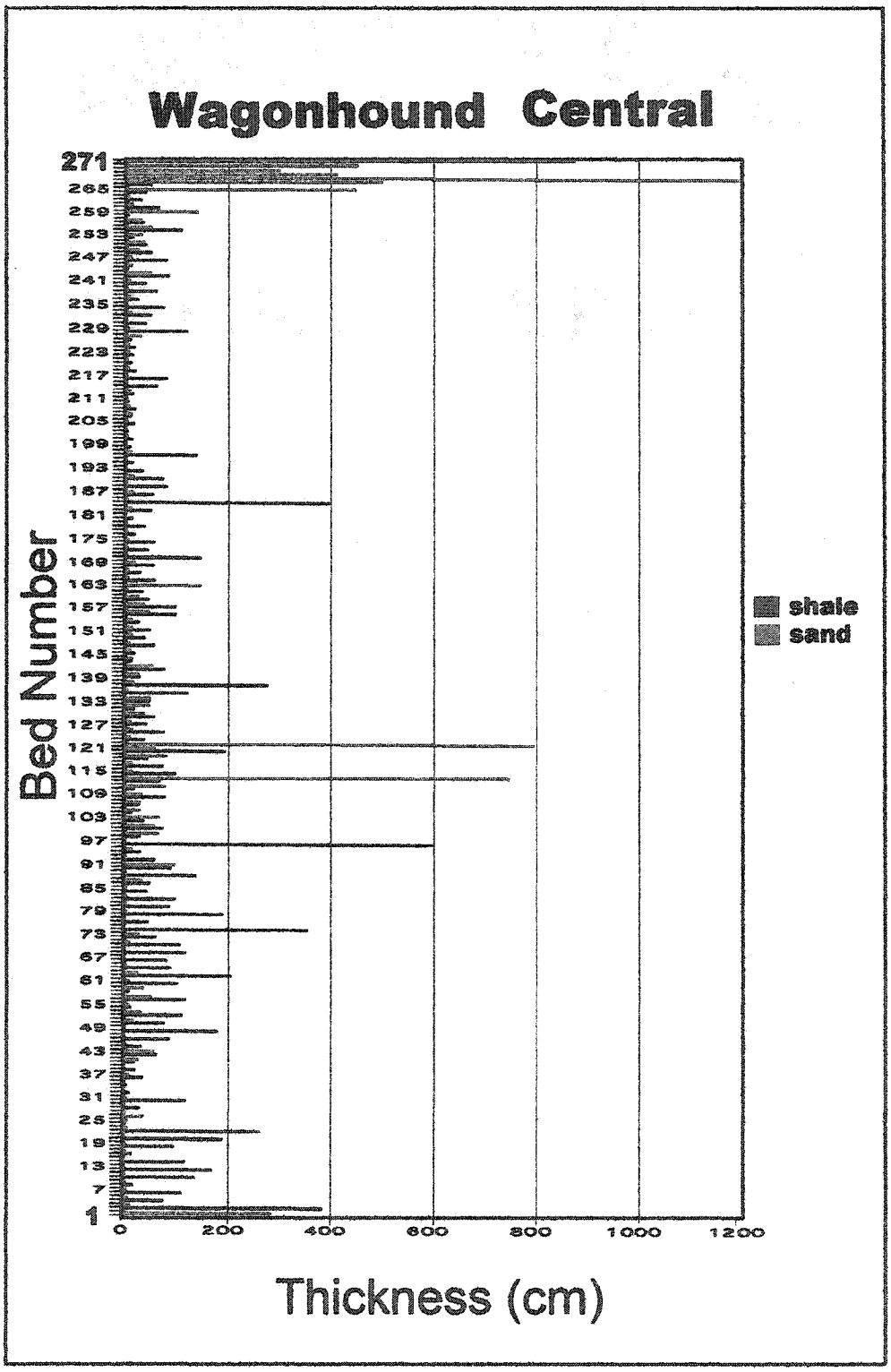

Figure 50. Thickness data for Wagonhound Central.

Reproduced with permission of the copyright owner. Further reproduction prohibited without permission.

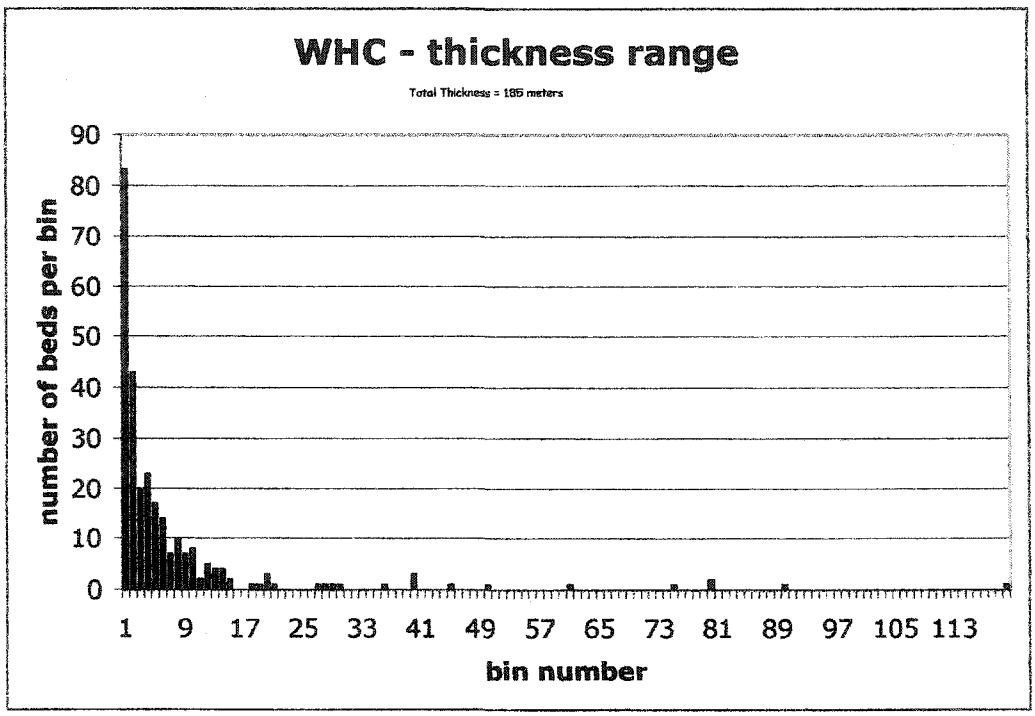

Figure 51. Thickness data arranged by bin for WHC.

Rare Events and the Sherman Statistic

The Sherman statistic is a way to evaluate whether the distribution of events are periodic or random (Sherman, 1957) and in this case, the amount of time between the events. Each thickness layer is an event whether it be sand or shale. On average the most common thickness was 10-15 cm. Layers with a thickness greater than 15 cm had the potential to be rare. For this study, a high percentage (> 70% for most sections) of the rare events were shale beds. It is assumed that these thick shale beds are portions of the random storm bed succession that have been "censored" by obliquity and precessional modulation. Their storm beds are represented by essentially invisible diastems; the sampling site was too far seaward and too deep for sand to be transported that far. In nearly every case, a thin (2-4 cm) sand bed caps these thick shale layers. The sand bed that caps them is random, impulsive storm event like its predecessors, but sand reaches the study site because the precessional cycle is now in phase of shallower water or intensified sediment supply or both.

The distribution of the Sherman statistic is shown on Figure 52. The Sherman statistic is calculated and plotted on the graph against the number of rare events. High percentage values

Reproduced with permission of the copyright owner. Further reproduction prohibited without permission.

meant that events are clustered and episodic. Low percentage values means that the events are periodic. Values that fall somewhere in the middle means the data is ambiguous, neither episodic or periodic, possibly random (Craddock, 1968). Clearly WHC, WHN-2 and WHE-7 show that the rare events in those sections are periodic with high probability. WHE-3 and WHE-5 plotted between 95% and 98%, meaning those events are clustered and episodic. The average period of time between each rare event ranges from 4,000 to 6,000 years. Figures 53 through 57 show the plotted thickness data with those rare events for WHC, WHN-2, WHE-3, WHE-5 and WHE-7 that ultimately represented the nearly 40,000 yr and nearly 20,000 yr intervals. All sections had rare events associated with them and all thickness plots including rare events are located in Appendix F.

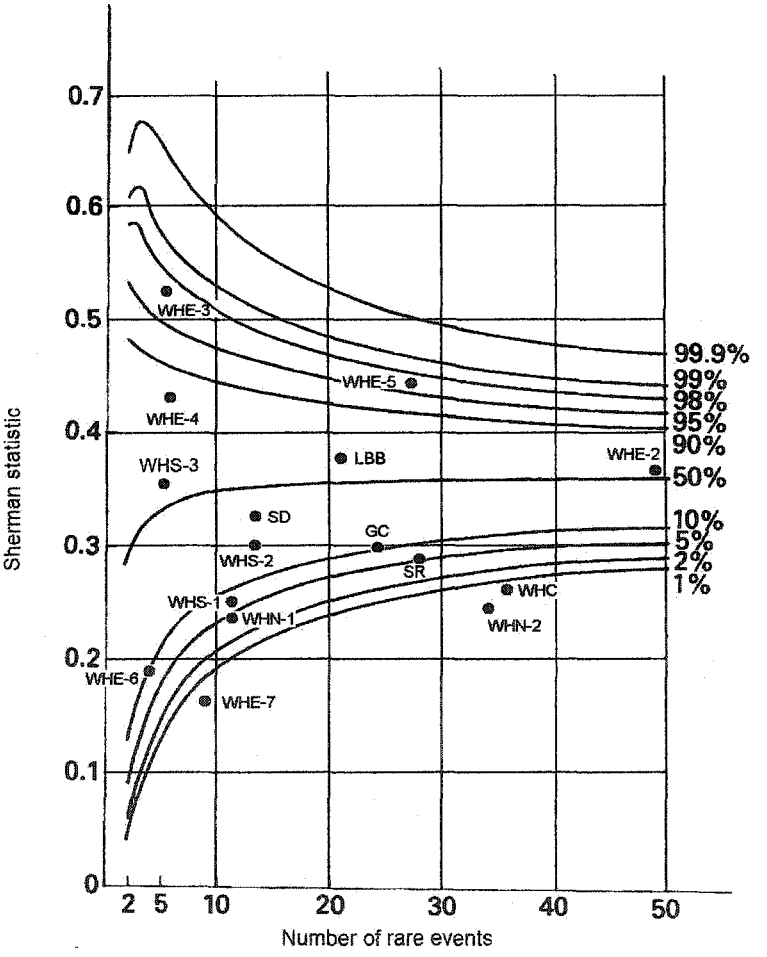

Figure 52. *Plot of Sherman statistic values for study area.* The percentiles of the distribution of Sherman's statistic for values of *n* (the number of rare events based on bed thickness; after Craddock, 1968).

Reproduced with permission of the copyright owner. Further reproduction prohibited without permission.

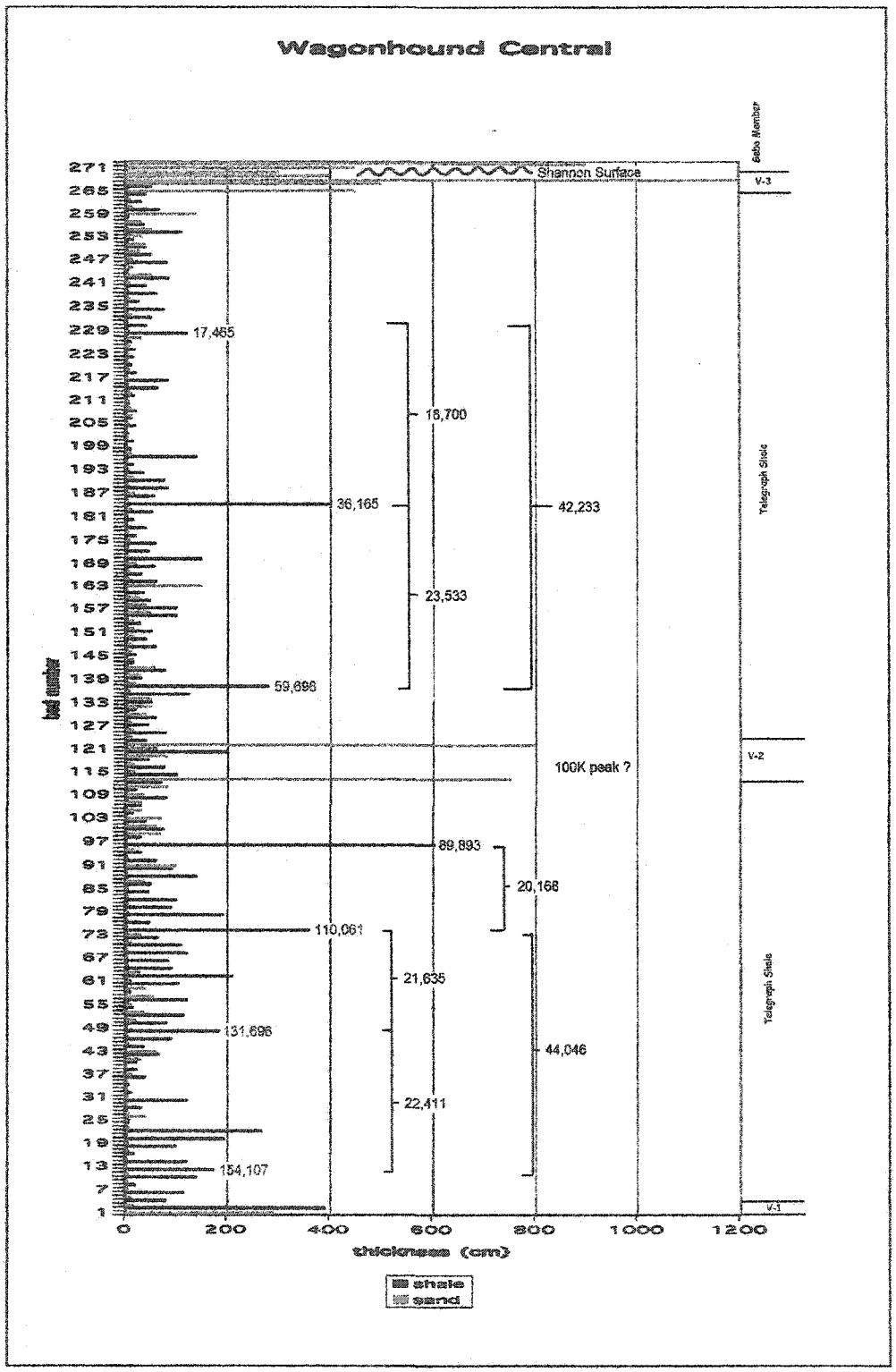

Figure 53. Wagonhound Central thickness data showing rare events with assigned time (red) and possible Milankovitch cycles (black).

Reproduced with permission of the copyright owner. Further reproduction prohibited without permission.

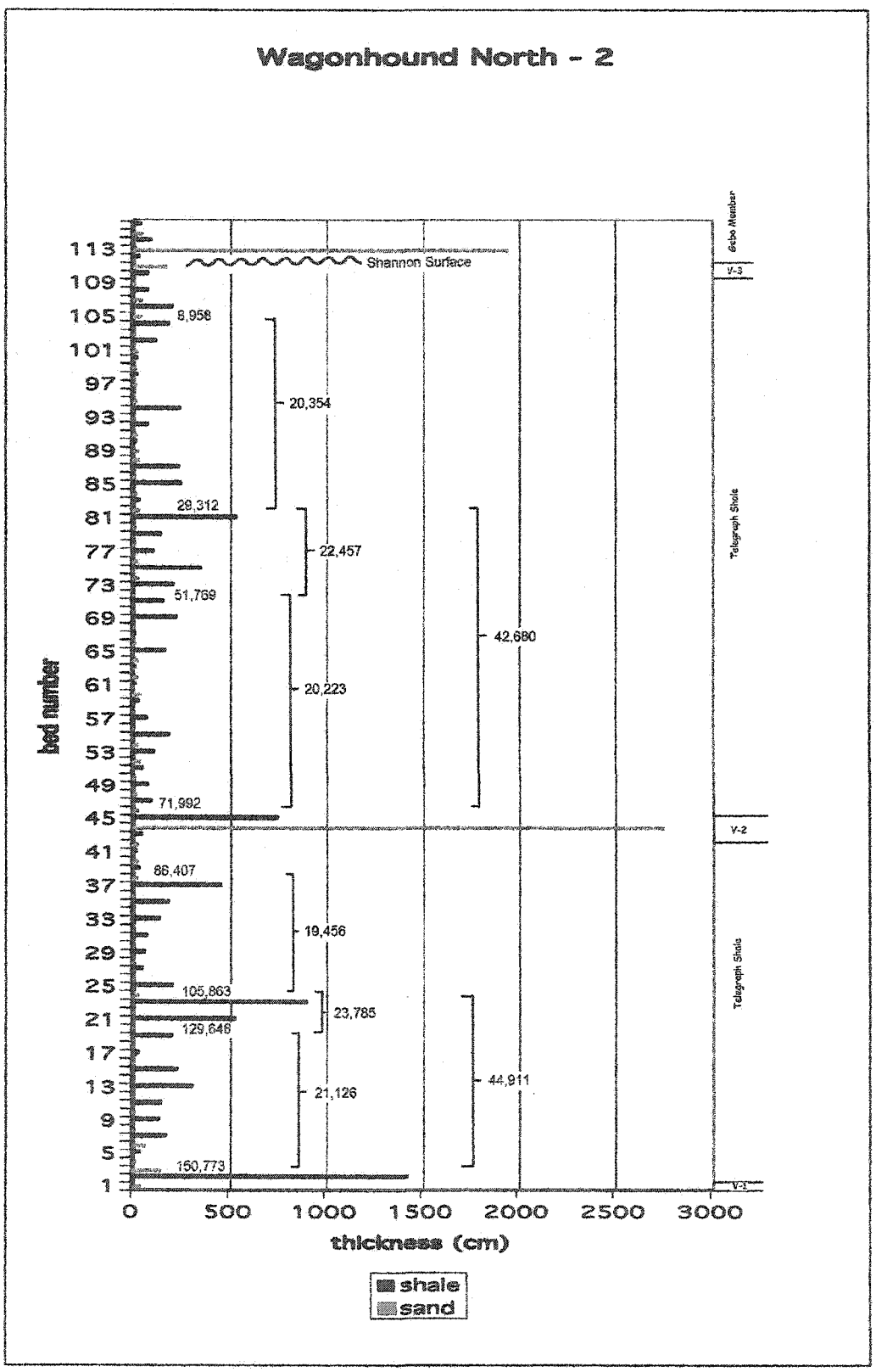

Figure 54. Wagonhound North - 2 thickness data showing rare events with assigned time (red) and possible Milankovitch cycles (black).

Reproduced with permission of the copyright owner. Further reproduction prohibited without permission.

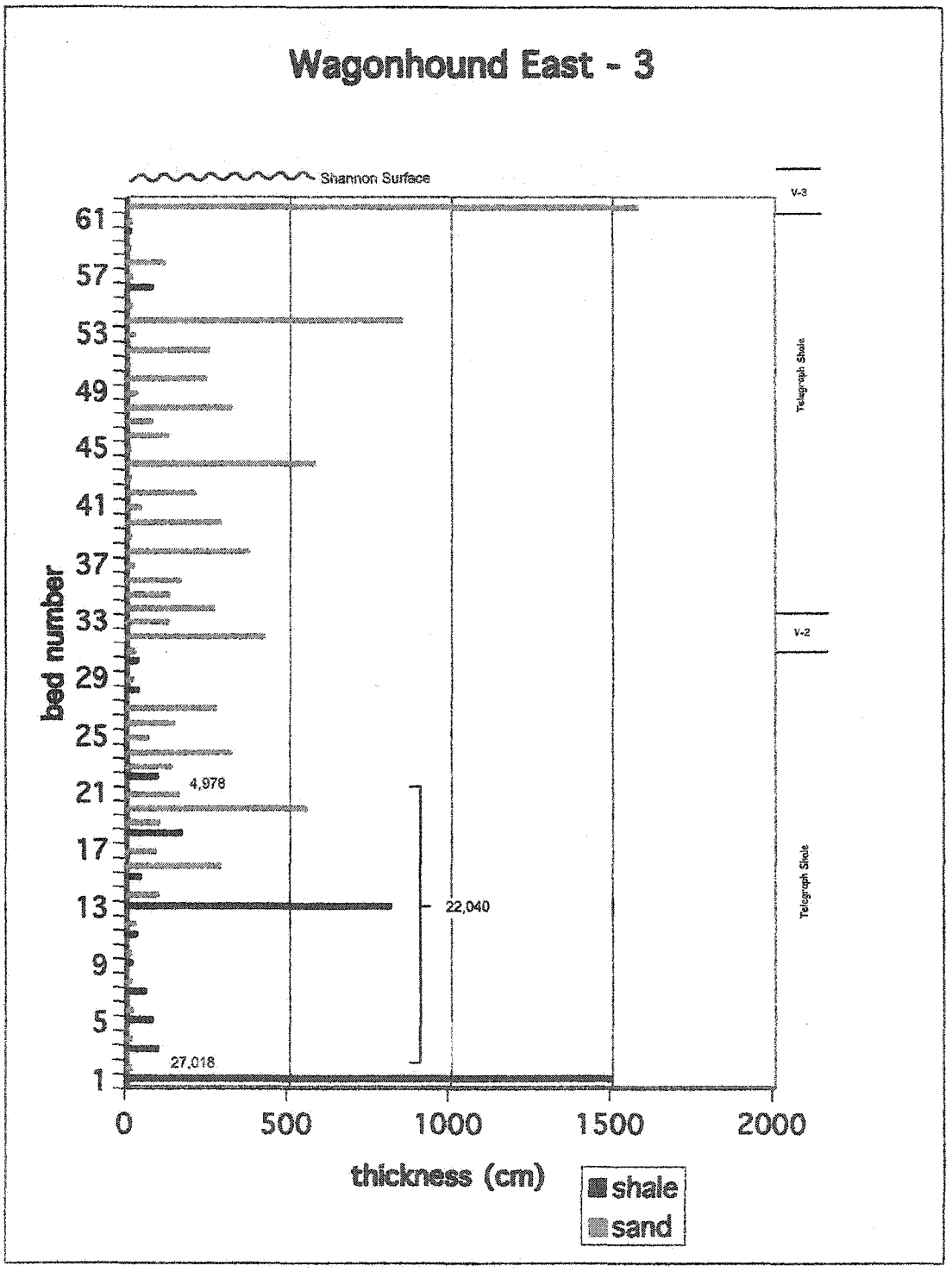

Figure 55. Wagonhound East - 3 thickness data showing rare events with assigned time (red) and possible Milankovitch cycles (black).

Reproduced with permission of the copyright owner. Further reproduction prohibited without permission.

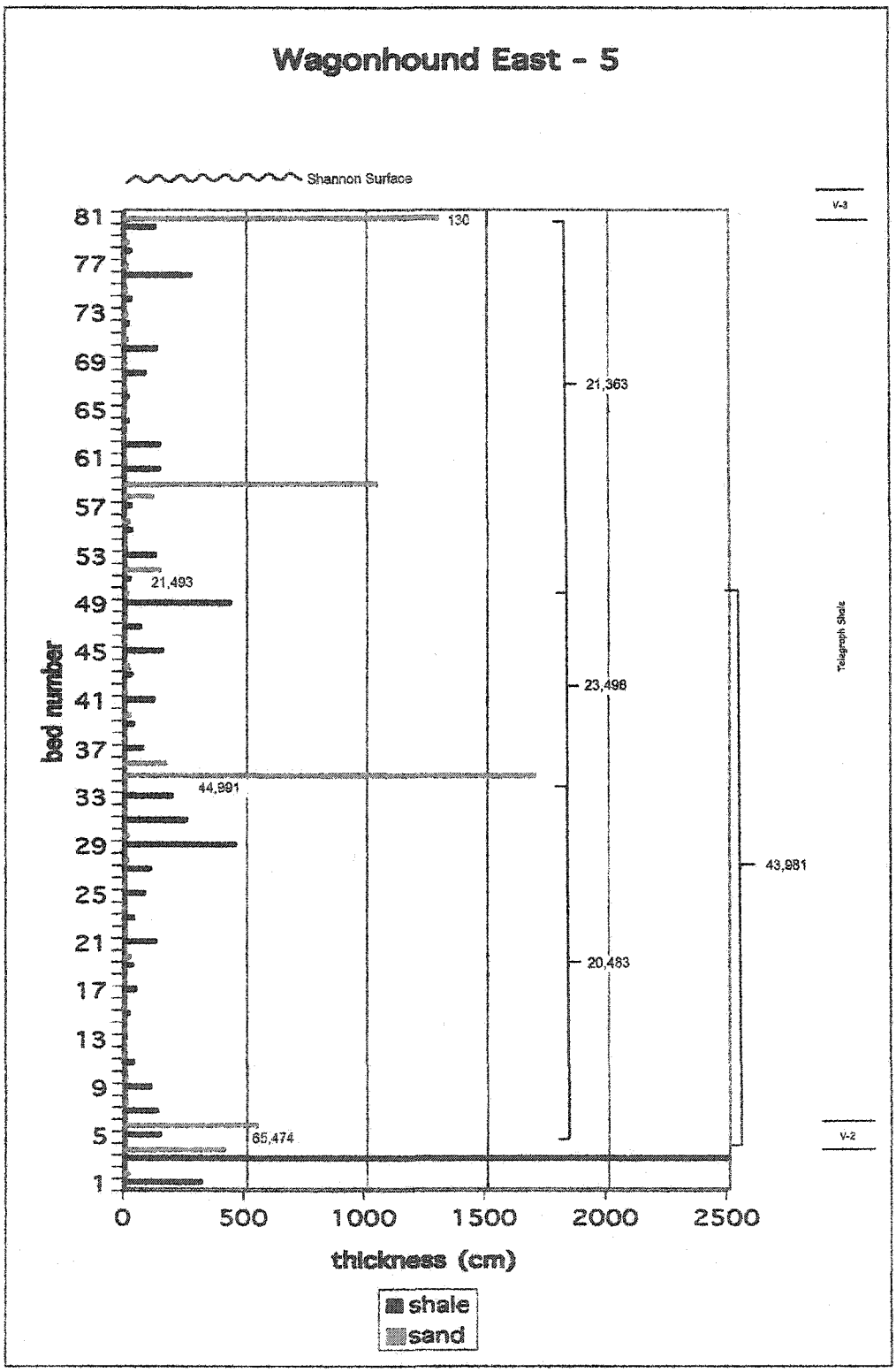

Figure 56. Wagonhound East - 5 thickness data showing rare events with assigned time (red) and possible Milankovitch cycles (black).

Reproduced with permission of the copyright owner. Further reproduction prohibited without permission.

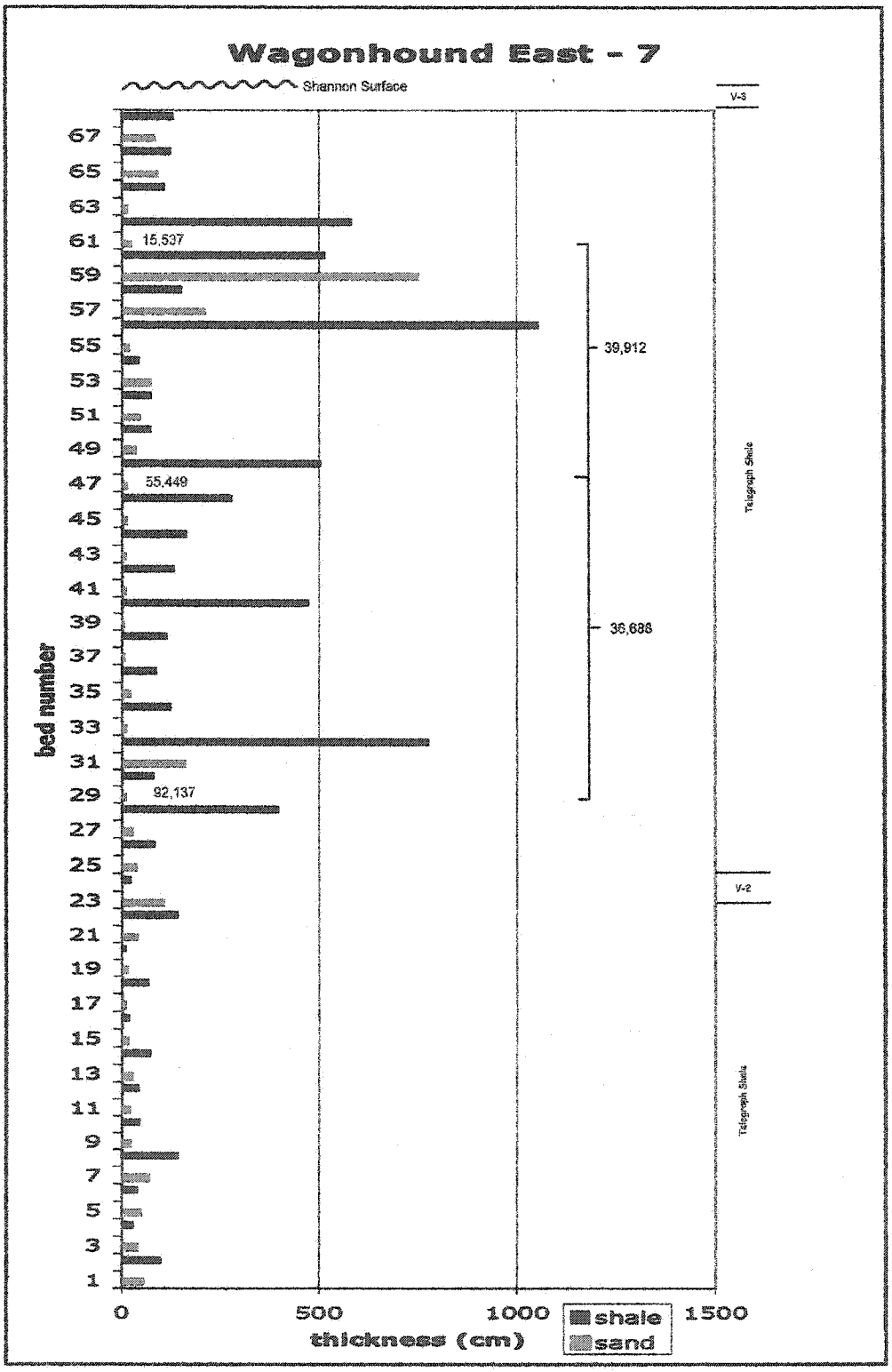

Figure 57. Wagonhound East - 7 thickness data showing rare events with assigned time (red) and possible Milankovitch cycles.

Reproduced with permission of the copyright owner. Further reproduction prohibited without permission.

Correlation of Precession Cycles

In this study, results indicate that Milankovitch cyclicity is present and two parameters were used generating results that were repeated in more than one section. Those parameters are grain size and thickness variation. Grain size data were collected in the lower Telegraph Creek Shale, approximately the lower third of the entire section, and data for the WHC and WHE-2 sections produced the best results with respect to the application of the Maximum Entropy Method (MEM). Those results clearly indicate that a very strong 40,000 yr (obliquity) peak and a strong 20,000 yr (precession) peak exist. With respect to thickness data, which were collected for the entire section, rare event data and Sherman statistic data indicated that WHC, WHN-3 and WHE-7 clearly showed rare events as being periodic. Those events correspond to 20,000 yr and 40,000 yr periods and these Milankovitch periodicities correlate (Figure 58). These cycles appear to follow the same pattern as the member units (see Figure 8). Although the Sherman statistic did not deem all sections as having periodic rare events, each section did have rare events according to the Powell Method (see Rare Events section) and an observation was done to determine if there were 20,000 yr and 40,000 yr intervals between those rare events.

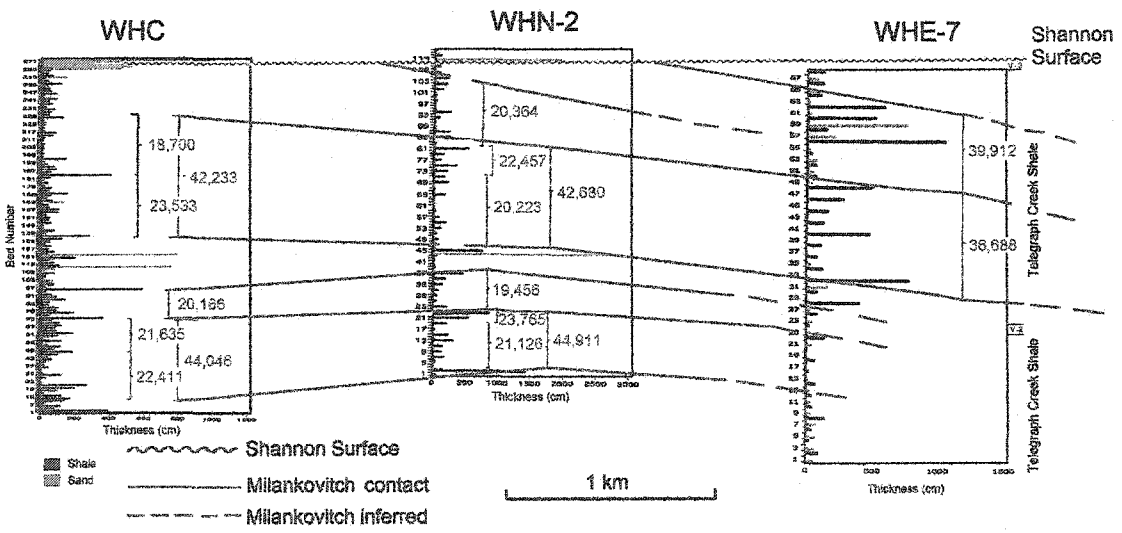

Figure 58. Milankovitch cycles correlated between WHC, WHN-2 and WHE-7.

In sections other than WHC, WHN-3 and WHE-7, rare events were also identified and the amount of time represented between those rare events were also determined. A visual inspection of those sections revealed time intervals between rare events, which coincide with the precessional cycle. The next step was to correlate these cycles and determine the spatial scales in which they correlate. How far basinward do they correlate, how far along paleoshoreline? Measured sections along a 6 km section of localized paleoshoreline around the Thermopolis Anticline

Reproduced with permission of the copyright owner. Further reproduction prohibited without permission.

included sections WHS-3 to WHN-2. Measured sections along a 100 km of regional paleoshoreline, or larger spatial scale included WHC, GC, LBB and SR. Measured sections along a 6 km localized shore normal transect included WHC and WHE-2 through WHE-7 (see Figure 14). Presentation of measured sections used for correlation is similar to those found in Figures 53 through 57. On these sections, the x-axis represents bed thickness and the y-axis represents bed number. Rare events and precessional cycles are noted on each section and all sections did show periodicity. Milankovitch cycles correlate along both the local and regional paleoshoreline (Plates 1 and 2) as do Milankovitch cycles out into the basin (Plate 3).

An offlapping pattern is not apparent in both the local and regional paleoshoreline sections (Plates 1 and 2), where truncation of a precessional cycle occurs in the WHS-2 section below both V-2 and V-3. Field reconnaissance of this area suggests that small scale normal faulting has occurred in this area. An offlapping pattern is also apparent in the shore normal section (Plate 3). In this case, the offlapping is occurring in a similar manner as the individual Virgelle tongues; however, they are not conformable with respect to the Virgelle tongues, instead they are truncated by the superjacent fourth order tongues of the Virgelle. This relationship is similar to the geometry predicted by the numerical simulations of Storms and Swift (2003; Figure 9) in which the lowstand beds envelope or "enshroud" the distal end of the tongue.

Reproduced with permission of the copyright owner. Further reproduction prohibited without permission.

DISCUSSION AND CONCLUSIONS

General

Four most important variables controlling stratigraphic geometry are sea level change, sediment input, grain size, and sediment transport intensity (Sloss, 1962). The next question is what are the driving forces behind these variables? In the Cretaceous Western Interior Seaway the loading of the crust by the Sevier Orogeny drives subsidence and this has been documented extensively (Kauffman and Caldwell; 1993; Beaumont et al., 1993; DeCelles, 2004). Changes in eustasy can be driven by tectonics or ice buildup or terrestrial water storage on a global scale. Climate changes along with ice sheet dynamics drive the accumulation and ablation of continental ice sheets. Sediment flux is driven by the availability of a source. The Sevier Mountain Range coupled with climate changes (i.e., stronger monsoons), would set the stage for variations in sediment supply to the Western Interior Seaway. Collectively these variables could potentially comprise time scales on the order of 10^3 to 10^4 years.

Several forcing mechanisms were considered when testing the hypothesis for this project; eustasy, local tectonics, lobe-switching, and sediment supply (Table 2). Spectral analysis of the grain size data indicates cyclic variation at two frequencies, with a 2:1 ratio of periods. This relationship is seen as strong evidence for a precession to obliquity relationship and for orbital forcing as the cause of the cycles. Orbital forcing is considered to be an allocyclic phenomenon, or a force from outside the basin. Local tectonics and lobe-switching are considered autocyclic phenomena, or forces within the basin, which at this point can be dismissed as possible mechanisms. Eustasy and sediment supply are the remaining mechanisms, which need explanation with regard to allocyclicity. Both eustasy and sediment supply can be driven by orbital variations. Eustatic changes in sea level are often attributed to changes in ice volume. Precessional cycles cause varying degrees of solar radiation to the Earth's surface, ultimately varying the growth and ablation of continental ice sheets, thus rising or lowering sea level (Ruddiman, 2000). During the Cretaceous it has been determined that ice may have been present, but in a minimal quantity (Miller et al., 2004). Ice that may have existed during the Cretaceous would have been constrained to higher elevations and would have had minimal effect on sea level changes (Miller et al., 2004). An explanation for sea level change in the Cretaceous is hydrospheric water storage, or fluctuations of lake and groundwater volume (Jacobs and Sahagian, 1995). Intensified monsoons, which take significant volumes of water from the oceans via evaporation, transfers that water in the form of precipitation onto the continents, is then stored in lakes and groundwater systems. The calculated volume transfer suggests that sea level could fluctuate on the order of 2 to 8 meters (Jacobs and Sahagian, 1995). Intensified monsoons, with

Reproduced with permission of the copyright owner. Further reproduction prohibited without permission.

the increased amount of precipitation would also be a cause for fluctuations in sediment supply and have been interpreted as the mechanism for cyclicity seen in this study.

Monsoons as the Forcing Mechanism

Milankovitch cyclicity has been shown to be present within the Telegraph Creek Shale between V-1 and V-2 as well as between V-2 and V-3. The results of this study have been interpreted to be increases in sediment supply due to orbital forcing. The expected 5:1 precession to eccentricity ratio expressed on the eastern portion of the basin was not observed on the western portion; however; a 2:1 of precession to obliquity was present and the 41,000 year obliquity cycle was dominant, a contradiction to the carbonate systems where the 23,000 year precessional cycle is dominant.

The modern day Asian monsoon system has been studied in detail and has been traced back in time to at least the pre-Quaternary. It has revealed orbitally forced changes in monsoon intensity (Bloemendal and deMenocal, 1989; Quade et al., 1989; Clemens et al., 1991). The Upper Triassic tropical Pangean has also been studied and has shown 'megamonsoon' circulation associated with the Tethy's Ocean (Parrish and Curtis, 1982; Crowley et al., 1989; Parrish, 1993; Kutzback, 1994). A study using the external insolation as a forcing mechanism has shown that summer insolation reaches a maximum at the precessional frequency in the north-tropical latitudes creating periodically intensified monsoons. This forcing mechanism is known as the orbital monsoon hypothesis (Kutzbach, 1981). The more intense modern monsoon systems are located in the northern hemisphere where land masses are large and elevated (Ruddiman, 2001).

Using the above notions, the following interpretations have been made for this study: (1) Monsoons that are generated from both the Pacific Ocean and Gulf of Mexico would form low pressure systems over the elevated Sevier Mountain range which would then serve as the source terrain for sediment supply into the Western Interior Basin, (2) Prior to the onset of the intensified monsoons every 23,000 years, sea level would be in at a position where storm wave base could reach further into the basin. These intensified monsoonal systems would bring large amounts of sediment into the basin as well as a significant amount of precipitation. The large amount of water storage generated by these monsoons would be stored in lake and groundwater systems (Jacobs and Sahagian, 1995) and potentially lower relative sea level, pushing storm wave base eastward allowing for the deposition of coarser grained material, (3) The 41,000 years signal is often expressed at higher latitudes and considering the paleolatitude of the central portion of the Western Interior Seaway, which was approximately 30 degrees North, this is the explanation for the expression of both the precessional and the obliquity signal. (4) Milankovitch cyclicity

Reproduced with permission of the copyright owner. Further reproduction prohibited without permission.

(precession and obliquity) can be correlated along paleoshoreline as well as into the basin at least a local level (i.e. on the western portion of the Bighorn Basin).

Milankovitch Studies in a Clastic Environment

Studies involving the recognition of Milankovitch cyclicity in a clastic environment, using thickness data coupled with grain size analysis have not previously been undertaken for the Cretaceous Western Interior Seaway. Earlier studies have mostly been concerned with the deep-water carbonate settings of the Seaway's eastern margin where Milankovitch cyclicity is clearly present and thickness data and lithology are the parameters used. The Cenomanian-Turonian Bridge Creek Limestone Member of the Greenhorn Formation in central Colorado is a classic example of Milankovitch cyclicity using lithologic as well as chemical data. Alternating siliciclastic deposits and hemipelagic carbonate beds (shale-limestone couplets) appear to be rhythmic, and spectral analysis of thickness data and percent carbon indicate cycles in the Milankovitch frequency band, specifically the precessional : eccentricity or 5:1 ratio (Sageman et al., 1997).

The use of thickness data as a parameter of Milankovitch-scale cyclicity has been carried over to this project; grain size data has been substituted for a lithologic parameter. Spectral analysis of the grain size data has produced results at Milankovitch frequencies, only in this clastic setting the ratio was 2:1. In other words, the carbonate rich eastern portion of the basin has been previously shown to reveal the precession : eccentricity cycles, and in this study the clastic-rich (sands and silts) western portion of the basin has revealed precession : obliquity cycles. Age control on the Bridge Creek Member is not clearly established, although a range of 0.6 to 3 Ma is suggested as the upper and lower limits of possibility. An age range including approximately 2.5 million years of time would certainly have the potential to produce the eccentricity cycle, however, obliquity was not as apparent in the Bridge Creek data. The interval of focus for this study encompasses approximately 250,000 years of time. Precession and obliquity are apparent but the eccentricity cycle was not seen. This is not to say that the eccentricity cycle was not recorded on the eastern margin; thicker sections would allow more time to be represented and would have the potential for eccentricity cycles to be revealed.

Another study which included the use of clastics in the recognition of Milankovitch cyclicity was within the Fort Hays Limestone (Coniancian) of Colorado, which used percent carbonate and percent organic matter in combination with clastic composition (Ricken, 1996). It was noted by this author that orbital signals are not well documented as well as not well developed on the western side of the Western Interior Seaway due to low carbonate production. This would suggest that Milankovitch cyclicity is only made apparent in depositional systems where

Reproduced with permission of the copyright owner. Further reproduction prohibited without permission.

carbonate is present. This study has shown that a parameter other than carbonate or organic carbon, namely variation in grain size, can be used to study Milankovitch cyclicity in a clastic depositional environment with little to no carbonate production.

The interval of interest was between V-1 and the Shannon Surface where the 41,000 obliquity cycle and the 21,000 precession cycle were found within the Telegraph Creek Shale both above and below the V-2 sandstone tongue. The Virgelle tongues may be the result of and represent the 100,000 year eccentricity cycle; however, further research needs to be conducted in order to confirm this interpretation.

One of the goals of this research was to show that an easily measured parameter, thickness variation, used in several other environments (eastern portion of the Western Interior Seaway) can be used in a nearly pure clastic environment. It was also a goal of this research to find a second proxy (grain size variation) which had not been used previously and could potentially be shown to be unique to clastic environments or shown to be useful in other environments with respect to the recognition of Milankovitch cyclicity. Locally, with respect to the Bighorn Basin, Milankovitch has been shown to be present as well correlated along paleoshoreline and at least 10 km into the basin (Plates 1-3). The work completed here could be used as a model in which to test Milankovitch cyclicity in the Powder River Basin, located further east in Western Interior Basin and possibly correlate along a more regional scale. Once a firm timeline has been established for the Western Interior Basin, this model could be used in other Cretaceous basins and correlation on a global scale would be the next natural step.

Grain Size and Thickness Data as Parameters for Milankovitch Studies

In this study, grain size proved to be a valuable tool for recognizing Milankovitch cyclicity where sedimentary structures are limited. Although several studies have been completed using chemical proxies to show Milankovitch cyclicity (Fischer, 1993; Ricken, 1996; Sageman et al., 1997), this is the first study to use grain size as a proxy in clastic sediments of the western portion of the Western Interior Seaway. Grain size data were also useful in determining sedimentation rates, which ultimately produced a timeline for each section. The assumption here was that sedimentation rate was constant throughout the entire section, and that these same sedimentation rates occurred along paleoshoreline as well as offshore. For those sections other than WHC, WHN-2 and WHE-7, where the Sherman statistic deemed them not periodic, a grain size study for those particular sections may produce a different sedimentation rate, therefore a difference timeline and one more conducive to showing Milankovitch cyclicity.

Reproduced with permission of the copyright owner. Further reproduction prohibited without permission.

Thickness data proved to be useful for sections that had both shale and sand beds. It is necessary to measure each and every bed very carefully and very meticulously in order to determine which thickness would ultimately be rare and therefore become a rare event and correlatable among sections. Although several studies have been completed using spectral analysis of thickness data, this is the first study to use the Powell Method and Sherman statistic in a geologic setting. Conventional studies involving Milankovitch cyclicity have been completed using either varved lake sediments (Olsen, 1986) or carbonate sediments (Fischer, 1993; Sageman et al., 1997). This study has shown that Milankovitch cyclicity can not only be found in clastics via grain size and thickness data, but that these cycles can also be correlated along paleoshoreline and into the basin. Future studies will include more detailed grain size analysis and a larger geographic area.

Reproduced with permission of the copyright owner. Further reproduction prohibited without permission.

REFERENCES CITED

Armstrong, R. L., 1968, Sevier orogenic belt in Nevada and Utah: Geological Society of America Bulletin, v. 79, p. 429-458.

Arthur, M. A. and S. O. Schlanger, 1979, Cretaceous "oceanic anoxic events" as causal factors in development of reef-reservoired giant oil fields: American Association of Petroleum Geologists Bulletin, v. 63, p. 870-885.

Asquith, D. O., 1970, Depositional topography and major marine environments, Late Cretaceous, Wyoming: American Association of Petroleum Geologists Bulletin, v. 54, p. 1184-1224.

Barnard, P., 1973, Mesozoic floras: Paleontological Association of London, v. 12, p. 175-188.

Barron, E. J. and W. M. Washington, 1982, Cretaceous climate: a comparison of atmospheric simulations with the geologic record: Paleogeography, Paleoclimatology and Paleoecology, v. 40, p. 103-133.

Barron, P., 1983, A warm, equable Cretaceous: the nature of the problem: Earth Science Reviews, v. 19, p. 305-338.

Bartholomew, D. J., 1954, Note on the use of Sherman's statistic as a test of randomness: Biometrika, v. 41, p. 556-558.

Beaumont, C. G., M. Quinlin, and G. S. Stockmal, 1993, The Evolution of the Western Interior Basin: Causes, Consequences and Unsolved Problems, *in* W.G.E. Caldwell and E.G. Kauffman, eds., Evolution of the Western Interior Basin. Geological Association of Canada Special Paper 39, p. 97-117.

Bhattacharya, J. and R. Walker, 1991, Allostratigraphic subdivision of the Upper Cretaceous Dunvegan, Shaftebury and Kaskapau Formations in the Northwestern Alberta Subsurface: Bulletin of Canadian Petroleum Geology, v. 39, p. 161-191.

Bloemendal, J. and P. deMenocal, 1989, Evidence for change in the periodicity of tropical climate cycles at 2.4 Myr from whole-core magnetic susceptibility measurements: Nature, v. 342, p. 897-900.

Reproduced with permission of the copyright owner. Further reproduction prohibited without permission.

Boyd, R., Suter, J., and S. Penland, 1989, Sequence stratigraphy of the Mississippi Delta: Transactions-Gulf Coast Association of Geological Societies, v. 39, p.331-340.

Brass, G . W., J. R. Southam, and W. H. Peterson, 1982, Warm saline bottom water in the ancient ocean: Nature, v. 296, p. 620-623.

Chamberlain, T. C., 1909, Diastrophism as the ultimate basis of correlation: Journal of Geology, v. 17, p. 685-693.

Clemens, S., W. Prell, D. Murray, G. Shimmield, and G. Weeden, 1991, Forcing mechanisms of the Indian Ocean monsoon: Nature, v. 353, p. 720-725.

Craddock, J. M., 1968, Statistics in the computer age: English University Press, London.

Crowley, T. J., W. T. Hyde, and D. A. Short, 1989, Seasonal cycle variations on the supercontinent of Pangea: implications for Early Permian vertebrate extinctions: Geology, v. 17, p. 457-460.

Crowley T. J. and G. R. North, 1991, Paleoclimatology: New York, Oxford University Press, p. 339.

Curray, J. R., F. J. Emmel, and P. J. S. Crampton, 1969, Holocene history of a strand Plain, *in* A. A. Castañares and F. B. Phleger, eds., Lagunas Mem. Simp. Internat. Lagunas Costeras. Univ. Nac. Autonoma De Mexico Mexico City, p. 63-100.

D'Argenio, B., V. Ferreri, A. Raspini, S. Amodio, and F. P. Buonocunto, 1999, Cyclostratigraphy of a carbonate platform as a tool for high-precision correlation: Tectonophysics, v. 315, p. 357-384.

DeCelles, P. G., 2004, Late Jurassic to Eocene evolution of the Cordilleran thrust belt and foreland basin system, western U.S.A.: American Journal of Science, v. 304, p. 105-168.

DeCelles, P. G., and K. N. Giles, 1996, Foreland basin systems: Basin Research, v. 8, p. 105-123.

deBoer, P. L., 1983, Aspects of Middle Cretaceous pelagic sedimentation in S. Europe: Geol. Ultraiectina 31.

Reproduced with permission of the copyright owner. Further reproduction prohibited without permission.

deBoer, P. L., and D. G. Smith, 1994, Orbital forcing and cyclic sequences, *in* P. L. de Boer and D. G. Smith, eds., Orbital Forcing and Cyclic Sequences: International Association of Sedimentologists Special Publication 19, p. 1-14.

Devlin W. J., K. W. Rudolph, C. A. Shaw, and K. D. Ehman, 1993, The effect of the tectonic and eustatic cycles on accommodation and sequence-stratigraphic framework in the Upper Cretaceous foreland basin of southwestern Wyoming: International Association of Sedimentology Special Publications, v. 18, p. 501-520.

Duff, P. D., A. Hallam, and E. K. Walton, 1967, Cyclic Sedimentation. Elsevier, Amsterdam, p. 280.

Elder, W. P., E. R. Gustason, and B. B. Sageman, 1994, Correlation of basinal carbonate cycles to nearshore parasequences in the Late Cretaceous Greenhorn seaway, Western Interior U.S.A.: Geological Society of America Bulletin, v. 106, p. 892-902.

Emery, W. J. and R. E. Thompson, 1997, Data Analysis Methods in Physical Oceanography. Elsevier Science, p. 658.

Fischer, A. G., 1993, Cyclostratigraphy of Cretaceous Chalk-Marl Sequences, *in* W.G.E. Caldwell and E.G. Kauffman, eds., Evolution of the Western Interior Basin. Geological Association of Canada Special Paper 39, p. 283-295.

Fitzsimmons, R. and S. Johnson, 2000, Forced regressions: recognition, architecture and genesis in the Campanian of the Bighorn Basin, Wyoming, *in* D. Hunt and R. L. Gawthorpe, eds., Sedimentary Responses to Forced Regressions, London, v. 172, p. 113-139.

Folk, R. L., 1968, Petrology of sedimentary rocks, University of Texas, Austin, p. 170.

Gale, A. S., J. Hardenbol, B. Hathway, W. J. Kennedy, J. R. Young, and V. Phansalkar, 2002, Global correlation of Cenomanian (Upper Cretaceous) sequences: evidence for Milankovitch control on sea level: Geology, v. 30, p. 291-294.

Gill, J. R. and W. A. Cobban, 1966a, The Red Bird section of the Upper Cretaceous Pierre Shale in Wyoming: United States Geological Survey Professional Papers, 393-A.

Reproduced with permission of the copyright owner. Further reproduction prohibited without permission.

Gill, J. R. and W. A. Cobban, 1966b, Regional unconformity in Late Cretaceous, Wyoming: United States Geological Survey Professional Papers, 550-B.

Gill, J. R. and W. A. Cobban, 1973, Stratigraphy and geologic history of the Montana Group and equivalent rocks, Montana, Wyoming, and North and South Dakota: U.S. Department of the Interior Geological Survey professional Paper 776, p. 1-37.

Grabau, W. A., 1913, Principles of stratigraphy. New York, Dover facsimile edition, p. 1185.

Hampson, G. J. and Storms, J. E. A., 2003, Geomorphological and sequence stratigraphic variability in wave-dominated, shoreface-shelf parasequences. Sedimentology, v. 50, p. 667-701.

Heller, P. L., C. L. Angevine, and W. S. Winslow, 1988, Two-phase stratigraphic model of foreland basin sequences: Geology, v. 14, p. 501-504.

Herbert, T. D., J. Gee, and S. DiDonna, 1999, Precessional cycles in Upper Cretaceous pelagic sediments of the South Atlantic: Long term patterns from high frequency climate variations: Geological Society of America Special Paper 332, p. 105-120.

Houston, W. S., J. E. Huntoon, and D. L. Kamola, 2000, Modeling of Cretaceous foreland-basin parasequences, Utah, with implications for timing of Sevier thrusting: Geology, v. 28, p. 267-270.

Howell, J. A. and S. S. Flint, 2003, Siliciclastic case study: the Book Cliffs, *in* A. Coe, ed., The Sedimentary Record of Sea-level Change, p. 135-255.

Jacobs, D. K., and D. L. Sahagian, 1993, Climate-induced fluctuations in sea level during non-glacial times: Nature, v. 361, p. 710-712.

Jacobs, D. K. and D. L. Sahagian, 1995, Milankovitch fluctuations in sea level and recent trends in sea-level change: ice may not always be the answer, *in* B. U. Haq, ed., Sequence Stratigraphy and Depositional Response to Eustatic, Tectonic and Climatic Forcing, p. 329-366.

Jordan, T. E., 1988, Thrust loads and foreland basin evolution, western United States: American Association of Petroleum Geologists Bulletin, v. 65, p. 2506-2520.

Reproduced with permission of the copyright owner. Further reproduction prohibited without permission.

Jordan, T. E., 1995, Retroarc and related foreland basins, *in* C. Busby and R. V. Ingersoll, eds., Tectonics of Sedimentary Basins, Oxford, Blackwell Science, p. 579.

Kauffman, E. G., 1973, Evolutionary rates and biostratigraphy: Geological Society of America Abstracts, v. 5, p. 688.

Kauffman, E. G., 1977, Upper Cretaceous cyclothems, biotas and environments, Rock Canyon Anticline, Pueblo, Colorado: The Mountain Geologist, v. 14, p. 129-142.

Kauffman, E. G., and W. G. E. Caldwell, 1993, The Western Interior Basin in space and time, *in* W.G.E. Caldwell and E.G. Kauffman, eds., Evolution of the Western Interior Basin. Geological Association of Canada Special Paper 39, p. 1-30.

Kauffman, E. G., B. B. Sageman, W. P. Elder, J. I. Kirkland, and T. Villamil, 1993, Cretaceous molluscan biostratigraphy and biogeography, Western Interior Basin, North America, *in* W.G.E. Caldwell and E.G. Kauffman, eds., Evolution of the Western Interior Basin. Geological Association of Canada Special Paper 39, p. 397-434.

King, P., 1959, the Evolution of North America, Princeton University Press, p. 190.

Klug, B., 1994, The Mesaverde Group (Campanian) in the Bighorn Basin of Wyoming/Montana, USA: Facies arcitecture and sequence stratigraphic evolution of a foreland basin fill: Bonn University Dissertation, p.199.

Kominz, M. A., and G. C. Bond, 1990, A new method of testing periodicity in cyclic sediments: application to the Newark Supergroup: Earth and Planetary Science Letters, v. 98, p. 233-244.

Krystinik, L. F., and B. B. DeJarnett, 1995, Lateral variability of sequence stratigraphic framework in the Campanian and Lower Maastrichtian of the Western Interior Seaway, *in* J.C. Van Wagoner and G. T. Bertram, eds., Sequence Stratigraphy of Foreland Basin Deposits: Outcrop and Subsurface Examples from the Cretaceous of North America.. American Association of Petroleum Geologists Bulletin, p. 11-25.

Reproduced with permission of the copyright owner. Further reproduction prohibited without permission.

Kump, L. R. and R. L. Slingerland, 1999, Circulation and stratification of the early Turonian Western Interior Seaway: Sensitivity to a variety of forcings: Geological Society of America Special Paper 332, p. 181-190.

Kutzbach, J. E. and R. G. Gillmore, 1989, Pangean climates: megamonsoons of the megacontinent: Journal of Geophysical Research, v. 94, p. 3341-3357.

Kutzbach, J. E., 1981, Monsoon climate of the early Holocene: climate experiment with earth's orbital parameters for 9000 years ago: Science, v. 214, p. 59-61.

Kutzbach, J. E., 1994, Idealized Pangean climates: sensitivity to orbital change, *in* G. D. Klein, ed., Tectonics and Sedimentation during Accretion, Zenith, and Breakup of a Continent: Geological Society of America Special Paper 288, p. 41-55.

Laferriere, A. P., and D. E. Hattin, 1987, Effects of climate, tectonics, and sea-level changes on rhythmic bedding patterns in the Niobrara Formation (Upper Cretaceous), U.S. Western Interior: Geology, v. 15, p. 233-236.

Lamb, H. H., 1972, Climate: Present, Past and Future, Volume I: Methuen, London.

Miller, K. G., P. J. Surgarman, J. V. Browning, M. A. Kominz, R. K. Olsen, M. D. Feigenson, and J. C. Hernandez, 2004, Upper Cretaceous sequences and sea-level history, New Jersey coastal plain: Geological Society of America Bulletin, v. 116, p. 368-393.

Mutterlose, J., 1992, Biostratigraphy and paleobiogeography of Early Cretaceous calcareous nannofossils: Cretaceous Research, v. 18, p. 167-189.

Niedoroda, A. W., D. J. P. Swift, and J. A. Thorne, 1989, Modeling shelf storm beds: controls of bed thickness and bedding sequence, *in* R. A. Morton and D. Nummedal, eds., Shelf Sedimentation, Shelf Sequence and Related Hydrocarbon Accumulation: Gulf Coast Section, Society of Economic Paleontologists and Mineralogists Proceedings, 7th Annual Research Conference, p. 15-39.

Reproduced with permission of the copyright owner. Further reproduction prohibited without permission.

O'Byrne, C., and S. Flint, 1995, Sequence, parasequence and intraparasequence architecture of the Grassy Member, Blackhawk Formation, Book Cliffs, Utah. Sequence Stratigraphy of Foreland Basin Deposits: *in* J.C. Van Wagoner and G.T. Bertram, eds., Outcrop and Subsurface Examples from the Cretaceous of North America: American Association of Petroleum Geologists Bulletin, p. 225-255.

Obradovich, J. D., 1988, A different perspective on glauconite as a geochronometer: Paleoceanography, v. 3, p. 757-770.

Obradovich, J. D., 1993, A Cretaceous time scale, *in* W.G.E. Caldwell and E.G. Kauffman, eds., Evolution of the Western Interior Basin. Geological Association of Canada Special Paper 39, p. 379-396.

Obradovich, J. D., and W. A. Cobban, 1975, A time scale for the late Cretaceous of western North America, *in* W.G.E. Caldwell and E.G. Kauffman, eds., Evolution of the Western Interior Basin. Geological Association of Canada Special Paper 39, p. 31-54.

Olsen, P. E., 1986, A 40-million year lake record of early Mesozoic orbital climatic forcing: Science, v. 234, p. 842-848.

Parrish, J. T. and R. L. Curtis, 1982, Atmospheric circulation, upwelling, and organic-rich rocks in the Mesozoic and Cenozoic Eras: Palaeogeography, Palaeoceanography, Palaeoecology, v. 40, p. 31-66.

Parrish, J. T. and R. A. Spicer, 1988, Middle Cretaceous wood from the Nanushuk Group, central North Slope, Alaska: Paleontology, v. 31, p. 19-34.

Parrish, J. T., 1993, Climate of the Supercontinent Pangea: Journal of Geology, v. 101, p. 215-233.

Peach, B. N., 1988, Some of the relations of paleontology to geology illustrated chiefly by examples from the Scottish rocks: Proc. Roy. Phys. Soc Edinburghv 9, p 1-24.

Peper, T., F. Beekman, and S. Cloetingh, 1992, Consequences of thrusting and intraplate stress for vertical motions in foreland basins and peripheral areas: Geophysical Journal International, v. 11, p. 104-126.

Reproduced with permission of the copyright owner. Further reproduction prohibited without permission.

Pitman, W. C., 1978, The relationship between eustasy and stratigraphic sequences on continental margins: Geological Society of America Bulletin, v. 89, p. 1839-1843.

Plint, A. G., 1996, Marine and nonmarine systems tract in fourth-order sequences in the Early-Middle Cenomanian, Dunvegan Alloformation, northeastern British Columbia, Canada, *in* J. A. Howell and J. F. Aitken, eds.,, High resolution Sequence Stratigraphy: Innovations and Applications: Geological Society Special Publication No. 104, 159-191.

Press, W. H., W. T. Vetterling, S. A. Teukolsky, and B. P. Flannery, 1992, Numerical recipes in Fortran 77, Press Syndicate of the University of Cambridge, p. 933.

Quade, J., T. E. Cerling, and J. R. Bowman, 1989, Development of Asian monsoon revealed by marked ecological shift during the latest Miocene in northern Pakistan: Nature, v. 342, p. 163-166.

Reinhardt, L. and W. Ricken, 2000, The stratigraphic and geochemical record of playa cycles: monitoring a Pangaean monsoon-like system (Triassic, Middle Keuper, S. Germany): Palaeogeography, Palaeoclimatology, Palaeoecology, v. 161, p. 205-227.

Ricken, W., 1996, Bedding rhythms and cyclic sequences as documented in organic carbon-carbonate patters, Upper Cretaceous, Western Interior, U.S: Sedimentary Geology, v. 102, p. 131-154.

Ruddiman, W. F., 2001, Earth's Climate Past and Present: W. H. Freeman Company, p. 465.

Ryan, W. B. F. and M. B. Cita, 1976, Ignorance concerning episodes of oceanwide stagnation: Marine Geology, v. 23, p. 197-215.

Ryer, T. A., 1993, Speculations on the origins of Mid-Cretaceous clastic wedges, Central Rocky Mountain Region, United States, *in* W.G.E. Caldwell and E.G. Kauffman, eds., Evolution of the Western Interior Basin. Geological Association of Canada Special Paper 39, p. 189-198.

Sageman, B. B., J. Rich, M. A. Arthur, G. E. Birchfield, and W. E. Dean, 1997, Evidence for Milankovitch periodicities in Cenomanian-Turonian lithologic and geochemical cycles, Western Interior, U.S.A.: Journal of Sedimentary Research, v. 67, no. 2, p. 286-302.

Reproduced with permission of the copyright owner. Further reproduction prohibited without permission.

Schwans, P., 1995, Controls on sequence stacking and fluvial to shallow marine architecture in a foreland basin *in* J. C. Van Wagoner and G. T. Bertram, eds., Outcrop and Subsurface Examples from the Cretaceous of North America: American Association of Petroleum Geologists Bulletin, p. 55-102.

Schwarzacher, W., 1964, Searching for long cycles in short sections: Mathmatical Geology, v. 26, no. 7, p. 759-768.

Sherman, B., 1950, A random variable related to the spacing of sample values: The Annals of Mathmatical Statistics, v. 21, p. 339-361.

Sherman, B., 1957, Percentiles of the Omega Statistic: The Annals of Mathematical Statistics, v. 28, p. 259-261.

Slingerland, R., L. R. Kump, M. A. Arthur, P. J. Fawcett, B. B. Sageman, and E. J. Barron, 1996, Estuarine circulation in the Turonian-Western Interior seaway of North America: Geological Society of America Bulletin, v. 108, p. 941-952.

Sloss, L. L., 1962, Stratigraphical models in exploration: Journal of Sedimentary Petrology, v. 32, p. 415-422.

Sloss, L. L., 1963, Sequences in the cratonic interior of North America: Geological Society of America Bulletin, v. 74, p. 93-114.

Storms, J. E. A.,and D. J. P. Swift, 2003, Architecture of Shallow marine sequences: insights from Numerical Modeling. Basin Research.

Swift, D. J. P. and B. S. Parsons, 1999, Shannon sandstone of the Powder River Basin: orthodoxy and revisionism in stratigraphic thought, *in* K. Bergman and J. Snedden, eds., Isolated Shallow Marine Sandbodies: Sequence Stratigraphic Analysis and Sedimentological Interpretation: SEPM Special Publication 64, p. 55-84.

Swift, D. J. P., S. Phillips, and J. A. Thorne, 1991, Sedimentation on continental margins, *in* D. J. P. Swift, R. W.Tillman and G. O. Oertel, eds., Shelf sand and sandstone types: Geometry, facies and distribution: Int. Assoc. Sedimentologists Special Paper 14, p. 62-152.

Reproduced with permission of the copyright owner. Further reproduction prohibited without permission.

Swift, D. J. P., B. S. Parsons, A. Foyle, and G. F. Oertel, 2003, Between beds and sequences: stratigraphic organization at intermediate scales in the Quaternary of the Virginia coast, U.S.A.: Sedimentology, v. 50, p. 81-112.

Thorne, J. A., 1988, Modeling storm bed genesis: oceanography or geology-which one holds the key? SEPM program workshop on quantitative dynamic stractigraphy, Deckers, Colorado, p. 12.

Thorne, J. A., E. Grace, D. J. P.Swift, and A. W. Niedoroda, 1991, Sedimentation on continental shelves, part III. The depositional fabric: an analytical approach to stratification and facies. In press *in* D. J. P. Swift, R. W. Tillman and G. O. Oertel, eds., Shelf sand and sandstone types: Geometry, facies and distribution: Int. Assoc. Sedimentologists Special Paper 14.

Tuenter, E., S. L. Weber, F. J. Hilgen, and L. J. Lourens, 2003, The response of the African summer monsoon to remote and local forcing due to precession and obliquity: Global and Planetary Change, v. 36, p. 219-235.

Ulrych, T. J., and T. N. Bishop, 1975, Maximum entropy spectral analysis and autoregressive recomposition: Geophysics and Space Physics, v. 13, p. 183-200.

Vail, P. R., R. M. Mitchum, and S. Thompson III, 1977, Seismic stratigraphy and global changes of sea level, part 3: relative changes of sea level from coastal onlap, *in* C.W. Payton, ed., Seismic stratigraphy application to hydrocarbon exploration: AAPG Memoir 26, p. 63-97.

Van Wagoner, J. C., H. Posamentier, R. M. Mitchum Jr., P. R.Vail, J. F. Sarg, T. S. Loutit, and J. Hardenbol, 1988, An overview of the fundamentals of sequence stratigraphy and Key definitions of sequence stratigraphy, p. 39-47, *in* C. K.Wilgus, B. S. Hastings, C. G. St. C. Kendall, H. W. Posamentier, C. A. Ross, and J.C. Van Wagoner, eds., Sea-level Changes: An Integrated Approach: Tulsa, Soc. Econ. Palon. Mineral. Spec. Publ. 42., p. 407.

Van Wagoner, J.C., R. M. Mitchum, K. M. Campion, and V. D. Rahmanian, 1990, Siliciclastic sequence stratigraphy in well logs, cores, and outcrops: AAPG Methods in Exploration Series, No. 7.

Reproduced with permission of the copyright owner. Further reproduction prohibited without permission.

Wang, B, S. C. Clemens, and P. Liu, 2003, Contrasting the Indian and East Asian monsoons: implications on geologic timescales: Marine Geology, v. 210, p. 5021.

Wilde, P., and W. B. N. Berry, 1982, Progressive ventilation of the oceans – Potential for return to anoxic conditions in the post-Paleozoic, *in* S. O. Schlanger and M. B. Cita, eds, Nature and Origin of Cretaceous Carbon-rich Facies, p. 209-224.

Williams, G. D., and C. R. Stelk, 1975, Speculations on the Cretaceous paleogeography of North America, *in* W. G. E. Caldwell, ed., The Cretaceous System in the Western Interior of North America: Geological Association of Canada Special Paper 13, p. 1-20.

Wiltschko, D. V., and J. A. Dorr Jr., 1983, Timing of deformation in overthrust belt and foreland of Idaho, Wyoming and Utah: American Association of Petroleum Geologists Bulletin, v. 67, p. 1304-1322.

Wheatcroft, R. A., and D. E. Drake, 2003, Post-depositional alteration and preservation of sedimentary event layers on continental margins: The role of episodic sedimentation: Marine Geology, v. 199, p. 123-137.

Yoshida, S., A. Willis, and A. D. Miall, 1996, Tectonic Control of Nested Sequence Architecture in the Castlegate Sandstone (Upper Cretaceous), Book Cliffs, Utah: Journal of Sedimentary Research, v. 66, p. 737-748.

Zhang, Y., D. J. P. Swift, A. W. Niedoroda, C. W. Reid, and J. A. Thorne, 1997, Simulation of sedimentary facies on the Northern California Shelf: implications for an analytical theory of facies differentiation: Geology, v. 27, p. 635-638.

Reproduced with permission of the copyright owner. Further reproduction prohibited without permission.

APPENDIX A

MEASURED SECTIONS

Reproduced with permission of the copyright owner. Further reproduction prohibited without permission.

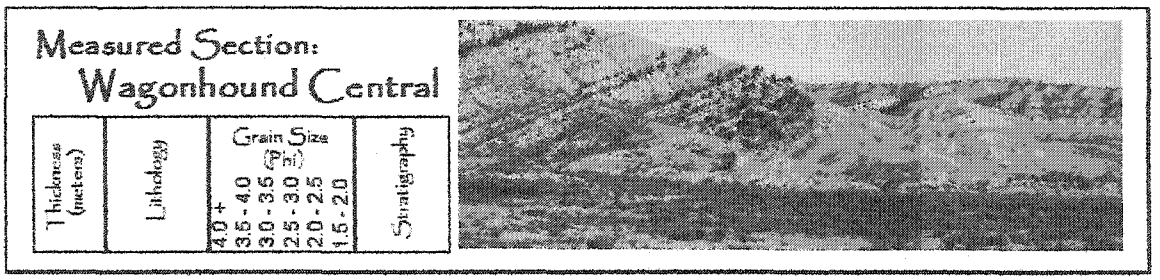

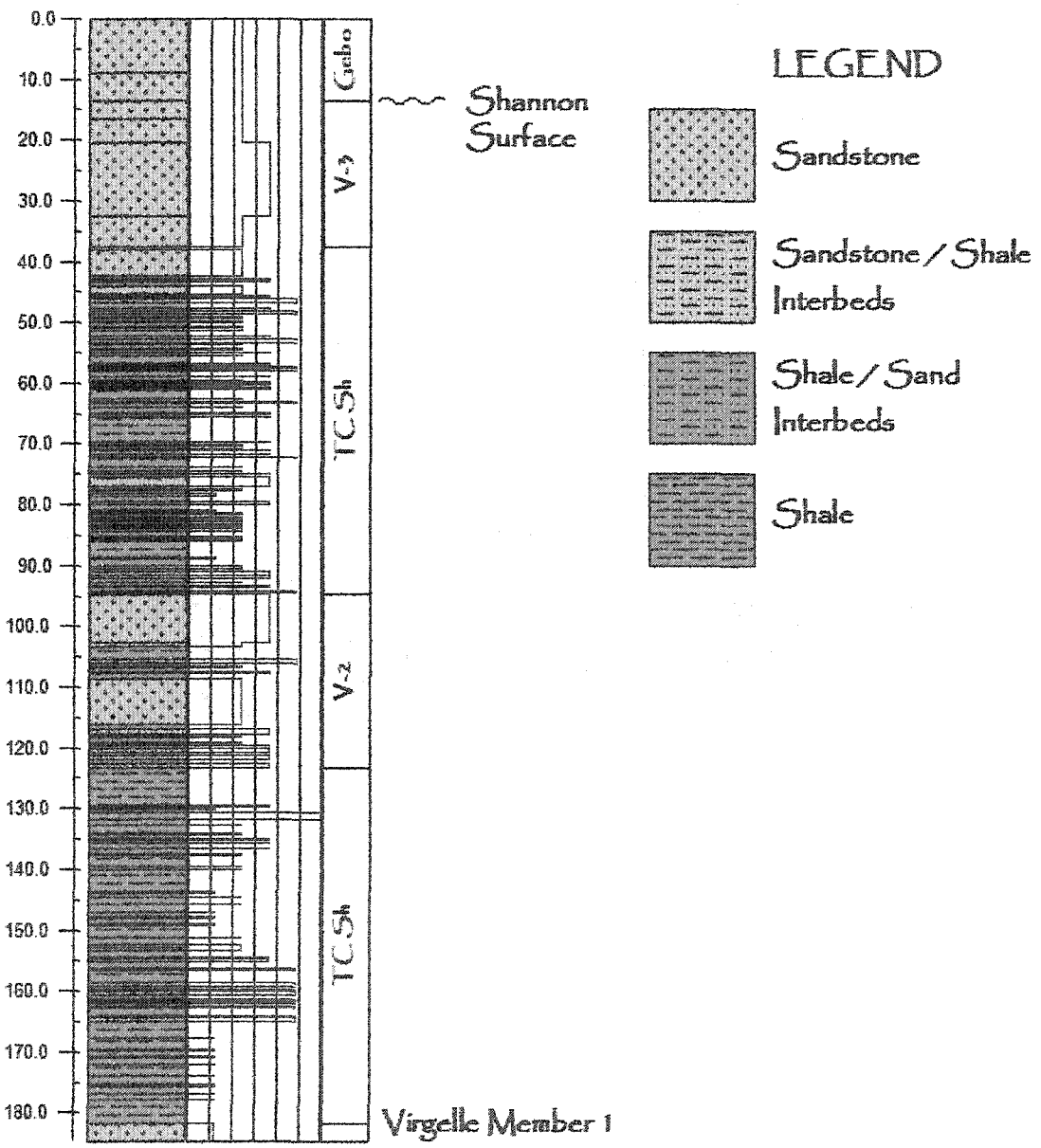

Reproduced with permission of the copyright owner. Further reproduction prohibited without permission.

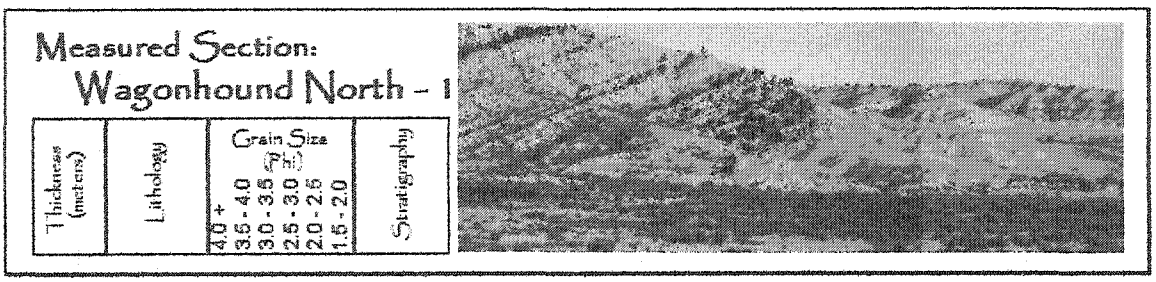

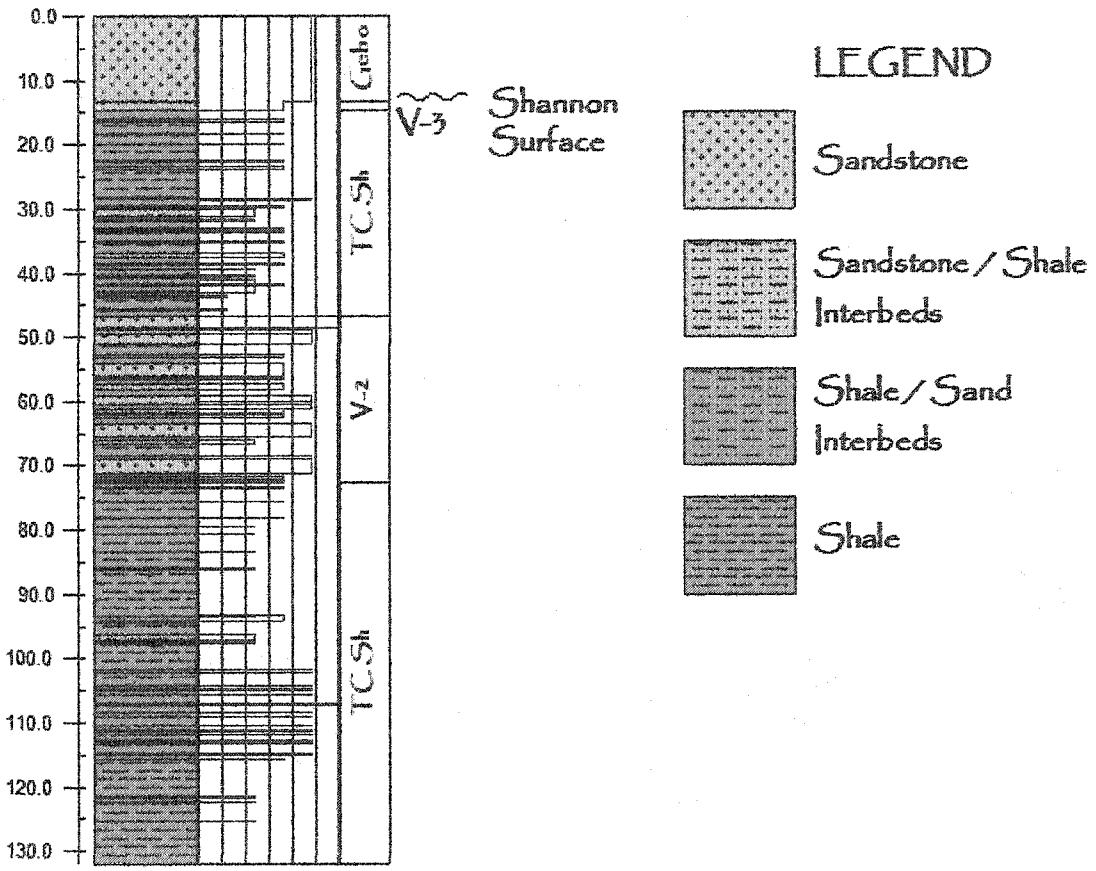

Reproduced with permission of the copyright owner. Further reproduction prohibited without permission.

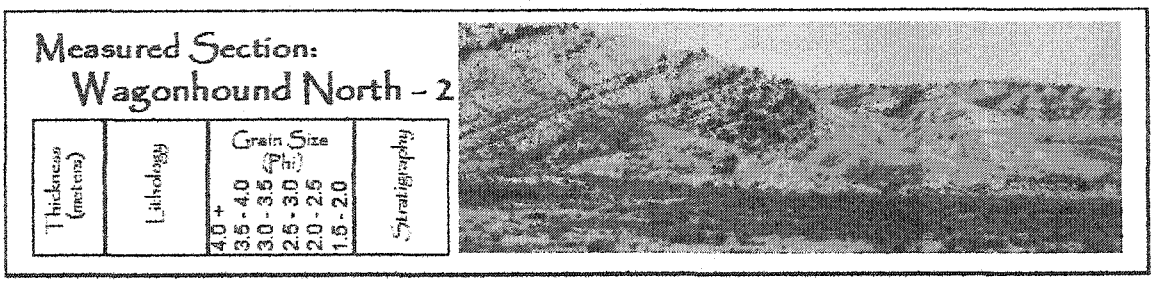

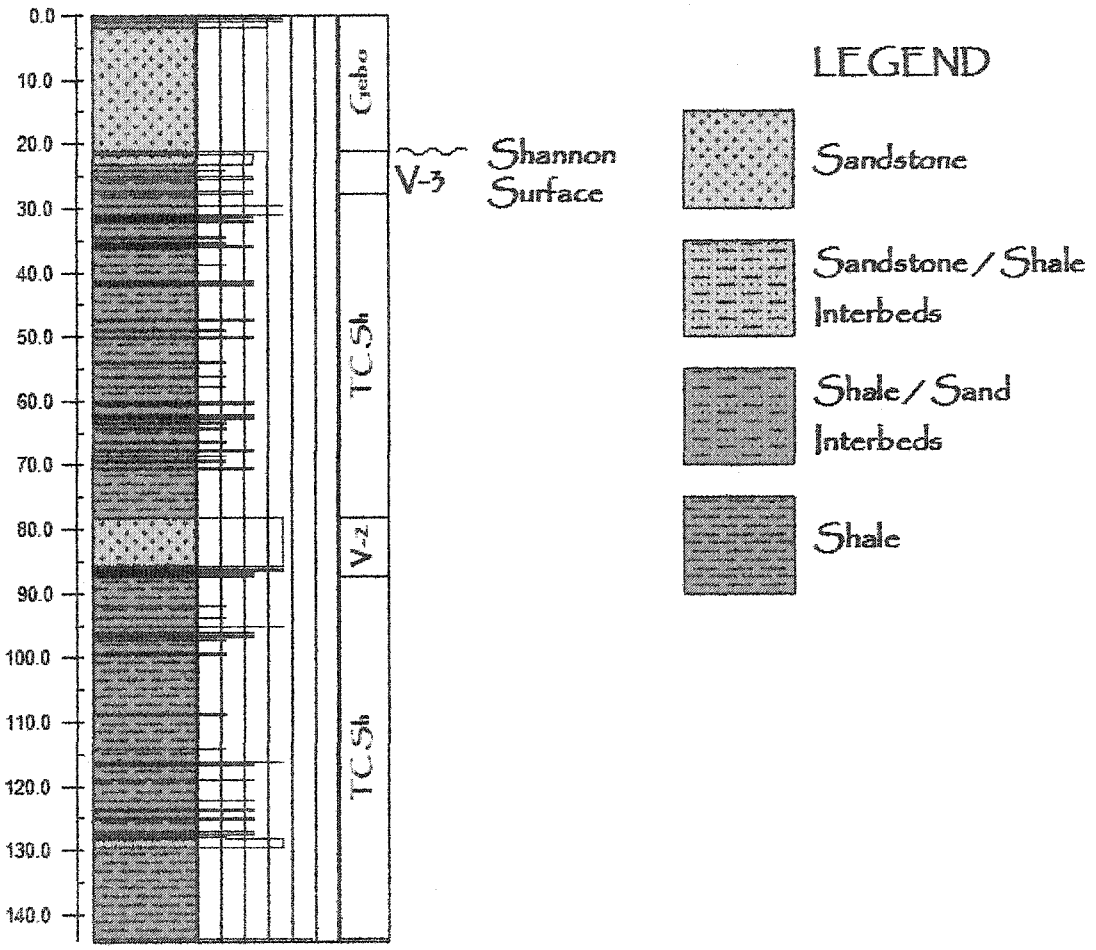

Reproduced with permission of the copyright owner. Further reproduction prohibited without permission.

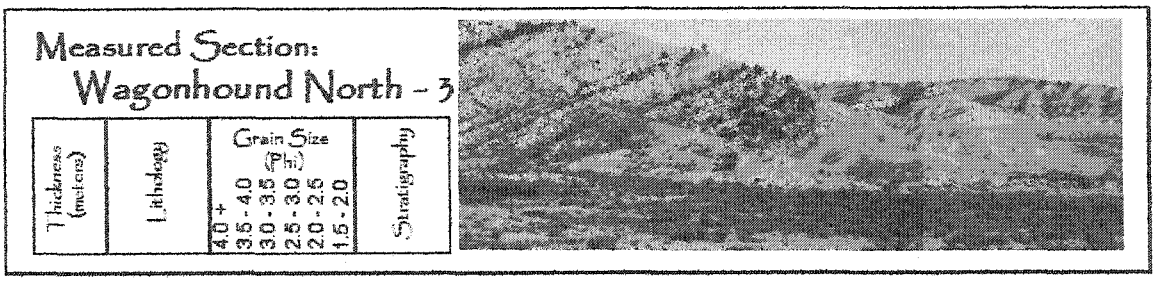

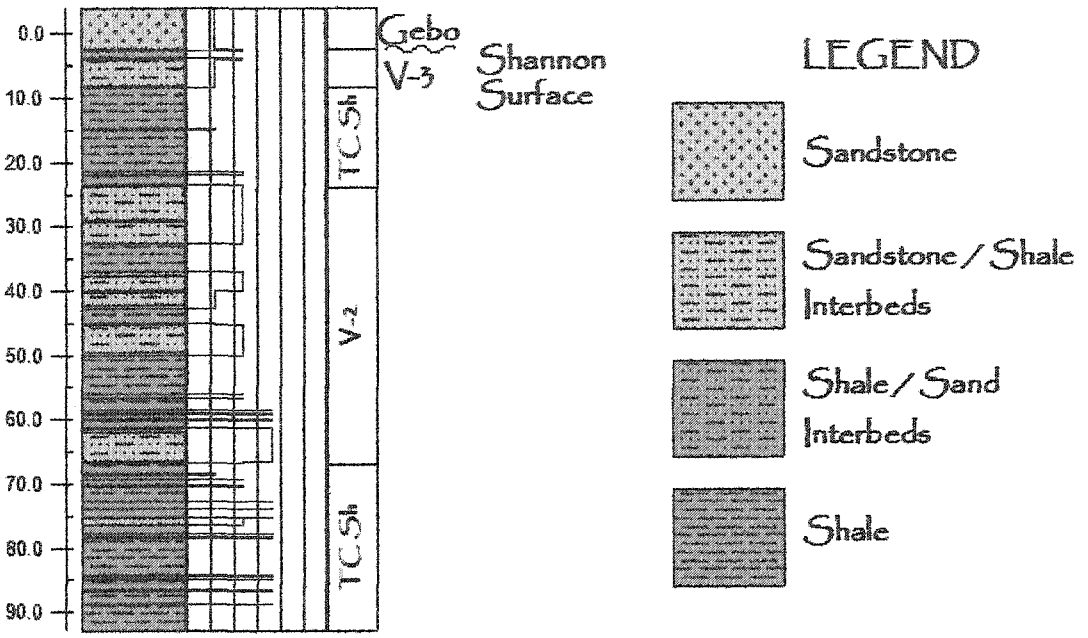

Reproduced with permission of the copyright owner. Further reproduction prohibited without permission.

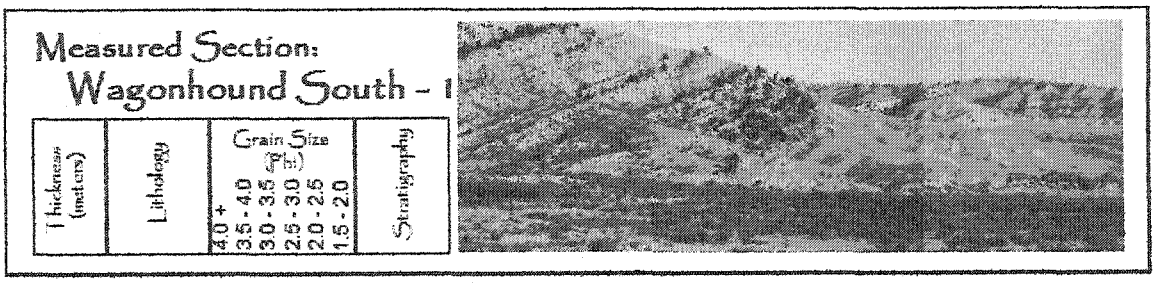

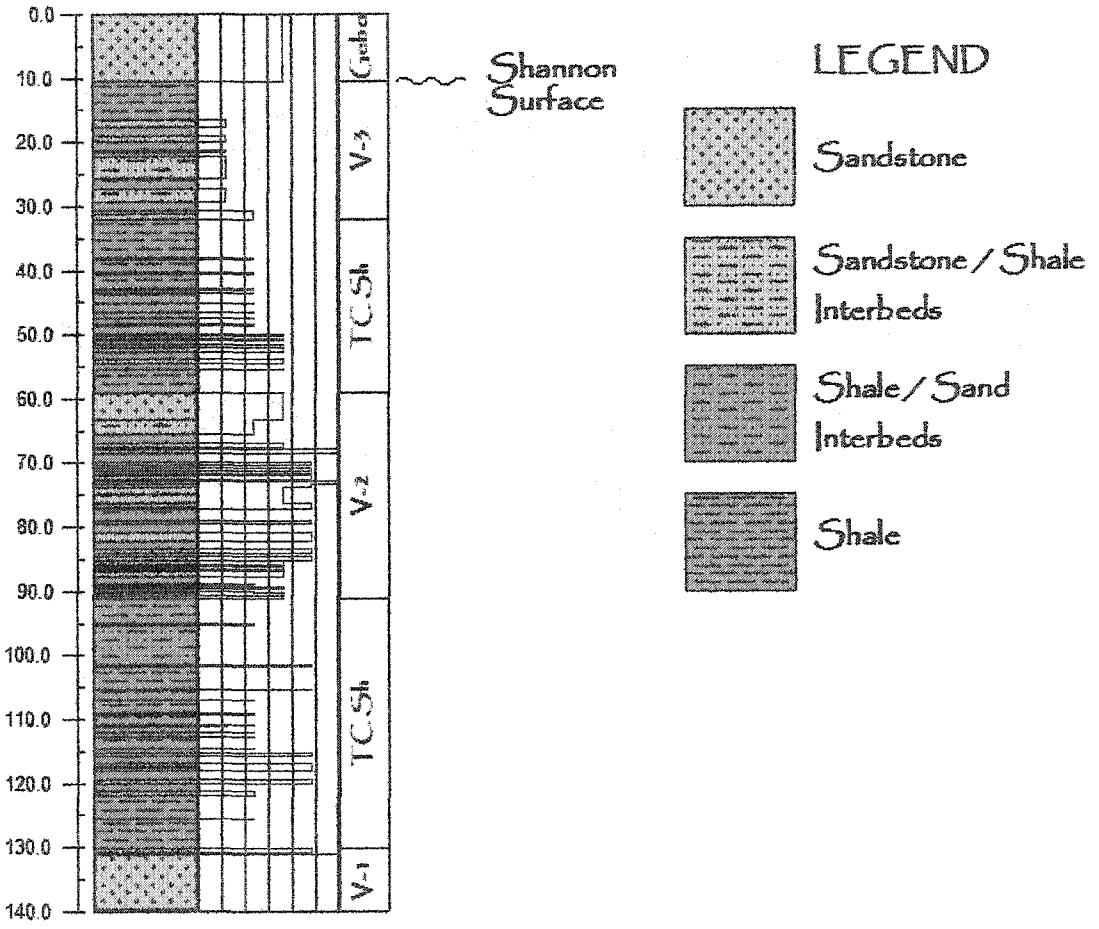

Reproduced with permission of the copyright owner. Further reproduction prohibited without permission.

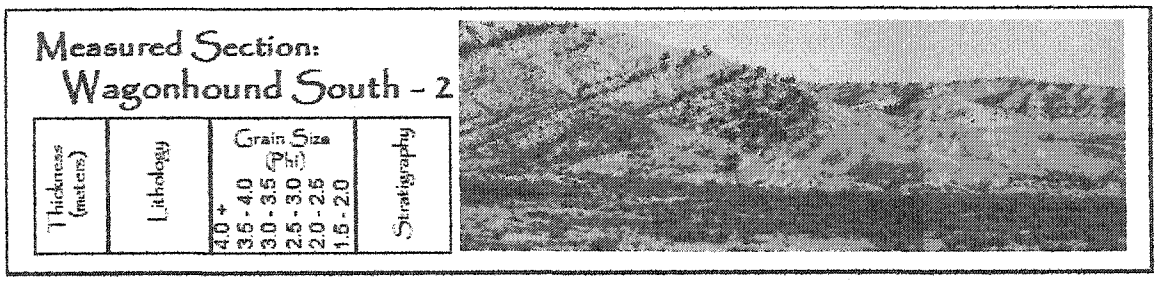

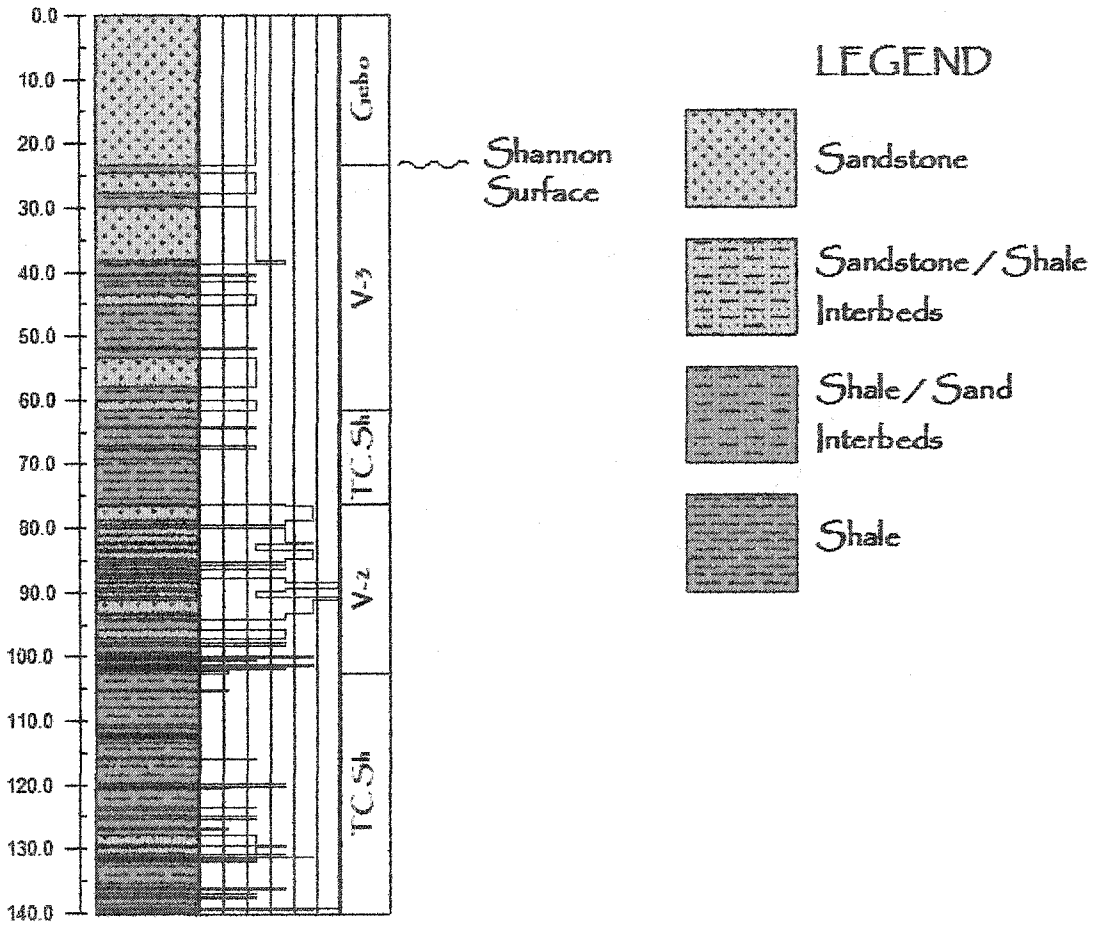

Reproduced with permission of the copyright owner. Further reproduction prohibited without permission.

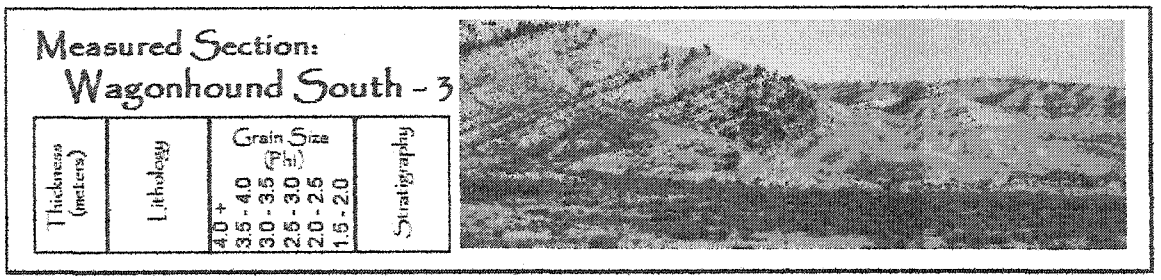

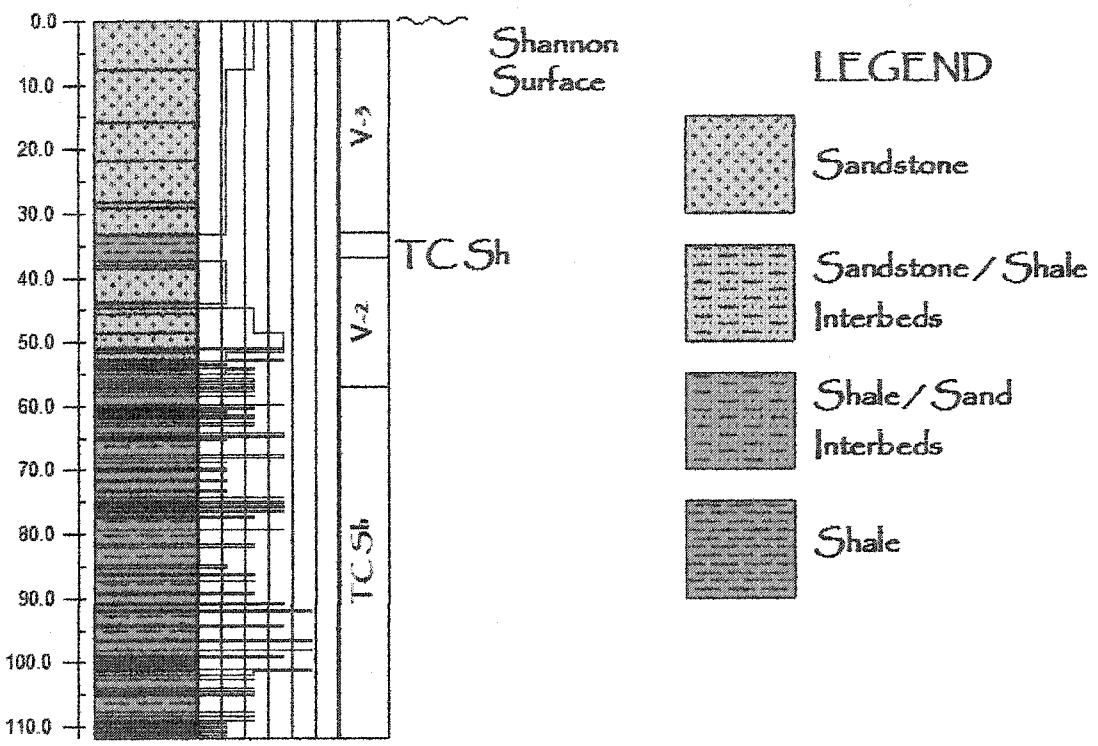

Reproduced with permission of the copyright owner. Further reproduction prohibited without permission.

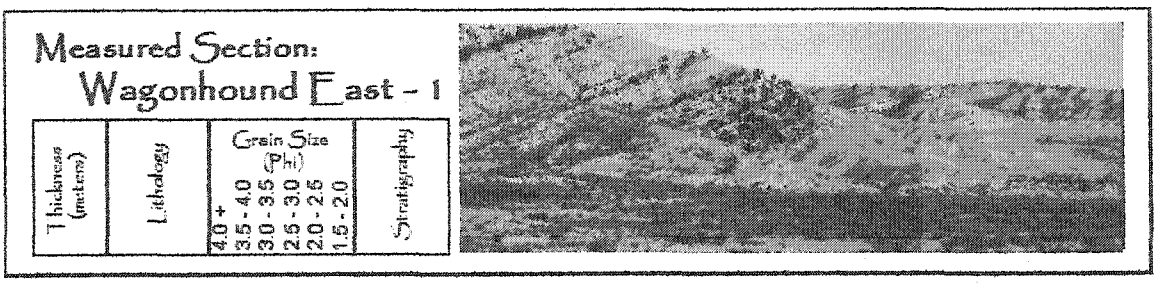

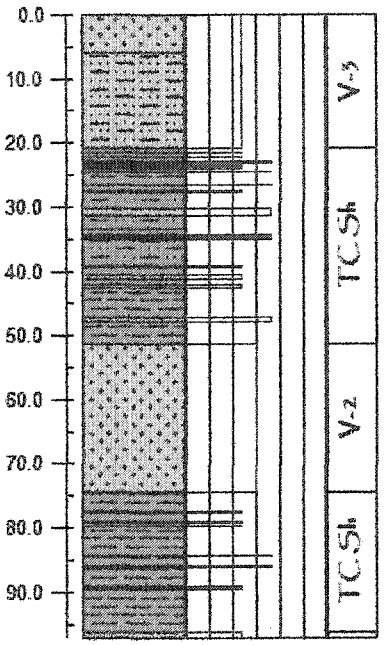

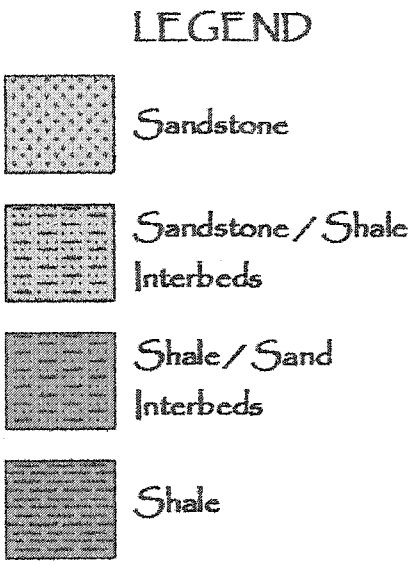

Reproduced with permission of the copyright owner. Further reproduction prohibited without permission.

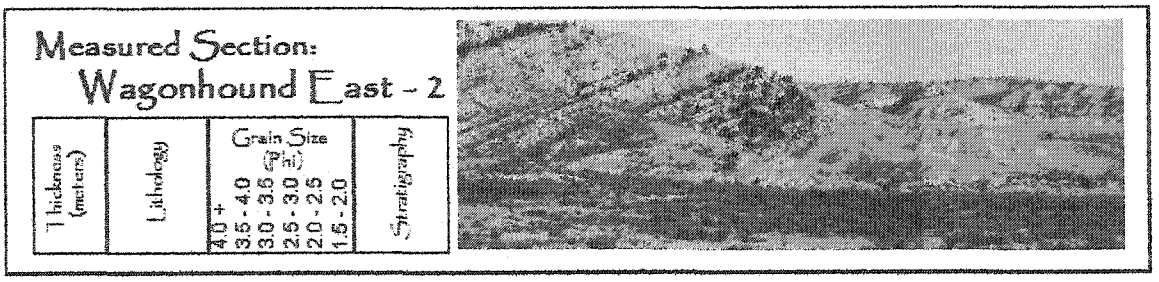

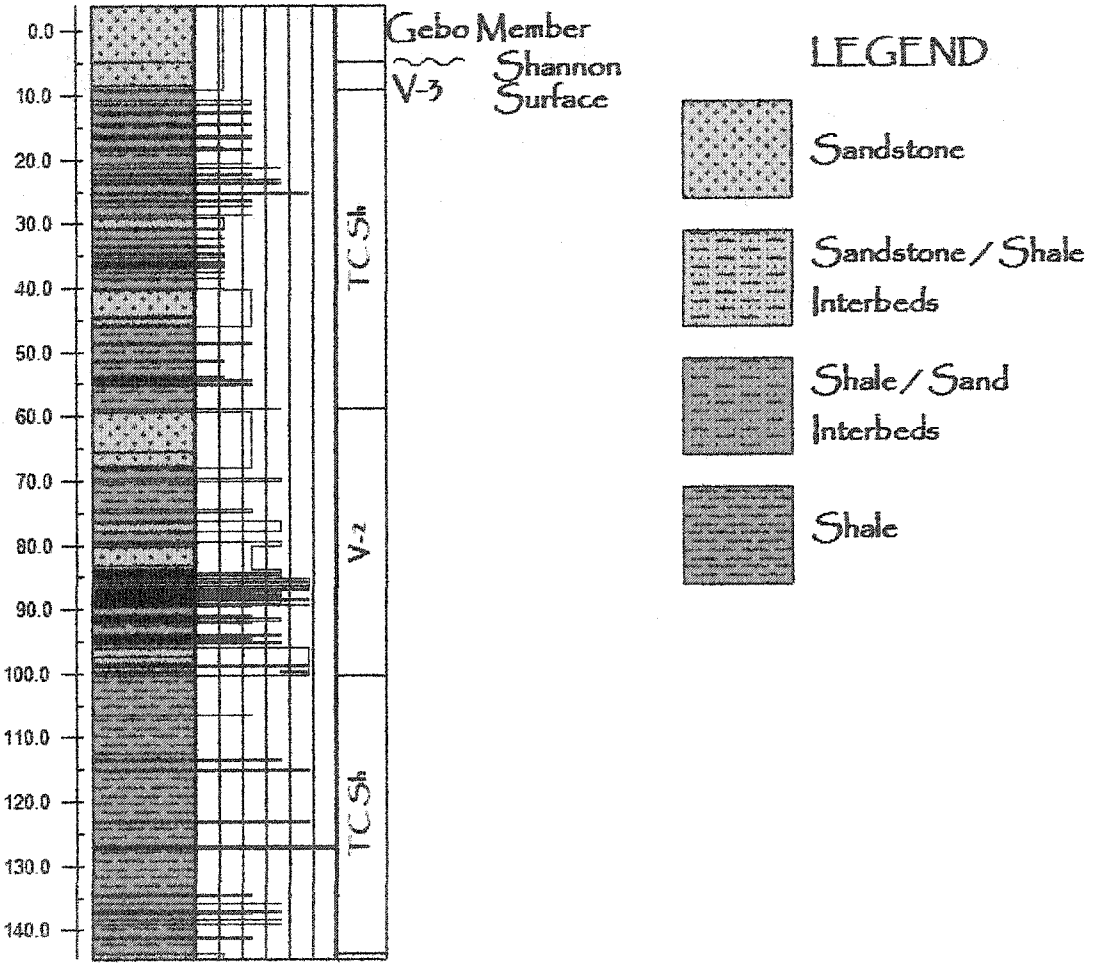

Reproduced with permission of the copyright owner. Further reproduction prohibited without permission.

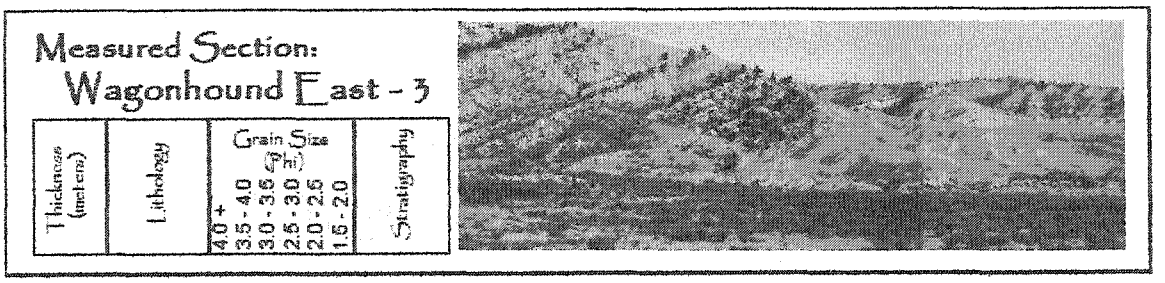

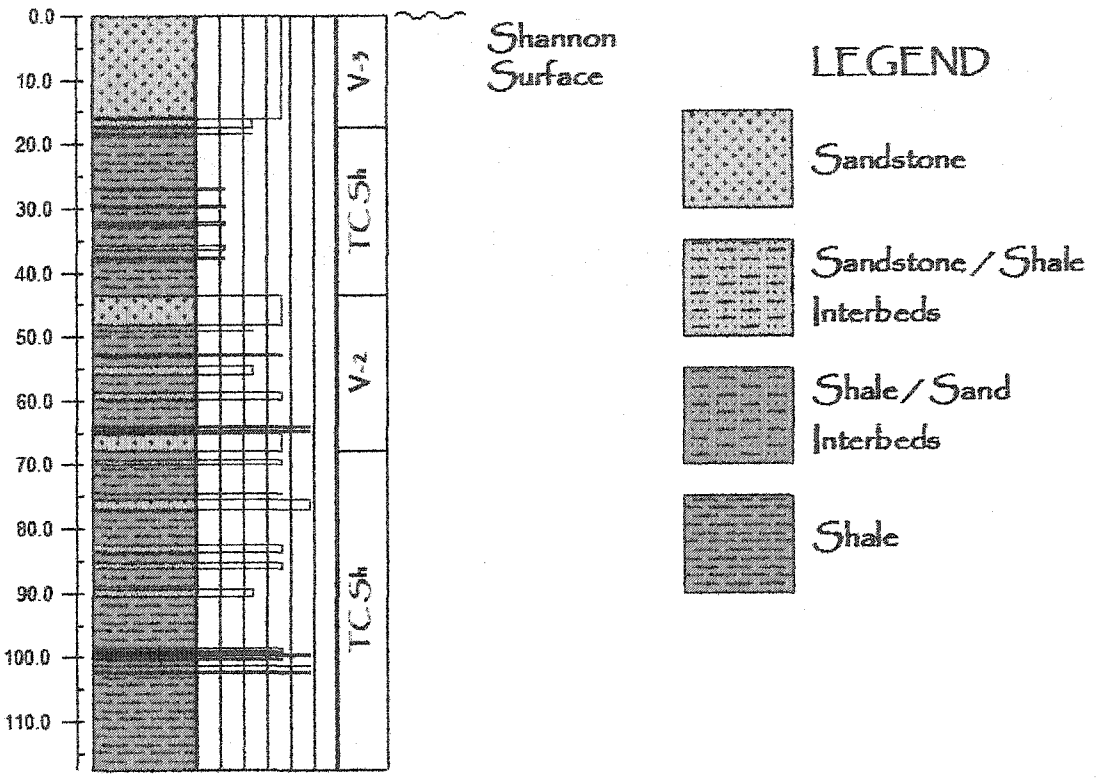

Reproduced with permission of the copyright owner. Further reproduction prohibited without permission.

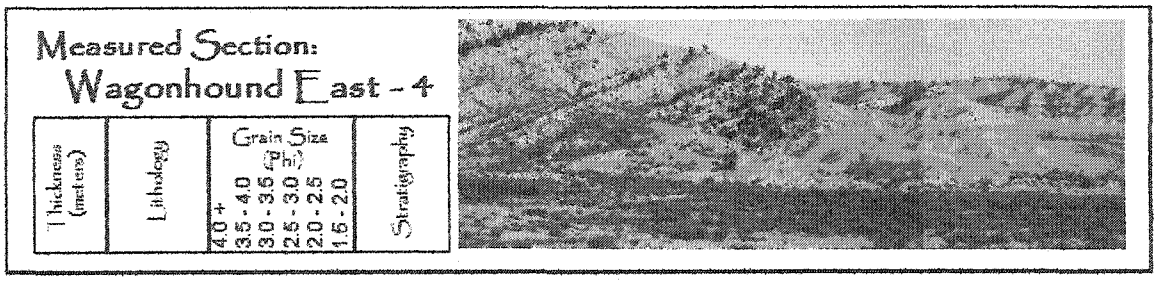

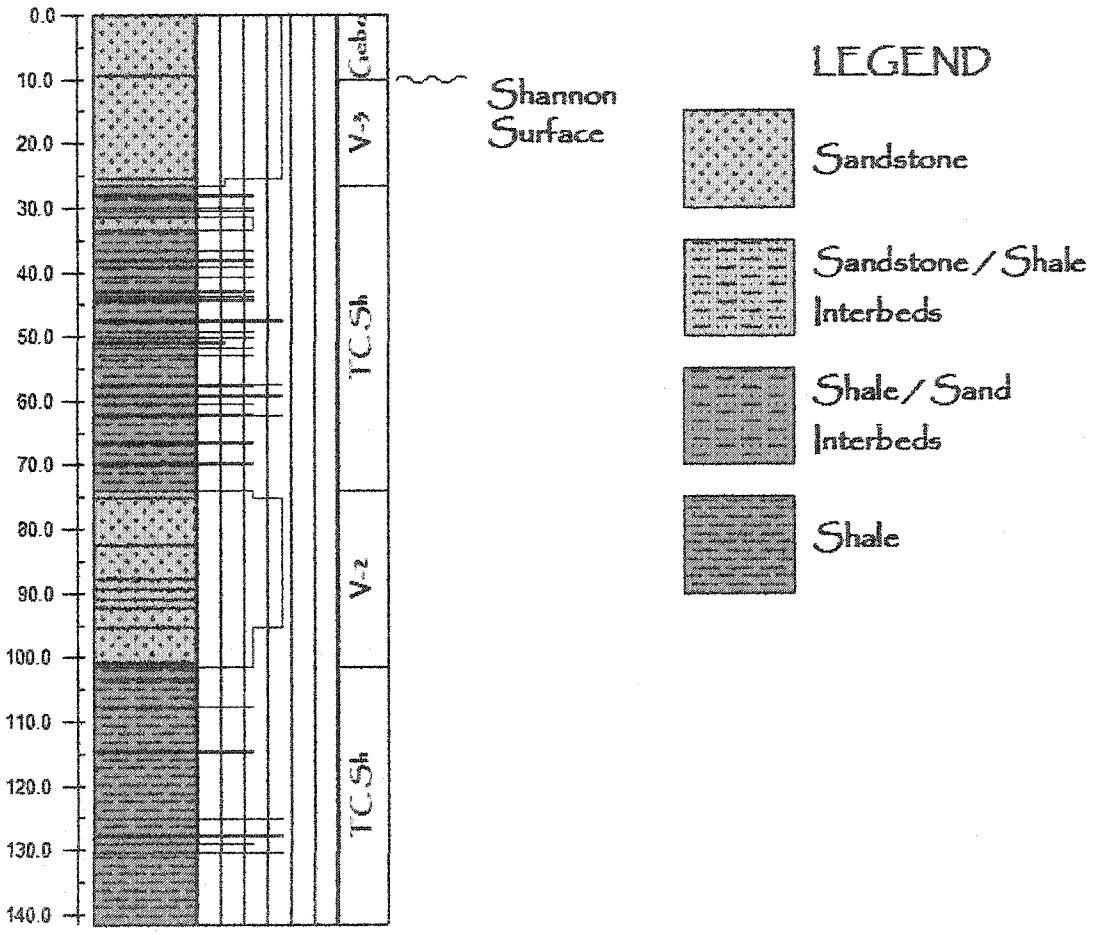

Reproduced with permission of the copyright owner. Further reproduction prohibited without permission.

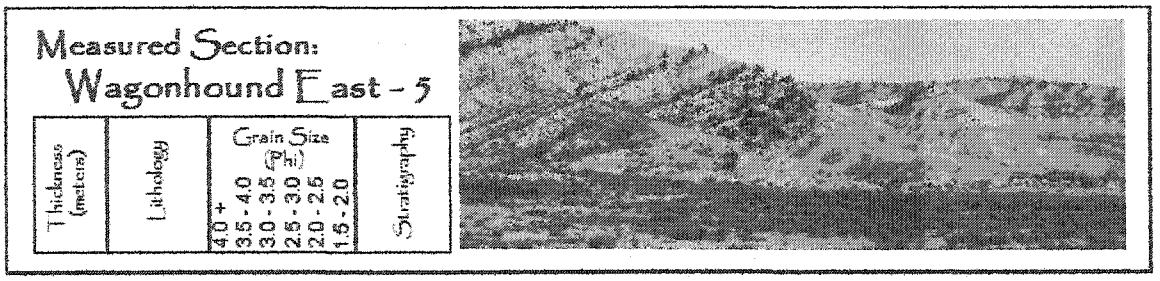

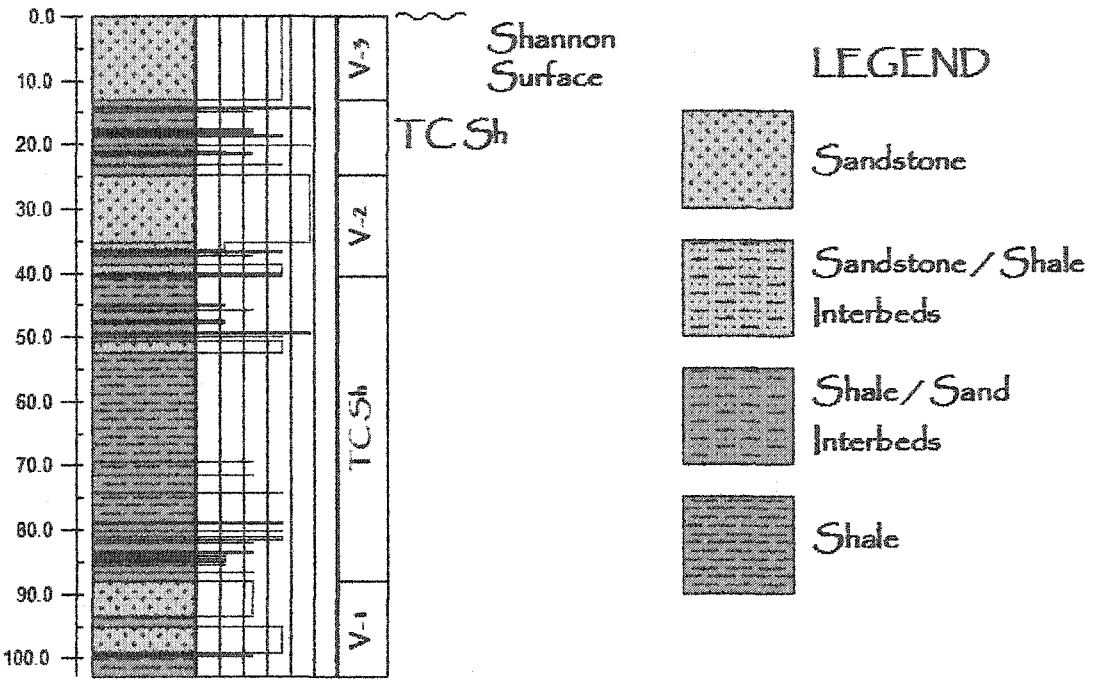

Reproduced with permission of the copyright owner. Further reproduction prohibited without permission.

Measured Section: Wagonhound East - 6

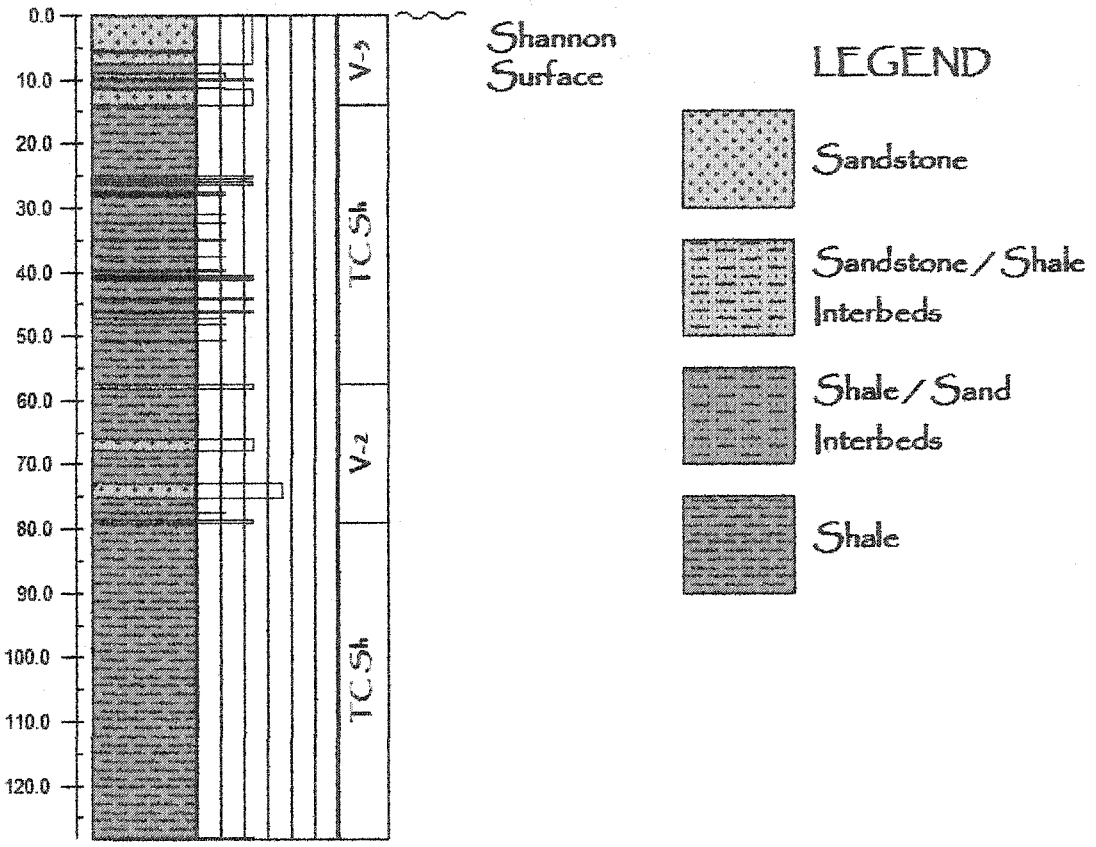

Reproduced with permission of the copyright owner. Further reproduction prohibited without permission.

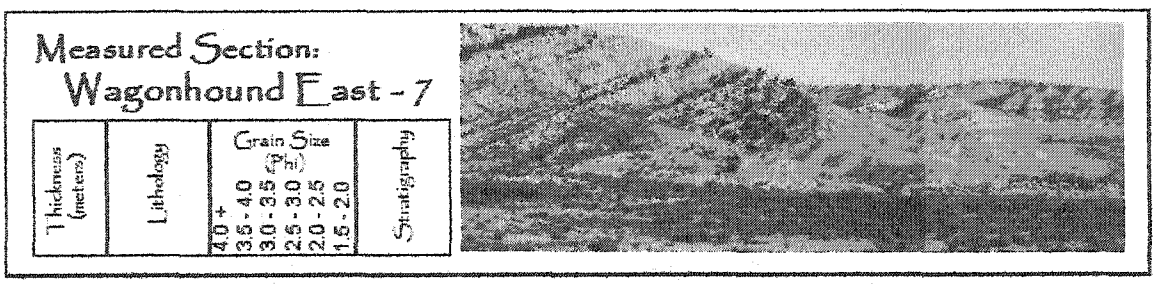

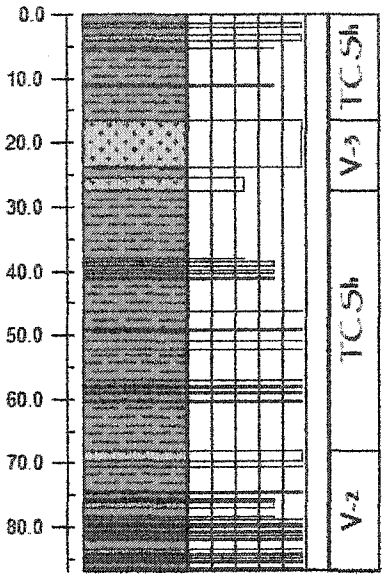

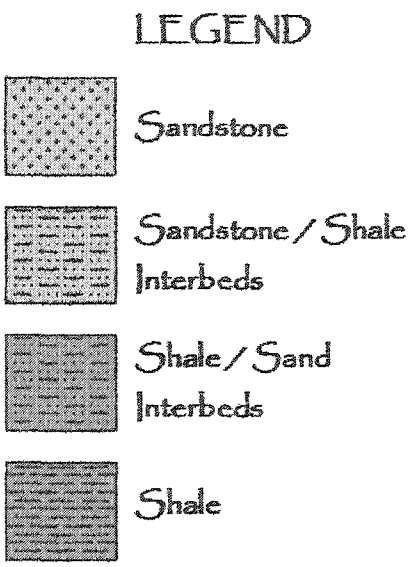

Reproduced with permission of the copyright owner. Further reproduction prohibited without permission.

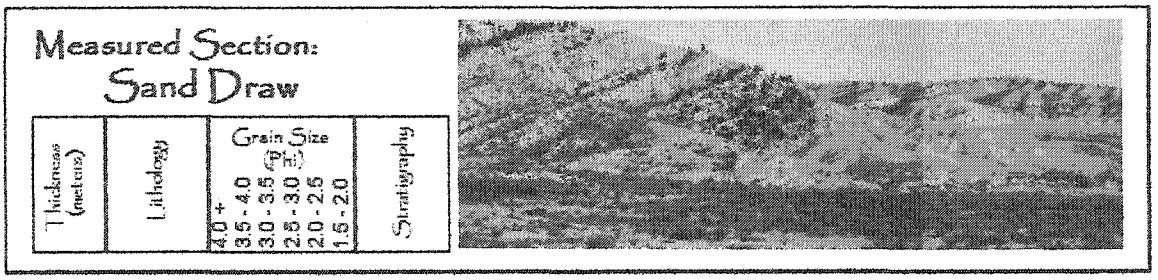

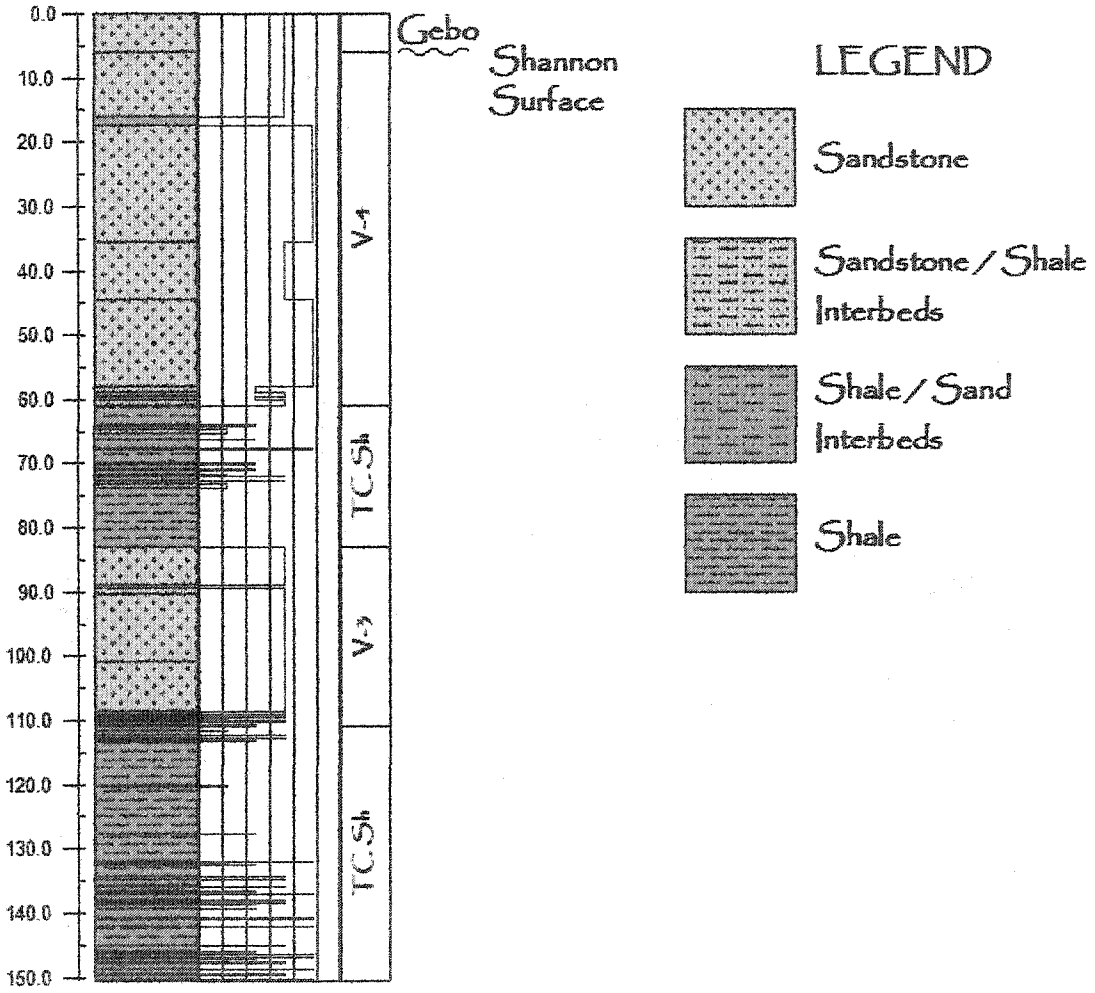

Reproduced with permission of the copyright owner. Further reproduction prohibited without permission.

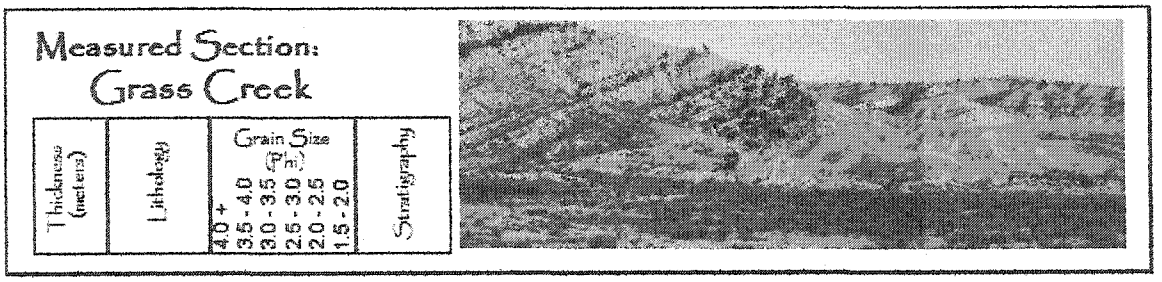

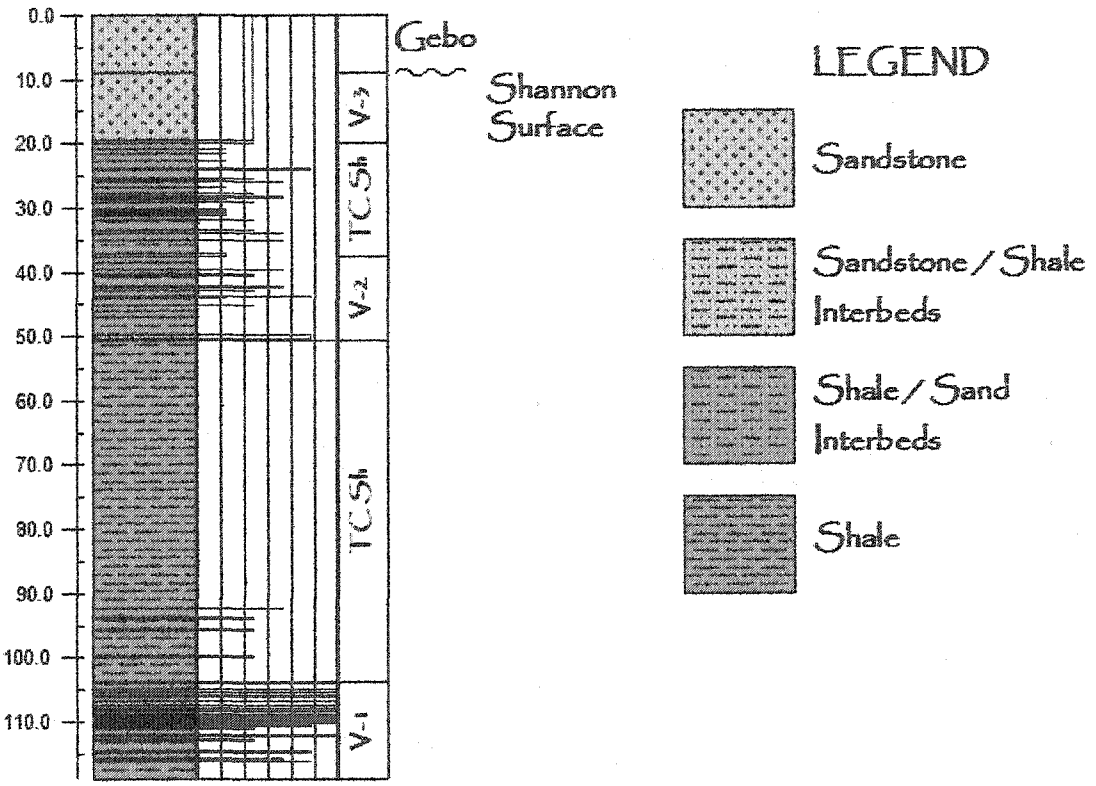

Reproduced with permission of the copyright owner. Further reproduction prohibited without permission.

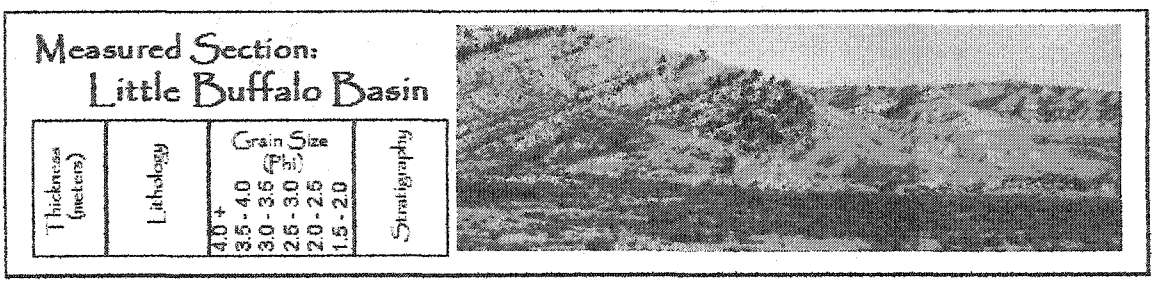

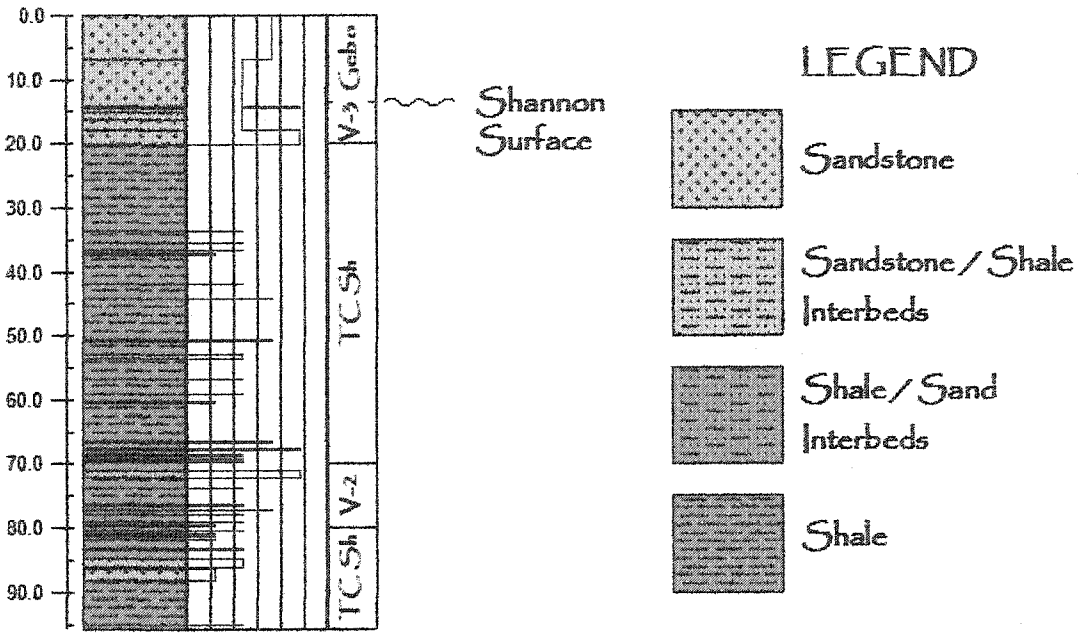

Reproduced with permission of the copyright owner. Further reproduction prohibited without permission.

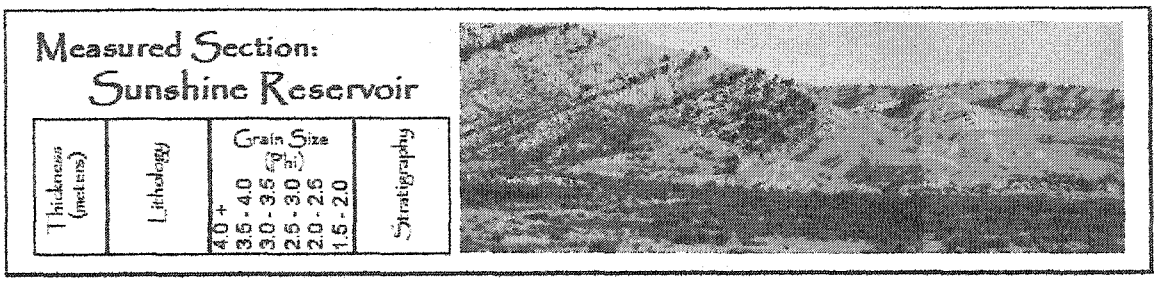

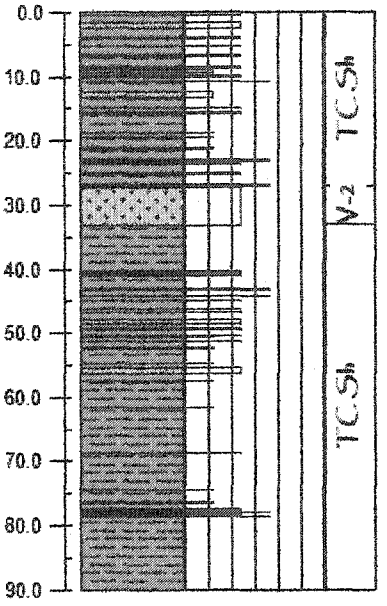

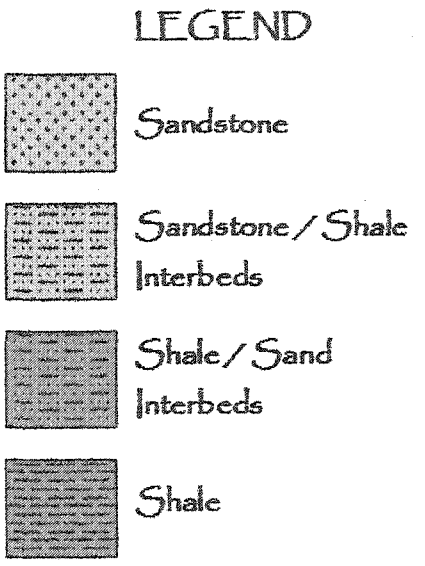

Reproduced with permission of the copyright owner. Further reproduction prohibited without permission.

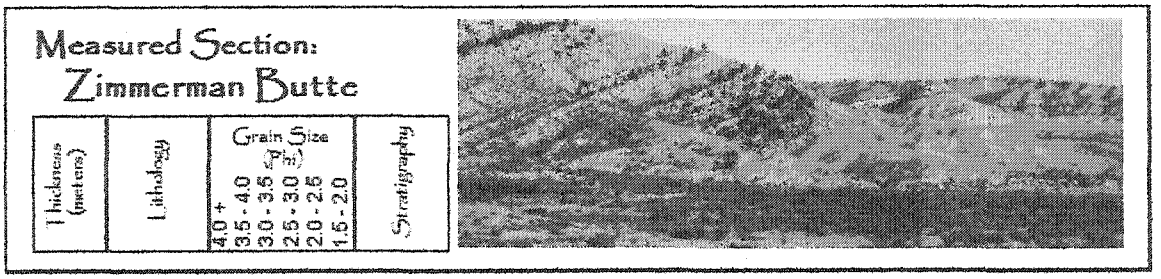

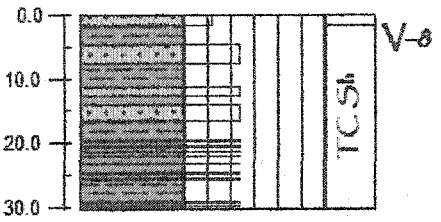

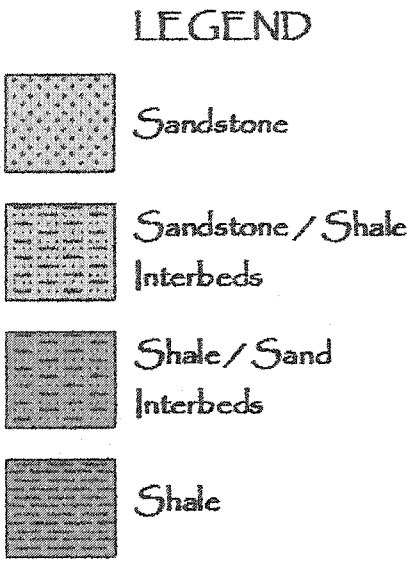

Reproduced with permission of the copyright owner. Further reproduction prohibited without permission.

APPENDIX B

PROCEDURES FOR GRAIN SIZE ANALYSIS

Reproduced with permission of the copyright owner. Further reproduction prohibited without permission.

Procedure for Grain Size Analysis

(modified from Folk, 1968)

1. Assign an SDL # (Sediment Dynamics Lab #, unique for each sample).
2. Crush original sample to 1-2cm pieces.
3. In a 1000-1400ml beaker, place crushed sample + 10grams Sodium sulfite + D.I. water. Fill with D.I. water to approximately 300-400ml.
4. Let sample sit for at least 48-72 hours.
5. Boil sample for 3 hours.
6. A: If sample has broken down enough, take off hotplate and let cool.
   B: If sample has NOT broken down, this becomes a "problem child" and must continue to boil until enough material has broken down.
7. Flush sample 3 times (more if water does not become clear after 3 flushes). Do this by decanting off water in container with syringe then filling container about halfway with D.I. water, mixing thoroughly and letting sit for 24 hours. Repeat two more times.
8. After the third flush, fill with D.I. water again and boil for one hour.
9. Wet sieve sample through the zero phi sieve. This separates the broken down material from the un-broken down material. Place un-broken material is placed back in original sample bag.
10. Let sample settle, decant, and place entire sample (more if necessary) into a 250ml beaker.
11. If the amount of material in the beaker exceeds 100 ml, then use a 400ml beaker.
12. Sonify for 4min.
13. Weigh a larger beaker (labeled SDL# <63) and a smaller beaker (labeled SDL# >63).
14. After sonifying, immediately wet sieve through the 125micron/63micron sieve stack. What falls through the 63micron sieve will be collected in the SDL# <63 beaker. What remains on the 125 & 63micron sieves will be placed in the SDL# >63micron beaker. Place both beakers in the oven to dry.
15. After material in both beakers (from step #14) are dry AND cool, weigh again and place on data sheet.
16. The material in the SDL# >63 beaker will be run through the dry sieve stack and all data placed on the data sheet.
17. The material that is collected in the pan (at the bottom of the sieve stack) will be placed in a triangle container and labeled SDL# PAN.
18. The material in the SDL# <63 beaker will be crushed gently with the mortar and pestle and placed in a triangle container and labeled SDL# <63.
19. The material from steps 17 & 18 will be combined together in the triangle container that is labeled SDL# PAN.
20. The PAN sample will then be run through the particle counter.
21. Combine SDL# >63 and particle counter data in excel spreadsheet and calculate the mean to be used for statistical analysis.

Reproduced with permission of the copyright owner. Further reproduction prohibited without permission.

APPENDIX C

RAW DATA (GRAIN SIZE, SAND, SILT, AND CLAY FRACTIONS)

Reproduced with permission of the copyright owner. Further reproduction prohibited without permission.

Wagonhound Central

length (m)	"tuned" time (yrs)	grain size (phi)	sand fraction	silt fraction	clay fraction
57.0	0	6.29	3.86	88.79	7.35
56.5	789	6.11	2.28	96.44	1.28
56.0	1578	6.33	1.92	93.11	4.96
55.5	2367	6.19	1.21	97.84	0.94
55.0	3156	6.53	1.07	90.04	8.88
54.5	3945	4.03	51.84	45.11	3.05
54.0	4734	5.44	14.59	75.87	9.5
53.5	5523	5.42	10.74	85.34	3.91
53.0	6312	5.70	5.22	85.43	9.31
52.5	7101	5.28	16.48	78.92	4.58
52.0	7890	5.38	11.18	85.77	3.05
51.5	8679	5.63	15.03	80.3	4.66
51.0	9468	5.37	11.37	85.34	3.29
50.5	10257	5.45	12.42	80.54	7.02
50.0	11046	5.29	22.80	73.88	3.31
49.5	11835	5.23	17.62	75.43	6.92
49.0	12624	5.55	5.20	90.96	3.83
48.5	13413	5.33	16.66	78.52	4.81
48.0	14202	5.99	6.16	91.5	2.35
47.5	14991	4.81	32.79	63.23	3.96
47.0	15780	5.38	27.50	68.84	3.66
46.5	16569	5.40	22.28	73.86	3.85
46.0	17358	5.74	0.00	96.28	3.72
45.5	18147	6.04	0.40	93.5	6.1
45.0	18936	5.80	2.42	90.83	6.73
44.5	19725	4.48	41.21	57.85	0.95
44.0	20514	5.44	7.58	91.82	0.59
43.5	21303	5.11	17.96	76.58	5.43
43.0	22092	5.65	10.68	80.7	8.59
42.5	22881	4.42	50.63	47.76	1.6
42.0	23670	4.78	40.05	56.5	3.44
41.5	24459	5.97	0.00	92.43	7.55
41.0	25248	6.14	0.00	97.83	2.17
40.5	26037	5.97	0.00	98.12	1.89
40.0	26826	6.19	4.11	94.41	1.48
39.5	27615	5.59	2.91	95.54	1.55
39.0	28404	5.75	1.05	97.13	1.82
38.5	29193	5.71	4.33	95.32	0.36
38.0	29982	6.26	0.00	94.54	5.45
37.5	30771	5.23	16.45	77.66	5.86
37.0	31560	5.88	3.75	93.5	2.75

Reproduced with permission of the copyright owner. Further reproduction prohibited without permission.

length (m)	"tuned" time (yrs)	grain size (phi)	sand fraction	silt fraction	clay fraction
36.5	32349	5.74	1.61	98.13	0.16
36.0	33138	5.59	1.15	98.01	0.83
35.5	33927	5.57	8.47	91.15	0.38
35.0	34716	5.39	9.04	88.18	2.78
34.5	35505	5.37	7.14	89.85	3
34.0	36294	5.52	9.05	86.98	3.96
33.5	37083	5.47	13.59	83.6	2.8
33.0	37872	5.35	8.95	87.78	3.27
32.5	38661	5.08	27.09	64.66	8.2
32.0	39450	5.10	21.50	68.41	10.09
31.5	40239	5.12	16.50	79.79	3.68
31.0	41028	5.14	16.80	78.01	5.17
30.5	41817	5.21	10.02	87.7	2.27
30.0	42606	5.00	29.44	68.05	2.5
29.5	43395	5.27	8.36	89.66	1.97
29.0	44184	4.63	38.81	58.76	2.42
28.5	44973	4.90	31.43	64.1	4.45
28.0	45762	4.85	35.14	61.57	3.29
27.5	46551	4.58	42.15	54.63	3.21
27.0	47340	4.97	24.84	72.8	2.38
26.5	48129	4.88	31.36	65.54	3.1
26.0	48918	4.81	30.58	65.65	3.75
25.5	49707	4.95	25.98	70.18	3.83
25.0	50496	4.93	32.10	63.72	4.17
24.5	51285	4.77	34.67	60.44	4.87
24.0	52074	5.25	18.80	78.59	2.61
23.5	52863	5.00	29.38	66.11	4.49
23.0	53652	4.82	34.52	62.11	3.36
22.5	54441	5.28	23.05	70.36	6.57
22.0	55230	4.81	31.10	66.72	2.17
21.5	56019	5.44	16.81	78.87	4.32
21.0	56808	5.82	7.90	86.17	5.91
20.5	57597	5.79	3.32	94.75	1.93
20.0	58386	5.92	0.25	96.16	3.58
19.5	59175	5.41	14.03	83.21	2.76
19.0	59964	5.23	22.64	73.68	3.68
18.5	60753	5.32	14.63	81.66	3.71
18.0	61542	5.62	9.59	85.03	5.36
17.5	62331	5.50	9.36	85.01	5.61
17.0	63120	5.15	25.88	69.85	4.26
16.5	63909	5.23	26.27	69.56	4.17
16.0	64698	5.63	13.72	73.2	13.02
15.5	65487	5.41	19.08	79.36	1.56

Reproduced with permission of the copyright owner. Further reproduction prohibited without permission.

length (m)	"tuned" time (yrs)	grain size (phi)	sand fraction	silt fraction	clay fraction
15.0	66276	4.36	44.25	54.09	1.66
14.5	67065	5.12	23.62	75.61	0.77
14.0	67854	5.04	17.00	81.21	1.95
13.5	68643	5.64	7.05	91.6	1.36
13.0	69432	5.52	4.97	93.82	1.22
12.5	70221	5.52	17.55	78.39	4.06
12.0	71010	4.96	21.33	76.87	1.79
11.5	71799	4.98	8.35	91.64	0.01
11.0	72588	5.41	10.89	87.35	1.76
10.5	73377	5.67	2.78	94.42	2.8
10.0	74166	5.26	9.74	88.88	1.38
9.5	74955	4.47	36.16	63.77	0.09
9.0	75744	5.42	8.23	89.18	2.58
8.5	76533	5.51	7.60	90.73	1.66
8.0	77322	5.35	9.01	88.71	2.28
7.5	78111	5.53	8.54	87.55	3.9
7.0	78900	5.65	9.50	88.48	2.01
6.5	79689	5.50	7.39	90	2.61
6.0	80478	5.48	7.77	90.04	2.2
5.5	81267	5.51	10.22	87.12	2.67
5.0	82056	5.60	5.27	92.47	2.26
4.5	82845	5.09	21.89	75.58	2.52
4.0	83634	4.94	26.46	71.24	2.3
3.5	84423	4.74	31.08	64.42	4.46
3.0	85212	4.79	28.51	70.27	1.22
2.5	86001	5.62	18.41	81.58	0.01
2.0	86790	4.68	15.68	84.24	0.08
1.5	87579	3.98	57.89	37.87	4.21
1.0	88368	4.31	48.08	50.64	1.29
0.5	89157	3.88	57.13	38.91	3.94
0.0	89946	3.56	70.89	29.11	0

Reproduced with permission of the copyright owner. Further reproduction prohibited without permission.

Wagonhound South – 3

length (m)	"tuned" time (yrs)	grain size (phi)	sand fraction	silt fraction	clay fraction
52.0	0	6.10	0.12	90.82	9.03
51.5	789	5.41	3.4	88.38	8.18
51.0	1578	6.41	0.51	95.11	4.38
50.5	2367	5.51	1	97.97	1.03
50.0	3156	6.19	0.19	94.99	4.81
49.5	3945	5.32	2.04	95.49	2.46
49.0	4734	5.36	9.32	83.41	7.23
48.5	5523	5.49	11.31	80.87	7.79
48.0	6312	5.00	30.86	61.9	7.19
47.5	7101	5.16	22.59	70.98	6.41
47.0	7890	5.52	4.56	89.29	6.12
46.5	8679	5.61	13.01	79.8	7.16
46.0	9468	5.44	13.22	79.68	7.07
45.5	10257	5.20	18.04	75.73	6.21
45.0	11046	5.22	17.03	78.67	4.29
44.5	11835	4.95	23.58	71.65	4.76
44.0	12624	5.13	28.4	59.45	12.06
43.5	13413	5.19	25.09	67.5	7.37
43.0	14202	5.29	18.22	67.84	13.82
42.5	14991	5.15	21.19	71.02	7.74
42.0	15780	5.22	17.12	73.87	8.96
41.5	16569	5.36	21.86	67.98	10.11
41.0	17358	5.51	10.15	79.45	10.35
40.5	18147	5.35	18.61	73.27	8.08
40.0	18936	5.56	9.51	80.65	9.78
39.5	19725	5.51	14.41	73.55	11.98
39.0	20514	5.48	7.25	89.07	3.68
38.5	21303	5.65	6.82	91.58	1.6
38.0	22092	5.20	24.55	65.61	9.78
37.5	22881	5.66	12.78	76.28	10.9
37.0	23670	5.65	14.13	73.71	12.09
36.5	24459	5.47	16.57	74.42	8.99
36.0	25248	5.99	2.55	86.28	11.13
35.5	26037	5.84	2.44	92.58	4.97
35.0	26826	6.01	0.77	90.19	9
34.5	27615	5.36	1.51	97.04	1.45
34.0	28404	5.03	7.62	91.4	0.98
33.5	29193	5.54	2.86	96.22	0.92
33.0	29982	5.94	0.94	96.43	2.63
32.5	30771	5.77	5.16	89.45	5.37
32.0	31560	5.72	1.04	95.79	3.18

Reproduced with permission of the copyright owner. Further reproduction prohibited without permission.

length (m)	"tuned" time (yrs)	grain size (phi)	sand fraction	silt fraction	clay fraction
31.5	32349	5.75	0.6	99.24	0.16
31.0	33138	5.93	0.47	98.1	1.43
30.5	33927	5.88	1.01	98.18	0.82
30.0	34716	5.55	6.36	86.83	6.77
29.5	35505	5.25	12.02	83.29	4.67
29.0	36294	5.50	14.58	77.73	7.65
28.5	37083	5.48	13.52	77.45	8.98
28.0	37872	5.50	8.29	85.46	6.22
27.5	38661	5.52	16.08	78.64	5.27
27.0	39450	5.37	18.74	74.13	7.1
26.5	40239	5.35	23.28	63.97	12.67
26.0	41028	5.47	9.66	88.49	1.84
25.5	41817	5.30	23.28	63.97	12.67
25.0	42606	5.22	31.26	62.33	6.39
24.5	43395	5.50	5.41	89.32	5.25
24.0	44184	4.71	43.44	49.05	7.47
23.5	44973	4.97	36.28	57.92	5.79
23.0	45762	5.19	24.45	61.77	13.68
22.5	46551	5.50	9.2	82.05	8.71
22.0	47340	4.98	32.4	57.19	10.35
21.5	48129	5.41	21.9	73.01	5.08
21.0	48918	5.43	12.96	78.62	8.38
20.5	49707	5.02	33.59	56.5	9.86
20.0	50496	5.46	5.53	94.09	0.39
19.5	51285	5.26	16.2	77.82	5.96
19.0	52074	5.97	4.46	86.59	8.93
18.5	52863	5.66	7.61	81.88	10.45
18.0	53652	5.58	8.33	83.12	8.52
17.5	54441	5.72	9.03	76.08	14.81
17.0	55230	5.65	14.93	74.47	10.57
16.5	56019	5.72	2.28	95.28	2.44
16.0	56808	5.75	7.19	85.83	6.95
15.5	57597	5.55	8.23	86.77	4.98
15.0	58386	5.58	4.51	92.87	2.61
14.5	59175	5.25	7.09	92.63	0.29
14.0	59964	5.46	7.84	89.36	2.8
13.5	60753	5.42	14.83	77.55	7.6
13.0	61542	5.51	3.36	91.81	4.82
12.5	62331	5.62	6.9	89.3	3.8
12.0	63120	5.50	10.02	79.08	10.83
11.5	63909	5.78	7.46	84.54	7.98
11.0	64698	5.72	4.08	88.87	7.03
10.5	65487	5.67	6.36	89.71	3.93

Reproduced with permission of the copyright owner. Further reproduction prohibited without permission.

length (m)	"tuned" time (yrs)	grain size (phi)	sand fraction	silt fraction	clay fraction
10.0	66276	5.92	2.52	84.9	12.51
9.5	67065	5.82	1.85	93.8	4.34
9.0	67854	5.81	4.25	89.99	5.75
8.5	68643	5.64	7.6	78.22	14.1
8.0	69432	5.58	7.57	83.2	9.2
7.5	70221	5.65	9.93	75.98	14
7.0	71010	5.53	8.38	77.02	14.49
6.5	71799	5.65	9.93	75.98	14
6.0	72588	5.73	4.64	88.44	6.91
5.5	73377	5.81	4.03	82.56	13.34
5.0	74166	5.93	5.03	89.33	5.63
4.5	74955	5.79	2.69	83.47	13.75
4.0	75744	5.60	8.71	80.56	10.68
3.5	76533	5.78	7.94	86.21	5.86
3.0	77322	5.63	8.57	83.04	8.36
2.5	78111	5.73	6.74	84.58	8.67
2.0	78900	5.59	6.81	82.07	11.05
1.5	79689	5.84	1.61	90.17	8.19
1.0	80478	5.73	2.13	92.38	5.48
0.5	81267	5.72	1.41	92.42	6.17
0.0	82056	5.90	1.2	95.18	3.61

Reproduced with permission of the copyright owner. Further reproduction prohibited without permission.

Wagonhound East – 2

length (m)	"tuned" time (yrs)	grain size (phi)	sand fraction	silt fraction	clay fraction
43.5	0	6.41	0.02	94.67	5.32
43.0	794	5.53	14.84	82.86	2.31
42.5	1588	5.18	3.51	95.29	1.19
42.0	2382	5.96	1.71	96.27	2.03
41.5	3176	5.61	8.44	84.96	6.58
41.0	3970	5.75	5.27	91.09	3.65
40.5	4764	5.71	0.74	94.49	4.77
40.0	5558	5.65	9.62	83.48	6.89
39.5	6352	5.87	3.58	91.4	5.01
39.0	7146	5.88	5.15	89.49	5.35
38.5	7940	5.54	9.22	84.37	6.39
38.0	8734	5.87	0.63	86.03	13.25
37.5	9528	5.55	9.35	81.43	9.16
37.0	10322	5.59	11.44	84.85	3.7
36.5	11116	5.35	22.81	68.77	8.4
36.0	11910	5.72	6.28	84.17	9.5
35.5	12704	5.74	9.22	80.47	10.27
35.0	13498	5.67	4.87	87.54	7.55
34.5	14292	5.23	2.87	92.41	4.7
34.0	15086	5.23	24.81	64.29	10.85
33.5	15880	5.55	6.61	83.38	9.94
33.0	16674	5.78	7.1	87.42	5.47
32.5	17468	5.50	10.79	81.44	7.73
32.0	18262	5.50	16.12	76.51	7.35
31.5	19056	5.77	9.49	79.72	10.75
31.0	19850	3.31	71.72	22.78	5.45
30.5	20644	3.16	76.28	19.23	4.45
30.0	21438	3.24	76.06	21.11	2.81
29.5	22232	4.49	40.48	56.77	2.75
29.0	23026	4.17	49.71	42.98	7.28
28.5	23820	6.01	9.65	76.93	13.39
28.0	24614	5.28	22.63	72.12	5.24
27.5	25408	5.80	11.31	82.48	6.2
27.0	26202	4.37	43.96	49.78	6.23
26.5	26996	5.21	24.36	69.54	6.07
26.0	27790	5.65	19.71	72.85	7.44
25.5	28584	4.53	40.95	51.28	7.71
25.0	29378	5.36	23.89	56.75	19.23
24.5	30172	5.91	12.07	70.62	17.24
24.0	30966	6.15	8.9	81.48	9.61
23.5	31760	3.95	56.43	39.5	4.05

Reproduced with permission of the copyright owner. Further reproduction prohibited without permission.

length (m)	"tuned" time (yrs)	grain size (phi)	sand fraction	silt fraction	clay fraction
23.0	32554	5.63	16.98	67.49	15.44
22.5	33348	3.09	77.35	18.04	4.57
22.0	34142	4.08	50.01	41.93	8
21.5	34936	3.48	68.15	26.06	5.72
21.0	35730	3.93	60.2	34.27	5.51
20.5	36524	4.20	47.17	50.37	2.45
20.0	37318	3.40	70.05	25.76	4.17
19.5	38112	4.08	54.52	39.88	5.59
19.0	38906	3.36	71.62	23.1	5.24
18.5	39700	3.16	77.21	19.41	3.36
18.0	40494	3.43	70.11	24.52	5.33
17.5	41288	3.13	76.68	20.46	2.85
17.0	42082	3.08	78.15	19.04	2.8
16.5	42876	4.85	36.22	51.77	11.96
16.0	43670	5.25	22.8	68.13	9.05
15.5	44464	4.45	39.08	48.44	12.35
15.0	45258	4.74	35.68	53.33	10.92
14.5	46052	6.03	4.12	90.39	5.48
14.0	46846	5.62	21.26	67.26	11.45
13.5	47640	5.30	17.11	74.5	8.37
13.0	48434	5.83	7.68	88.11	4.21
12.5	49228	5.96	9.62	82.16	8.21
12.0	50022	6.25	3.23	77.78	18.99
11.5	50816	6.09	9.1	78.96	11.92
11.0	51610	6.15	3.65	86.48	9.85
10.5	52404	6.36	0.39	90.08	9.52
10.0	53198	6.29	4.44	80.89	14.62
9.5	53992	5.00	27.17	68.09	3.73
9.0	54786	5.17	19.74	77.36	2.89
8.5	55580	5.71	3.56	94.48	1.94
8.0	56374	5.36	6.63	91.72	1.66
7.5	57168	5.09	25.26	69.42	5.3
7.0	57962	5.57	9.22	86.71	4.06
6.5	58756	5.11	25.3	70.25	4.44
6.0	59550	5.33	19.08	78.49	2.43
5.5	60344	5.30	19.59	76.9	3.51
5.0	61138	4.93	24.34	72.05	3.6
4.5	61932	4.86	33.86	53.8	12.24
4.0	62726	4.40	49.58	48.29	2.13
3.5	63520	4.91	32.85	62.78	4.35
3.0	64314	4.66	43.55	52.88	3.56
2.5	65108	4.84	35.49	59.93	4.56
2.0	65902	4.73	40.89	54.15	4.94

Reproduced with permission of the copyright owner. Further reproduction prohibited without permission.

length (m)	"tuned" time (yrs)	grain size (phi)	sand fraction	silt fraction	clay fraction
1.5	66696	6.13	0.57	99.17	0.25
1.0	67490	5.86	1.01	93.48	5.49
0.5	68284	5.46	9.78	88.83	1.39
0.0	69078	5.80	2.77	96.85	0.38

Reproduced with permission of the copyright owner. Further reproduction prohibited without permission.

APPENDIX D

GRAPHICAL PLOTS OF SAND, SILT AND CLAY FRACTIONS

Reproduced with permission of the copyright owner. Further reproduction prohibited without permission.

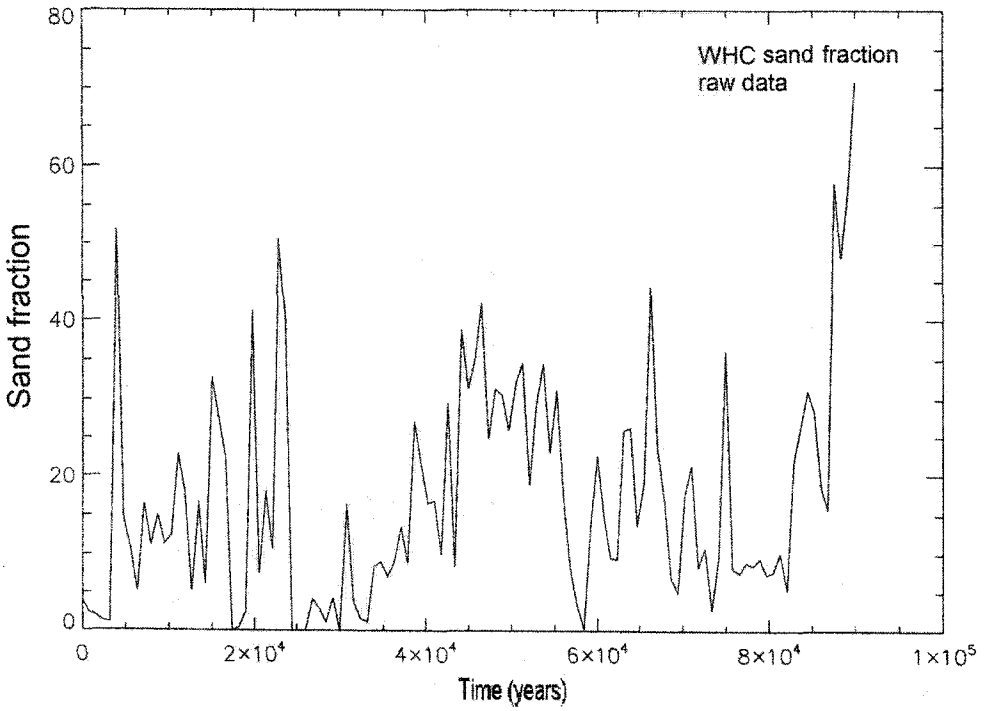

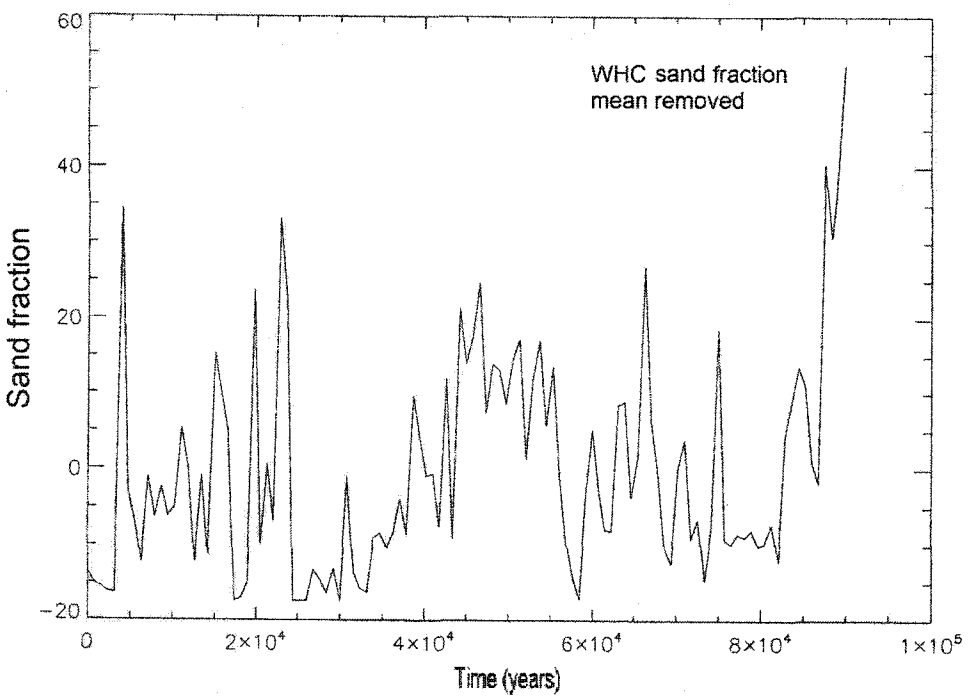

Reproduced with permission of the copyright owner. Further reproduction prohibited without permission.

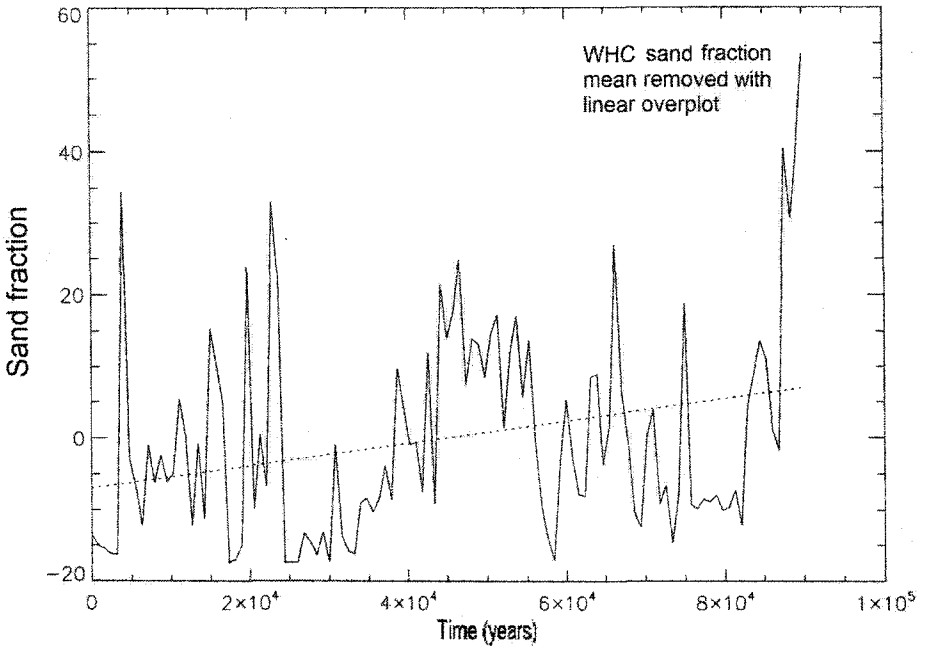

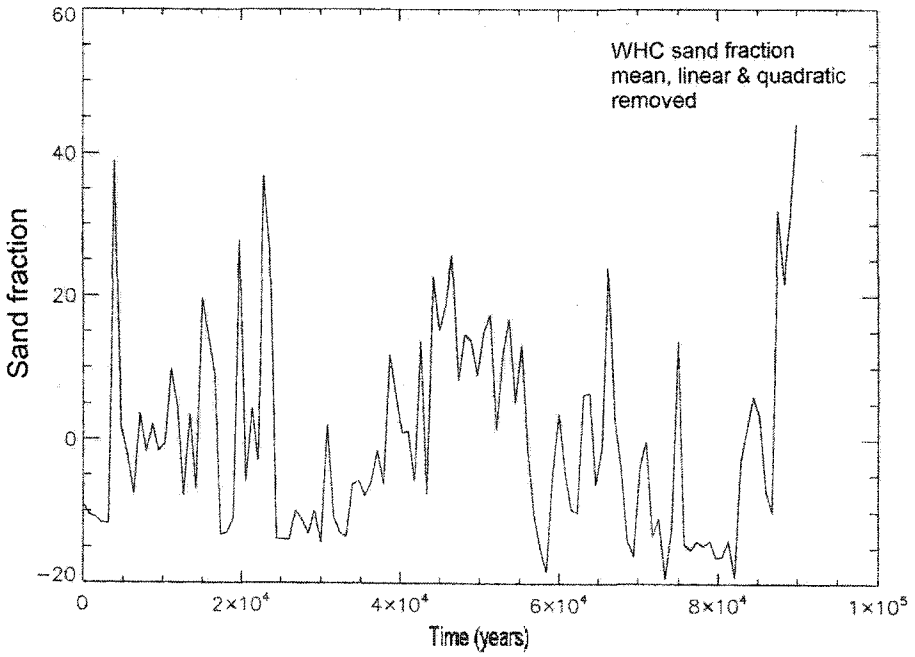

Reproduced with permission of the copyright owner. Further reproduction prohibited without permission.

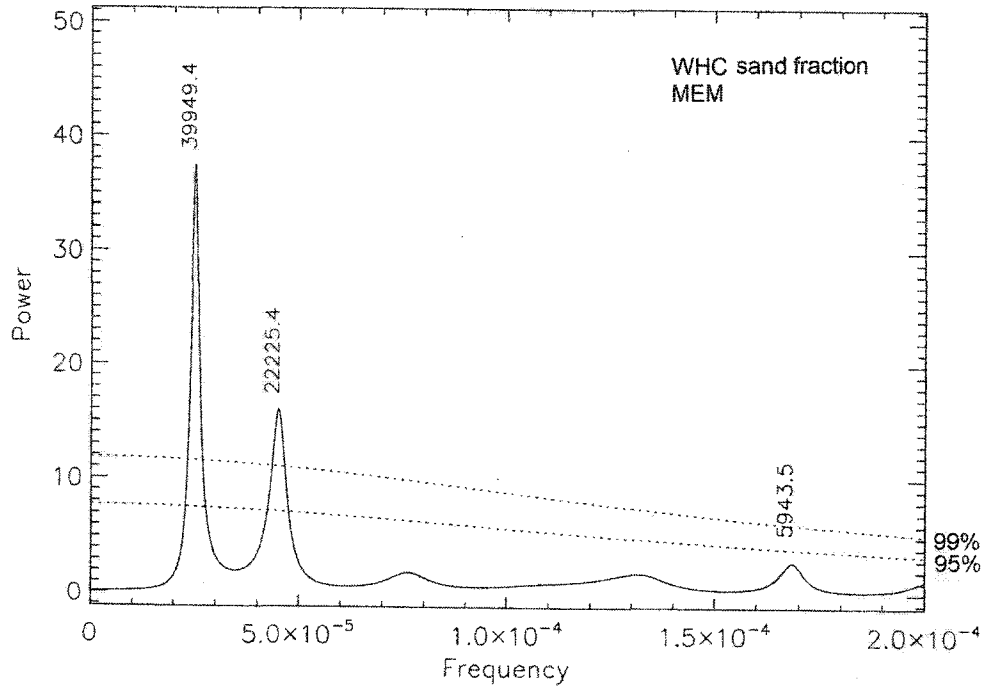

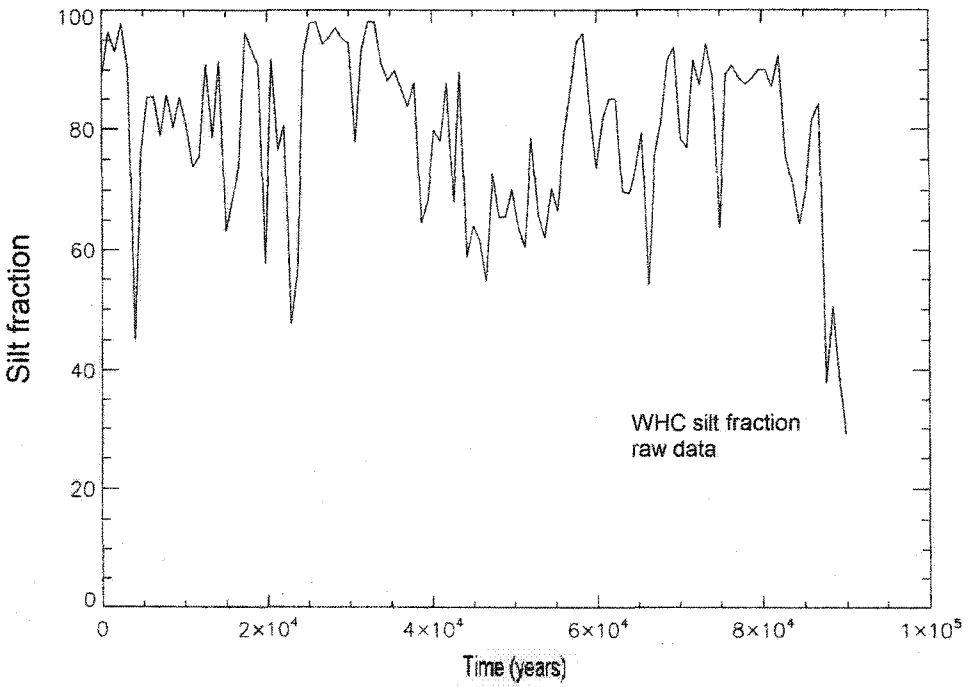

Reproduced with permission of the copyright owner. Further reproduction prohibited without permission.

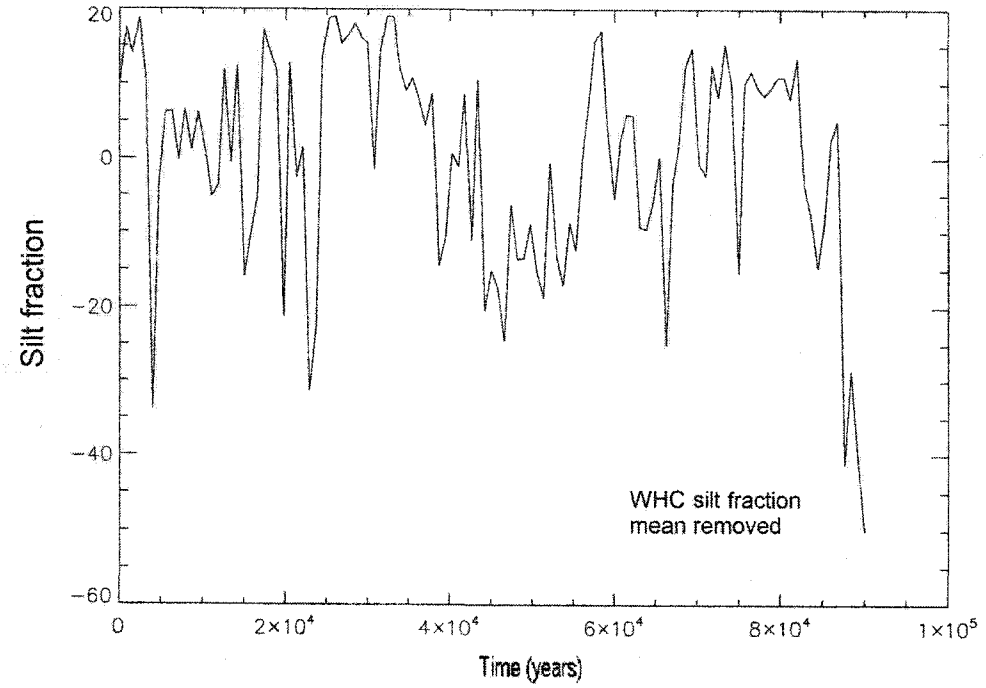

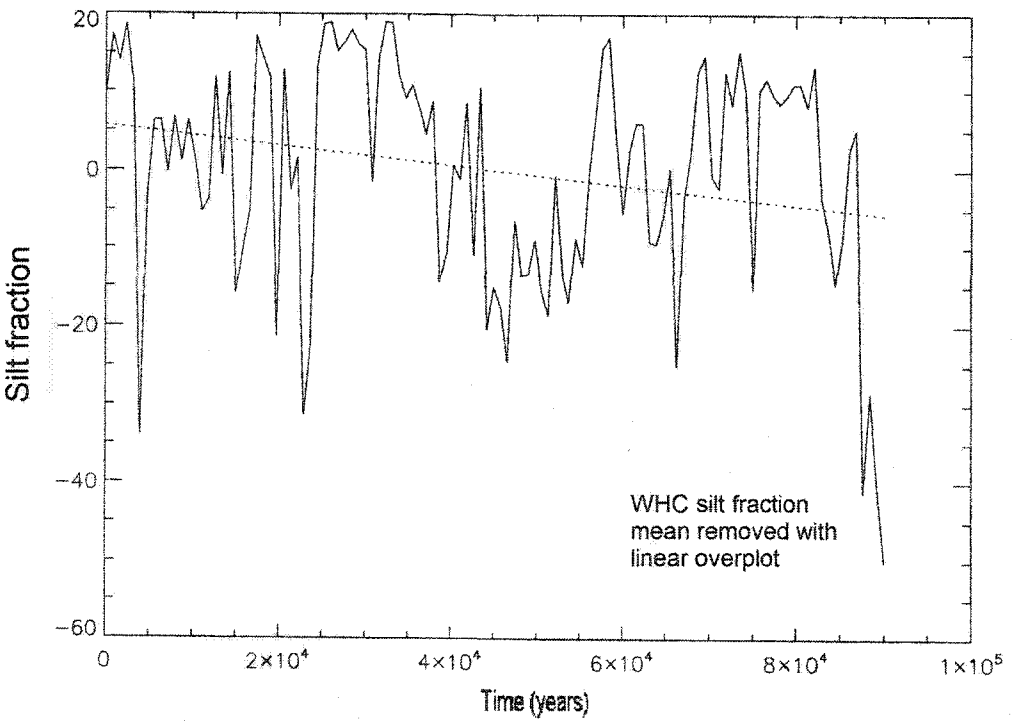

Reproduced with permission of the copyright owner. Further reproduction prohibited without permission.

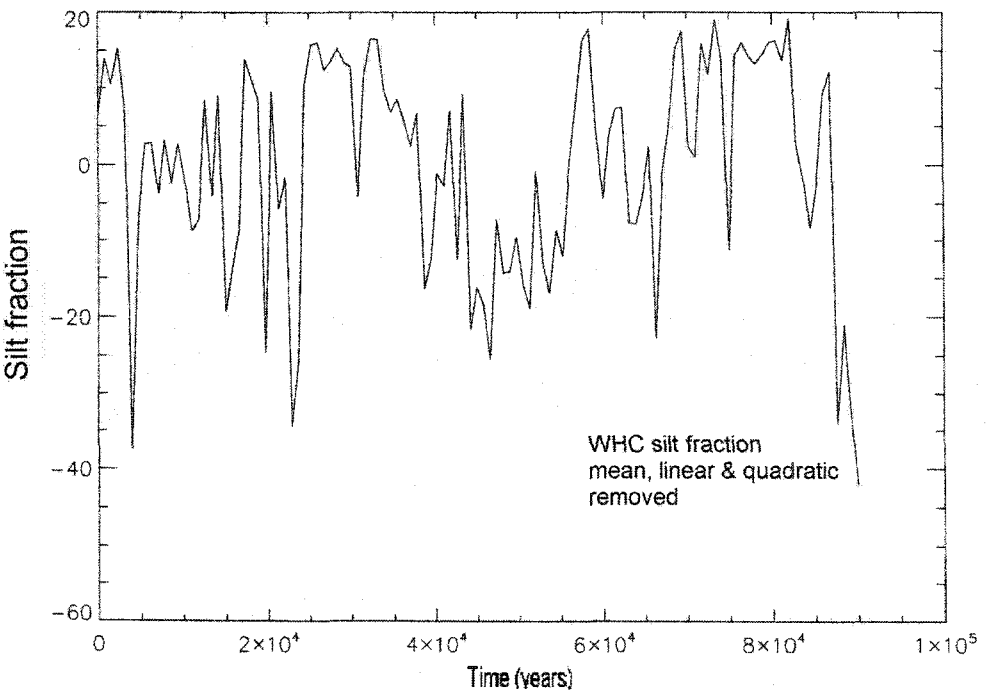

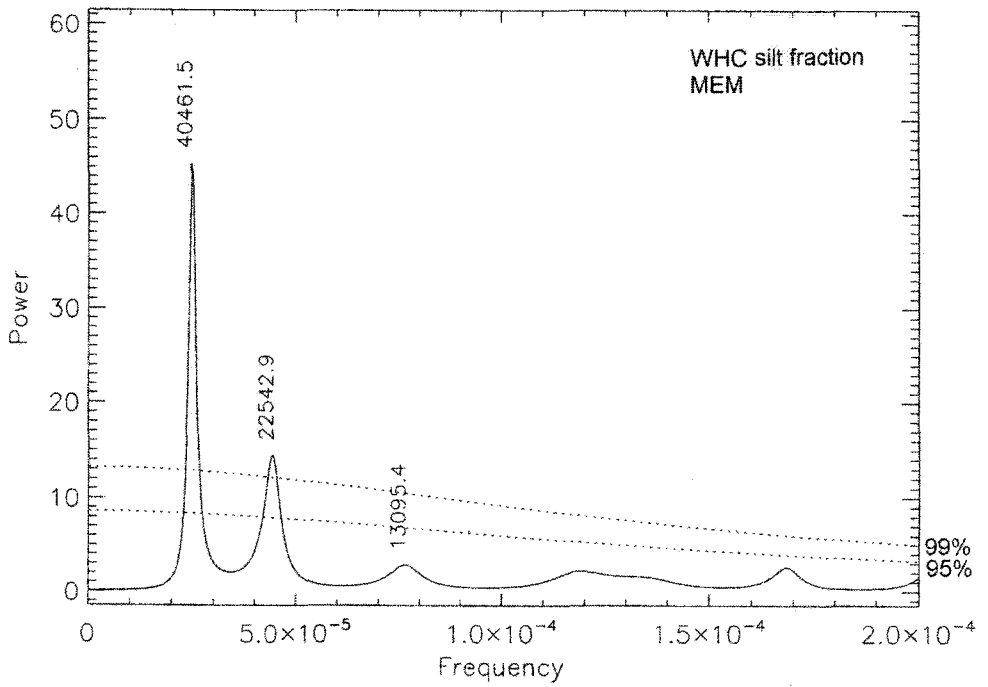

Reproduced with permission of the copyright owner. Further reproduction prohibited without permission.

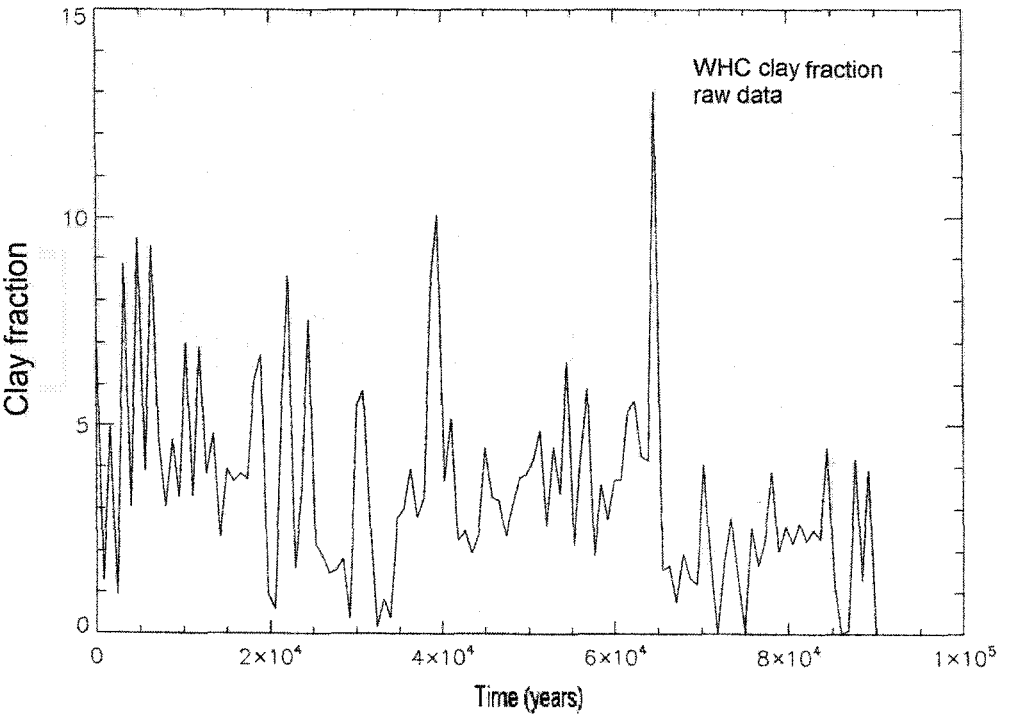

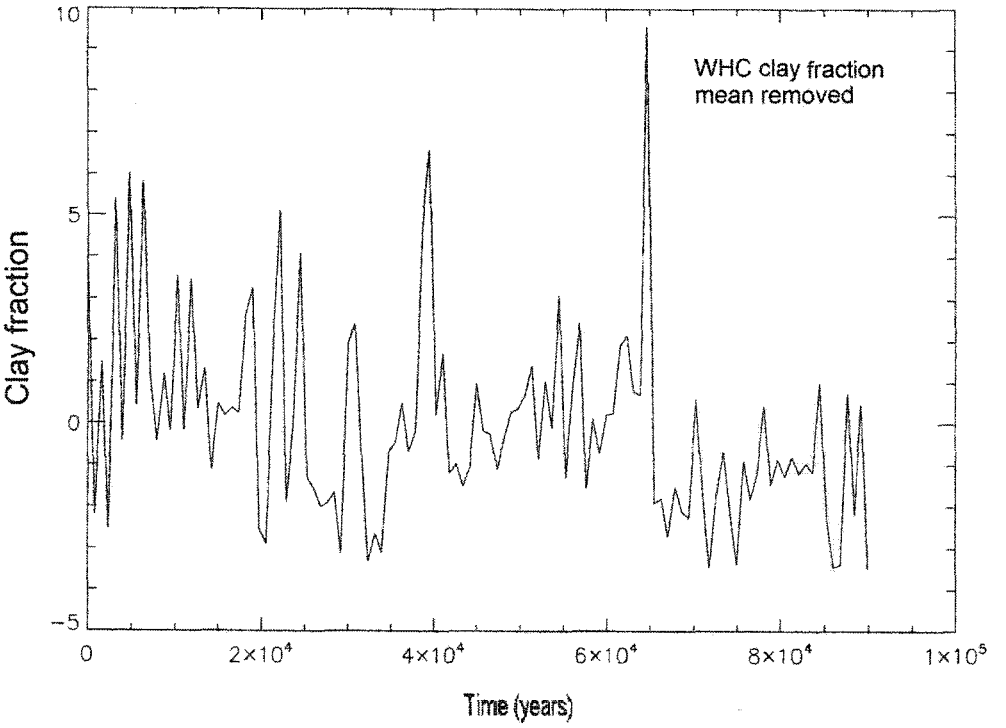

Reproduced with permission of the copyright owner. Further reproduction prohibited without permission.

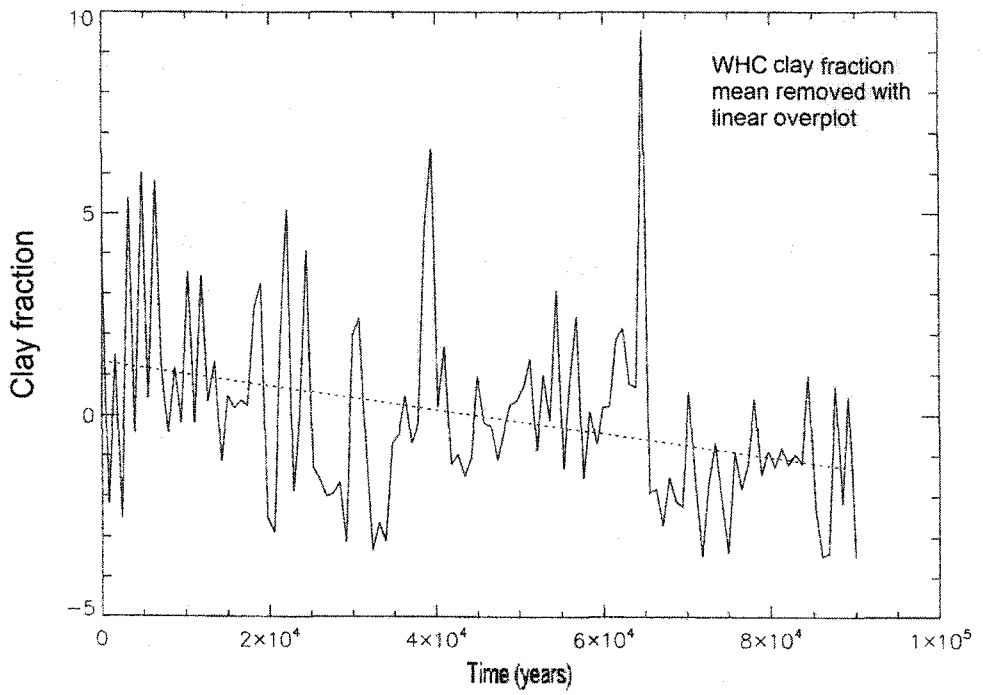

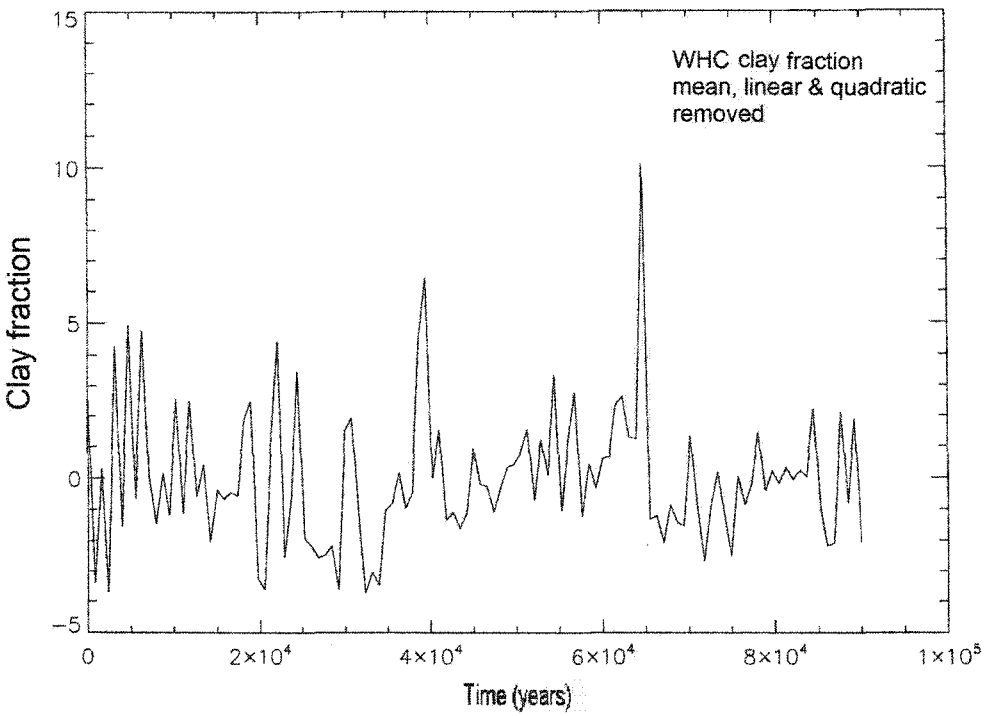

Reproduced with permission of the copyright owner. Further reproduction prohibited without permission.

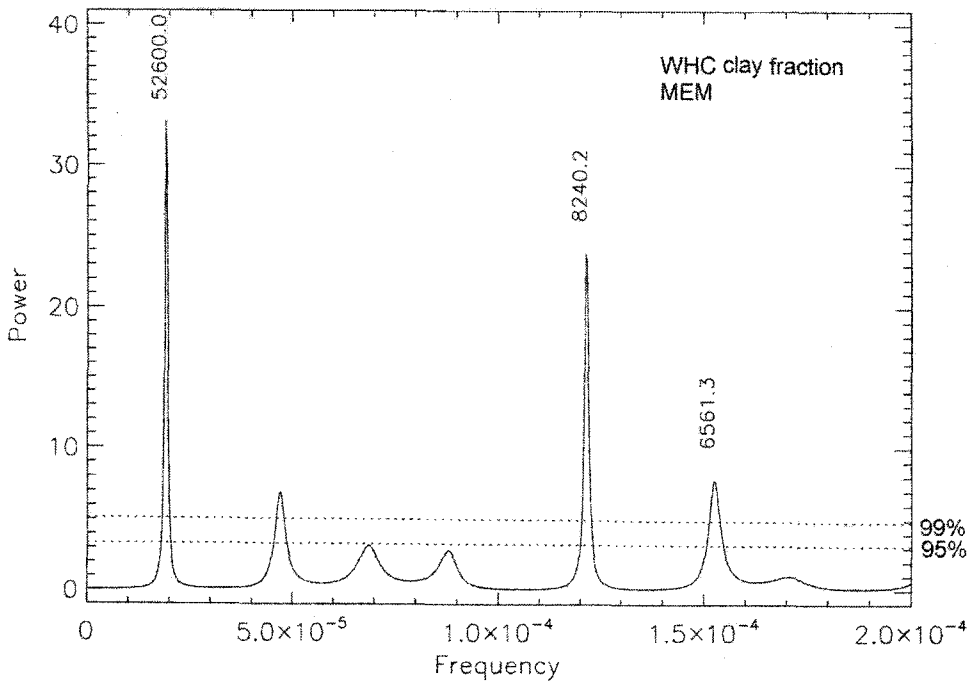

Reproduced with permission of the copyright owner. Further reproduction prohibited without permission.

APPENDIX E

CALCULATED TIMELINES

Reproduced with permission of the copyright owner. Further reproduction prohibited without permission.

Wagonhound Central

bed number	thickness (cm)	bin assignment	bin number	no. of beds per bin	indiv. Time (yrs)	cum. Time (yrs)
272	900	180	1	53	90.00	90.00
271	450	90	2	30	45.00	135.00
270	300	60	3	29	30.00	165.00
269	400	80	4	14	40.00	205.00
268	1200	220	5	5	120.00	325.00
267	500	100	6	15	50.00	375.00
266	50	10	7	10	833.33	1208.33
265	450	90	8	13	45.00	1253.33
264	40	8	9	4	666.67	1920.00
263	7	2	10	13	0.70	1920.70
262	30	6	11	4	500.00	2420.70
261	12	3	12	10	1.20	2421.90
260	65	13	13	4	1083.33	3505.23
259	140	28	14	3	14.00	3519.23
258	5	1	15	4	83.33	3602.57
257	30	6	16	7	3.00	3605.57
256	35	7	17	5	583.33	4188.90
255	50	10	18	2	5.00	4193.90
254	110	22	19	2	1833.33	6027.23
253	30	6	20	6	3.00	6030.23
252	15	3	21	1	250.00	6280.23
251	35	7	22	1	3.50	6283.73
250	40	8	23	3	666.67	6950.40
249	25	5	24	2	2.50	6952.90
248	50	10	25	3	833.33	7786.23
247	12	3	26	0	1.20	7787.43
246	80	16	27	0	1333.33	9120.77
245	13	3	28	4	1.30	9122.07
244	5	1	29	0	83.33	9205.40
243	50	10	30	2	5.00	9210.40
242	85	17	31	0	1416.67	10627.07
241	8	2	32	0	0.80	10627.87
240	40	8	33	0	666.67	11294.53
239	3	1	34	0	0.30	11294.83
238	60	12	35	1	1000.00	12294.83
237	8	2	36	0	0.80	12295.63
236	25	5	37	1	416.67	12712.30
235	3	1	38	0	0.30	12712.60
234	75	15	39	2	1250.00	13962.60
233	12	3	40	1	1.20	13963.80
232	50	10	41	0	833.33	14797.13
231	3	1	42	1	0.30	14797.43
230	40	8	43	0	666.67	15464.10
229	6	2	44	0	0.60	15464.70

Reproduced with permission of the copyright owner. Further reproduction prohibited without permission.

bed number	thickness (cm)	bin assignment	bin number	no. of beds per bin	indiv. Time (yrs)	cum. Time (yrs)
228	120	24	45	0	2000.00	17464.70
227	30	6	46	0	3.00	17467.70
226	10	2	47	0	166.67	17634.37
225	6	2	48	0	0.60	17634.97
224	18	4	49	0	300.00	17934.97
223	7	2	50	0	0.70	17935.67
222	15	3	51	0	250.00	18185.67
221	4	1	52	0	0.40	18186.07
220	10	2	53	0	166.67	18352.73
219	6	2	54	1	0.60	18353.33
218	20	4	55	0	333.33	18686.67
217	4	1	56	1	0.40	18687.07
216	82	17	57	0	1366.67	20053.73
215	2	1	58	1	0.20	20053.93
214	62	13	59	0	1033.33	21087.27
213	10	2	60	1	1.00	21088.27
212	16	4	61	0	266.67	21354.93
211	5	1	62	0	0.50	21355.43
210	6	2	63	0	100.00	21455.43
209	8	2	64	0	0.80	21456.23
208	20	4	65	0	333.33	21789.57
207	12	3	66	0	1.20	21790.77
206	12	3	67	0	200.00	21990.77
205	5	1	68	0	0.50	21991.27
204	18	4	69	0	300.00	22291.27
203	1	1	70	0	0.10	22291.37
202	5	1	71	0	83.33	22374.70
201	4	1	72	1	0.40	22375.10
200	15	3	73	0	250.00	22625.10
199	1	1	74	0	0.10	22625.20
198	10	2	75	0	166.67	22791.87
197	10	2	76	0	1.00	22792.87
196	140	28	77	0	2333.33	25126.20
195	2	1	78	1	0.20	25126.40
194	15	3	79	0	250.00	25376.40
193	2	1	80	2	0.20	25376.60
192	35	7	81	0	583.33	25959.93
191	15	3	82	0	1.50	25961.43
190	75	15	83	0	1250.00	27211.43
189	4	1	84	0	0.40	27211.83
188	82	17	85	0	1366.67	28578.50
187	15	3	86	0	1.50	28580.00
186	55	11	87	0	916.67	29496.67
185	4	1	88	0	0.40	29497.07
184	400	80	89	0	6666.67	36163.73

Reproduced with permission of the copyright owner. Further reproduction prohibited without permission.

bed number	thickness (cm)	bin assignment	bin number	no. of beds per bin	indiv. Time (yrs)	cum. Time (yrs)
183	10	2	90	2	1.00	36164.73
182	52	11	91	0	866.67	37031.40
181	1	1	92	0	0.10	37031.50
180	15	3	93	0	250.00	37281.50
179	1	1	94	0	0.10	37281.60
178	40	8	95	0	666.67	37948.27
177	5	1	96	0	0.50	37948.77
176	20	4	97	0	333.33	38282.10
175	6	2	98	0	0.60	38282.70
174	58	12	99	0	966.67	39249.37
173	5	1	100	1	0.50	39249.87
172	45	9	101	0	750.00	39999.87
171	5	1	102	0	0.50	40000.37
170	150	30	103	0	2500.00	42500.37
169	20	4	104	0	2.00	42502.37
168	57	12	105	0	950.00	43452.37
167	8	2	106	0	0.80	43453.17
166	30	6	107	0	500.00	43953.17
165	5	1	108	0	0.50	43953.67
164	60	12	109	0	1000.00	44953.67
163	150	30	110	0	15.00	44968.67
162	4	1	111	0	0.40	44969.07
161	35	7	112	0	583.33	45552.40
160	25	5	113	0	2.50	45554.90
159	48	10	114	0	800.00	46354.90
158	38	8	115	0	3.80	46358.70
157	100	20	116	0	1666.67	48025.37
156	48	10	117	0	4.80	48030.17
155	100	20	118	0	1666.67	49696.83
154	15	3	119	0	1.50	49698.33
153	28	6	120	0	466.67	50165.00
152	15	3	121	1	1.50	50166.50
151	50	10	122	0	833.33	50999.83
150	15	3	123	0	1.50	51001.33
149	40	8	124	0	666.67	51668.00
148	8	2	125	0	0.80	51668.80
147	58	12	126	0	966.67	52635.47
146	10	2	127	0	1.00	52636.47
145	20	4	128	0	333.33	52969.80
144	15	3	129	0	1.50	52971.30
143	15	3	130	0	250.00	53221.30
142	55	11	131	0	5.50	53226.80
141	78	16	132	0	1300.00	54526.80
140	28	6	133	0	2.80	54529.60
139	30	6	134	0	500.00	55029.60

Reproduced with permission of the copyright owner. Further reproduction prohibited without permission.

bed number	thickness (cm)	bin assignment	bin number	no. of beds per bin	indiv. Time (yrs)	cum. Time (yrs)
138	18	4	135	0	1.80	55031.40
137	280	56	136	0	4666.67	59698.07
136	6	2	137	0	0.60	59698.67
135	125	25	138	0	2083.33	61782.00
134	50	10	139	0	5.00	61787.00
133	50	10	140	0	833.33	62620.33
132	50	10	141	0	5.00	62625.33
131	20	4	142	0	333.33	62958.67
130	40	8	143	0	4.00	62962.67
129	58	12	144	0	966.67	63929.33
128	12	3	145	0	1.20	63930.53
127	44	9	146	0	733.33	64663.87
126	15	3	147	0	1.50	64665.37
125	78	16	148	0	1300.00	65965.37
124	10	2	149	0	1.00	65966.37
123	40	8	150	1	666.67	66633.03
122	800	160	151	0	80.00	66713.03
121	60	12	152	0	6.00	66719.03
120	200	40	153	0	3333.33	70052.37
119	80	16	154	0	8.00	70060.37
118	45	9	155	0	750.00	70810.37
117	15	3	156	0	1.50	70811.87
116	75	15	157	0	1250.00	72061.87
115	15	3	158	0	1.50	72063.37
114	100	20	159	0	1666.67	73730.03
113	750	150	160	1	75.00	73805.03
112	70	14	161	0	1166.67	74971.70
111	80	16	162	0	8.00	74979.70
110	20	4	163	0	333.33	75313.03
109	35	7	164	0	3.50	75316.53
108	80	16	165	0	1333.33	76649.87
107	30	6	166	0	3.00	76652.87
106	30	6	167	0	500.00	77152.87
105	30	6	168	0	3.00	77155.87
104	15	3	169	0	250.00	77405.87
103	70	14	170	0	7.00	77412.87
102	38	8	171	0	633.33	78046.20
101	60	12	172	0	6.00	78052.20
100	75	15	173	0	1250.00	79302.20
99	68	14	174	0	6.80	79309.00
98	30	6	175	0	500.00	79809.00
97	3	1	176	0	0.30	79809.30
96	605	121	177	0	10083.33	89892.63
95	15	3	178	0	1.50	89894.13
94	31	7	179	0	516.67	90410.80

Reproduced with permission of the copyright owner. Further reproduction prohibited without permission.

bed number	thickness (cm)	bin assignment	bin number	no. of beds per bin	indiv. Time (yrs)	cum. Time (yrs)
93	4	1	180	1	0.40	90411.20
92	60	12	181	0	1000.00	91411.20
91	100	20	182	0	10.00	91421.20
90	92	19	183	0	1533.33	92954.53
89	3	1	184	0	0.30	92954.83
88	140	28	185	0	2333.33	95288.17
87	35	7	186	0	3.50	95291.67
86	50	10	187	0	833.33	96125.00
85	5	1	188	0	0.50	96125.50
84	45	9	189	0	750.00	96875.50
83	5	1	190	0	0.50	96876.00
82	100	20	191	0	1666.67	98542.67
81	5	1	192	0	0.50	98543.17
80	90	18	193	0	1500.00	100043.17
79	5	1	194	0	0.50	100043.67
78	193	39	195	0	3216.67	103260.33
77	2	1	196	0	0.20	103260.53
76	48	10	197	0	800.00	104060.53
75	2	1	198	0	0.20	104060.73
74	360	72	199	0	6000.00	110060.73
73	30	6	200	0	3.00	110063.73
72	63	13	201	0	1050.00	111113.73
71	12	3	202	0	1.20	111114.93
70	111	23	203	0	1850.00	112964.93
69	4	1	204	0	0.40	112965.33
68	122	25	205	0	2033.33	114998.67
67	3	1	206	0	0.30	114998.97
66	85	17	207	0	1416.67	116415.63
65	5	1	208	0	0.50	116416.13
64	92	19	209	0	1533.33	117949.47
63	28	6	210	0	2.80	117952.27
62	210	42	211	0	3500.00	121452.27
61	10	2	212	0	1.00	121453.27
60	105	21	213	0	1750.00	123203.27
59	40	8	214	0	4.00	123207.27
58	10	2	215	0	166.67	123373.93
57	55	11	216	0	5.50	123379.43
56	120	24	217	0	2000.00	125379.43
55	10	2	218	0	1.00	125380.43
54	15	3	219	0	250.00	125630.43
53	35	7	220	1	3.50	125633.93
52	115	23			1916.67	127550.60
51	20	4			2.00	127552.60
50	81	17			1350.00	128902.60
49	2	1			0.20	128902.80

Reproduced with permission of the copyright owner. Further reproduction prohibited without permission.

bed number	thickness (cm)	bin assignment	bin number	no. of beds per bin	indiv. Time (yrs)	cum. Time (yrs)
48	184	37			3066.67	131969.47
47	3	1			0.30	131969.77
46	90	18			1500.00	133469.77
45	5	1			0.50	133470.27
44	35	7			583.33	134053.60
43	60	12			6.00	134059.60
42	65	13			1083.33	135142.93
41	30	6			3.00	135145.93
40	22	5			366.67	135512.60
39	3	1			0.30	135512.90
38	23	5			383.33	135896.23
37	12	3			1.20	135897.43
36	38	8			633.33	136530.77
35	4	1			0.40	136531.17
34	7	2			116.67	136647.83
33	3	1			0.30	136648.13
32	12	3			200.00	136848.13
31	6	2			0.60	136848.73
30	122	25			2033.33	138882.07
29	3	1			0.30	138882.37
28	32	7			533.33	139415.70
27	7	2			0.70	139416.40
26	40	8			4.00	139420.40
25	8	2			0.80	139421.20
24	5	1			83.33	139504.53
23	8	2			0.80	139505.33
22	267	54			4450.00	143955.33
21	3	1			0.30	143955.63
20	195	39			3250.00	147205.63
19	5	1			0.50	147206.13
18	100	20			1666.67	148872.80
17	5	1			0.50	148873.30
16	17	4			283.33	149156.63
15	3	1			0.30	149156.93
14	122	25			2033.33	151190.27
13	3	1			0.30	151190.57
12	175	35			2916.67	154107.23
11	5	1			0.50	154107.73
10	140	28			2333.33	156441.07
9	5	1			0.50	156441.57
8	20	4			333.33	156774.90
7	5	1			0.50	156775.40
6	115	23			1916.67	158692.07
5	10	2			1.00	158693.07
4	80	16			1333.33	160026.40

Reproduced with permission of the copyright owner. Further reproduction prohibited without permission.

bed number	thickness (cm)	bin assignment	bin number	no. of beds per bin	indiv. Time (yrs)	cum. Time (yrs)
3	15	3			1.50	160027.90
2	390	78			6500.00	166527.90
1	290	58			29.00	166556.90

Reproduced with permission of the copyright owner. Further reproduction prohibited without permission.

Wagonhound North –1

bed number	thickness (cm)	bin assignment	bin number	no. of beds per bin	indiv. Time (yrs)	cum. Time (yrs)
148	1340	268	1	26	134.00	134.00
147	119	24	2	14	11.90	145.90
146	151	31	3	10	2516.67	2662.57
145	27	6	4	4	2.70	2665.27
144	20	4	5	6	2.00	2667.27
143	165	33	6	8	2750.00	5417.27
142	21	5	7	6	2.10	5419.37
141	150	30	8	2	2500.00	7919.37
140	108	22	9	3	10.80	7930.17
139	148	30	10	4	2466.67	10396.83
138	28	6	11	2	2.80	10399.63
137	69	14	12	4	1150.00	11549.63
136	28	6	13	4	2.80	11552.43
135	441	89	14	5	7350.00	18902.43
134	30	6	15	1	3.00	18905.43
133	112	23	16	4	1866.67	20772.10
132	22	5	17	0	2.20	20774.30
131	132	27	18	0	2200.00	22974.30
130	11	3	19	1	1.10	22975.40
129	50	10	20	2	833.33	23808.73
128	20	4	21	0	2.00	23810.73
127	116	24	22	2	1933.33	25744.07
126	11	3	23	3	1.10	25745.17
125	34	7	24	3	566.67	26311.83
124	12	3	25	1	1.20	26313.03
123	145	29	26	1	2416.67	28729.70
122	30	6	27	1	3.00	28732.70
121	148	30	28	0	2466.67	31199.37
120	62	13	29	3	6.20	31205.57
119	110	22	30	4	1833.33	33038.90
118	21	5	31	1	2.10	33041.00
117	62	13	32	2	1033.33	34074.33
116	10	2	33	2	1.00	34075.33
115	79	16	34	0	1316.67	35392.00
114	17	4	35	1	1.70	35393.70
113	28	6	36	1	466.67	35860.37
112	15	3	37	1	1.50	35861.87
111	70	14	38	2	1166.67	37028.53
110	40	8	39	1	4.00	37032.53
109	95	19	40	0	1583.33	38615.87
108	23	5	41	0	2.30	38618.17
107	43	9	42	1	716.67	39334.83
106	7	2	43	0	0.70	39335.53
105	195	39	44	0	3250.00	42585.53
104	9	2	45	0	0.90	42586.43
103	6	2	46	1	100.00	42686.43
102	3	1	47	0	0.30	42686.73
101	290	58	48	0	4833.33	47520.07

Reproduced with permission of the copyright owner. Further reproduction prohibited without permission.

bed number	thickness (cm)	bin assignment	bin number	no. of beds per bin	indiv. Time (yrs)	cum. Time (yrs)
100	178	36	49	0	17.80	47537.87
99	32	7	50	1	533.33	48071.20
98	60	12	51	1	6.00	48077.20
97	10	2	52	1	166.67	48243.87
96	160	32	53	0	16.00	48259.87
95	165	33	54	0	2750.00	51009.87
94	29	6	55	0	2.90	51012.77
93	113	23	56	0	1883.33	52896.10
92	20	4	57	1	2.00	52898.10
91	15	3	58	1	250.00	53148.10
90	10	2	59	0	1.00	53149.10
89	2	1	60	0	33.33	53182.43
88	13	3	61	0	1.30	53183.73
87	67	14	62	0	1116.67	54300.40
86	100	20	63	0	10.00	54310.40
85	76	16	64	0	1266.67	55577.07
84	157	32	65	0	15.70	55592.77
83	50	10	66	0	833.33	56426.10
82	6	2	67	0	0.60	56426.70
81	5	1	68	0	83.33	56510.03
80	60	12	69	0	6.00	56516.03
79	23	5	70	0	383.33	56899.37
78	52	11	71	0	5.20	56904.57
77	120	24	72	0	2000.00	58904.57
76	173	35	73	0	17.30	58921.87
75	57	12	74	0	950.00	59871.87
74	55	11	75	0	5.50	59877.37
73	185	37	76	0	3083.33	62960.70
72	13	3	77	0	1.30	62962.00
71	35	7	78	0	583.33	63545.33
70	227	46	79	0	22.70	63568.03
69	45	9	80	0	750.00	64318.03
68	1	1	81	0	0.10	64318.13
67	2	1	82	0	33.33	64351.47
66	35	7	83	1	3.50	64354.97
65	35	7	84	0	583.33	64938.30
64	25	5	85	0	2.50	64940.80
63	71	15	86	0	1183.33	66124.13
62	14	3	87	0	1.40	66125.53
61	210	42	88	0	3500.00	69625.53
60	6	2	89	1	0.60	69626.13
59	250	50	90	0	4166.67	73792.80
58	3	1	91	0	0.30	73793.10
57	126	26	92	0	2100.00	75893.10
56	2	1	93	0	0.20	75893.30
55	122	25	94	0	2033.33	77926.63
54	2	1	95	0	0.20	77926.83
53	260	52	96	0	4333.33	82260.17
52	4	1	97	0	0.40	82260.57
51	253	51	98	0	4216.67	86477.23

Reproduced with permission of the copyright owner. Further reproduction prohibited without permission.

bed number	thickness (cm)	bin assignment	bin number	no. of beds per bin	indiv. Time (yrs)	cum. Time (yrs)
50	12	3	99	0	1.20	86478.43
49	736	148	100	0	12266.67	98745.10
48	12	3	101	0	1.20	98746.30
47	68	14	102	0	1133.33	99879.63
46	10	2	103	0	1.00	99880.63
45	190	38	104	0	3166.67	103047.30
44	3	1	105	0	0.30	103047.60
43	45	9	106	0	750.00	103797.60
42	10	2	107	0	1.00	103798.60
41	412	83	108	0	6866.67	110665.27
40	7	2	109	0	0.70	110685.97
39	46	10	110	0	766.67	111432.63
38	5	1	111	0	0.50	111433.13
37	190	38	112	1	3166.67	114599.80
36	5	1	113	0	0.50	114600.30
35	57	12	114	0	950.00	115550.30
34	5	1	115	0	0.50	115550.80
33	77	16	116	0	1283.33	116834.13
32	2	1	117	0	0.20	116834.33
31	143	29	118	0	2383.33	119217.67
30	10	2	119	0	1.00	119218.67
29	112	23	120	0	1866.67	121085.33
28	4	1	121	0	0.40	121085.73
27	62	13	122	0	1033.33	122119.07
26	2	1	123	0	0.20	122119.27
25	144	29	124	0	2400.00	124519.27
24	4	1	125	0	0.40	124519.67
23	78	16	126	0	1300.00	125819.67
22	10	2	127	0	1.00	125820.67
21	49	10	128	0	816.67	126637.33
20	1	1	129	0	0.10	126637.43
19	100	20	130	0	1666.67	128304.10
18	3	1	131	0	0.30	128304.40
17	32	7	132	0	533.33	128837.73
16	3	1	133	1	0.30	128838.03
15	147	30	134	0	2450.00	131288.03
14	2	1	135	0	0.20	131288.23
13	38	8	136	0	633.33	131921.57
12	2	1	137	0	0.20	131921.77
11	61	13	138	0	1016.67	132938.43
10	8	2	139	0	0.80	132939.23
9	560	112	140	0	9333.33	142272.57
8	3	1	141	0	0.30	142272.87
7	30	6	142	0	500.00	142772.87
6	2	1	143	0	0.20	142773.07
5	68	14	144	0	1133.33	143906.40
4	3	1	145	0	0.30	143906.70
3	282	57	146	0	4700.00	148606.70
2	2	1	147	0	0.20	148606.90
1	662	133	148	1	11033.33	159640.23

Reproduced with permission of the copyright owner. Further reproduction prohibited without permission.

Wagonhound North – 2

bed number	thickness (cm)	bin assignment	bin number	no. of beds per bin	ind. Time (yrs)	cum. Time (yrs)
116	41	9	1	6	683.33	683.33
115	44	9	2	16	4.40	687.73
114	93	19	3	13	1550.00	2237.73
113	1940	387	4	7	194.00	2431.73
112	32	7	5	10	533.33	2965.07
111	173	35	6	6	17.30	2982.37
110	77	16	7	6	1283.33	4265.70
109	13	3	8	2	1.30	4267.00
108	77	16	9	3	1283.33	5550.33
107	43	9	10	2	4.30	5554.63
106	204	41	11	1	3400.00	8954.63
105	34	7	12	0	3.40	8958.03
104	185	37	13	2	3083.33	12041.37
103	8	2	14	0	0.80	12042.17
102	119	24	15	2	1983.33	14026.50
101	19	4	16	4	1.90	14027.40
100	25	5	17	0	416.67	14444.07
99	14	3	18	0	1.40	14445.47
98	22	5	19	2	366.67	14812.13
97	13	3	20	0	1.30	14813.43
96	10	2	21	0	166.67	14980.10
95	15	3	22	1	1.50	14981.60
94	244	49	23	1	4066.67	19048.27
93	8	2	24	1	0.80	19049.07
92	77	16	25	0	1283.33	20332.40
91	19	4	26	0	1.90	20334.30
90	19	4	27	1	316.67	20650.97
89	26	6	28	2	2.60	20653.57
88	30	6	29	1	3.00	20656.57
87	239	48	30	1	3983.33	24639.90
86	12	3	31	0	1.20	24641.10
85	247	50	32	1	4116.67	28757.77
84	13	3	33	0	1.30	28759.07
83	33	7	34	1	550.00	29309.07
82	26	6	35	2	2.60	29311.67
81	533	107	36	0	8883.33	38195.00
80	12	3	37	2	1.20	38196.20
79	143	29	38	1	2383.33	40579.53
78	12	3	39	0	1.20	40580.73
77	108	22	40	0	1800.00	42380.73
76	24	5	41	2	2.40	42383.13
75	352	71	42	0	5866.67	48249.80
74	21	5	43	1	2.10	48251.90
73	211	43	44	0	3516.67	51768.57
72	6	2	45	0	0.60	51769.17
71	158	32	46	2	2633.33	54402.50
70	9	2	47	0	0.90	54403.40
69	226	46	48	1	3766.67	58170.07

Reproduced with permission of the copyright owner. Further reproduction prohibited without permission.

bed number	thickness (cm)	bin assignment	bin number	no. of beds per bin	ind. Time (yrs)	cum. Time (yrs)
68	10	2	49	1	1.00	58171.07
67	11	3	50	1	183.33	58354.40
66	16	4	51	0	1.60	58356.00
65	168	34	52	0	2800.00	61156.00
64	22	5	53	0	2.20	61158.20
63	11	3	54	0	183.33	61341.53
62	20	4	55	0	2.00	61343.53
61	14	3	56	0	233.33	61576.87
60	32	7	57	0	3.20	61580.07
59	30	6	58	0	500.00	62080.07
58	8	2	59	0	0.80	62080.87
57	74	15	60	0	1233.33	63314.20
56	4	1	61	0	0.40	63314.60
55	188	38	62	1	3133.33	66447.93
54	25	5	63	0	2.50	66450.43
53	111	23	64	0	1850.00	68300.43
52	34	7	65	0	3.40	68303.83
51	52	11	66	0	866.67	69170.50
50	11	3	67	0	1.10	69171.60
49	76	16	68	0	1266.67	70438.27
48	17	4	69	0	1.70	70439.97
47	93	19	70	0	1550.00	71989.97
46	24	5	71	1	2.40	71992.37
45	750	150	72	0	12500.00	84492.37
44	2752	551	73	0	275.20	84767.57
43	46	10	74	0	766.67	85534.23
42	23	5	75	0	2.30	85536.53
41	19	4	76	0	316.67	85853.20
40	22	5	77	0	2.20	85855.40
39	33	7	78	0	550.00	86405.40
38	23	5	79	0	2.30	86407.70
37	454	91	80	0	7566.67	93974.37
36	6	2	81	0	0.60	93974.97
35	185	37	82	0	3083.33	97058.30
34	4	1	83	0	0.40	97058.70
33	138	28	84	0	2300.00	99358.70
32	4	1	85	0	0.40	99359.10
31	72	15	86	0	1200.00	100559.10
30	3	1	87	0	0.30	100559.40
29	62	13	88	0	1033.33	101592.73
28	6	2	89	0	0.60	101593.33
27	50	10	90	0	833.33	102426.67
26	6	2	91	1	0.60	102427.27
25	206	42	92	0	3433.33	105860.60
24	28	6	93	0	2.80	105863.40
23	900	180	94	0	15000.00	120863.40
22	7	2	95	0	0.70	120864.10
21	527	108	96	0	8783.33	129647.43
20	8	2	97	0	0.80	129648.23

Reproduced with permission of the copyright owner. Further reproduction prohibited without permission.

bed number	thickness (cm)	bin assignment	bin number	no. of beds per bin	ind. Time (yrs)	cum. Time (yrs)
19	203	41	98	0	3383.33	133031.57
18	3	1	99	0	0.30	133031.87
17	30	6	100	0	500.00	133531.87
16	10	2	101	0	1.00	133532.87
15	229	46	102	0	3816.67	137349.53
14	4	1	103	0	0.40	137349.93
13	310	62	104	0	5166.67	142516.60
12	6	2	105	0	0.60	142517.20
11	147	30	106	1	2450.00	144967.20
10	7	2	107	1	0.70	144967.90
9	135	27	108	0	2250.00	147217.90
8	7	2	109	0	0.70	147218.60
7	174	35	110	0	2900.00	150118.60
6	62	13	111	0	6.20	150124.80
5	38	8	112	0	633.33	150758.13
4	13	3	113	0	1.30	150759.43
3	140	28	114	0	14.00	150773.43
2	1422	285	115	0	23700.00	174473.43
1	39	8	116	0	3.90	174477.33

Reproduced with permission of the copyright owner. Further reproduction prohibited without permission.

Wagonhound North – 3

bed number	thickness (cm)	bin assignment	bin number	no. of beds per bin	ind.time (yrs)	cum.time (yrs)
69	250	50	1	10	25.00	25.00
68	15	3	2	7	250.00	275.00
67	11	3	3	6	1.10	276.10
66	100	20	4	1	1666.67	1942.77
65	35	7	5	4	3.50	1946.27
64	410	82	6	3	6833.33	8779.60
63	25	5	7	2	2.50	8782.10
62	630	126	8	0	10500.00	19282.10
61	28	6	9	2	2.80	19284.90
60	645	129	10	1	10750.00	30034.90
59	30	6	11	1	3.00	30037.90
58	178	36	12	2	2966.67	33004.57
57	24	5	13	1	2.40	33006.97
56	525	105	14	0	8750.00	41756.97
55	8	2	15	0	0.80	41757.77
54	353	71	16	1	5883.33	47641.10
53	6	2	17	0	0.60	47641.70
52	430	86	18	0	7166.67	54808.37
51	60	12	19	0	6.00	54814.37
50	245	49	20	2	4083.33	58897.70
49	25	5	21	0	2.50	58900.20
48	205	41	22	2	3416.67	62316.87
47	30	6	23	0	3.00	62319.87
46	240	48	24	1	4000.00	66319.87
45	11	3	25	1	1.10	66320.97
44	435	87	26	0	7250.00	73570.97
43	45	9	27	0	4.50	73575.47
42	600	120	28	1	10000.00	83575.47
41	3	1	29	0	0.30	83575.77
40	63	13	30	0	1050.00	84625.77
39	3	1	31	0	0.30	84626.07
38	195	39	32	0	3250.00	87876.07
37	5	1	33	0	0.50	87876.57
36	35	7	34	0	583.33	88459.90
35	12	3	35	1	1.20	88461.10
34	80	16	36	2	1333.33	89794.43
33	20	4	37	0	2.00	89796.43
32	120	24	38	0	2000.00	91796.43
31	21	5	39	1	2.10	91798.53
30	42	9	40	0	4.20	91802.73
29	470	94	41	2	7833.33	99636.07
28	8	2	42	0	0.80	99636.87
27	176	36	43	0	2933.33	102570.20
26	12	3	44	0	1.20	102571.40
25	60	12	45	0	1000.00	103571.40
24	10	2	46	1	1.00	103572.40
23	100	20	47	0	1666.67	105239.07
22	10	2	48	1	1.00	105240.07

Reproduced with permission of the copyright owner. Further reproduction prohibited without permission.

bed number	thickness (cm)	bin assignment	bin number	no. of beds per bin	ind.time (yrs)	cum.time (yrs)
21	230	46	49	1	3833.33	109073.40
20	5	1	50	1	0.50	109073.90
19	110	22	51	0	1833.33	110907.23
18	3	1	52	0	0.30	110907.53
17	138	28	53	0	2300.00	113207.53
16	3	1	54	0	0.30	113207.83
15	110	22	55	0	1833.33	115041.17
14	12	3	56	0	1.20	115042.37
13	125	25	57	0	2083.33	117125.70
12	5	1	58	0	0.50	117126.20
11	54	11	59	0	900.00	118026.20
10	3	1	60	0	0.30	118026.50
9	589	118	61	0	9816.67	127843.17
8	7	2	62	0	0.70	127843.87
7	48	10	63	0	800.00	128643.87
6	2	1	64	0	0.20	128644.07
5	175	35	65	0	2916.67	131560.73
4	7	2	66	0	0.70	131561.43
3	204	41	67	0	3400.00	134961.43
2	3	1	68	0	0.30	134961.73
1	423	85	69	0	7050.00	142011.73

Reproduced with permission of the copyright owner. Further reproduction prohibited without permission.

Wagonhound South – 1

bed number	thickness (cm)	bin assignment	bin number	no. of beds per bin	indiv. Time (yrs)	cum. Time (yrs)
131	1050	210	1	11	105.00	105.00
130	60	12	2	12	1000.00	1105.00
129	113	23	3	7	11.30	1116.30
128	150	30	4	8	2500.00	3616.30
127	75	15	5	6	7.50	3623.80
126	150	30	6	4	2500.00	6123.80
125	20	4	7	4	2.00	6125.80
124	72	15	8	5	1200.00	7325.80
123	330	66	9	5	33.00	7358.80
122	150	30	10	4	2500.00	9858.80
121	198	40	11	3	19.80	9878.60
120	158	32	12	4	15.80	9894.40
119	25	5	13	3	416.67	10311.07
118	100	20	14	3	10.00	10321.07
117	602	121	15	5	10033.33	20354.40
116	20	4	16	1	2.00	20356.40
115	195	39	17	3	3250.00	23606.40
114	26	6	18	0	2.60	23609.00
113	242	49	19	1	4033.33	27642.33
112	17	4	20	1	1.70	27644.03
111	38	8	21	1	633.33	28277.37
110	13	3	22	1	1.30	28278.67
109	157	32	23	3	2616.67	30895.33
108	5	1	24	1	0.50	30895.83
107	125	25	25	1	2083.33	32979.17
106	10	2	26	3	1.00	32980.17
105	80	16	27	2	1333.33	34313.50
104	10	2	28	2	1.00	34314.50
103	84	17	29	1	1400.00	35714.50
102	30	6	30	5	3.00	35717.50
101	145	29	31	1	2416.67	38134.17
100	10	2	32	2	1.00	38135.17
99	55	11	33	0	916.67	39051.83
98	15	3	34	1	1.50	39053.33
97	75	15	35	0	1250.00	40303.33
96	4	1	36	0	0.40	40303.73
95	45	9	37	0	750.00	41053.73
94	60	12	38	1	6.00	41059.73
93	120	24	39	1	2000.00	43059.73
92	60	12	40	1	6.00	43065.73
91	92	19	41	0	1533.33	44599.07
90	15	3	42	0	1.50	44600.57
89	360	72	43	1	6000.00	50600.57
88	403	81	44	0	40.30	50640.87
87	242	49	45	0	24.20	50665.07
86	136	28	46	0	2266.67	52931.73
85	65	13	47	0	6.50	52938.23
84	20	4	48	0	333.33	53271.57

Reproduced with permission of the copyright owner. Further reproduction prohibited without permission.

bed number	thickness (cm)	bin assignment	bin number	no. of beds per bin	ind.time (yrs)	cum.time (yrs)
83	70	14	49	2	7.00	53278.57
82	130	26	50	0	2166.67	55445.23
81	45	9	51	0	4.50	55449.73
80	55	11	52	0	916.67	56366.40
79	35	7	53	0	3.50	56369.90
78	47	10	54	0	783.33	57153.23
77	8	2	55	0	0.80	57154.03
76	15	3	56	0	250.00	57404.03
75	85	17	57	0	8.50	57412.53
74	25	5	58	0	416.67	57829.20
73	45	9	59	0	4.50	57833.70
72	40	8	60	0	4.00	57837.70
71	110	22	61	0	11.00	57848.70
70	130	26	62	0	13.00	57861.70
69	70	14	63	0	7.00	57868.70
68	35	7	64	0	3.50	57872.20
67	190	38	65	0	3166.67	61038.87
66	45	9	66	1	4.50	61043.37
65	135	27	67	0	2250.00	63293.37
64	138	28	68	0	13.80	63307.17
63	112	23	69	0	1866.67	65173.83
62	65	13	70	0	6.50	65180.33
61	39	8	71	0	650.00	65830.33
60	70	14	72	1	7.00	65837.33
59	8	2	73	0	133.33	65970.67
58	74	15	74	1	7.40	65978.07
57	25	5	75	1	416.67	66394.73
56	7	2	76	0	0.70	66395.43
55	20	4	77	1	2.00	66397.43
54	30	6	78	0	500.00	66897.43
53	84	17	79	0	8.40	66905.83
52	114	23	80	0	1900.00	68805.83
51	23	5	81	1	2.30	68808.13
50	25	5	82	0	2.50	68810.63
49	35	7	83	0	583.33	69393.97
48	25	5	84	0	2.50	69396.47
47	47	10	85	0	783.33	70179.80
46	10	2	86	0	1.00	70180.80
45	45	9	87	0	4.50	70185.30
44	15	3	88	0	250.00	70435.30
43	39	8	89	0	3.90	70439.20
42	381	77	90	0	6350.00	76789.20
41	8	2	91	0	0.80	76790.00
40	10	2	92	1	166.67	76956.67
39	16	4	93	0	1.60	76958.27
38	610	122	94	0	10166.67	87124.93
37	4	1	95	0	0.40	87125.33
36	16	4	96	0	266.67	87392.00
35	4	1	97	0	0.40	87392.40
34	368	74	98	0	6133.33	93525.73

Reproduced with permission of the copyright owner. Further reproduction prohibited without permission.

bed number	thickness (cm)	bin assignment	bin number	no. of beds per bin	ind.time (yrs)	cum.time (yrs)
33	4	1	99	0	0.40	93526.13
32	150	30	100	0	2500.00	96026.13
31	7	2	101	0	0.70	96026.83
30	215	43	102	0	3583.33	99610.17
29	20	4	103	0	2.00	99612.17
28	154	31	104	0	2566.67	102178.83
27	3	1	105	0	0.30	102179.13
26	5	1	106	0	83.33	102262.47
25	7	2	107	0	0.70	102263.17
24	103	21	108	0	1716.67	103979.83
23	3	1	109	0	0.30	103980.13
22	62	13	110	0	1033.33	105013.47
21	2	1	111	0	0.20	105013.67
20	4	1	112	0	66.67	105080.33
19	2	1	113	0	0.20	105080.53
18	166	34	114	0	2766.67	107847.20
17	9	2	115	0	0.90	107848.10
16	73	15	116	0	1216.67	109064.77
15	35	7	117	0	3.50	109068.27
14	126	26	118	0	2100.00	111168.27
13	40	8	119	0	4.00	111172.27
12	15	3	120	0	1.50	111173.77
11	50	10	121	1	5.00	111178.77
10	150	30	122	1	2500.00	113678.77
9	55	11	123	0	5.50	113684.27
8	133	27	124	0	2216.67	115900.93
7	47	10	125	0	4.70	115905.63
6	373	75	126	0	6216.67	122122.30
5	14	3	127	0	1.40	122123.70
4	460	92	128	0	7666.67	129790.37
3	58	12	129	0	5.80	129796.17
2	30	6	130	0	500.00	130296.17
1	853	171	131	0	85.30	130381.47

Reproduced with permission of the copyright owner. Further reproduction prohibited without permission.

Wagonhound South – 2

bed number	thickness (cm)	bin assignment	bin number	no. of beds per bin	ind. Time (yrs)	cum. Time (yrs)
142	2347	470	1	27	234.70	234.70
141	112	23	2	13	1866.67	2101.37
140	326	65	3	7	32.60	2133.97
139	193	39	4	7	3216.67	5350.53
138	846	170	5	5	84.60	5435.13
137	61	13	6	8	6.10	5441.23
136	159	32	7	3	2650.00	8091.23
135	12	3	8	2	1.20	8092.43
134	88	18	9	3	1466.67	9559.10
133	8	2	10	5	0.80	9559.90
132	210	42	11	4	21.00	9580.90
131	146	30	12	2	14.60	9595.50
130	661	133	13	3	66.10	9661.60
129	27	6	14	2	2.70	9664.30
128	156	32	15	3	2600.00	12264.30
127	442	89	16	3	44.20	12308.50
126	205	41	17	4	3416.67	15725.17
125	163	33	18	2	16.30	15741.47
124	259	52	19	1	25.90	15767.37
123	19	4	20	2	1.90	15769.27
122	269	54	21	0	26.90	15796.17
121	46	10	22	0	4.60	15800.77
120	178	36	23	2	17.80	15818.57
119	340	68	24	2	5666.67	21485.23
118	269	54	25	1	26.90	21512.13
117	84	17	26	1	1400.00	22912.13
116	30	6	27	0	3.00	22915.13
115	217	44	28	0	21.70	22936.83
114	79	16	29	1	7.90	22944.73
113	49	10	30	2	816.67	23761.40
112	120	24	31	0	12.00	23773.40
111	118	24	32	3	11.80	23785.20
110	16	4	33	1	1.60	23786.80
109	86	18	34	1	8.60	23795.40
108	26	6	35	0	2.60	23798.00
107	122	25	36	1	12.20	23810.20
106	28	6	37	0	2.80	23813.00
105	60	12	38	0	1000.00	24813.00
104	53	11	39	1	5.30	24818.30
103	73	15	40	0	1216.67	26034.97
102	31	7	41	1	3.10	26038.07
101	40	8	42	2	666.67	26704.73
100	70	14	43	1	7.00	26711.73
99	100	20	44	1	10.00	26721.73
98	29	6	45	0	2.90	26724.63
97	96	20	46	0	9.60	26734.23
96	46	10	47	0	4.60	26738.83

Reproduced with permission of the copyright owner. Further reproduction prohibited without permission.

bed number	thickness (cm)	bin assignment	bin number	no. of beds per bin	ind.time (yrs)	cum.time (yrs)
95	210	42	48	0	21.00	26759.83
94	20	4	49	1	2.00	26761.83
93	68	14	50	1	6.80	26768.63
92	157	32	51	0	2616.67	29385.30
91	145	29	52	2	14.50	29399.80
90	63	13	53	0	1050.00	30449.80
89	44	9	54	2	4.40	30454.20
88	115	23	55	0	11.50	30465.70
87	52	11	56	0	866.67	31332.37
86	22	5	57	1	2.20	31334.57
85	2	1	58	1	33.33	31367.90
84	9	2	59	0	0.90	31368.80
83	25	5	60	0	416.67	31785.47
82	10	2	61	0	1.00	31786.47
81	71	15	62	0	1183.33	32969.80
80	21	5	63	0	2.10	32971.90
79	3	1	64	0	50.00	33021.90
78	15	3	65	1	1.50	33023.40
77	9	2	66	0	150.00	33173.40
76	29	6	67	0	2.90	33176.30
75	19	4	68	1	316.67	33492.97
74	54	11	69	0	5.40	33498.37
73	249	50	70	0	4150.00	37648.37
72	13	3	71	0	1.30	37649.67
71	244	49	72	0	4066.67	41716.33
70	3	1	73	0	0.30	41716.63
69	283	57	74	0	4716.67	46433.30
68	47	10	75	0	4.70	46438.00
67	85	17	76	1	1416.67	47854.67
66	21	5	77	0	2.10	47856.77
65	35	7	78	0	583.33	48440.10
64	9	2	79	0	0.90	48441.00
63	78	16	80	0	1300.00	49741.00
62	6	2	81	0	0.60	49741.60
61	212	43	82	0	3533.33	53274.93
60	22	5	83	0	2.20	53277.13
59	20	4	84	0	333.33	53610.47
58	3	1	85	0	0.30	53610.77
57	377	76	86	0	6283.33	59894.10
56	8	2	87	0	0.80	59894.90
55	39	8	88	0	650.00	60544.90
54	3	1	89	1	0.30	60545.20
53	14	3	90	0	233.33	60778.53
52	10	2	91	0	1.00	60779.53
51	290	58	92	0	4833.33	65612.87
50	2	1	93	0	0.20	65613.07
49	42	8	94	0	700.00	66313.07
48	14	3	95	0	1.40	66314.47
47	75	15	96	0	1250.00	67564.47

Reproduced with permission of the copyright owner. Further reproduction prohibited without permission.

bed number	thickness (cm)	bin assignment	bin number	no. of beds per bin	ind.time (yrs)	cum.time (yrs)
46	7	2	97	0	0.70	67565.17
45	44	9	98	0	733.33	68298.50
44	2	1	99	0	0.20	68298.70
43	150	30	100	0	2500.00	70798.70
42	6	2	101	0	0.60	70799.30
41	92	19	102	0	1533.33	72332.63
40	2	1	103	0	0.20	72332.83
39	170	34	104	0	17.00	72349.83
38	3	1	105	0	0.30	72350.13
37	1	1	106	0	16.67	72366.80
36	2	1	107	0	0.20	72367.00
35	128	26	108	0	12.80	72379.80
34	3	1	109	0	0.30	72380.10
33	32	7	110	0	3.20	72383.30
32	3	1	111	0	0.30	72383.60
31	5	1	112	0	0.50	72384.10
30	2	1	113	0	0.20	72384.30
29	29	6	114	0	2.90	72387.20
28	2	1	115	0	0.20	72387.40
27	16	4	116	0	266.67	72654.07
26	3	1	117	0	0.30	72654.37
25	2	1	118	0	33.33	72687.70
24	3	1	119	0	0.30	72688.00
23	2	1	120	0	33.33	72721.33
22	4	1	121	0	0.40	72721.73
21	83	17	122	0	8.30	72730.03
20	260	52	123	0	4333.33	77063.37
19	85	17	124	0	8.50	77071.87
18	17	4	125	0	283.33	77355.20
17	4	1	126	0	0.40	77355.60
16	51	11	127	0	850.00	78205.60
15	7	2	128	0	0.70	78206.30
14	59	12	129	0	983.33	79189.63
13	11	3	130	0	1.10	79190.73
12	4	1	131	0	66.67	79257.40
11	2	1	132	0	0.20	79257.60
10	79	16	133	1	1316.67	80574.27
9	6	2	134	0	0.60	80574.87
8	64	13	135	0	1066.67	81641.53
7	13	3	136	0	1.30	81642.83
6	10	2	137	0	1.00	81643.83
5	3	1	138	0	0.30	81644.13
4	2	1	139	0	33.33	81677.47
3	4	1	140	0	0.40	81677.87
2	48	10	141	0	800.00	82477.87
1	27	6	142	0	2.70	82480.57

Reproduced with permission of the copyright owner. Further reproduction prohibited without permission.

Wagonhound South – 3

bed number	thickness (cm)	bin assignment	bin number	no. of beds per bin	ind. Time (yrs)	cum. Time (yrs)
136	750	150	1	19	75.00	75.00
137	820	164	2	15	82.00	157.00
136	600	120	3	8	60.00	217.00
136	640	128	4	8	64.00	281.00
134	90	18	5	7	9.00	290.00
133	430	86	6	11	43.00	333.00
132	410	82	7	2	41.00	374.00
131	60	12	8	8	6.00	380.00
130	60	12	9	4	6.00	386.00
129	520	104	10	4	52.00	438.00
128	16	4	11	2	1.60	439.60
127	80	16	12	8	1333.33	1772.93
126	95	19	13	6	9.50	1782.43
125	280	56	14	1	28.00	1810.43
124	230	46	15	3	23.00	1833.43
123	30	6	16	2	500.00	2333.43
122	40	8	17	1	4.00	2337.43
121	130	26	18	1	13.00	2350.43
120	15	3	19	3	1.50	2351.93
119	45	9	20	1	750.00	3101.93
118	28	6	21	0	2.80	3104.73
117	40	8	22	1	666.67	3771.40
116	15	3	23	0	1.50	3772.90
115	65	13	24	0	6.50	3779.40
114	10	2	25	1	1.00	3780.40
113	60	12	26	2	1000.00	4780.40
112	48	10	27	1	4.80	4785.20
111	60	12	28	1	1000.00	5785.20
110	30	6	29	0	3.00	5788.20
109	25	5	30	1	416.67	6204.87
108	50	10	31	0	5.00	6209.87
107	65	13	32	1	1083.33	7293.20
106	12	3	33	0	1.20	7294.40
105	2	1	34	0	0.20	7294.60
104	130	26	35	0	2166.67	9461.27
103	7	2	36	0	0.70	9461.97
102	50	10	37	1	833.33	10295.30
101	12	3	38	2	1.20	10296.50
100	30	6	39	0	500.00	10796.50
99	8	2	40	0	0.80	10797.30
98	10	2	41	0	166.67	10963.97
97	6	2	42	1	0.60	10964.57
96	30	6	43	0	500.00	11464.57
95	22	5	44	0	2.20	11466.77
94	25	5	45	1	416.67	11883.43
93	5	1	46	1	0.50	11883.93
92	60	12	47	0	1000.00	12883.93

Reproduced with permission of the copyright owner. Further reproduction prohibited without permission.

bed number	thickness (cm)	bin assignment	bin number	no. of beds per bin	ind.time (yrs)	cum.time (yrs)
91	60	12	48	1	6.00	12889.93
90	110	22	49	0	1833.33	14723.27
89	40	8	50	0	4.00	14727.27
88	20	4	51	0	333.33	15060.60
87	20	4	52	0	2.00	15062.60
86	16	4	53	0	266.67	15329.27
85	30	6	54	0	3.00	15332.27
84	225	45	55	0	22.50	15354.77
83	44	9	56	2	4.40	15359.17
82	62	13	57	0	1033.33	16392.50
81	5	1	58	0	0.50	16393.00
80	98	20	59	0	1633.33	18026.33
79	7	2	60	0	0.70	18027.03
78	28	6	61	0	466.67	18493.70
77	8	2	62	0	0.80	18494.50
76	140	28	63	0	2333.33	20827.83
75	4	1	64	0	0.40	20828.23
74	156	32	65	0	2600.00	23428.23
73	15	3	66	0	1.50	23429.73
72	93	19	67	0	1550.00	24979.73
71	5	1	68	0	0.50	24980.23
70	55	11	69	0	916.67	25896.90
69	23	5	70	0	2.30	25899.20
68	60	12	71	0	1000.00	26899.20
67	12	3	72	0	1.20	26900.40
66	58	12	73	0	966.67	27867.07
65	18	4	74	0	1.80	27868.87
64	72	15	75	0	1200.00	29068.87
63	7	2	76	0	0.70	29069.57
62	185	37	77	0	3083.33	32152.90
61	4	1	78	0	0.40	32153.30
60	240	48	79	0	4000.00	36153.30
59	40	8	80	0	4.00	36157.30
58	280	56	81	0	4666.67	40823.97
57	35	7	82	1	3.50	40827.47
56	85	17	83	0	1416.67	42244.13
55	35	7	84	0	3.50	42247.63
54	80	16	85	0	8.00	42255.63
53	8	2	86	1	0.80	42256.43
52	190	38	87	0	3166.67	45423.10
51	14	3	88	0	1.40	45424.50
50	150	30	89	0	2500.00	47924.50
49	22	5	90	0	2.20	47926.70
48	95	19	91	0	1583.33	49510.03
47	20	4	92	0	2.00	49512.03
46	190	38	93	0	19.00	49531.03
45	38	8	94	0	3.80	49534.83
44	208	42	95	0	20.80	49555.63
43	25	5	96	0	2.50	49558.13

Reproduced with permission of the copyright owner. Further reproduction prohibited without permission.

bed number	thickness (cm)	bin assignment	bin number	no. of beds per bin	ind.time (yrs)	cum.time (yrs)
42	125	25	97	0	12.50	49570.63
41	10	2	98	0	1.00	49571.63
40	75	15	99	0	1250.00	50821.63
39	30	6	100	0	3.00	50824.63
38	45	9	101	0	4.50	50829.13
37	37	8	102	0	616.67	51445.80
36	45	9	103	0	4.50	51450.30
35	50	10	104	1	833.33	52283.63
34	30	6	105	0	3.00	52286.63
33	65	13	106	0	6.50	52293.13
32	75	15	107	0	1250.00	53543.13
31	5	1	108	0	0.50	53543.63
30	135	27	109	0	2250.00	55793.63
29	5	1	110	0	0.50	55794.13
28	25	5	111	0	416.67	56210.80
27	3	1	112	0	0.30	56211.10
26	64	13	113	0	1066.67	57277.77
25	6	2	114	0	0.60	57278.37
24	26	6	115	0	433.33	57711.70
23	5	1	116	0	0.50	57712.20
22	65	13	117	0	1083.33	58795.53
21	5	1	118	0	0.50	58796.03
20	68	14	119	0	1133.33	59929.37
19	3	1	120	1	0.30	59929.67
18	20	4	121	0	333.33	60263.00
17	4	1	122	0	0.40	60263.40
16	54	11	123	0	900.00	61163.40
15	3	1	124	0	0.30	61163.70
14	15	3	125	0	250.00	61413.70
13	5	1	126	0	0.50	61414.20
12	40	8	127	0	666.67	62080.87
11	3	1	128	1	0.30	62081.17
10	18	4	129	0	300.00	62381.17
9	6	2	130	0	0.60	62381.77
8	6	2	131	0	100.00	62481.77
7	2	1	132	0	0.20	62481.97
6	40	8	133	0	666.67	63148.63
5	8	2	134	0	0.80	63149.43
4	30	6	135	0	500.00	63649.43
3	4	1	136	0	0.40	63649.83
2	6	2	137	0	100.00	63749.83
1	4	1	138	0	0.40	63750.23

Reproduced with permission of the copyright owner. Further reproduction prohibited without permission.

Wagonhound East – 1

bed number	thickness (cm)	bin assignment	bin number	no. of beds per bin	ind. Time (yrs)	cum. Time (yrs)
51	605	121	1	1	60.50	60.50
50	1470	293	2	7	147.00	207.50
49	70	14	3	1	1166.67	1374.17
48	10	2	4	5	1.00	1375.17
47	60	12	5	5	1000.00	2375.17
46	8	2	6	4	0.80	2375.97
45	80	16	7	0	1333.33	3709.30
44	19	4	8	0	1.90	3711.20
43	25	5	9	0	416.67	4127.87
42	22	5	10	0	2.20	4130.07
41	25	5	11	1	416.67	4546.73
40	22	5	12	2	2.20	4548.93
39	30	6	13	0	500.00	5048.93
38	6	2	14	1	0.60	5049.53
37	200	40	15	0	3333.33	8382.87
36	7	2	16	3	0.70	8383.57
35	100	20	17	0	10.00	8393.57
34	19	4	18	1	1.90	8395.47
33	250	50	19	1	25.00	8420.47
32	110	22	20	2	1833.33	10253.80
31	210	42	21	0	21.00	10274.80
30	92	19	22	2	1533.33	11808.13
29	10	2	23	0	1.00	11809.13
28	30	6	24	0	500.00	12309.13
27	18	4	25	0	1.80	12310.93
26	412	83	26	0	6866.67	19177.60
25	30	6	27	0	3.00	19180.60
24	108	22	28	0	1800.00	20980.60
23	80	16	29	2	8.00	20988.60
22	90	18	30	0	1500.00	22488.60
21	55	11	31	0	5.50	22494.10
20	450	90	32	0	7500.00	29994.10
19	78	16	33	0	7.80	30001.90
18	325	65	34	0	5416.67	35418.57
17	2320	464	35	0	232.00	35650.57
16	295	59	36	0	4916.67	40567.23
15	25	5	37	0	2.50	40569.73
14	145	29	38	0	2416.67	42986.40
13	8	2	39	0	0.80	42987.20
12	60	12	40	1	1000.00	43987.20
11	7	2	41	0	0.70	43987.90
10	440	88	42	1	7333.33	51321.23
9	17	4	43	0	1.70	51322.93
8	145	29	44	0	2416.67	53739.60
7	20	4	45	0	2.00	53741.60
6	300	60	46	0	5000.00	58741.60
5	5	1	47	0	0.50	58742.10
4	30	6	48	0	500.00	59242.10

Reproduced with permission of the copyright owner. Further reproduction prohibited without permission.

bed number	thickness (cm)	bin assignment	bin number	no. of beds per bin	ind.time (yrs)	cum.time (yrs)
3	12	3	49	0	1.20	59243.30
2	660	132	50	1	11000.00	70243.30
1	100	20	51	0	10.00	70253.30

Reproduced with permission of the copyright owner. Further reproduction prohibited without permission.

Wagonhound East – 2

bed number	thickness (cm)	bin assignment	bin number	ind. Time (yrs)	cum. Time (yrs)
201	469	94	1	46.90	46.90
200	369	74	2	36.90	83.80
199	60	12	3	6.00	89.80
198	169	34	4	2816.67	2906.47
197	59	12	5	5.90	2912.37
196	122	25	6	2033.33	4945.70
195	22	5	7	2.20	4947.90
194	153	31	8	2550.00	7497.90
193	40	8	9	4.00	7501.90
192	158	32	10	2633.33	10135.23
191	7	2	11	0.70	10135.93
190	6	2	12	100.00	10235.93
189	6	2	13	0.60	10236.53
188	10	2	14	166.67	10403.20
187	7	2	15	0.70	10403.90
186	148	30	16	2466.67	12870.57
185	8	2	17	0.80	12871.37
184	20	4	18	333.33	13204.70
183	16	4	19	1.60	13206.30
182	205	41	20	3416.67	16622.97
181	4	1	21	0.40	16623.37
180	55	11	22	916.67	17540.03
179	5	1	23	0.50	17540.53
178	92	19	24	1533.33	19073.87
177	4	1	25	0.40	19074.27
176	20	4	26	333.33	19407.60
175	3	1	27	0.30	19407.90
174	60	12	28	1000.00	20407.90
173	10	2	29	1.00	20408.90
172	40	8	30	666.67	21075.57
171	15	3	31	1.50	21077.07
170	138	28	32	2300.00	23377.07
169	30	6	33	3.00	23380.07
168	100	20	34	1666.67	25046.73
167	8	2	35	0.80	25047.53
166	72	15	36	1200.00	26247.53
165	18	4	37	1.80	26249.33
164	125	25	38	2083.33	28332.67
163	3	1	39	0.30	28332.97
162	40	8	40	666.67	28999.63
161	6	2	41	0.60	29000.23
160	150	30	42	15.00	29015.23
159	12	3	43	1.20	29016.43
158	8	2	44	133.33	29149.77
157	7	2	45	0.70	29150.47
156	136	28	46	2266.67	31417.13
155	4	1	47	0.40	31417.53
154	120	24	48	2000.00	33417.53

Reproduced with permission of the copyright owner. Further reproduction prohibited without permission.

bed number	thickness (cm)	bin assignment	bin number	no. of beds per bin	ind.time (yrs)
153	8	2	49	0.80	33418.33
152	105	21	50	1750.00	35168.33
151	16	4	51	1.60	35169.93
150	10	2	52	166.67	35336.60
149	48	10	53	4.80	35341.40
148	70	14	54	1166.67	36508.07
147	5	1	55	0.50	36508.57
146	140	28	56	2333.33	38841.90
145	10	2	57	1.00	38842.90
144	20	4	58	333.33	39176.23
143	14	3	59	1.40	39177.63
142	62	13	60	1033.33	40210.97
141	12	3	61	1.20	40212.17
140	78	16	62	1300.00	41512.17
139	8	2	63	0.80	41512.97
138	167	34	64	2783.33	44296.30
137	6	2	65	0.60	44296.90
136	416	84	66	6933.33	51230.23
135	18	4	67	1.80	51232.03
134	130	26	68	13.00	51245.03
133	25	5	69	2.50	51247.53
132	250	50	70	4166.67	55414.20
131	26	6	71	2.60	55416.80
130	250	50	72	4166.67	59583.47
129	22	5	73	2.20	59585.67
128	220	44	74	3666.67	63252.33
127	4	1	75	0.40	63252.73
126	25	5	76	416.67	63669.40
125	12	3	77	1.20	63670.60
124	8	2	78	133.33	63803.93
123	10	2	79	1.00	63804.93
122	10	2	80	166.67	63971.60
121	12	3	81	1.20	63972.80
120	38	8	82	633.33	64606.13
119	13	3	83	1.30	64607.43
118	365	73	84	6083.33	70690.77
117	20	4	85	2.00	70692.77
116	35	7	86	583.33	71276.10
115	170	34	87	17.00	71293.10
114	666	134	88	11133.33	82426.43
113	36	8	89	3.60	82430.03
112	168	34	90	2800.00	85230.03
111	38	8	91	3.80	85233.83
110	433	87	92	43.30	85277.13
109	35	7	93	3.50	85280.63
108	142	29	94	2366.67	87647.30
107	27	6	95	2.70	87650.00
106	147	30	96	14.70	87664.70
105	156	32	97	15.60	87680.30
104	32	7	98	3.20	87683.50

Reproduced with permission of the copyright owner. Further reproduction prohibited without permission.

bed number	thickness (cm)	bin assignment	bin number	no. of beds per bin	ind.time (yrs)
103	27	6	99	2.70	87686.20
102	297	60	100	29.70	87715.90
101	70	14	101	7.00	87722.90
100	28	6	102	2.80	87725.70
99	25	5	103	2.50	87728.20
98	1	1	104	16.67	87744.87
97	13	3	105	1.30	87746.17
96	2	1	106	33.33	87779.50
95	27	6	107	2.70	87782.20
94	3	1	108	50.00	87832.20
93	9	2	109	0.90	87833.10
92	17	4	110	1.70	87834.80
91	17	4	111	1.70	87836.50
90	14	3	112	233.33	88069.83
89	43	9	113	4.30	88074.13
88	5	1	114	83.33	88157.47
87	47	10	115	4.70	88162.17
86	10	2	116	166.67	88328.83
85	39	8	117	3.90	88332.73
84	4	1	118	0.40	88333.13
83	7	2	119	0.70	88333.83
82	1	1	120	16.67	88350.50
81	4	1	121	0.40	88350.90
80	3	1	122	50.00	88400.90
79	12	3	123	1.20	88402.10
78	25	5	124	416.67	88818.77
77	15	3	125	1.50	88820.27
76	5	1	126	83.33	88903.60
75	19	4	127	1.90	88905.50
74	3	1	128	50.00	88955.50
73	6	2	129	0.60	88956.10
72	3	1	130	50.00	89006.10
71	30	6	131	3.00	89009.10
70	5			83.33	89092.43
69	6	1	132	0.60	89093.03
68	1	2	133	16.67	89109.70
67	6	2	134	0.60	89110.30
66	20	4	135	2.00	89112.30
65	11	3	136	183.33	89295.63
64	8	2	137	0.80	89296.43
63	30	6	138	3.00	89299.43
62	2	1	139	33.33	89332.77
61	6	2	140	0.60	89333.37
60	6	2	141	100.00	89433.37
59	14	3	142	1.40	89434.77
58	7	2	143	116.67	89551.43
57	11	3	144	1.10	89552.53
56	142	29	145	2366.67	91919.20
55	14	3	146	1.40	91920.60
54	20	4	147	333.33	92253.93

Reproduced with permission of the copyright owner. Further reproduction prohibited without permission.

bed number	thickness (cm)	bin assignment	bin number	no. of beds per bin	ind.time (yrs)
53	11	3	148	1.10	92255.03
52	8	2	149	133.33	92388.37
51	11	3	150	1.10	92389.47
50	13	3	151	1.30	92390.77
49	14	3		233.33	92624.10
48	16	4		1.60	92625.70
47	86	18		1433.33	94059.03
46	13	3		1.30	94060.33
45	39	8		650.00	94710.33
44	10	2		1.00	94711.33
43	11	3		183.33	94894.67
42	12	3		1.20	94895.87
41	38	8		633.33	95529.20
40	13	8		1.30	95530.50
39	69	14		1150.00	96680.50
38	138	28		13.80	96694.30
37	120	24		12.00	96706.30
36	10	2		1.00	96707.30
35	13	3		1.30	96708.60
34	19	4		316.67	97025.27
33	63	13		6.30	97031.57
32	31	7		516.67	97548.23
31	33	7		3.30	97551.53
30	630	126		10500.00	108051.53
29	10	2		1.00	108052.53
28	578	116		9633.33	117685.87
27	7	2		0.70	117686.57
26	85	17		1416.67	119103.23
25	22	5		2.20	119105.43
24	142	29		2366.87	121472.10
23	18	4		1.80	121473.90
22	800	160		13333.33	134807.23
21	24	5		2.40	134809.63
20	352	71		5866.67	140676.30
19	20	4		2.00	140678.30
18	22	5		366.67	141044.97
17	15	3		1.50	141046.47
16	705	141		11750.00	152796.47
15	10	2		1.00	152797.47
14	130	26		2166.67	154964.13
13	5	1		0.50	154964.63
12	94	19		1566.67	156531.30
11	25	5		2.50	156533.80
10	25	5		416.67	156950.47
9	7	2		0.70	156951.17
8	91	19		1516.67	158467.83
7	3	1		0.30	158468.13
6	57	12		950.00	159418.13
5	3	1		0.30	159418.43
4	220	44		3666.67	163085.10

Reproduced with permission of the copyright owner. Further reproduction prohibited without permission.

bed number	thickness (cm)	bin assignment	bin number	no. of beds per bin	ind.time (yrs)
3	6	2		0.60	163085.70
2	230	46		3833.33	166919.03
1	110	22		11.00	166930.03

Reproduced with permission of the copyright owner. Further reproduction prohibited without permission.

Wagonhound East – 3

bed number	thickness (cm)	bin assignment	bin number	no. of beds per bin	ind. Time (yrs)	cum. Time (yrs)
62	1579	316	1	0	157.90	157.90
61	15	3	2	5	1.50	159.40
60	12	3	3	7	200.00	359.40
59	9	2	4	4	0.90	360.30
58	115	23	5	3	11.50	371.80
57	16	4	6	2	1.60	373.40
56	78	16	7	3	1300.00	1673.40
55	15	3	8	1	1.50	1674.90
54	849	170	9	1	84.90	1759.80
53	25	5	10	0	2.50	1762.30
52	252	51	11	0	25.20	1787.50
51	8	2	12	1	0.80	1788.30
50	243	49	13	0	24.30	1812.60
49	29	6	14	1	2.90	1815.50
48	320	64	15	0	32.00	1847.50
47	77	16	16	3	7.70	1855.20
46	125	25	17	0	12.50	1867.70
45	10	2	18	1	1.00	1868.70
44	578	116	19	0	57.80	1926.50
43	10	2	20	4	1.00	1927.50
42	206	42	21	0	20.60	1948.10
41	40	8	22	0	4.00	1952.10
40	285	57	23	1	28.50	1980.60
39	10	2	24	0	1.00	1981.60
38	373	75	25	1	37.30	2018.90
37	22	5	26	2	2.20	2021.10
36	162	33	27	1	16.20	2037.30
35	130	26	28	0	13.00	2050.30
34	267	54	29	0	26.70	2077.00
33	126	26	30	1	12.60	2089.60
32	418	84	31	0	41.80	2131.40
31	22	5	32	1	2.20	2133.60
30	33	7	33	1	550.00	2683.60
29	18	4	34	1	1.80	2685.40
28	35	7	35	0	583.33	3268.73
27	274	55	36	0	27.40	3296.13
26	146	30	37	0	14.60	3310.73
25	66	14	38	0	6.60	3317.33
24	321	65	39	0	32.10	3349.43
23	134	27	40	0	13.40	3362.83
22	96	20	41	0	1600.00	4962.83
21	159	32	42	1	15.90	4978.73
20	554	111	43	0	55.40	5034.13
19	99	20	44	0	9.90	5044.03
18	168	34	45	0	2800.00	7844.03
17	87	18	46	0	8.70	7852.73
16	290	58	47	0	29.00	7881.73

Reproduced with permission of the copyright owner. Further reproduction prohibited without permission.

bed number	thickness (cm)	bin assignment	bin number	no. of beds Per bin	ind. Time (yrs)	cum. Time (yrs)
15	45	9	48	0	750.00	8631.73
14	98	20	49	1	9.80	8641.53
13	817	164	50	0	13616.67	22258.20
12	27	6	51	1	2.70	22260.90
11	31	7	52	0	516.67	22777.57
10	11	3	53	0	1.10	22778.67
9	17	4	54	1	283.33	23062.00
8	14	3	55	1	1.40	23063.40
7	60	12	56	0	1000.00	24063.40
6	19	4	57	1	1.90	24065.30
5	79	16	58	1	1316.67	25381.97
4	15	3	59	0	1.50	25383.47
3	98	20	60	0	1633.33	27016.80
2	13	3	61	0	1.30	27018.10
1	1500	300	62	0	25000.00	52018.10

Reproduced with permission of the copyright owner. Further reproduction prohibited without permission.

Wagonhound East – 4

bed number	thickness (cm)	bin assignment	bin number	no. of beds per bin	ind. Time (yrs)	cum. Time (yrs)
79	950	190	1	10	95.00	95.00
78	1600	320	2	17	160.00	255.00
77	100	20	3	7	10.00	265.00
76	150	30	4	1	2500.00	2765.00
75	12	3	5	1	1.20	2766.20
74	200	40	6	2	3333.33	6099.53
73	25	5	7	0	2.50	6102.03
72	200	40	8	0	20.00	6122.03
71	320	64	9	0	5333.33	11455.37
70	5	1	10	0	0.50	11455.87
69	150	30	11	0	2500.00	13955.87
68	7	2	12	1	0.70	13956.57
67	108	22	13	4	1800.00	15756.57
66	3	1	14	0	0.30	15756.87
65	145	29	15	0	2416.67	18173.53
64	10	2	16	1	1.00	18174.53
63	201	41	17	0	3350.00	21524.53
62	15	3	18	1	1.50	21526.03
61	65	13	19	0	1083.33	22609.37
60	3	1	20	2	0.30	22609.67
59	65	13	21	0	1083.33	23693.00
58	4	1	22	1	0.40	23693.40
57	10	2	23	0	166.67	23860.07
56	4	1	24	1	0.40	23860.47
55	300	60	25	2	30.00	23890.47
54	6	2	26	0	0.60	23891.07
53	170	34	27	1	2833.33	26724.40
52	4	1	28	0	0.40	26724.80
51	90	18	29	1	1500.00	28224.80
50	8	2	30	6	0.80	28225.60
49	63	13	31	0	1050.00	29275.60
48	8	2	32	0	0.80	29276.40
47	80	16	33	1	1333.33	30609.73
46	4	1	34	1	0.40	30610.13
45	98	20	35	0	1633.33	32243.47
44	15	3	36	1	1.50	32244.97
43	443	89	37	0	7383.33	39628.30
42	10	2	38	0	1.00	39629.30
41	10	2	39	0	166.67	39795.97
40	8	2	40	2	0.80	39796.77
39	150	30	41	1	2500.00	42296.77
38	5	1	42	0	0.50	42297.27
37	125	25	43	0	2083.33	44380.60
36	4	1	44	0	0.40	44381.00
35	150	30	45	0	2500.00	46881.00
34	7	2	46	0	0.70	46881.70
33	12	3	47	0	200.00	47081.70

Reproduced with permission of the copyright owner. Further reproduction prohibited without permission.

bed number	thickness (cm)	bin assignment	bin number	no. of beds Per bin	ind. Time (yrs)	cum. Time (yrs)
32	3	1	48	1	0.30	47082.00
31	420	84	49	0	7000.00	54082.00
30	19	4	50	0	1.90	54083.90
29	30	6	51	0	500.00	54583.90
28	10	2	52	0	1.00	54584.90
27	15	3	53	0	250.00	54834.90
26	10	2	54	0	1.00	54835.90
25	407	82	55	0	6783.33	61619.23
24	120	24	56	0	12.00	61631.23
23	720	144	57	0	72.00	61703.23
22	520	104	58	0	52.00	61755.23
21	180	36	59	0	18.00	61773.23
20	150	30	60	1	15.00	61788.23
19	150	30	61	0	15.00	61803.23
18	28	6	62	0	2.80	61806.03
17	56	12	63	0	5.60	61811.63
16	10	2	64	1	1.00	61812.63
15	65	13	65	0	6.50	61819.13
14	165	33	66	0	16.50	61835.63
13	450	90	67	0	7500.00	69335.63
12	6	2	68	0	0.60	69336.23
11	680	136	69	0	11333.33	80669.57
10	10	2	70	0	1.00	80670.57
9	1037	208	71	0	17283.33	97953.90
8	14	3	72	0	1.40	97955.30
7	240	48	73	0	4000.00	101955.30
6	14	3	74	0	1.40	101956.70
5	121	25	75	0	2016.67	103973.37
4	8	2	76	0	0.80	103974.17
3	134	27	77	0	2233.33	106207.50
2	8	2	78	0	0.80	106208.30
1	1116	224	79	0	18600.00	124808.30

Reproduced with permission of the copyright owner. Further reproduction prohibited without permission.

Wagonhound East – 5

bed number	thickness (cm)	bin assignment	bin number	no. of beds per bin	ind. Time (yrs)	cum. Time (yrs)
81	1300	260	1	8	130.00	130.00
80	130	26	2	11	2166.67	2296.67
79	20	4	3	7	2.00	2298.67
78	30	6	4	11	500.00	2798.67
77	16	4	5	4	1.60	2800.27
76	280	56	6	6	4666.67	7466.93
75	12	3	7	1	1.20	7468.13
74	30	6	8	3	500.00	7968.13
73	14	3	9	0	1.40	7969.53
72	20	4	10	1	333.33	8302.87
71	16	4	11	0	1.60	8304.47
70	138	28	12	0	2300.00	10604.47
69	10	2	13	0	1.00	10605.47
68	90	18	14	1	1500.00	12105.47
67	12	3	15	1	1.20	12106.67
66	20	4	16	0	333.33	12440.00
65	3	1	17	1	0.30	12440.30
64	20	4	18	1	333.33	12773.63
63	4	1	19	0	0.40	12774.03
62	150	30	20	0	2500.00	15274.03
61	10	2	21	0	1.00	15275.03
60	150	30	22	2	2500.00	17776.03
59	1050	210	23	0	105.00	17880.03
58	120	24	24	1	12.00	17892.03
57	30	6	25	1	500.00	18392.03
56	20	4	26	1	2.00	18394.03
55	30	6	27	1	500.00	18894.03
54	10	2	28	2	1.00	18895.03
53	130	26	29	0	2166.67	21061.70
52	150	30	30	4	15.00	21076.70
51	25	5	31	0	416.67	21493.37
50	16	4	32	1	1.60	21494.97
49	440	88	33	0	7333.33	28828.30
48	10	2	34	1	1.00	28829.30
47	70	14	35	0	1166.67	29995.97
46	4	1	36	0	0.40	29996.37
45	160	32	37	0	2666.67	32663.03
44	20	4	38	0	2.00	32665.03
43	30	6	39	0	500.00	33165.03
42	10	2	40	1	1.00	33166.03
41	125	25	41	0	2083.33	35249.37
40	25	5	42	0	2.50	35251.87
39	40	8	43	0	666.67	35918.53
38	8	2	44	0	0.80	35919.33
37	76	15	45	0	1250.00	37169.33
36	170	34	46	0	17.00	37186.33
35	1700	340	47	0	170.00	37356.33

Reproduced with permission of the copyright owner. Further reproduction prohibited without permission.

bed number	thickness (cm)	bin assignment	bin number	no. of beds per bin	ind. Time (yrs)	cum. Time (yrs)
34	10	2	48	0	1.00	37357.33
33	200	40	49	0	3333.33	40690.67
32	6	2	50	0	0.60	40691.27
31	258	52	51	0	4300.00	44991.27
30	16	4	52	1	1.60	44992.87
29	460	92	53	0	7666.67	52659.53
28	14	3	54	0	1.40	52660.93
27	108	22	55	0	1800.00	54460.93
26	4	1	56	1	0.40	54461.33
25	85	17	57	0	1416.67	55878.00
24	5	1	58	0	0.50	55878.50
23	40	8	59	0	666.67	56545.17
22	12	3	60	0	1.20	56546.37
21	132	27	61	0	2200.00	58746.37
20	25	5	62	0	2.50	58748.87
19	35	7	63	0	583.33	59332.20
18	5	1	64	1	0.50	59332.70
17	50	10	65	0	833.33	60166.03
16	3	1	66	0	0.30	60166.33
15	20	4	67	0	333.33	60499.67
14	4	1	68	0	0.40	60500.07
13	7	2	69	0	116.67	60616.73
12	6	2	70	0	0.60	60617.33
11	40	8	71	0	666.67	61284.00
10	10	2	72	0	1.00	61285.00
9	110	22	73	0	1833.33	63118.33
8	12	3	74	0	1.20	63119.53
7	138	28	75	0	2300.00	65419.53
6	550	110	76	0	55.00	65474.53
5	150	30	77	0	2500.00	67974.53
4	415	83	78	0	41.50	68016.03
3	25	5	79	0	416.67	68432.70
2	12	3	80	0	1.20	68433.90
1	320	64	81	0	5333.33	73767.23

Reproduced with permission of the copyright owner. Further reproduction prohibited without permission.

Wagonhound East – 6

bed number	thickness (cm)	bin assignment	bin number	no. of beds per bin	ind. Time (yrs)	cum. Time (yrs)
57	550	110	1	5	55.00	55.00
56	20	4	2	10	2.00	57.00
55	180	36	3	2	18.00	75.00
54	155	31	4	6	2583.33	2658.33
53	70	14	5	0	7.00	2665.33
52	15	3	6	1	250.00	2915.33
51	20	4	7	1	2.00	2917.33
50	120	24	8	0	2000.00	4917.33
49	16	4	9	3	1.60	4918.93
48	250	50	10	1	25.00	4943.93
47	1115	223	11	0	18583.33	23527.27
46	45	9	12	0	4.50	23531.77
45	48	10	13	1	4.80	23536.57
44	45	9	14	2	4.50	23541.07
43	100	20	15	1	10.00	23551.07
42	34	7	16	0	3.40	23554.47
41	20	4	17	0	333.33	23887.80
40	10	2	18	0	1.00	23888.80
39	280	56	19	0	28.00	23916.80
38	5	1	20	2	0.50	23917.30
37	130	26	21	1	13.00	23930.30
36	6	2	22	0	0.60	23930.90
35	260	52	23	0	26.00	23956.90
34	10	2	24	1	1.00	23957.90
33	260	52	25	0	26.00	23983.90
32	10	2	26	1	1.00	23984.90
31	200	40	27	0	20.00	24004.90
30	10	2	28	0	1.00	24005.90
29	70	14	29	0	1166.67	25172.57
28	5	1	30	0	0.50	25173.07
27	30	6	31	1	500.00	25673.07
26	5	1	32	0	0.50	25673.57
25	15	3	33	0	250.00	25923.57
24	10	2	34	1	1.00	25924.57
23	288	58	35	0	28.80	25953.37
22	20	4	36	1	2.00	25955.37
21	190	38	37	0	19.00	25974.37
20	6	2	38	1	0.60	25974.97
19	97	20	39	0	1616.67	27591.63
18	10	2	40	1	1.00	27592.63
17	75	15	41	0	1250.00	28842.63
16	4	1	42	0	0.40	28843.03
15	252	51	43	0	4200.00	33043.03
14	10	2	44	0	1.00	33044.03
13	695	139	45	0	11583.33	44627.37
12	65	13	46	2	6.50	44633.87
11	780	156	47	0	13000.00	57633.87
10	168	34	48	0	16.80	57650.67

Reproduced with permission of the copyright owner. Further reproduction prohibited without permission.

bed number	thickness (cm)	bin assignment	bin number	no. of beds per bin	ind. Time (yrs)	cum. Time (yrs)
9	520	104	49	0	52.00	57702.67
8	228	46	50	1	22.80	57725.47
7	228	46	51	1	22.80	57748.27
6	5	1	52	2	0.50	57748.77
5	103	21	53	0	1716.67	59465.43
4	42	9	54	0	4.20	59469.63
3	10	2	55	0	1.00	59470.63
2	4903	981	56	1	81716.67	141187.30
1	16	4	57	0	1.60	141188.90

Reproduced with permission of the copyright owner. Further reproduction prohibited without permission.

Wagonhound East – 7

bed number	thickness (cm)	bin assignment	bin number	no. of beds per bin	ind. Time (yrs)	cum. Time (yrs)
68	127	26	1	2	2116.67	2116.67
67	80	16	2	10	8.00	2124.67
66	120	24	3	4	2000.00	4124.67
65	88	18	4	3	8.80	4133.47
64	104	21	5	3	1733.33	5866.80
63	10	2	6	2	1.00	5867.80
62	580	116	7	2	9666.67	15534.47
61	21	5	8	5	2.10	15536.57
60	510	102	9	2	8500.00	24036.57
59	750	150	10	1	75.00	24111.57
58	148	30	11	0	2466.67	26578.23
57	210	42	12	0	21.00	26599.23
56	1050	210	13	2	17500.00	44099.23
55	15	3	14	4	1.50	44100.73
54	40	8	15	0	666.67	44767.40
53	70	14	16	3	7.00	44774.40
52	70	14	17	1	1166.67	45941.07
51	40	8	18	1	4.00	45945.07
50	70	14	19	1	1166.67	47111.73
49	30	6	20	1	3.00	47114.73
48	500	100	21	1	8333.33	55448.07
47	7	2	22	1	0.70	55448.77
46	275	55	23	0	4583.33	60032.10
45	9	2	24	2	0.90	60033.00
44	160	32	25	0	2666.67	62699.67
43	6	2	26	2	0.60	62700.27
42	129	26	27	0	2150.00	64850.27
41	6	2	28	2	0.60	64850.87
40	470	94	29	0	7833.33	72684.20
39	3	1	30	1	0.30	72684.50
38	110	22	31	0	1833.33	74517.83
37	3	1	32	2	0.30	74518.13
36	83	17	33	0	1383.33	75901.47
35	18	4	34	0	1.80	75903.27
34	120	24	35	0	2000.00	77903.27
33	8	2	36	0	0.80	77904.07
32	775	155	37	0	12916.67	90820.73
31	157	32	38	0	15.70	90836.43
30	78	16	39	0	1300.00	92136.43
29	7	2	40	0	0.70	92137.13
28	395	79	41	0	6583.33	98720.47
27	22	5	42	1	2.20	98722.67
26	80	16	43	0	1333.33	100056.00
25	32	7	44	0	3.20	100059.20
24	20	4	45	0	333.33	100392.53
23	100	20	46	0	10.00	100402.53
22	138	28	47	0	2300.00	102702.53
21	32	7	48	0	3.20	102705.73

Reproduced with permission of the copyright owner. Further reproduction prohibited without permission.

bed number	thickness (cm)	bin assignment	bin number	no. of beds per bin	ind. Time (yrs)	cum. Time (yrs)
20	8	2	49	0	133.33	102839.07
19	10	2	50	0	1.00	102840.07
18	65	13	51	0	1083.33	103923.40
17	7	2	52	0	0.70	103924.10
16	15	3	53	0	250.00	104174.10
15	11	3	54	0	1.10	104175.20
14	70	14	55	1	1166.67	105341.87
13	24	5	56	0	2.40	105344.27
12	40	8	57	0	666.67	106010.93
11	15	3	58	0	1.50	106012.43
10	42	9	59	0	700.00	106712.43
9	19	4	60	0	1.90	106714.33
8	140	28	61	0	2333.33	109047.67
7	64	13	62	0	6.40	109054.07
6	36	8	63	0	600.00	109654.07
5	46	10	64	0	4.60	109658.67
4	26	6	65	0	433.33	110092.00
3	37	8	66	0	3.70	110095.70
2	95	19	67	0	1583.33	111679.03
1	42	9	68	0	4.20	111683.23

Reproduced with permission of the copyright owner. Further reproduction prohibited without permission.

Sand Draw

bed number	thickness (cm)	bin assignment	bin number	no. of beds per bin	ind. Time (yrs)	cum. Time (yrs)
119	600	120	1	25	60.00	60.00
118	10	2	2	14	1.00	61.00
117	150	30	3	14	15.00	76.00
116	1800	360	4	7	180.00	256.00
115	900	180	5	8	90.00	346.00
114	1350	270	6	3	135.00	481.00
113	90	18	7	0	9.00	490.00
112	40	8	8	2	4.00	494.00
111	22	5	9	2	2.20	496.20
110	50	10	10	2	5.00	501.20
109	90	18	11	4	9.00	510.20
108	300	60	12	4	5000.00	5510.20
107	20	4	13	1	2.00	5512.20
106	60	12	14	4	1000.00	6512.20
105	55	11	15	0	5.50	6517.70
104	85	17	16	1	1416.67	7934.37
103	4	1	17	3	0.40	7934.77
102	150	30	18	5	2500.00	10434.77
101	14	3	19	0	1.40	10436.17
100	200	40	20	0	3333.33	13769.50
99	42	9	21	0	4.20	13773.70
98	70	14	22	0	1166.67	14940.37
97	7	2	23	1	0.70	14941.07
96	68	14	24	0	1133.33	16074.40
95	20	4	25	0	2.00	16076.40
94	7	2	26	0	116.67	16193.07
93	10	2	27	0	1.00	16194.07
92	55	11	28	1	916.67	17110.73
91	2	1	29	0	0.20	17110.93
90	60	12	30	2	1000.00	18110.93
89	51	11	31	0	5.10	18116.03
88	920	184	32	0	15333.33	33449.37
87	600	120	33	0	60.00	33509.37
86	50	10	34	1	833.33	34342.70
85	90	18	35	0	9.00	34351.70
84	1050	210	36	0	105.00	34456.70
83	770	154	37	0	77.00	34533.70
82	3	1	38	0	50.00	34583.70
81	45	9	39	0	4.50	34588.20
80	6	2	40	1	100.00	34688.20
79	12	3	41	0	1.20	34689.40
78	12	3	42	0	200.00	34889.40
77	25	5	43	0	2.50	34891.90
76	15	3	44	0	250.00	35141.90
75	4	1	45	0	0.40	35142.30
74	15	3	46	0	250.00	35392.30
73	3	1	47	0	0.30	35392.60

Reproduced with permission of the copyright owner. Further reproduction prohibited without permission.

bed number	thickness (cm)	bin assignment	bin number	no. of beds per bin	ind. Time (yrs)	cum. Time (yrs)
72	15	3	48	0	250.00	35642.60
71	7	2	49	0	0.70	35643.30
70	15	3	50	0	250.00	35893.30
69	4	1	51	0	0.40	35893.70
68	40	8	52	0	666.67	36560.37
67	15	3	53	0	1.50	36561.87
66	5	1	54	0	83.33	36645.20
65	6	2	55	0	0.60	36645.80
64	55	11	56	0	916.67	37562.47
63	5	1	57	0	0.50	37562.97
62	65	13	58	0	1083.33	38646.30
61	8	2	59	1	0.80	38647.10
60	40	8	60	1	666.67	39313.77
59	5	1	61	0	0.50	39314.27
58	25	5	62	0	416.67	39730.93
57	15	3	63	0	1.50	39732.43
56	700	140	64	0	11666.67	51399.10
55	4	1	65	0	0.40	51399.50
54	740	148	66	0	12333.33	63732.83
53	3	1	67	0	0.30	63733.13
52	430	86	68	0	7166.67	70899.80
51	2	1	69	0	0.20	70900.00
50	25	5	70	0	416.67	71316.67
49	6	2	71	0	0.60	71317.27
48	20	4	72	0	333.33	71650.60
47	2	1	73	0	0.20	71650.80
46	170	34	74	0	2833.33	74484.13
45	2	1	75	0	0.20	74484.33
44	58	12	76	0	966.67	75451.00
43	2	1	77	0	0.20	75451.20
42	82	17	78	0	1366.67	76817.87
41	7	2	79	0	0.70	76818.57
40	15	3	80	0	250.00	77068.57
39	5	1	81	0	0.50	77069.07
38	78	16	82	0	1300.00	78369.07
37	4	1	83	0	0.40	78369.47
36	25	5	84	0	416.67	78786.13
35	6	2	85	0	0.60	78786.73
34	85	17	86	1	1416.67	80203.40
33	19	4	87	0	1.90	80205.30
32	10	2	88	0	166.67	80371.97
31	4	1	89	0	0.40	80372.37
30	20	4	90	0	333.33	80705.70
29	5	1	91	0	0.50	80706.20
28	8	2	92	0	133.33	80839.53
27	1	1	93	0	0.10	80839.63
26	3	1	94	0	50.00	80889.63
25	1	1	95	0	0.10	80889.73
24	70	14	96	0	1166.67	82056.40

Reproduced with permission of the copyright owner. Further reproduction prohibited without permission.

bed number	thickness (cm)	bin assignment	bin number	no. of beds per bin	ind. Time (yrs)	cum. Time (yrs)
23	1	1	97	0	0.10	82056.50
22	140	28	98	0	2333.33	84389.83
21	25	5	99	0	2.50	84392.33
20	112	23	100	0	1866.67	86259.00
19	2	1	101	0	0.20	86259.20
18	295	59	102	0	4916.67	91175.87
17	12	3	103	0	1.20	91177.07
16	90	18	104	0	1500.00	92677.07
15	18	4	105	0	1.80	92678.87
14	20	4	106	0	333.33	93012.20
13	9	2	107	0	0.90	93013.10
12	25	5	108	0	416.67	93429.77
11	12	3	109	0	1.20	93430.97
10	30	6	110	0	500.00	93930.97
9	28	6	111	0	2.80	93933.77
8	15	3	112	0	250.00	94183.77
7	22	5	113	0	2.20	94185.97
6	90	18	114	0	1500.00	95685.97
5	4	1	115	0	0.40	95686.37
4	60	12	116	0	1000.00	96686.37
3	15	3	117	0	1.50	96687.87
2	70	14	118	0	1166.67	97854.53
1	30	6	119	0	3.00	97857.53

Reproduced with permission of the copyright owner. Further reproduction prohibited without permission.

Grass Creek

bed number	thickness (cm)	bin assignment	bin number	no. of beds per bin	ind. Time (yrs)	cum. Time (yrs)
114	900	180	1	19	90.00	90.00
113	1050	210	2	15	105.00	195.00
112	8	2	3	10	0.80	195.80
111	30	6	4	9	500.00	695.80
110	4	1	5	9	0.40	696.20
109	90	18	6	6	1500.00	2196.20
108	4	1	7	3	0.40	2196.60
107	60	12	8	2	1000.00	3196.60
106	3	1	9	0	0.30	3196.90
105	110	22	10	2	1833.33	5030.23
104	12	3	11	2	1.20	5031.43
103	120	24	12	4	2000.00	7031.43
102	12	3	13	0	1.20	7032.63
101	10	2	14	1	166.67	7199.30
100	3	1	15	1	0.30	7199.60
99	135	27	16	4	2250.00	9449.60
98	3	1	17	1	0.30	9449.90
97	12	3	18	2	200.00	9649.90
96	4	1	19	2	0.40	9650.30
95	10	2	20	3	166.67	9816.97
94	6	2	21	0	0.60	9817.57
93	95	19	22	1	1583.33	11400.90
92	4	1	23	1	0.40	11401.30
91	80	16	24	3	1333.33	12734.63
90	2	1	25	0	0.20	12734.83
89	50	10	26	0	833.33	13568.17
88	25	5	27	1	2.50	13570.67
87	10	2	28	0	166.67	13737.33
86	2	1	29	0	0.20	13737.53
85	55	11	30	1	916.67	14654.20
84	2	1	31	0	0.20	14654.40
83	115	23	32	1	1916.67	16571.07
82	3	1	33	2	0.30	16571.37
81	30	6	34	1	500.00	17071.37
80	20	4	35	0	2.00	17073.37
79	15	3	36	1	250.00	17323.37
78	25	5	37	0	2.50	17325.87
77	60	12	38	0	1000.00	18325.87
76	5	1	39	0	0.50	18326.37
75	160	32	40	1	2666.67	20993.03
74	8	2	41	0	0.80	20993.83
73	30	6	42	0	500.00	21493.83
72	8	2	43	0	0.80	21494.63
71	120	24	44	0	2000.00	23494.63
70	4	1	45	0	0.40	23495.03
69	200	40	46	0	3333.33	26828.37
68	35	7	47	0	3.50	26831.87

Reproduced with permission of the copyright owner. Further reproduction prohibited without permission.

bed number	Thickness (cm)	bin assignment	bin number	no. of beds per bin	ind. Time (yrs)	cum. Time (yrs)
67	95	19	48	0	1583.33	28416.20
66	10	2	49	0	1.00	28416.20
65	100	20	50	0	1666.67	30082.87
64	4	1	51	0	0.40	30083.27
63	80	16	52	0	1333.33	31416.60
62	7	2	53	0	0.70	31417.30
61	165	33	54	1	2750.00	34167.30
60	22	5	55	0	2.20	34169.50
59	60	12	56	0	1000.00	35169.50
58	3	1	57	0	0.30	35169.80
57	80	16	58	0	1333.33	36503.13
56	3	1	59	0	0.30	36503.43
55	12	3	60	0	200.00	36703.43
54	1	1	61	0	0.10	36703.53
53	120	24	62	0	2000.00	38703.53
52	5	1	63	0	0.50	38704.03
51	100	20	64	0	1666.67	40370.70
50	90	18	65	0	9.00	40379.70
49	270	54	66	0	4500.00	44879.70
48	70	14	67	0	7.00	44886.70
47	10	2	68	0	166.67	45053.37
46	18	4	69	0	1.80	45055.17
45	4150	208	70	0	69166.67	114221.83
44	4	1	71	0	0.40	114222.23
43	150	30	72	0	2500.00	116722.23
42	22	5	73	0	2.20	116724.43
41	165	33	74	0	2750.00	119474.43
40	18	4	75	0	1.80	119476.23
39	380	76	76	1	6333.33	125809.57
38	20	4	77	0	2.00	125811.57
37	400	80	78	0	6666.67	132478.23
36	21	5	79	0	2.10	132480.33
35	85	17	80	1	1416.67	133897.00
34	50	10	81	0	5.00	133902.00
33	40	8	82	0	666.67	134568.67
32	35	7	83	0	3.50	134572.17
31	75	15	84	0	1250.00	135822.17
30	60	12	85	0	6.00	135828.17
29	40	8	86	0	666.67	136494.83
28	25	5	87	0	2.50	136497.33
27	10	2	88	0	166.67	136664.00
26	20	4	89	0	2.00	136666.00
25	35	7	90	0	583.33	137249.33
24	12	3	91	0	1.20	137250.53
23	15	3	92	0	250.00	137500.53
22	8	2	93	0	0.80	137501.33
21	18	4	94	0	300.00	137801.33
20	10	2	95	0	1.00	137802.33
19	20	4	96	0	333.33	138135.67

Reproduced with permission of the copyright owner. Further reproduction prohibited without permission.

bed number	thickness (cm)	bin assignment	bin number	no. of beds per bin	ind. Time (yrs)	cum. Time (yrs)
18	25	5	97	0	2.50	138138.17
17	20	4	98	0	333.33	138471.50
16	12	3	99	0	1.20	138472.70
15	30	6	100	0	500.00	138972.70
14	25	5	101	0	2.50	138975.20
13	28	6	102	0	466.67	139441.87
12	6	2	103	0	0.60	139442.47
11	98	20	104	0	1633.33	141075.80
10	15	3	105	0	1.50	141077.30
9	55	11	106	0	916.67	141993.97
8	20	4	107	0	2.00	141995.97
7	168	34	108	0	2800.00	144795.97
6	23	5	109	0	2.30	144798.27
5	80	16	110	0	1333.33	146131.60
4	30	6	111	0	3.00	146134.60
3	12	3	112	0	200.00	146334.60
2	8	2	113	0	0.80	146335.40
1	180	36	114	0	3000.00	149335.40

Reproduced with permission of the copyright owner. Further reproduction prohibited without permission.

Little Buffalo Basin

bed number	thickness (cm)	bin assignment	bin number	no. of beds per bin	ind. Time (yrs)	cum. Time (yrs)
73	660	132	1	10	66.00	66.00
72	750	150	2	9	75.00	143.00
71	15	3	3	6	1.50	144.50
70	60	12	4	2	6.00	150.50
69	5	1	5	2	0.50	151.00
68	120	24	6	4	12.00	163.00
67	160	32	7	0	16.00	179.00
66	230	46	8	4	23.00	202.00
65	1350	270	9	2	22500.00	22702.00
64	5	1	10	1	0.50	22702.50
63	170	34	11	0	2833.33	25535.83
62	4	1	12	5	0.40	25536.23
61	110	22	13	0	1833.33	27369.57
60	9	2	14	0	0.90	27370.47
59	40	8	15	1	666.67	28037.13
58	25	5	16	1	2.50	28039.63
57	450	90	17	0	7500.00	35539.63
56	4	1	18	0	0.40	35540.03
55	235	47	19	0	3916.67	39456.70
54	4	1	20	1	0.40	39457.10
53	650	130	21	0	10833.33	50290.43
52	9	2	22	2	0.90	50291.33
51	210	42	23	1	3500.00	53791.33
50	60	12	24	3	6.00	53797.33
49	320	64	25	0	5333.33	59130.67
48	9	2	26	1	0.90	59131.57
47	220	44	27	0	3666.67	62798.23
46	15	3	28	1	1.50	62799.73
45	116	23	29	0	1916.67	64716.40
44	7	2	30	0	0.70	64717.10
43	606	121	31	0	10083.33	74800.43
42	15	3	32	2	1.50	74801.93
41	100	20	33	1	1666.67	76468.60
40	30	6	34	1	3.00	76471.60
39	60	12	35	0	1000.00	77471.60
38	30	6	36	0	3.00	77474.60
37	30	6	37	0	500.00	77974.60
36	12	3	38	0	1.20	77975.80
35	25	5	39	0	416.67	78392.47
34	20	4	40	0	2.00	78394.47
33	130	26	41	0	2166.67	80561.13
32	110	22	42	1	11.00	80572.13
31	160	32	43	0	2666.67	83238.80
30	13	3	44	1	1.30	83240.10
29	250	50	45	0	4166.67	87406.77
28	12	3	46	1	1.20	87407.97
27	75	15	47	1	1250.00	88657.97

Reproduced with permission of the copyright owner. Further reproduction prohibited without permission.

bed number	thickness (cm)	bin assignment	bin number	no. of beds per bin	ind. Time (yrs)	cum. Time (yrs)
26	5	1	48	0	0.50	88658.47
25	58	12	49	0	966.67	89625.13
24	5	1	50	1	0.50	89625.63
23	45	9	51	0	750.00	90375.63
22	4	1	52	0	0.40	90376.03
21	50	10	53	0	833.33	91209.37
20	8	2	54	0	0.80	91210.17
19	18	4	55	0	300.00	91510.17
18	5	1	56	0	0.50	91510.67
17	60	12	57	0	1000.00	92510.67
16	5	1	58	0	0.50	92511.17
15	45	9	59	0	750.00	93261.17
14	7	2	60	0	0.70	93261.87
13	30	6	61	0	500.00	93761.87
12	7	2	62	0	0.70	93762.57
11	40	8	63	0	666.67	94429.23
10	8	2	64	1	0.80	94430.03
9	120	24	65	0	2000.00	96430.03
8	40	8	66	0	4.00	96434.03
7	120	24	67	0	2000.00	98434.03
6	140	28	68	0	14.00	98448.03
5	40	8	69	0	666.67	99114.70
4	165	33	70	0	16.50	99131.20
3	690	138	71	0	11500.00	110631.20
2	7	2	72	0	0.70	110631.90
1	80	16	73	0	1333.33	111965.23

Reproduced with permission of the copyright owner. Further reproduction prohibited without permission.

Sunshine Reservoir

bed number	thickness (cm)	bin assignment	bin number	no. of beds per bin	ind. Time (yrs)	cum. Time (yrs)
94	40	8	1	9	4.00	4.00
93	130	26	2	13	2166.67	2170.67
92	85	17	3	11	8.50	2179.17
91	126	25	4	10	2083.33	4262.50
90	30	6	5	4	3.00	4265.50
89	110	22	6	1	1833.33	6098.83
88	6	2	7	2	0.60	6099.43
87	150	30	8	4	2500.00	8599.43
86	8	2	9	0	0.80	8600.23
85	165	33	10	4	2750.00	11350.23
84	12	3	11	1	1.20	11351.43
83	40	8	12	2	666.67	12018.10
82	40	8	13	0	4.00	12022.10
81	50	10	14	2	833.33	12855.43
80	25	5	15	0	2.50	12857.93
79	50	10	16	0	833.33	13691.27
78	13	3	17	2	1.30	13692.57
77	150	30	18	1	2500.00	16192.57
76	100	20	19	0	10.00	16202.57
75	150	30	20	4	2500.00	18702.57
74	18	4	21	0	1.80	18704.37
73	60	12	22	3	1000.00	19704.37
72	18	4	23	0	1.80	19706.17
71	300	60	24	1	5000.00	24706.17
70	15	3	25	1	1.50	24707.67
69	50	10	26	2	833.33	25541.00
68	10	2	27	0	1.00	25542.00
67	5	1	28	0	83.33	25625.33
66	3	1	29	0	0.30	25625.63
65	150	30	30	6	2500.00	28125.63
64	20	4	31	0	2.00	28127.63
63	5	1	32	0	83.33	28210.97
62	2	1	33	2	0.20	28211.17
61	165	33	34	0	2750.00	30961.17
60	25	5	35	0	2.50	30963.67
59	20	4	36	0	333.33	31297.00
58	14	3	37	1	1.40	31298.40
57	150	30	38	0	2500.00	33798.40
56	14	3	39	0	1.40	33799.80
55	150	30	40	0	2500.00	36299.80
54	40	8	41	0	4.00	36303.80
53	20	4	42	0	333.33	36637.13
52	600	120	43	0	60.00	36697.13
51	700	140	44	2	11666.67	48363.80
50	15	3	45	0	1.50	48365.30
49	35	7	46	0	583.33	48948.63
48	15	3	47	0	1.50	48950.13

Reproduced with permission of the copyright owner. Further reproduction prohibited without permission.

bed number	thickness (cm)	bin assignment	bin number	no. of beds per bin	ind. Time (yrs)	cum. Time (yrs)
47	220	44	48	0	3666.67	52616.80
46	6	2	49	0	0.60	52617.40
45	100	20	50	0	1666.67	54284.07
44	8	2	51	0	0.80	54284.87
43	60	12	52	0	1000.00	55284.87
42	10	2	53	0	1.00	55285.87
41	130	26	54	0	2166.67	57452.53
40	35	7	55	0	3.50	57456.03
39	120	24	56	0	2000.00	59456.03
38	70	14	57	0	7.00	59463.03
37	70	14	58	0	1166.67	60629.70
36	14	3	59	0	1.40	60631.10
35	100	20	60	1	1666.67	62297.77
34	10	2	61	0	1.00	62298.77
33	15	3	62	0	250.00	62548.77
32	10	2	63	0	1.00	62549.77
31	55	11	64	0	916.67	63466.43
30	12	3	65	0	1.20	63467.63
29	85	17	66	0	1416.67	64884.30
28	20	4	67	0	2.00	64886.30
27	220	44	68	0	3666.67	68552.97
26	20	4	69	0	2.00	68554.97
25	50	10	70	0	833.33	69388.30
24	110	22	71	0	11.00	69399.30
23	100	20	72	0	1666.67	71065.97
22	7	2	73	0	0.70	71066.67
21	400	80	74	0	6666.67	77733.33
20	18	4	75	0	1.80	77735.13
19	700	140	76	0	11666.67	89401.80
18	6	2	77	0	0.60	89402.40
17	565	113	78	0	9416.67	98819.07
16	12	3	79	0	1.20	98820.27
15	185	37	80	1	3083.33	101903.60
14	7	2	81	0	0.70	101904.30
13	90	18	82	0	1500.00	103404.30
12	20	4	83	0	2.00	103406.30
11	25	5	84	0	416.67	103822.97
10	8	2	85	0	0.80	103823.77
9	5	1	86	0	83.33	103907.10
8	2	1	87	0	0.20	103907.30
7	5	1	88	0	83.33	103990.63
6	4	1	89	0	0.40	103991.03
5	25	5	90	0	416.67	104407.70
4	6	2	91	0	0.60	104408.30
3	20	4	92	0	333.33	104741.63
2	4	1	93	0	0.40	104742.03
1	110	22	94	0	1833.33	106575.37

Reproduced with permission of the copyright owner. Further reproduction prohibited without permission.

Zimmerman Butte

bed number	thickness (cm)	bin assignment	bin number	no. of beds per bin	ind. Time (yrs)	cum. Time (yrs)
28	150	30	1	5	15	15
27	300	60	2	4	5000	5015
26	3	1	3	2	0.3	5015.3
25	370	74	4	1	6166.666667	11181.96667
24	135	27	5	0	13.5	11195.46667
23	150	30	6	0	2500	13695.46667
22	250	50	7	0	25	13720.46667
21	300	60	8	2	5000	18720.46667
20	15	3	9	0	1.5	18721.96667
19	80	16	10	0	1333.333333	20055.3
18	10	2	11	0	1	20056.3
17	60	12	12	2	1000	21056.3
16	10	2	13	0	1	21057.3
15	60	12	14	0	1000	22057.3
14	8	2	15	0	0.8	22058.1
13	110	22	16	2	1833.333333	23891.43333
12	3	1	17	0	0.3	23891.73333
11	150	30	18	0	2500	26391.73333
10	6	2	19	0	0.6	26392.33333
9	80	16	20	0	1333.333333	27725.66667
8	12	3	21	0	1.2	27726.86667
7	350	70	22	1	5833.333333	33560.2
6	20	4	23	0	2	33562.2
5	40	8	24	0	666.6666667	34228.86667
4	5	1	25	0	0.5	34229.36667
3	4	1	26	0	66.66666667	34296.03333
2	3	1	27	1	0.3	34296.33333
1	40	8	28	0	666.6666667	34963

Reproduced with permission of the copyright owner. Further reproduction prohibited without permission.

APPENDIX F

THICKNESS DATA

Reproduced with permission of the copyright owner. Further reproduction prohibited without permission.

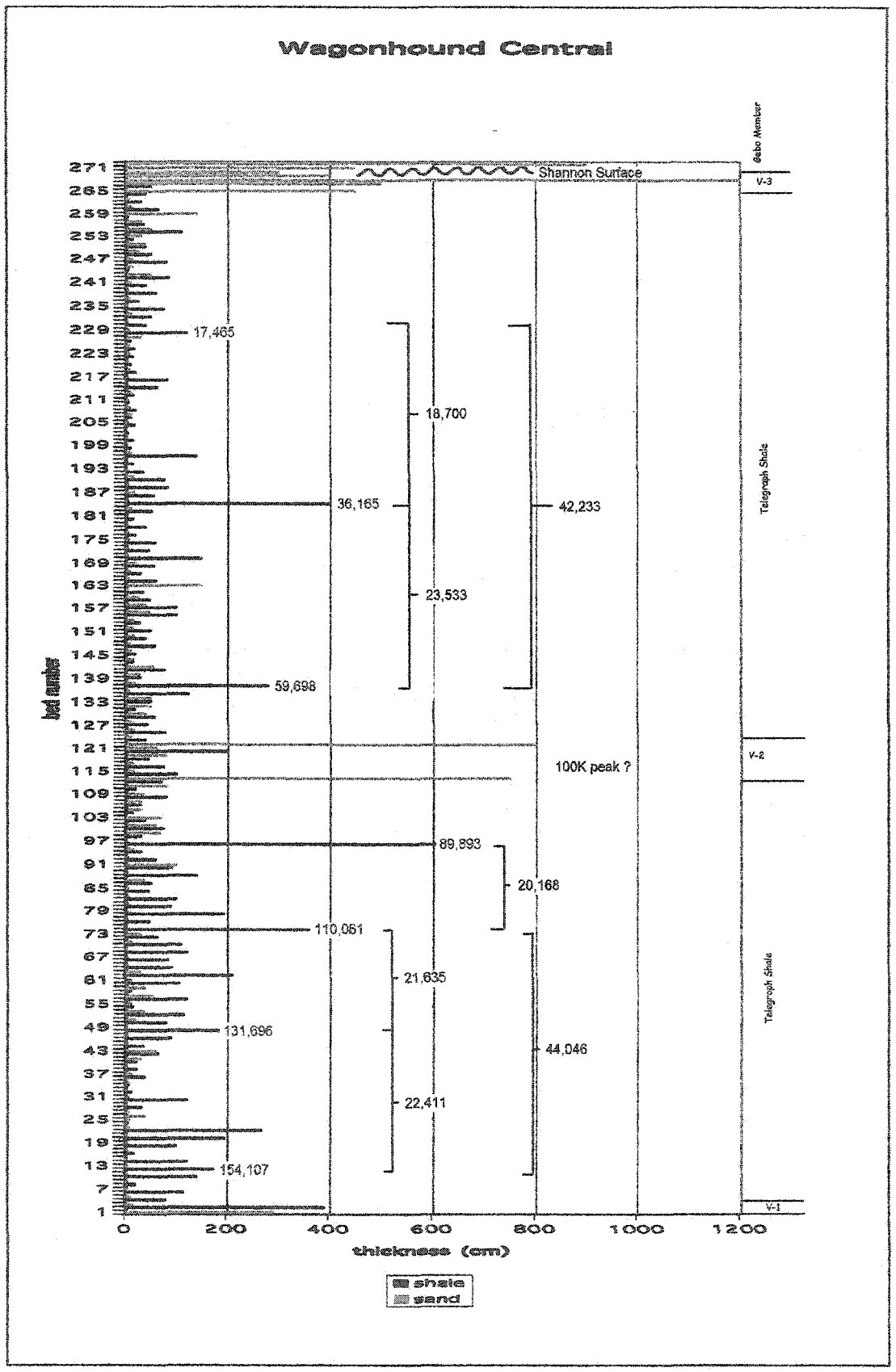

Reproduced with permission of the copyright owner. Further reproduction prohibited without permission.

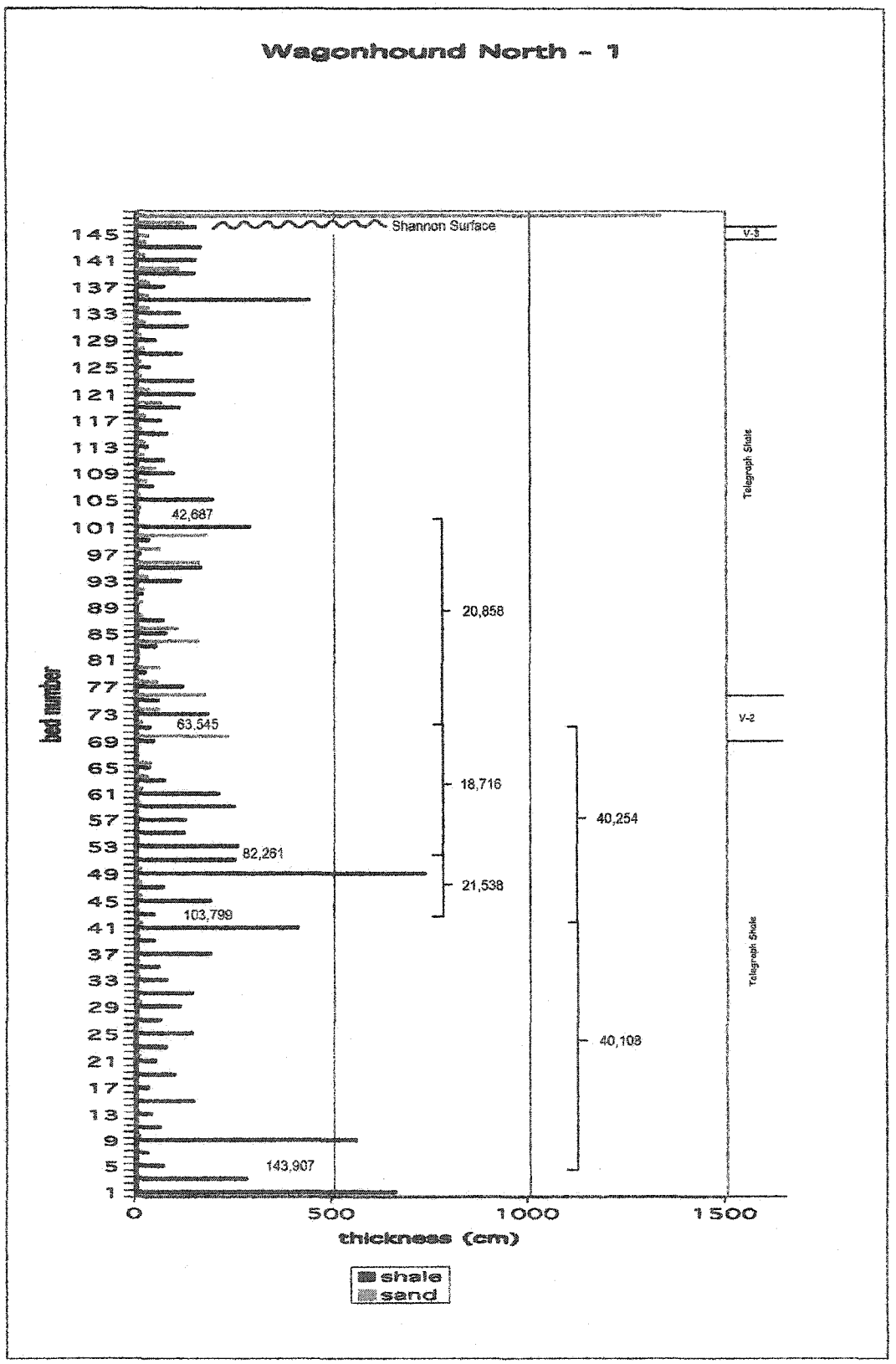

Reproduced with permission of the copyright owner. Further reproduction prohibited without permission.

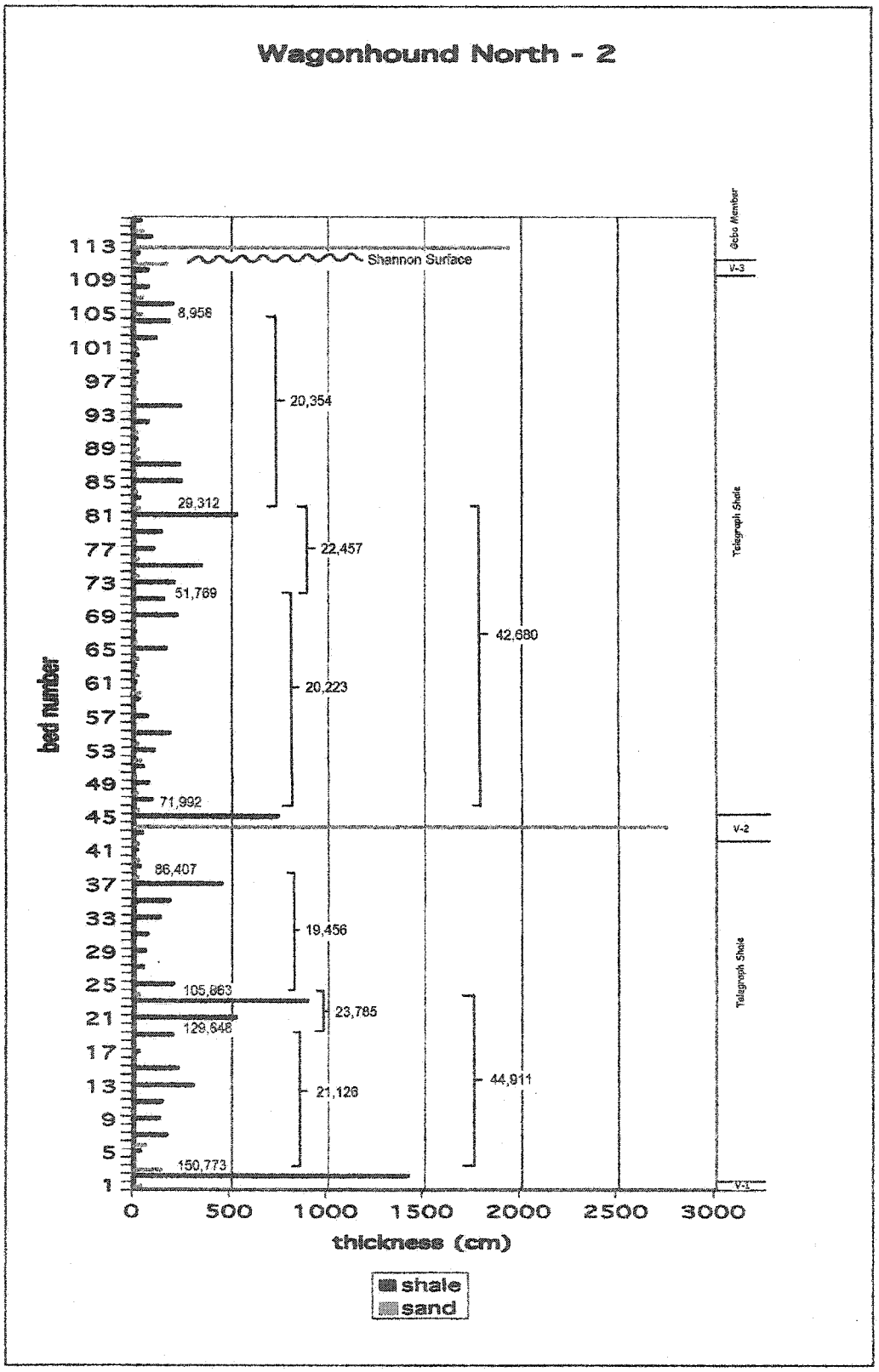

Reproduced with permission of the copyright owner. Further reproduction prohibited without permission.

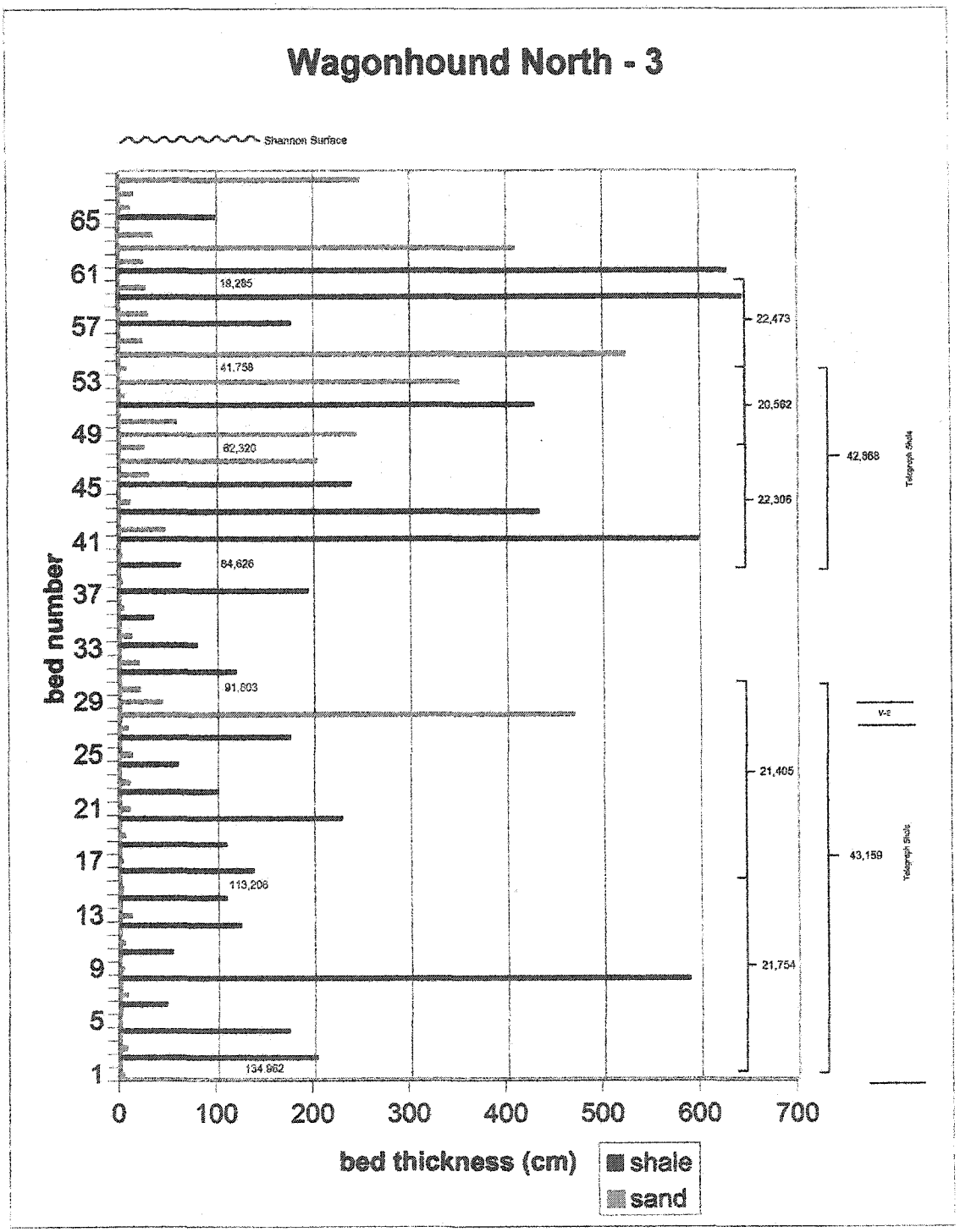

Reproduced with permission of the copyright owner. Further reproduction prohibited without permission.

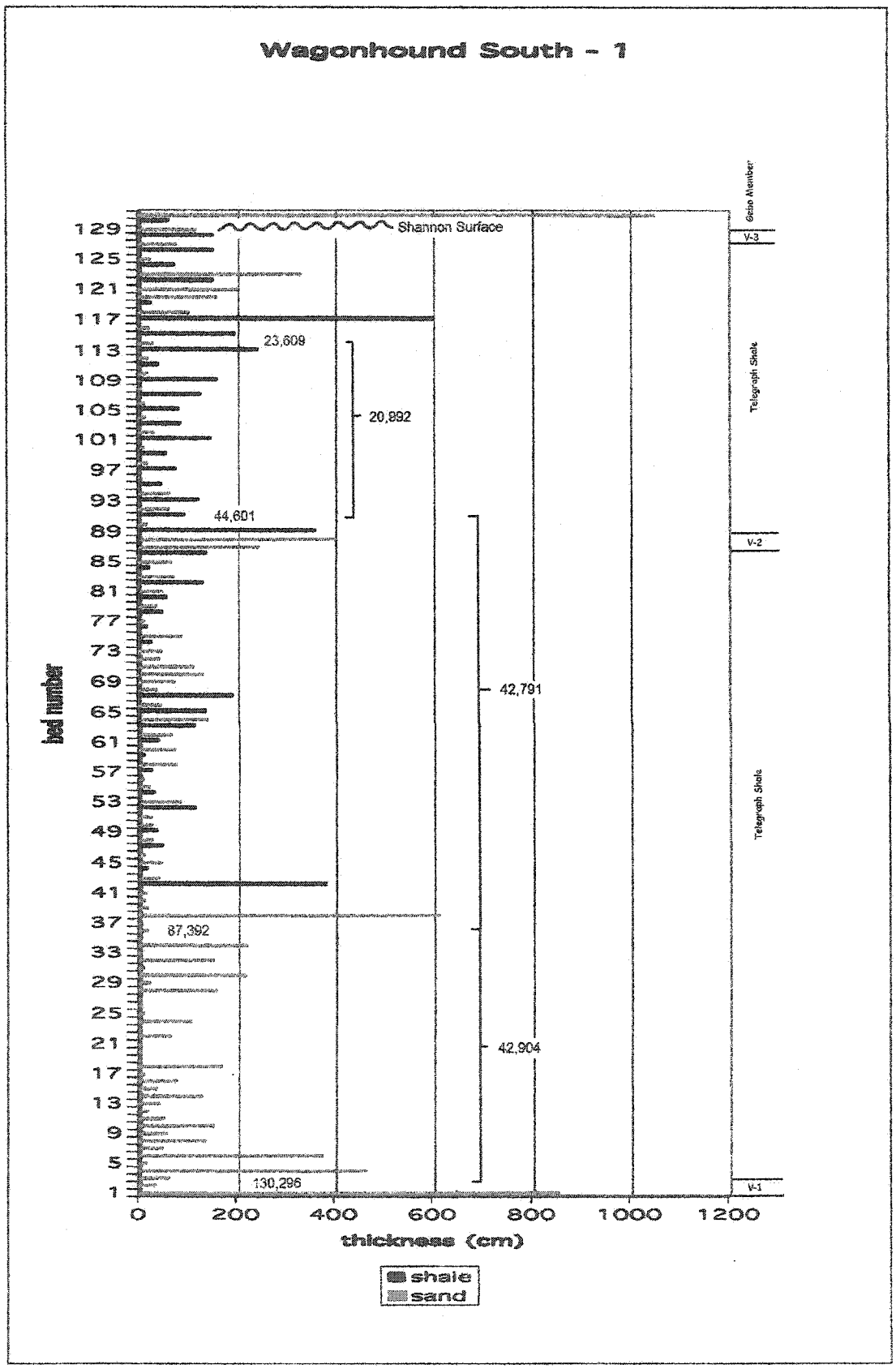

Reproduced with permission of the copyright owner. Further reproduction prohibited without permission.

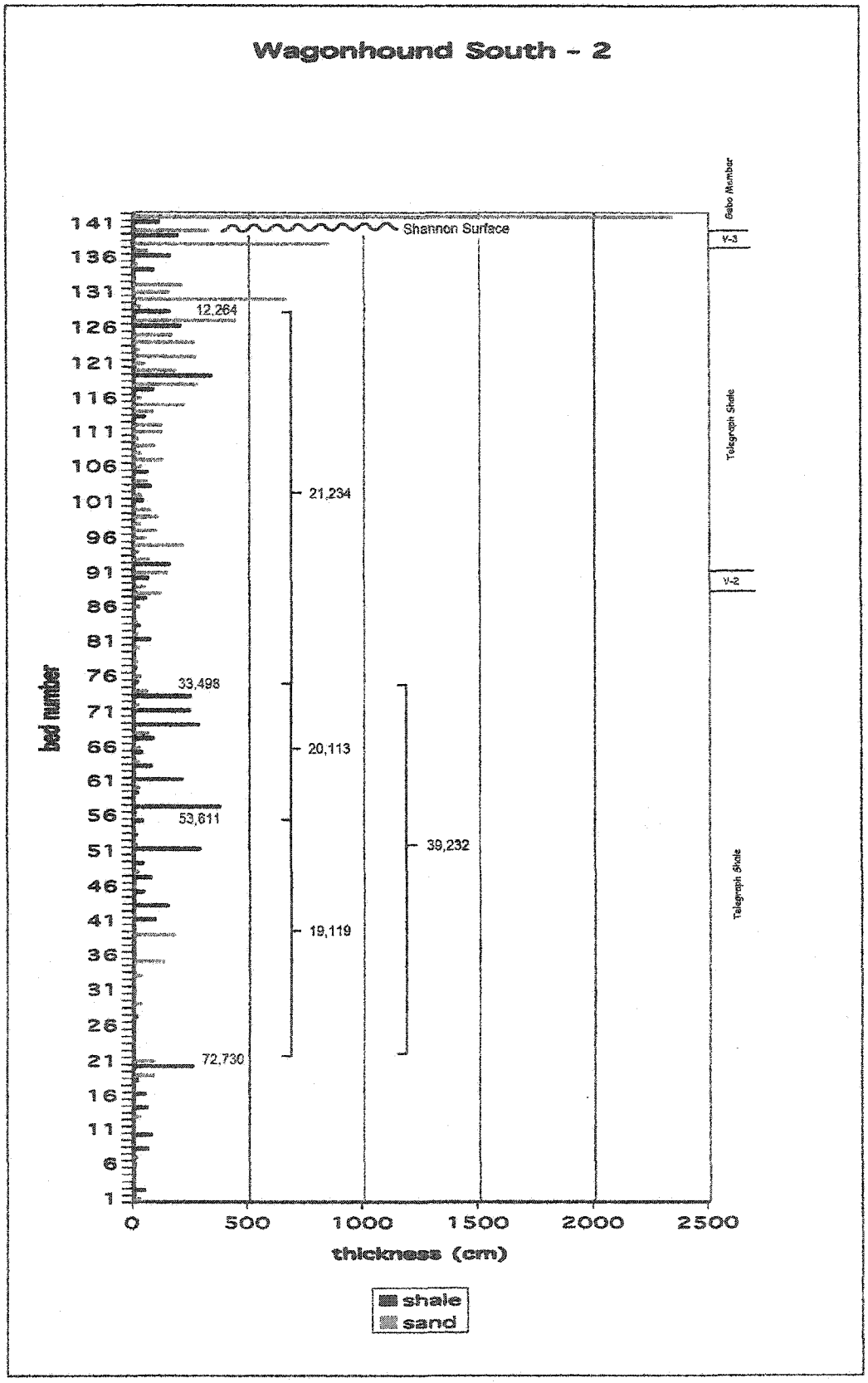

Reproduced with permission of the copyright owner. Further reproduction prohibited without permission.

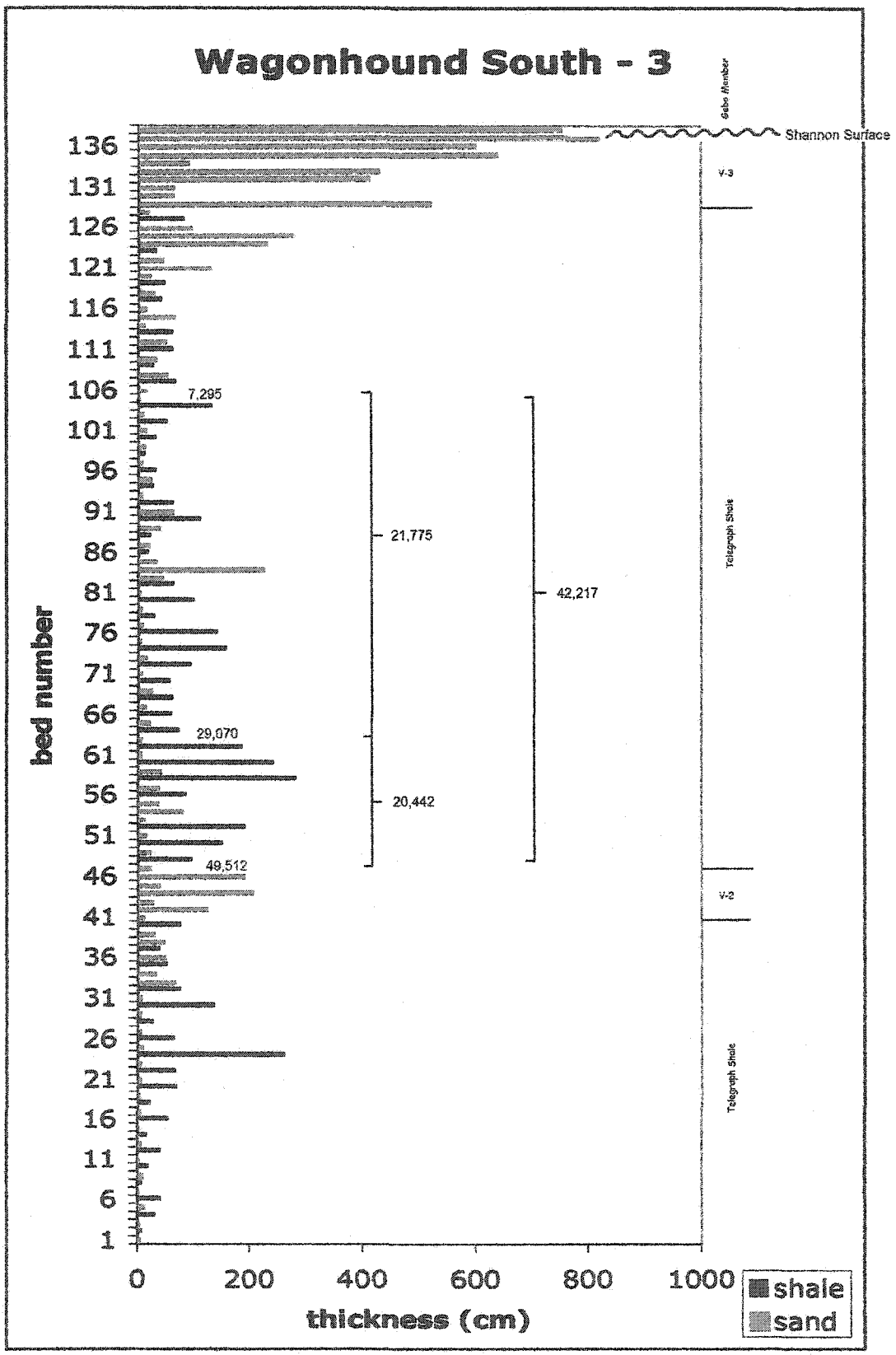

Reproduced with permission of the copyright owner. Further reproduction prohibited without permission.

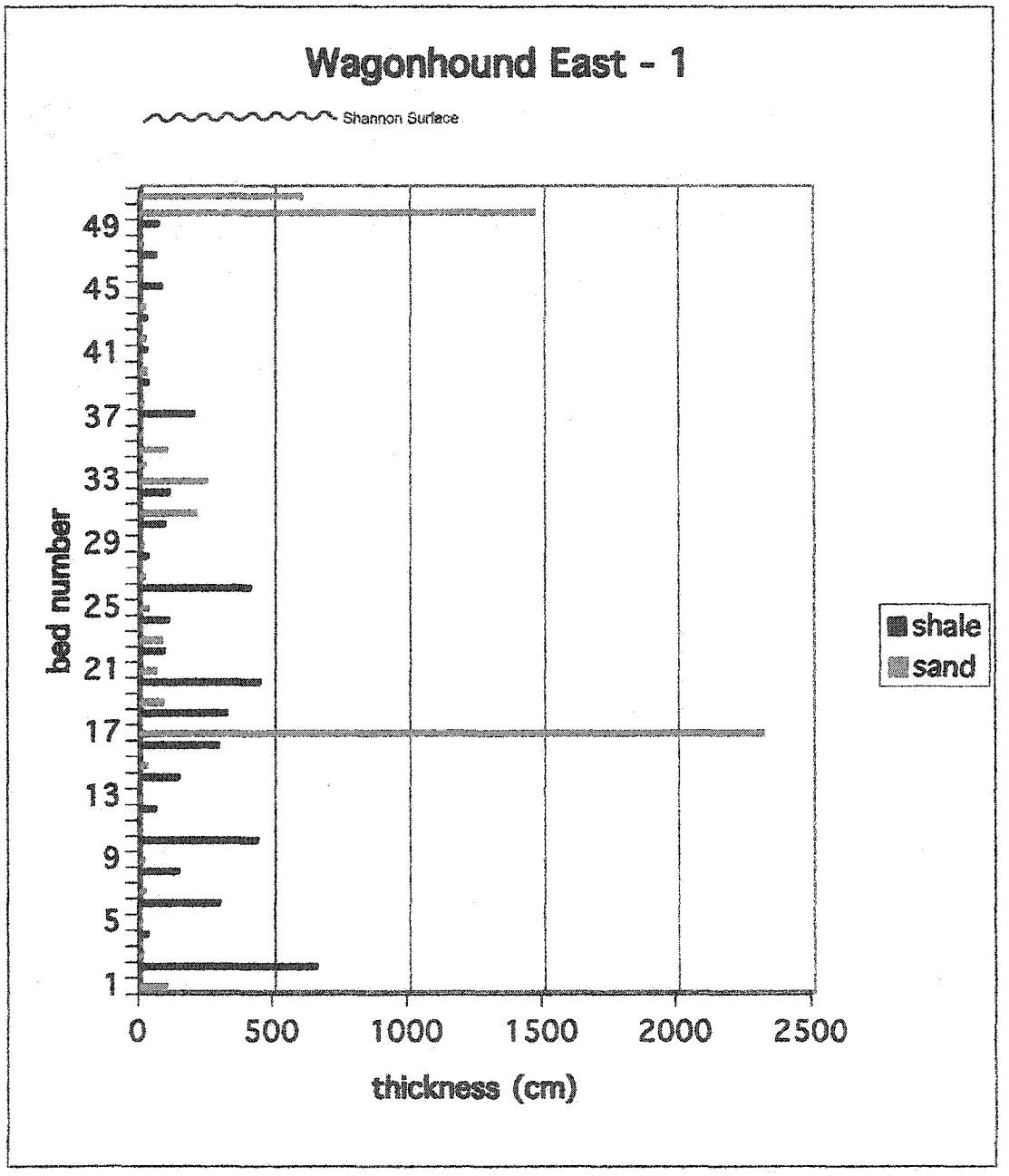

Reproduced with permission of the copyright owner. Further reproduction prohibited without permission.

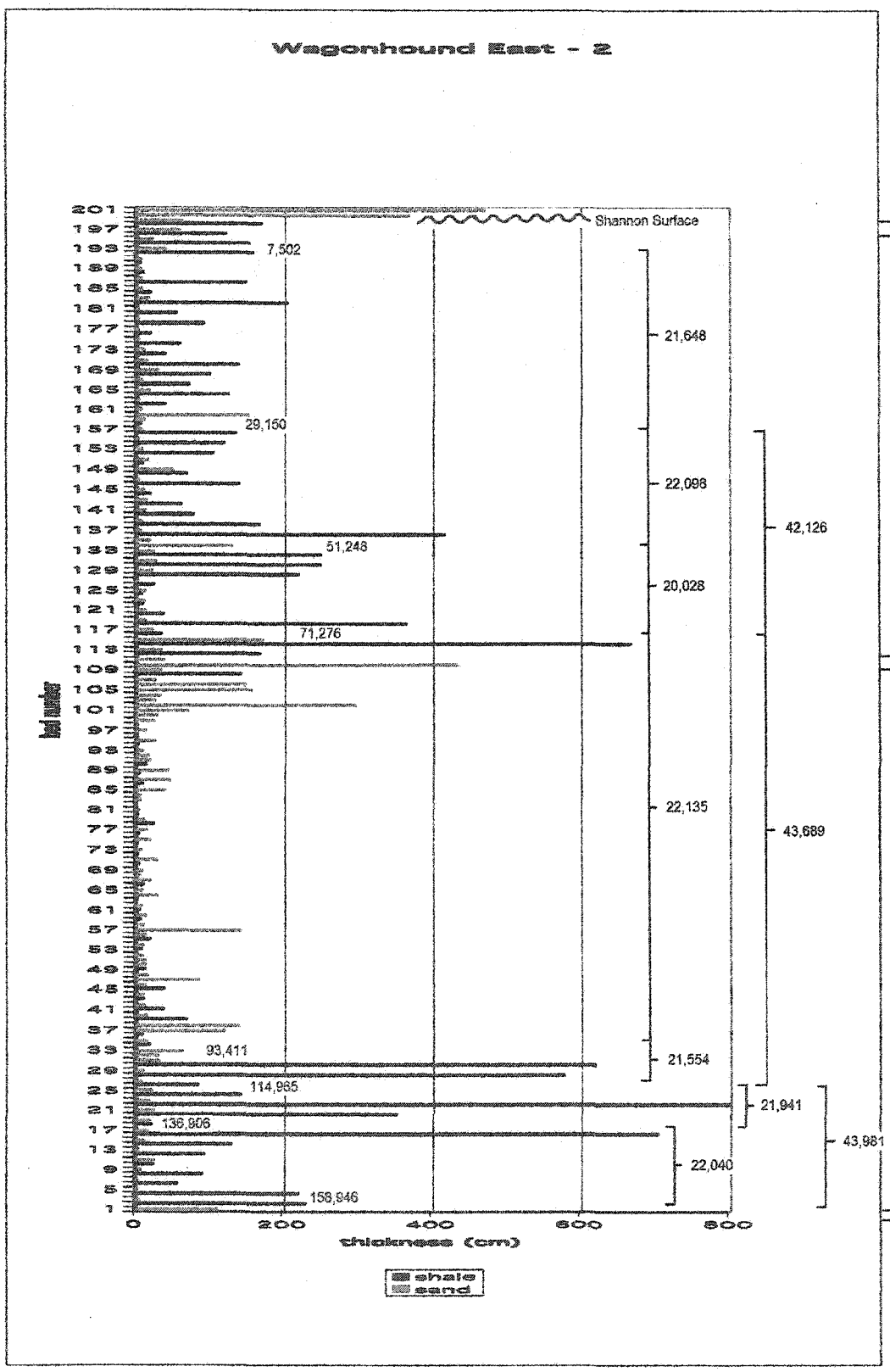

Reproduced with permission of the copyright owner. Further reproduction prohibited without permission.

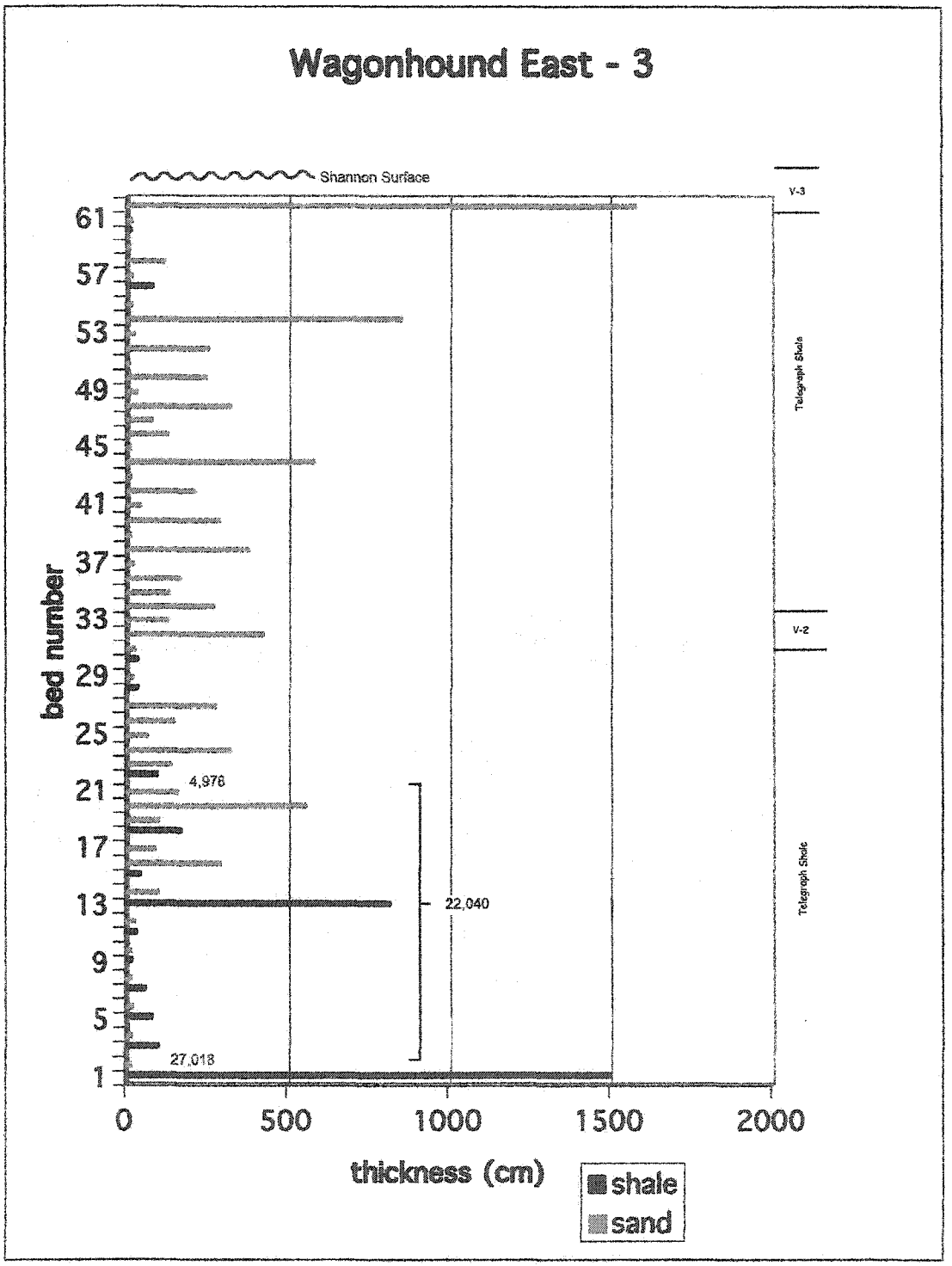

Reproduced with permission of the copyright owner. Further reproduction prohibited without permission.

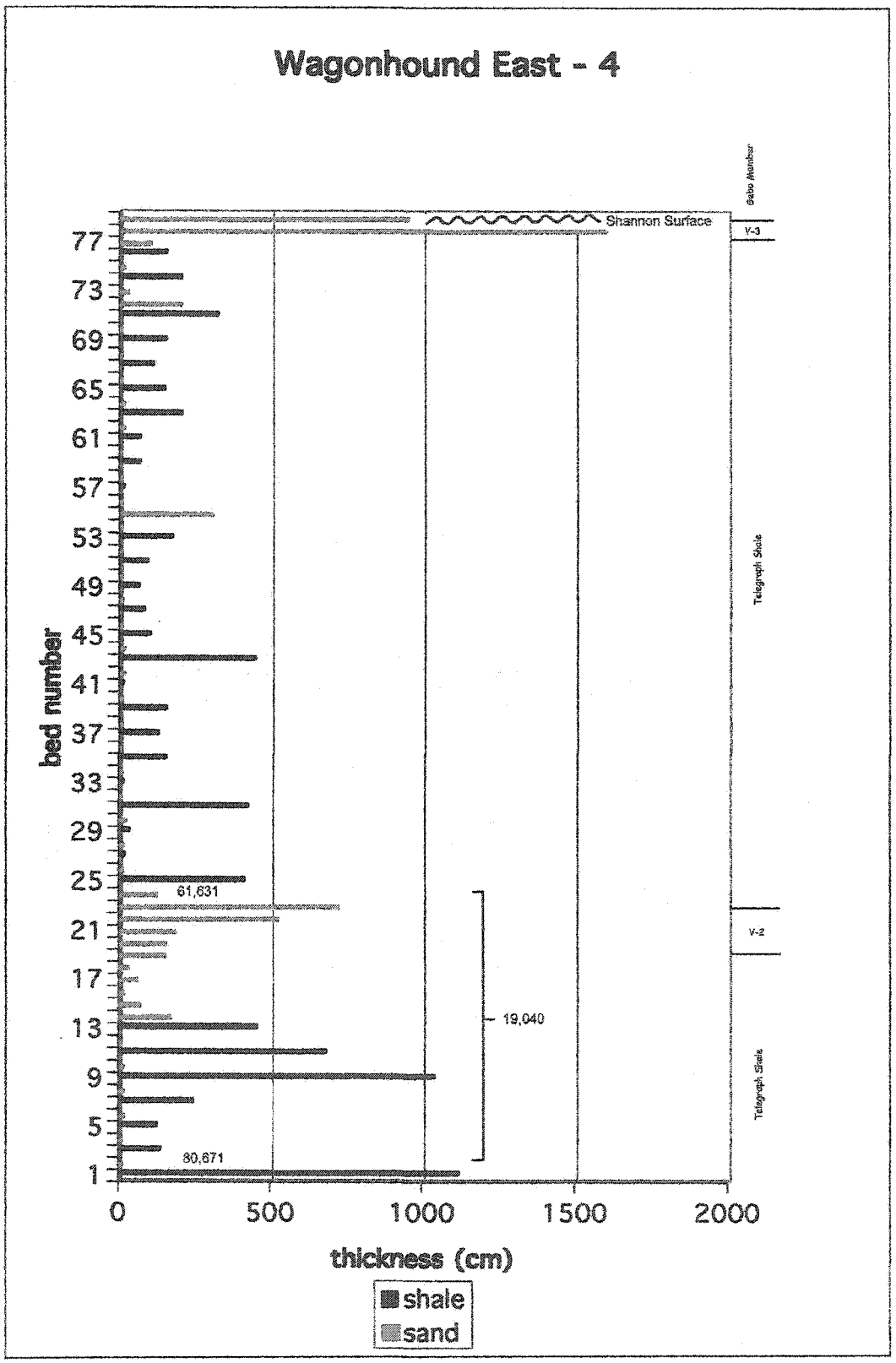

Reproduced with permission of the copyright owner. Further reproduction prohibited without permission.

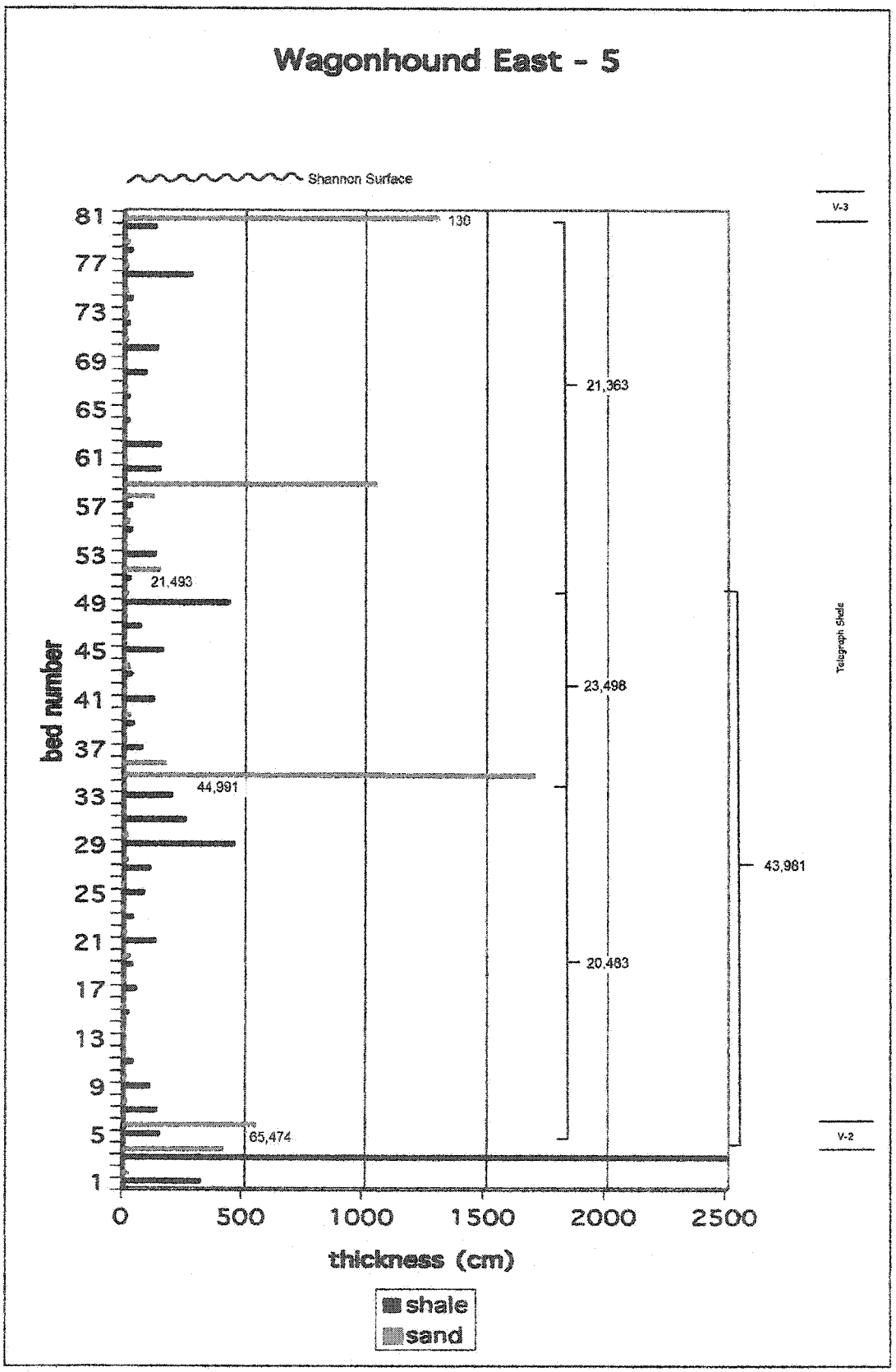

Reproduced with permission of the copyright owner. Further reproduction prohibited without permission.

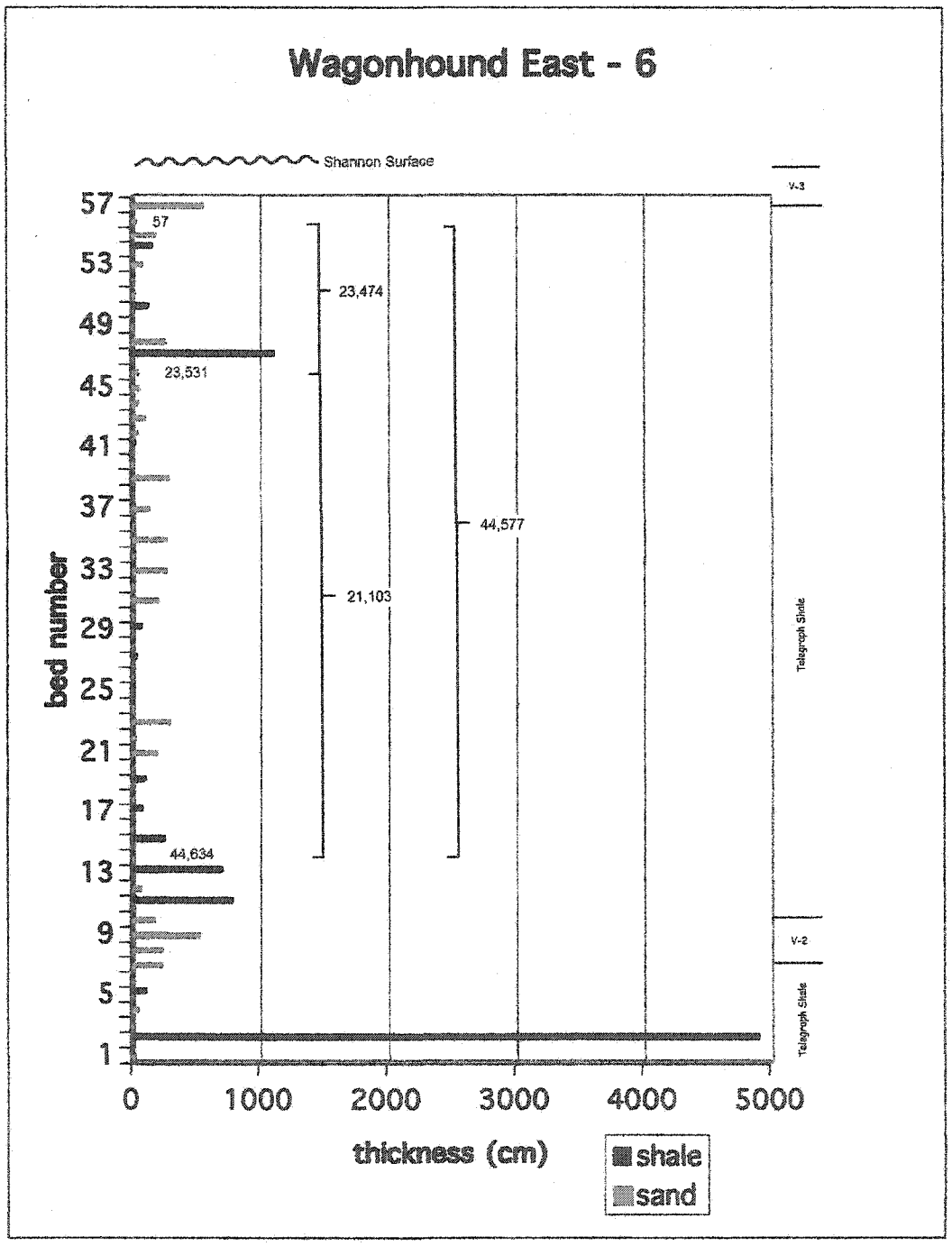

Reproduced with permission of the copyright owner. Further reproduction prohibited without permission.

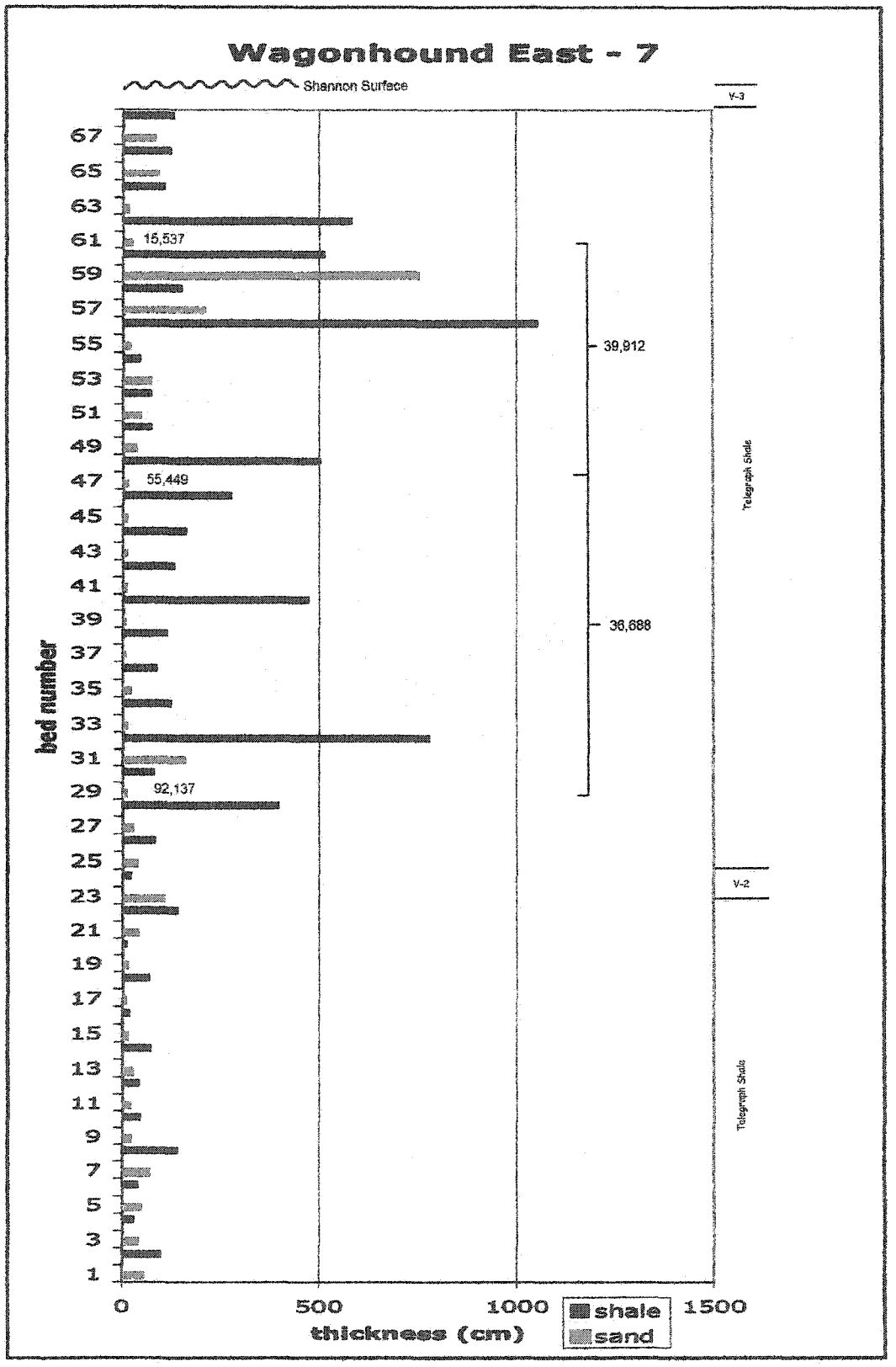

Reproduced with permission of the copyright owner. Further reproduction prohibited without permission.

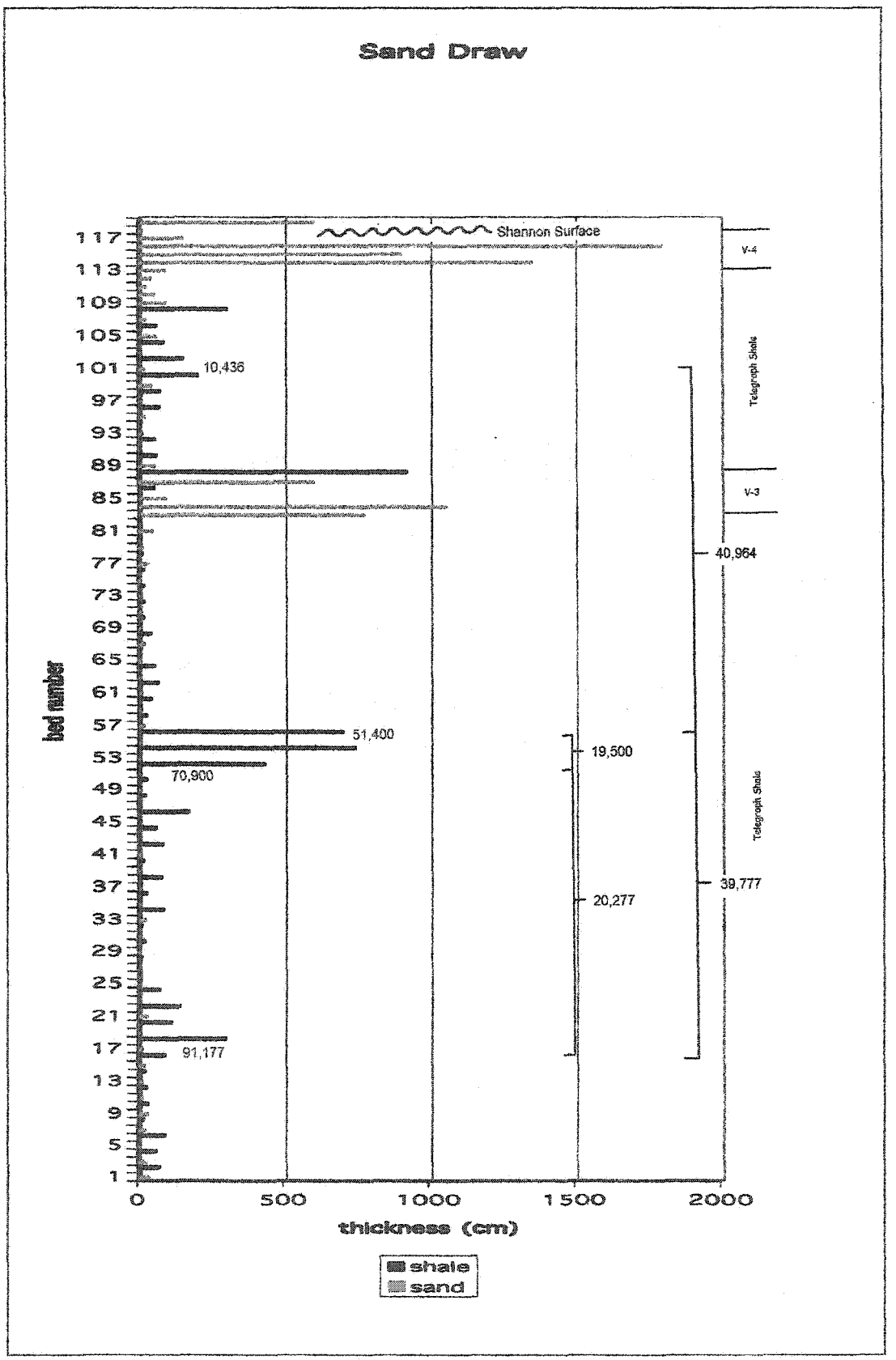

Reproduced with permission of the copyright owner. Further reproduction prohibited without permission.

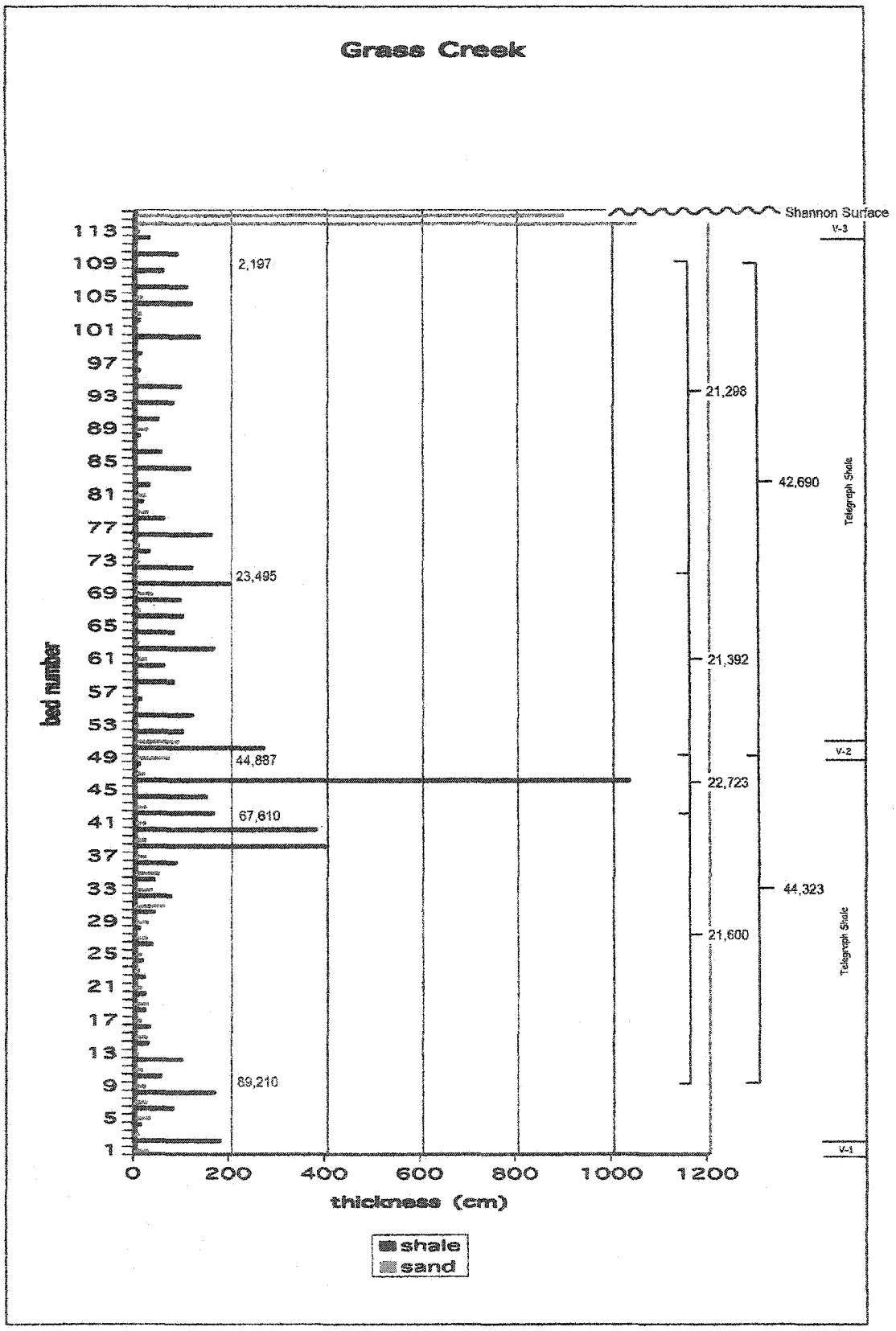

Reproduced with permission of the copyright owner. Further reproduction prohibited without permission.

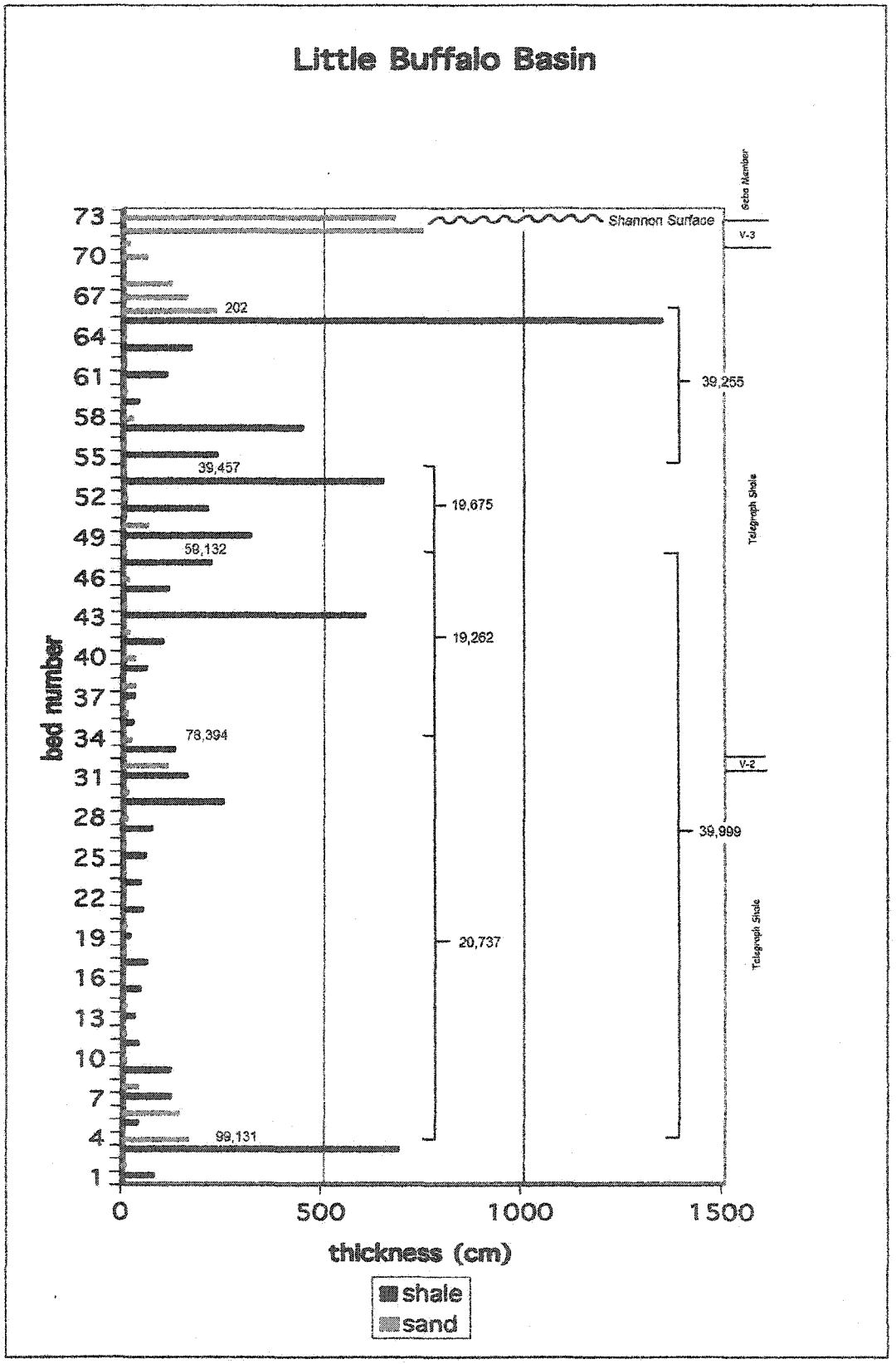

Reproduced with permission of the copyright owner. Further reproduction prohibited without permission.

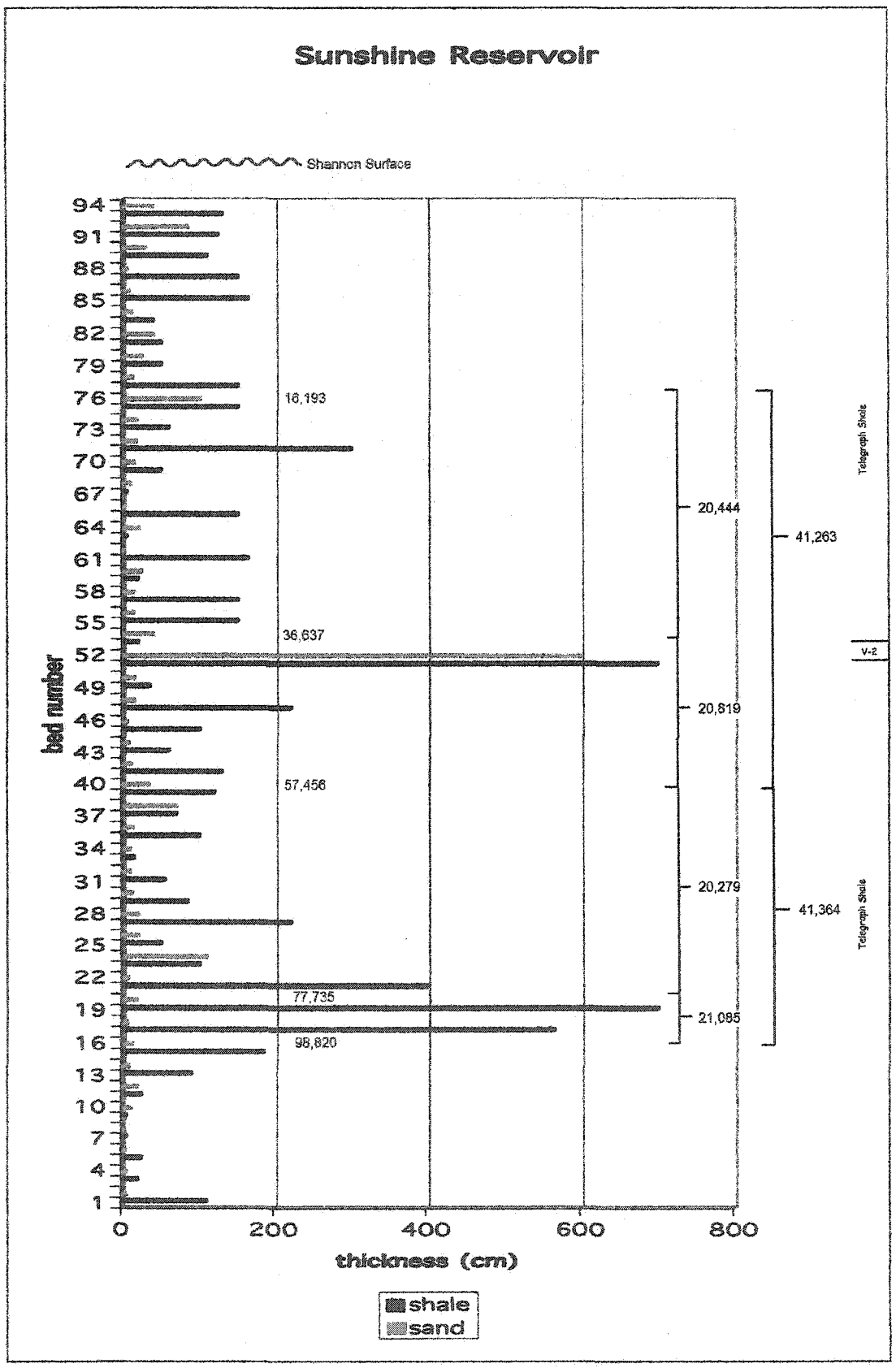

Reproduced with permission of the copyright owner. Further reproduction prohibited without permission.

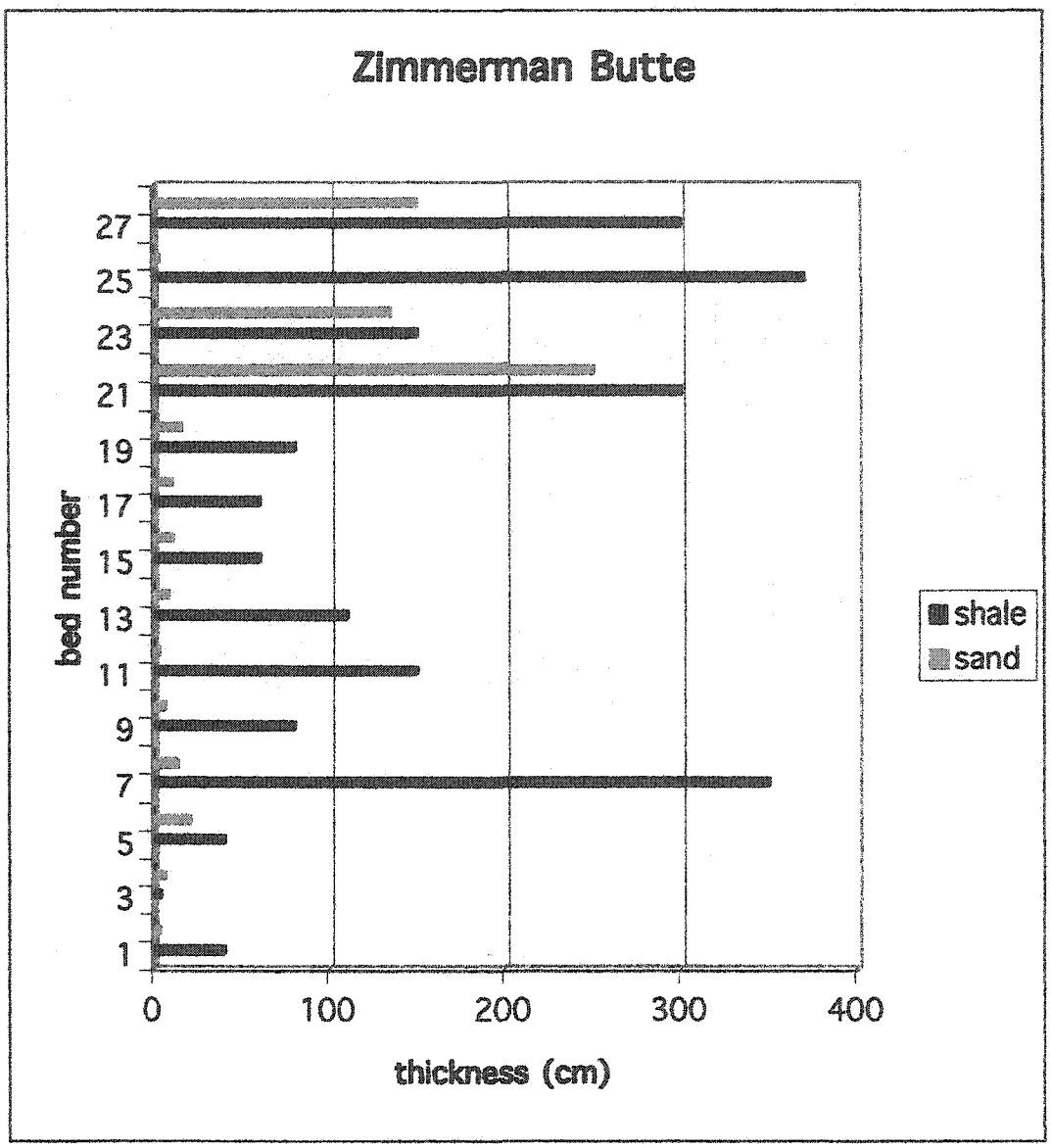

Reproduced with permission of the copyright owner. Further reproduction prohibited without permission.

APPENDIX G

BIN DATA

Reproduced with permission of the copyright owner. Further reproduction prohibited without permission.

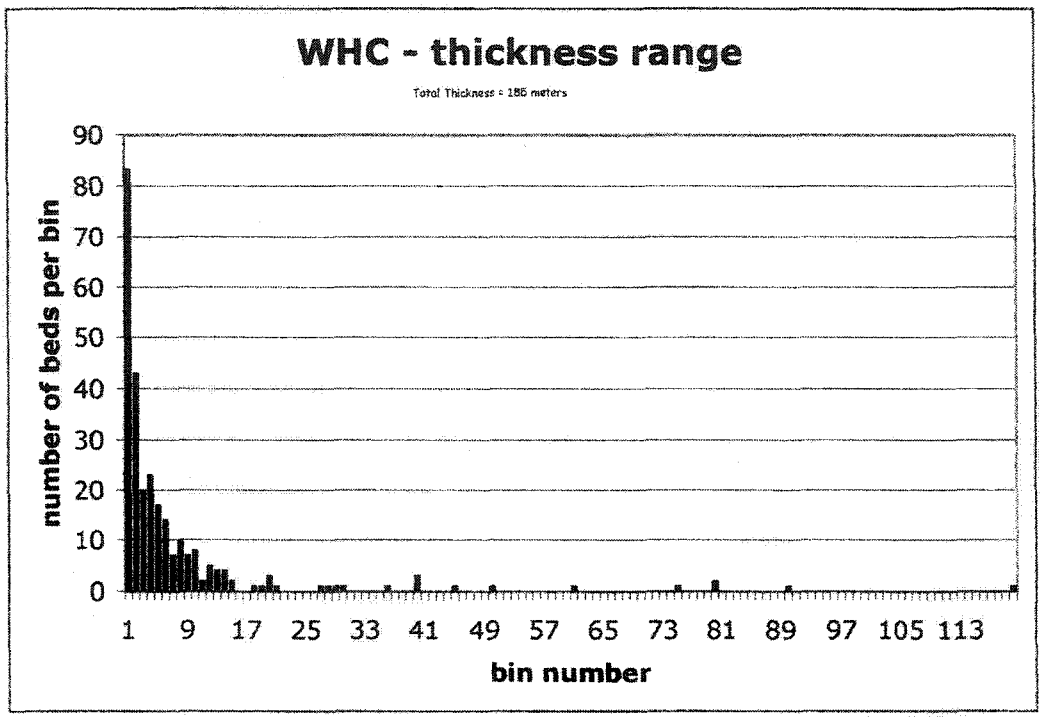

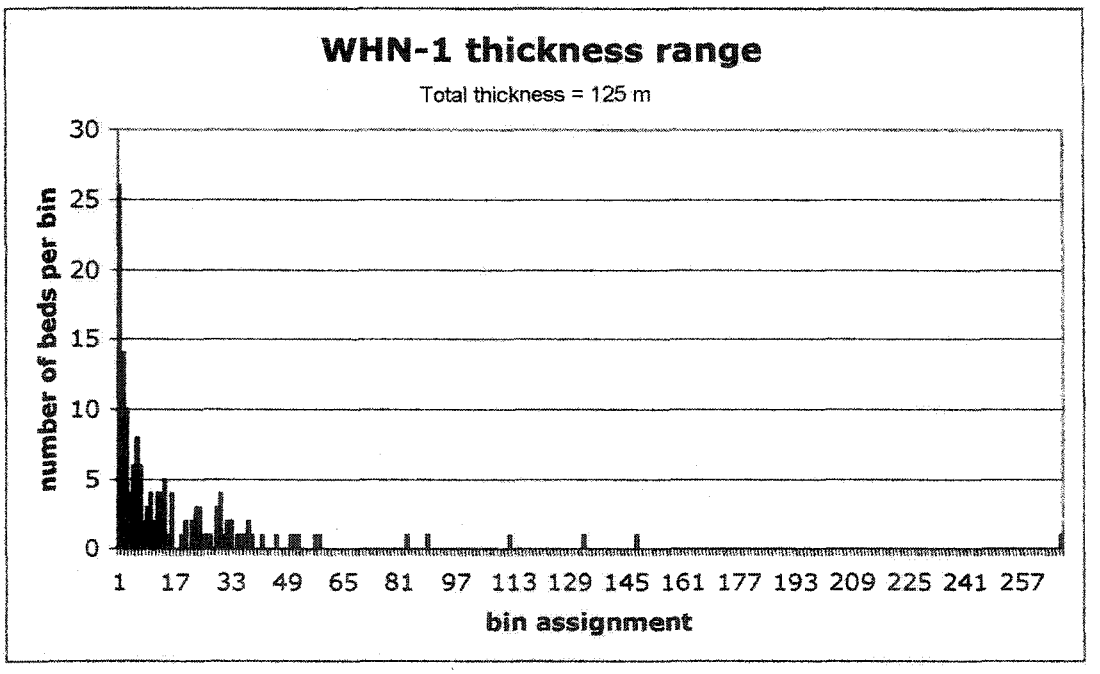

Reproduced with permission of the copyright owner. Further reproduction prohibited without permission.

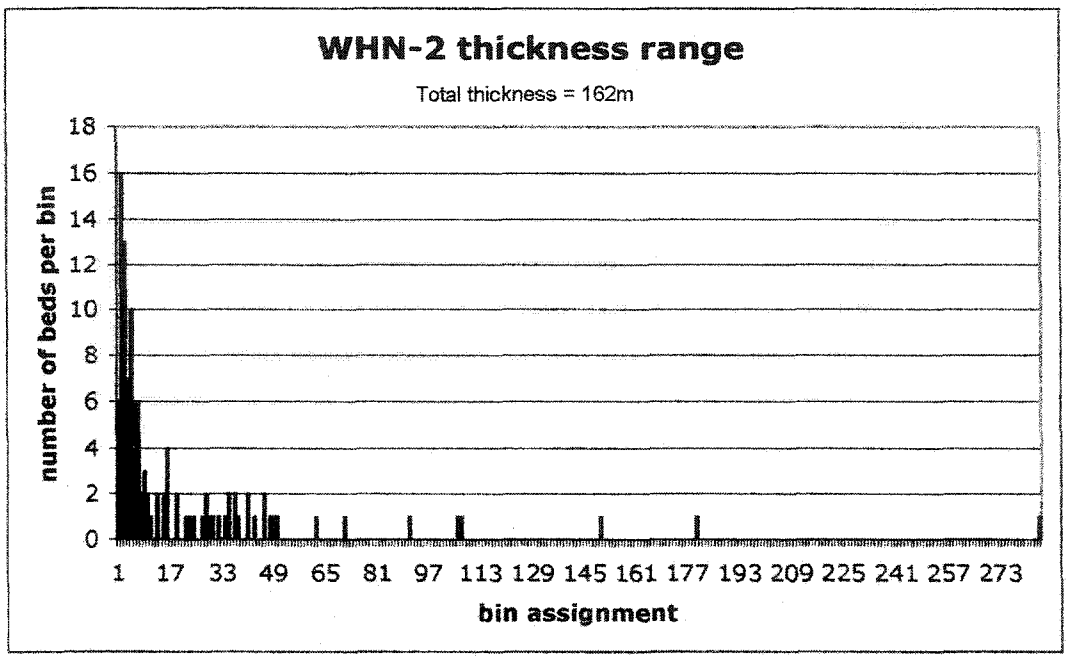

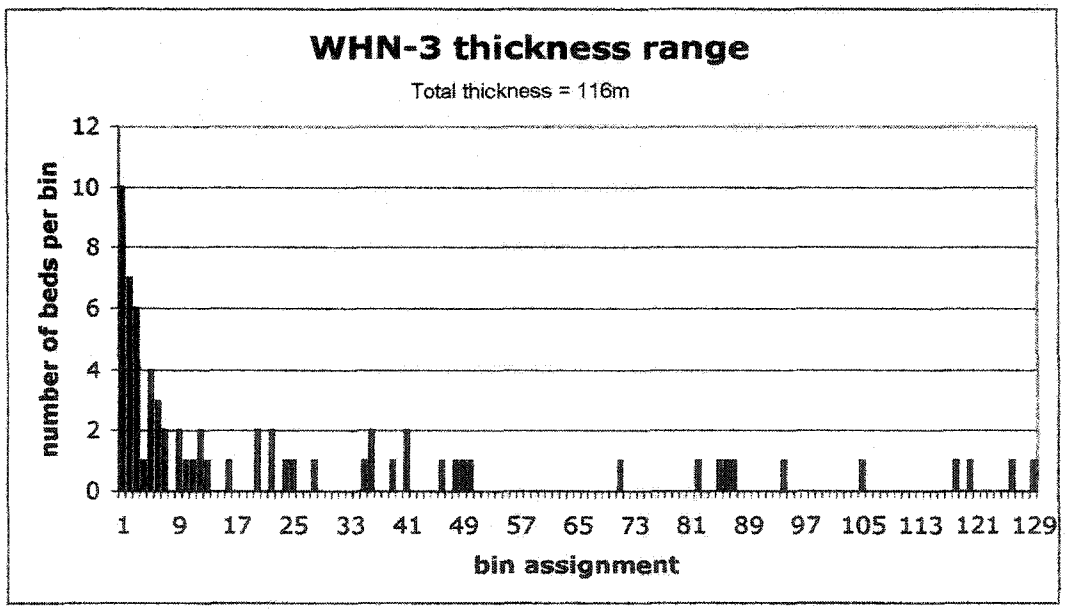

Reproduced with permission of the copyright owner. Further reproduction prohibited without permission.

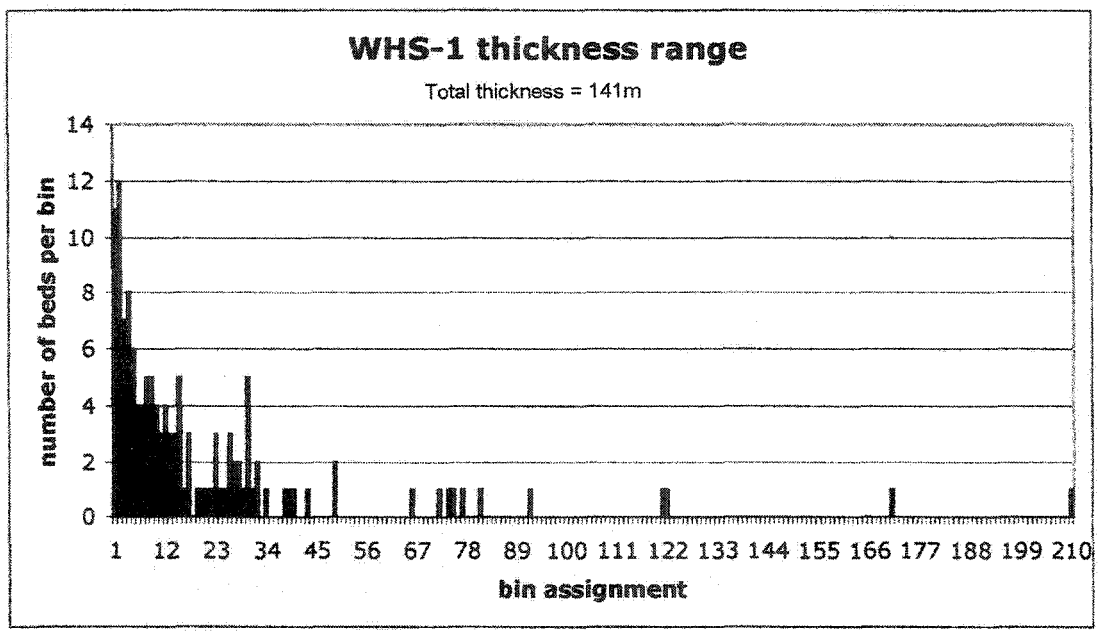

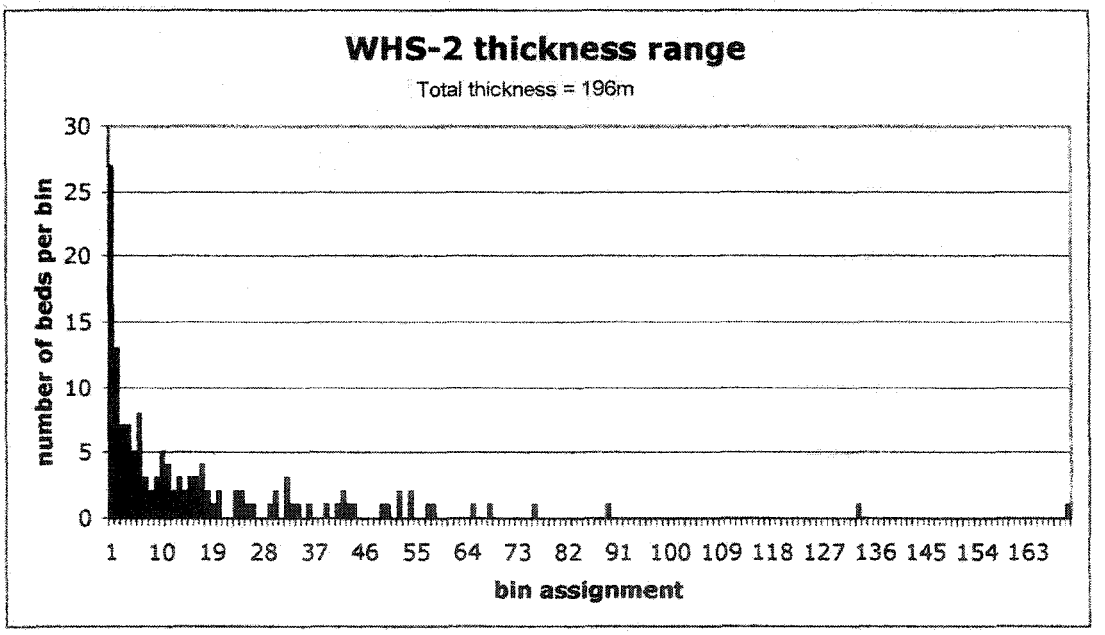

Reproduced with permission of the copyright owner. Further reproduction prohibited without permission.

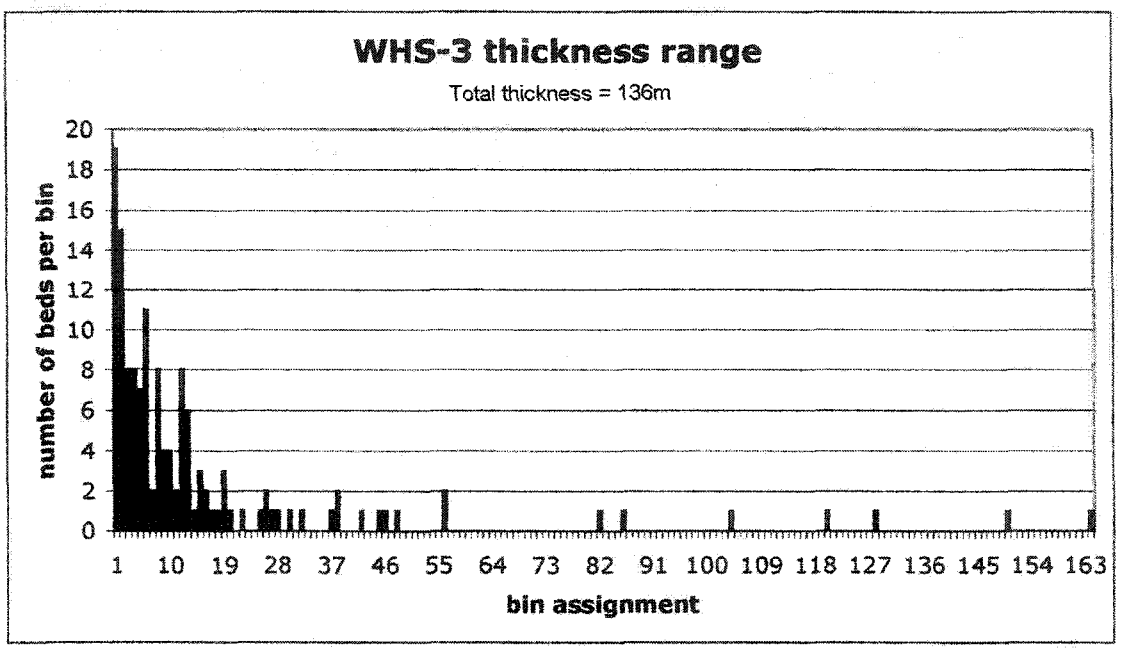

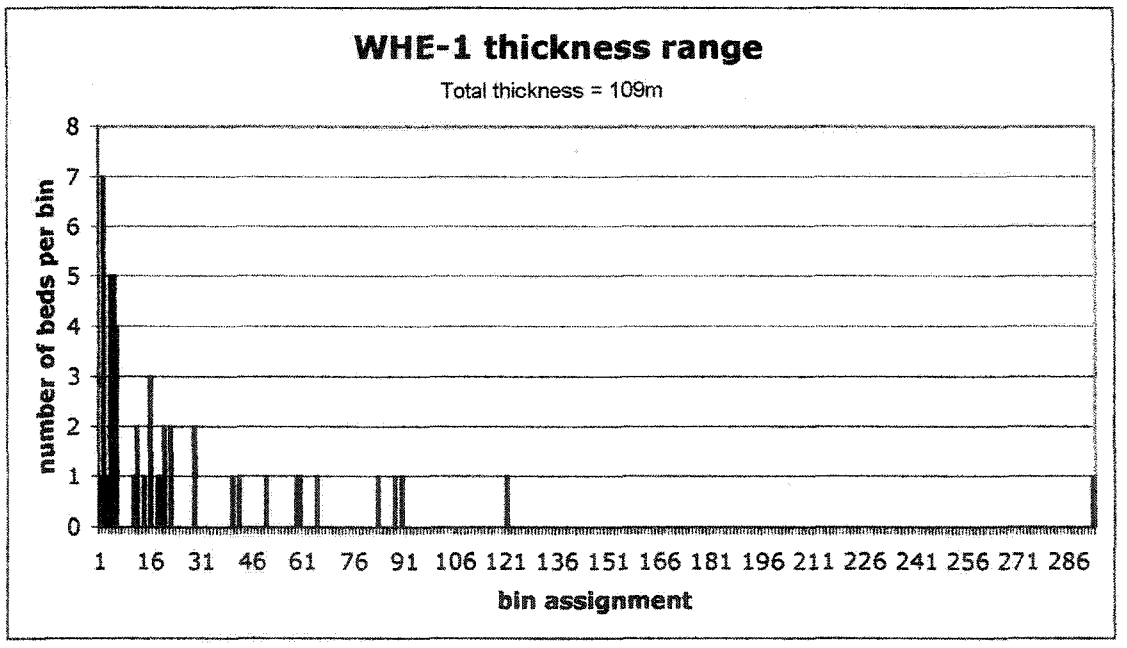

Reproduced with permission of the copyright owner. Further reproduction prohibited without permission.

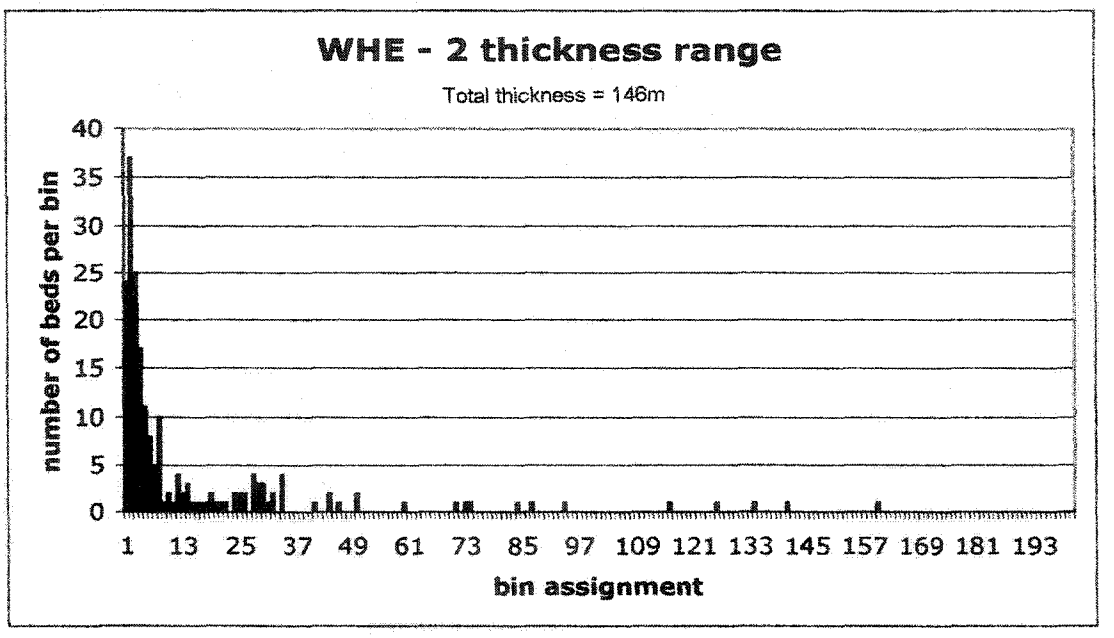

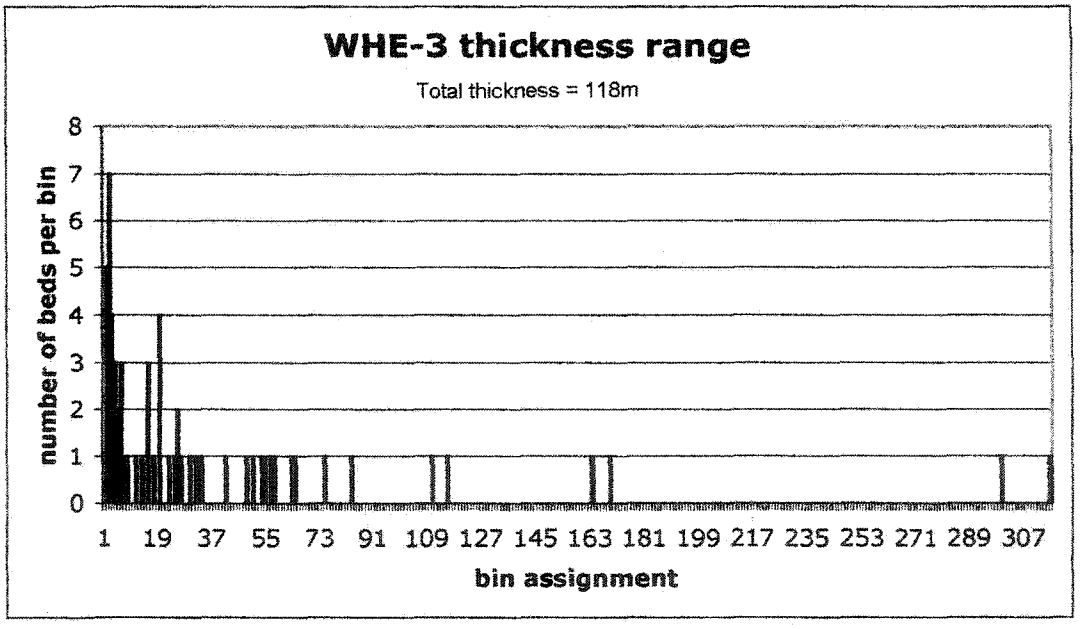

Reproduced with permission of the copyright owner. Further reproduction prohibited without permission.

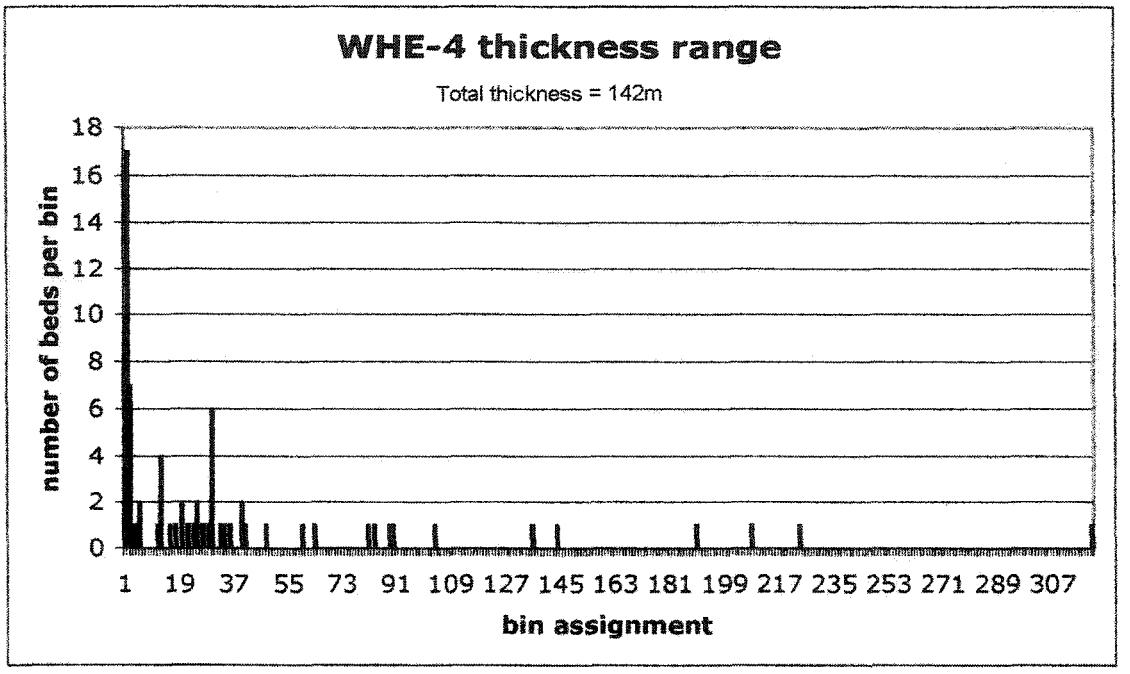

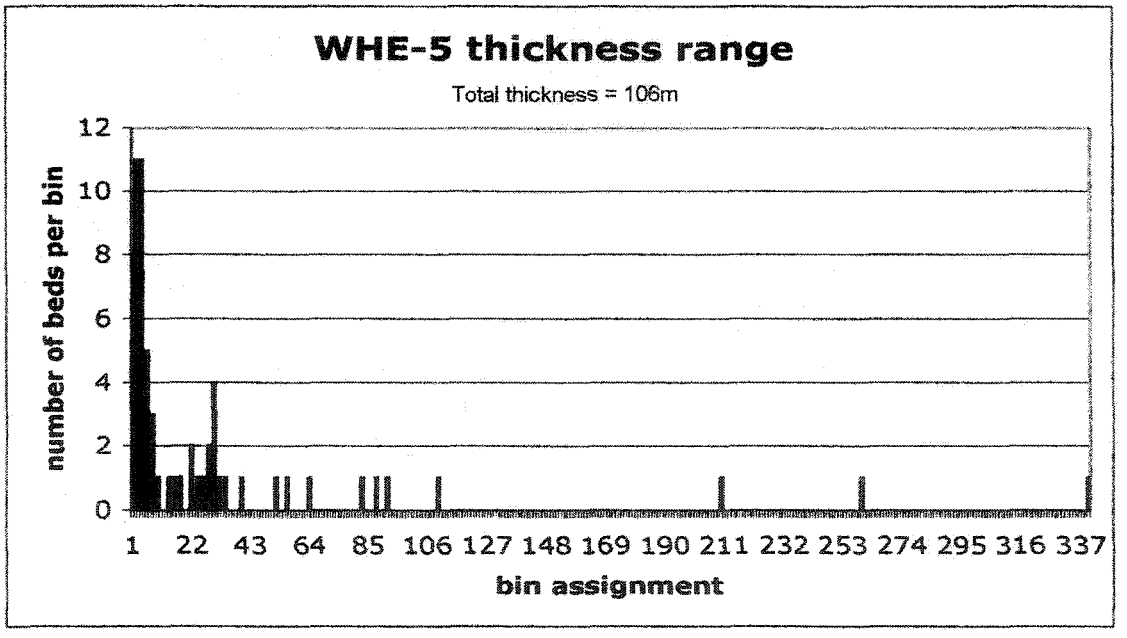

Reproduced with permission of the copyright owner. Further reproduction prohibited without permission.

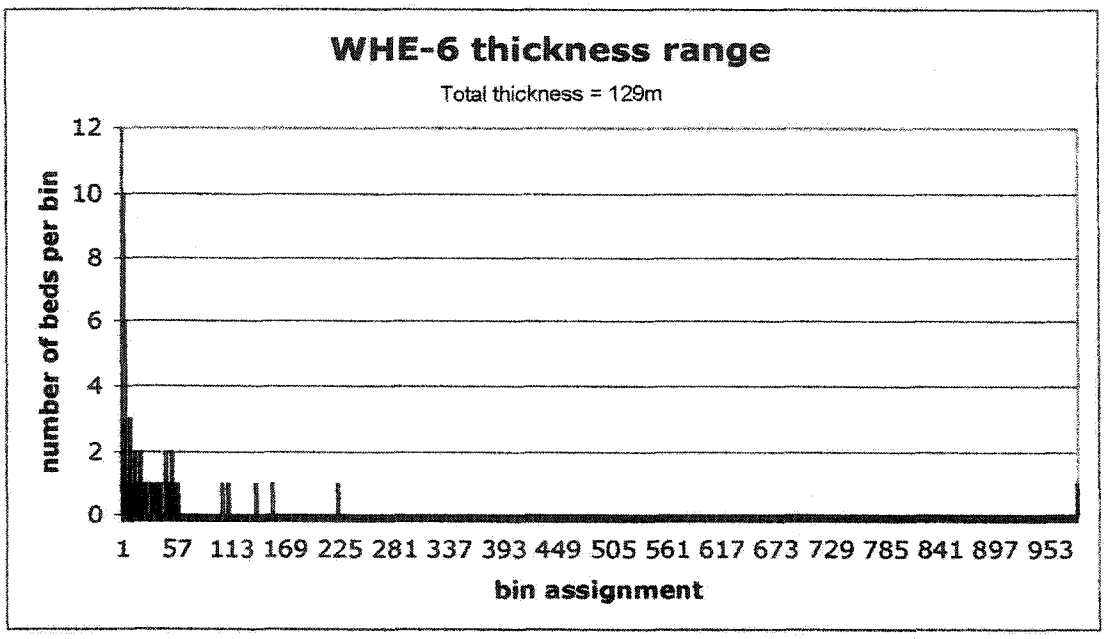

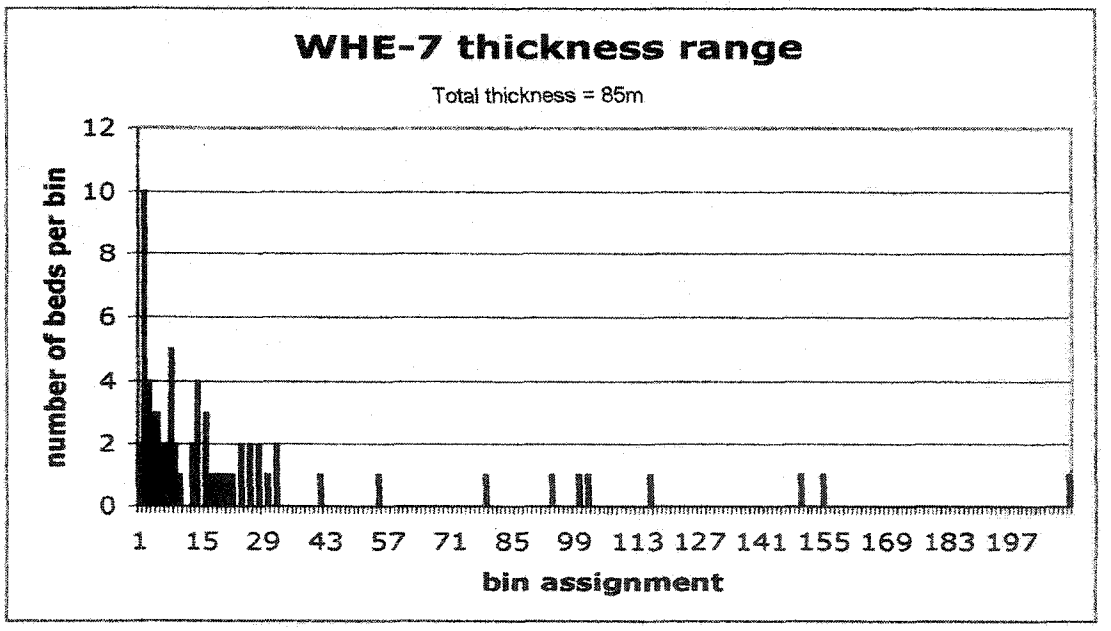

Reproduced with permission of the copyright owner. Further reproduction prohibited without permission.

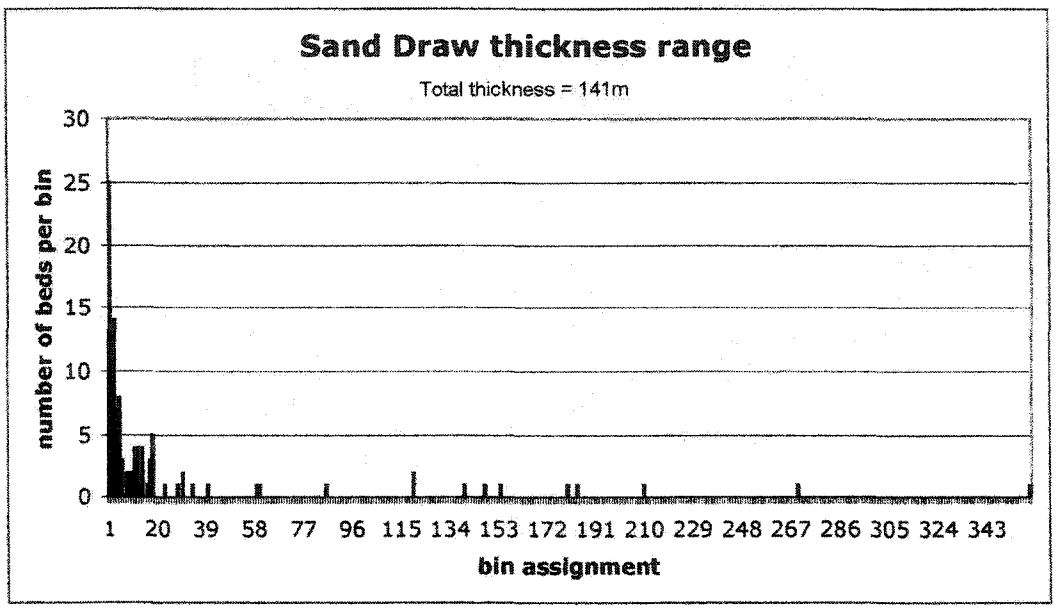

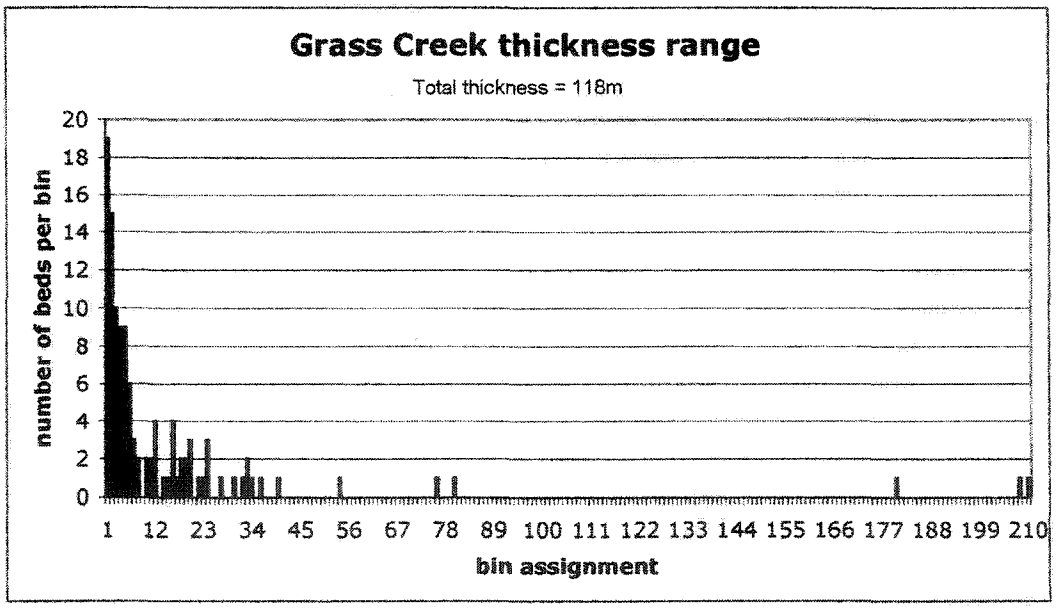

Reproduced with permission of the copyright owner. Further reproduction prohibited without permission.

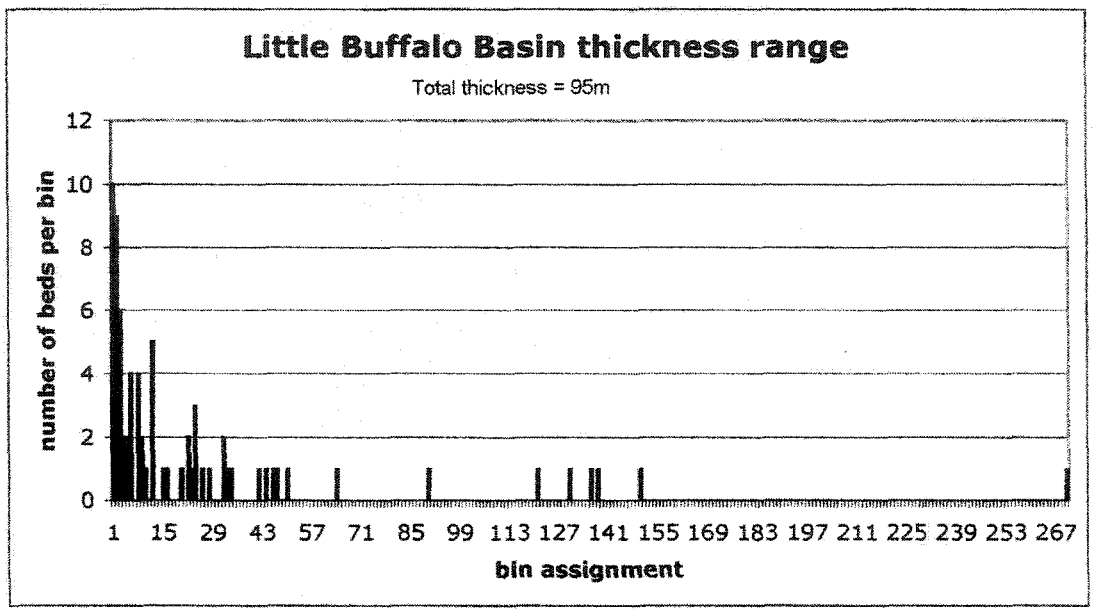

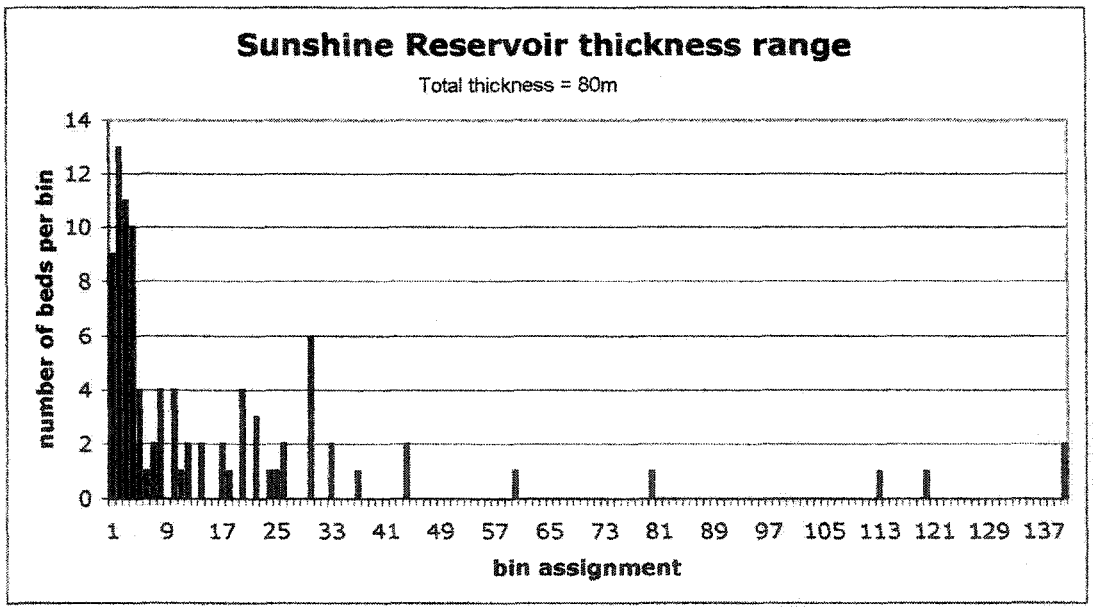

Reproduced with permission of the copyright owner. Further reproduction prohibited without permission.

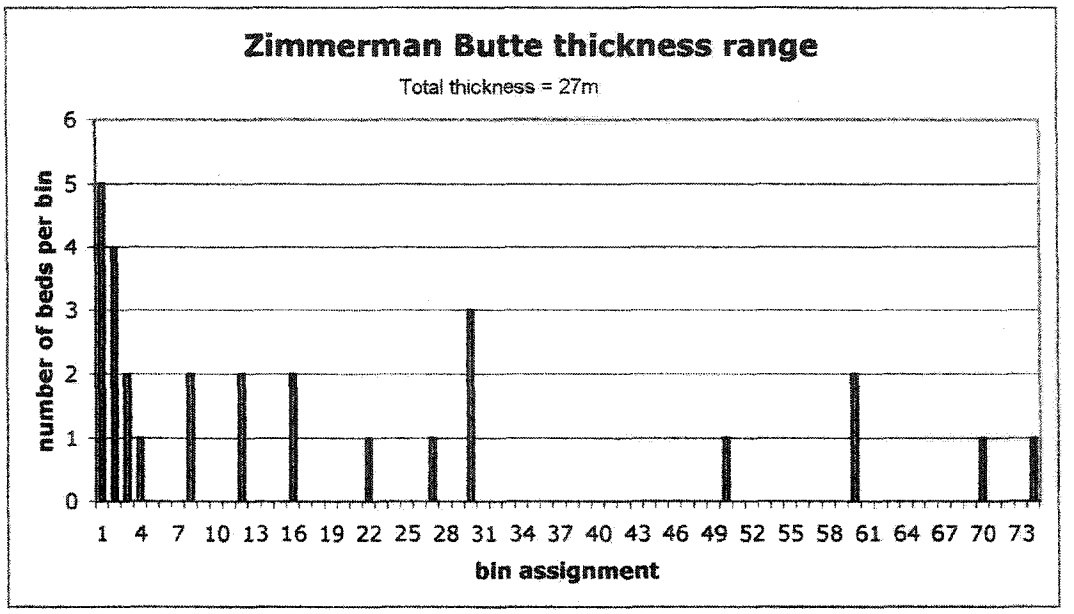

Reproduced with permission of the copyright owner. Further reproduction prohibited without permission.

VITA

KIMBERLY ANN JOHNSON

EDUCATION: Ph.D. in Geological Oceanography, January 1999 – May 2005
Old Dominion University, Norfolk, VA
GPA 3.70
Dissertation title: *Correlation and Causes of Fifth Order Cycles within the Bighorn Basin of Wyoming*

M.S. in Geology
Old Dominion University, Norfolk, VA, August 1995
GPA 3.58
Thesis title: *Late Cretaceous Foraminifera as Indicators of Sequence Boundaries, Book Cliffs, Utah, U.S.A. - Conducted under National Science Foundation Grant #NSF-EAR- 9304422*

B.S. in Geology\ Minor in Biology
Old Dominion University, Norfolk, VA, August 1992
GPA 2.8 overall; 3.3 in major

EXPERIENCE:

Research Assistant, Old Dominion University, 1/98 to 5/05
Under direct supervision of a Principle Investigator; responsible for field work, Including applying geologic principles, collection of sediment samples, laboratory work that consisted of sample processing, grain size analysis, permeability studies, statistical analysis, ground penetrating radar (GPR) and tomography analysis.

Teaching Assistant, University of Georgia, summers of 1993, 2000, 2001, 2002 and 2003
Field assistant for instructor of geology field course (Field Camp) mapping areas in Colorado, Utah, and New Mexico. Responsible for evaluating student geologic maps, organizing field trips, food and field supplies.

Adjunct Faculty, Old Dominion University, Norfolk, Virginia, 8/02 to present
Instructor for Geology and Introductory Oceanography lectures and labs. Responsible for oral presentations and lectures, preparing and administering tests as well as evaluating student performance.

Adjunct Faculty, Tidewater Community College, Virginia Beach Campus, 1/00 to present
Instructor for Geology and Introductory Oceanography lectures and labs. Responsible for oral presentations and lectures, preparing and administering tests as well as evaluating student performance. Conducted cruises on the R/V Matthew F. Maury and instructed students on the use of various oceanographic equipment.

Field Geologist/Site Manager, IT Corporation, NC and VA, 1/96 to 5/98
Responsible for all aspects of field work which included supervising drilling projects, soil and groundwater sampling, remediation system installation and maintenance as well as Phase I and Phase II environmental site assessments. Managerial duties included scheduling, preparing cost estimates and report writing. Responsible for up to 20 different sites.

Reproduced with permission of the copyright owner. Further reproduction prohibited without permission.